METABOLIC STUDIES OF THE HYPERTHERMOPHILIC ARCHAEON, *PYROCOCCUS FURIOSUS*, USING DNA MICROARRAYS

by

GERRIT JAN SCHUT, JR.

(Under Direction the of Michael W. W. Adams)

ABSTRACT

This research developed a DNA microarray-based system for *Pyrococcus furiosus* and used this molecular tool to generate data to increase the understanding of the physiology of *P. furiosus*. Initially microarrays containing 271 ORFs were constructed and were used to study the differential regulation of these ORFs in cells grown in the presence and absence of elemental sulfur (S^o). Most of the ORFs whose expression was down-regulated appeared to be related to the three multi-subunit hydrogenases in this organism, of which two are cytoplasmic and one is membrane bound. Down-regulation of the expression of these ORFs correlates well with the hydrogenase activities measured in cell-free extracts, indicating that none of these hydrogenases are directly involved in S^o metabolism. Two conserved hypothetical ORFs, now termed SipA and SipB (for sulfur-induced protein), were highly (>25-fold) up-regulated in S^o cultures and might participate in a novel S^o-reducing system. Using the methods developed by analyzing 271 ORFs, DNA microarrays were constructed for all 2065 ORFs annotated in the *P. furiosus* genome. These microarrays were used to analyze relative transcript levels in cells grown with peptide or with maltose as the primary carbon source. 126 ORFs showed differential

expression levels of more than 5-fold between the two culture conditions and 82 of these appeared to be part of operons, indicating substantial coordinated regulation. Most of the ORFs up-regulated in maltose-grown cultures appear to be involved in amino acid metabolism, an incomplete citric acid cycle and glycolysis. Many of the ORFs up-regulated in peptide cultures seem to be involved in the production of aryl and acyl acids from amino acids or encode enzymes involved in gluconeogenesis. The concentrations and types of aryl and acyl acids in spent growth media were consistent with the expression data. Interestingly, all ORFs encoding enzymes in the glycolysis and gluconeogenesis appeared to be monocistronic. The most strongly regulated were those encoding the enzymes glyceraldehyde-3-P dehydrogenase, phosphoglycerate kinase and fructose-1,6-bisphosphatase, suggesting that the glycolytic and gluconeogenic pathways in the *P. furiosus* are very tightly regulated.

INDEX WORDS: Hyperthermophile, archaea, *Pyrococcus furiosus*, DNA microarray, physiology, metabolism, glycolysis, gluconeogenesis, hydrogenase, 2-ketoacid ferredoxin oxidoreductase, organic acid, peptide, maltose, sulfur, carbohydrate

METABOLIC STUDIES OF THE HYPERTHERMOPHILIC ARCHAEON, *PYROCOCCUS FURIOSUS*, USING DNA MICROARRAYS

by

GERRIT JAN SCHUT, JR.

B.S., International Agricultural College Larenstein, Netherlands, 1991

Master of Agricultural Sciences, Wageningen Agricultural University, Netherlands, 1994

A Dissertation Submitted to the Graduate Faculty of The University of Georgia in Partial Fulfillment of the Requirements for the Degree

DOCTOR OF PHILOSOPHY

ATHENS, GEORGIA

2003

METABOLIC STUDIES OF THE HYPERTHERMOPHILIC ARCHAEON,

PYROCOCCUS FURIOSUS, USING DNA MICROARRAYS

by

GERRIT JAN SCHUT, JR.

Major Professor: M. W. W. Adams

Committee: L. G. Ljungdahl
W. B. Whitman
R. J. Maier
M. P. Terns

Electronic Version Approved:

Maureen Grasso
Dean of the Graduate School
The University of Georgia
May 2003

DEDICATION

I dedicate this dissertation to my parents, Gerrit Jan Schut Sr. and Jacomina Geertruida Schut-Jochems.

Ik wijd dit proefschrift aan mijn ouders Gerrit Jan Schut Sr. en Jacomina Geertruida Schut-Jochems

ACKNOWLEDGEMENTS

A Dutch dissertation normally contains a number of quotes about the research presented and about normal life. I have two quotes for the reader, and they can be applied to both this research and normal life. 1) Never blindly trust the materials you purchased, especially if the supplier claims that he or she is much better and cheaper than anyone else. 2) Genome sequence databases contain a wealth of information; but this does not mean you can count yourself “rich”. I have used this “rich” resource throughout my PhD research to increase the knowledge of the *Pyrococcus furiosus* physiology. I am now able to answer some of the question raised by literature concerning *P. furiosus* and related archaea, however at the same time I have generated many new questions. For example, a conserved hypothetical protein is of little interest when looked at in the genome sequence but a highly regulated conserved hypothetical can become an intriguing ‘question’. With this dissertation I am closing a chapter in my life which gave me a broad understanding of *P. furiosus* physiology and the use of the microarray technique.

A long list of people helped me through the years that I worked on my dissertation. I am very thankful to my supervisor Michael Adams for his “wonderful” guidance. I thank all members of the Adamslab (new and old), my committee, members of the Zhoulab at ORNL (Oakridge, TN), staff of the GAF facility (UGA), members of the Prattlab (UGA), and last but not least my wonderful wife Eleanor Green Schut.

TABLE OF CONTENTS

Page

LIST OF TABLES

Page

LIST OF FIGURES

Page

LIST OF ABBREVIATIONS

ACS - acetyl-CoA synthetase

Af - Aquifex

Afu, *Archaeoglobus fulgidus*

Ag - Archaeoglobus

AOR - aldehyde ferredoxin oxidoreductase

Ap - Aeropyrum

Ape - *Aeropyrum pernix.*

AF - Aquifex

CoASH - coenzyme A

EM - Embden-Meyerhof

ED - Entner-Douderhoff

FBA - fructose-1,6-bisphosphate aldolase

FBP - fructose-1,6-bisphosphatase

Fd - ferredoxin

FOR - formaldehyde ferredoxin oxidoreductase

GAPDH - glyceraldehydes-3-P dehydrogenase

GAPN - non-phosphorylating glyceraldehydes-3-phosphate dehydrogenase

GAPOR - glyceraldehydes-3-P ferredoxin oxidoreductase

GDH - glutamate dehydrogenase

GLK - glucokinase

IOR - indolepyruvate ferredoxin oxidoreductase

KGOR - 2-ketoglutarate ferredoxin oxidoreductase

Mac - *Methanosarcina acetivorans*

MBH - membrane bound hydrogenase

Mc - Methanocaldococcus

Mja - *Methanocaldococcus jannaschii*

Mka - *Methanopyrus kandleri*

Mma - *Methanosarcina maze*

Mp - Methanopyrus

Ms - Methanosarcina

Mth - *Methanothermobacter thermoautotrophicus*

Mt - Methanothermobacter

NAD - nicotinamide adenine dinucleotide

NADH - nicotinamide adenine dinucleotide (reduced)

NADP - nicotinamide adenine dinucleotide phosphate

NADPH - nicotinamide adenine dinucleotide phosphate (reduced)

ORF - open reading frame

P - Pyrococcus

Pab - *Pyrococcus abyssi*

Pae - *Pyrobaculum aerophilum*

Pb - Pyrobaculum

PFK - phosphofructokinase

Pfu - *Pyrococcus furiosus*

PGI - glucose-6-phosphate isomerase

PGK - phosphoglycerate kinase

PGM - phosphoglycerate mutase

Pho - *Pyrococcus horikoshii*

PK - pyruvate kinase

POR - pyruvate ferredoxin oxidoreductase

RT - reverse transcription reaction

Sl - *Sulfolobus*

Sso - *Sulfolobus solfataricus*

Sto - *Sulfolobus tokodaii*

Tac - *Themoplasma acidophilum*

Tc - *Thermococcus*

Tp - *Thermoplasma*

TPI - triosephosphate isomerase

TrmB - transcriptional regulator of mal operon

Tt - *Thermoproteus*

Tvo, *Thermoplasma volcanium*

VOR - isovalerate ferredoxin oxidoreductase

XOR - 2-ketoacid ferredoxin oxidoreductase

CHAPTER 1

INTRODUCTION AND LITERATURE REVIEW

Hyperthermophiles are usually defined as microorganisms with optimal growth temperatures of at least 80ºC, and most display little or no growth below 70ºC or so. Hyperthermophiles have been isolated from 'hotspots' located all over the world, such as hydrothermal vents, black or white smokers, solfataric fields, hot springs and even hot oil wells (172). With the isolation of *Pyrolobus fumarii*, the upper temperature of life has reached 113 ºC (15). In the last twenty years many different types of hyperthermophiles have been isolated, mainly due to the efforts of K.O. Stetter (Regensburg, Germany) and W. Zillig (München, Germany). All of them are prokaryotes and most belong to the domain of archaea (171). The archaea form the third phylogenetic domain of life in addition to the bacteria and the eukaryotes (191). The basis for this division is the comparison of 16S and 18S ribosomal RNA sequences. Based on the sequence differences, a phylogenetic tree, such as Figure 1.1, can be constructed assuming that all organisms are derived from a common ancestor (191). The domain of archaea is divided into two major phyla, the Crenarchaeota and the Euryarchaeota. A third phylum (Korarchaeota) has been proposed purely on the basis of 16S rRNA sequence data from environmental samples (9). However no organism from this potential phylum has ever been grown or characterized. Just before retiring, Stetter (and coworkers) added a new phylum to the archaea called Nanoarchaeota (66). The only species characterized in this new phylum is *Nanoarchaeum equitans*, a small (400 nm) cocci, obligately dependent for

growth on the presence of another archaeon belonging to the genus of *Ignicoccus*. Both host and symbiont have a growth range of 70ºC to 98ºC (66).

Most of the Crenarchaeota are hyperthermophiles or like some *Sulfolobus* species grow optimally above 70°C (171). The Euryarchaeota, on the other hand, display a much greater range of growth temperatures, and there are examples of mesophiles within the methanogens and the halophiles. Only two genera of bacteria contain species that are considered hyperthermophilic, and these are *Aquifex* and *Thermotoga*. Interestingly, both *Aquifex* and *Thermotoga* represent very deep phylogenetic branches of the bacterial domain, (Figure 1.1; (67, 69). Although species of these bacterial genera grow well above 80ºC, none of them are capable of growth at 100ºC or above, only archaea are able to grow at such high temperatures.

The hyperthermophiles show an enormous variation in their metabolic characteristics (154). There is no such thing as a typical hyperthermophilic metabolism. In fact, many of the metabolic properties of mesophilic bacteria are found in the hyperthermophilic archaea, although this group does not include a photoautotroph or a nitrogen fixer. The hyperthermophiles include examples of chemolithoautotrophs that couple H_2 oxidation to the reduction of CO_2 (methanogens), NO_3^- reduction to N_2 (denitrifiers), SO_4^{2-} (and other sulfur oxides) to H_2S (sulfate reducers), S^o to H_2S (sulfur reducers), and the reduction of O_2 (aerobic respirers) (68, 154). However, a large number of the hyperthermophiles that have been described are strict anaerobic heterotrophs. Most of them utilize complex peptides as a carbon source, often in a S^o-dependent matter (Table 1.1). A number of the hyperthermophiles are also capable of using carbohydrates as a growth substrate and starch appears to be the most preferred substrate (83).

In all life forms, whether eukaryotes, archaea or bacteria, there are two major types of pathway involved in the degradation of glucose to pyruvate, the Entner-Doudoroff (ED) and the Embden-Meyerhof (EM) pathway. Studies of the glycolytic pathway in archaea have focused mainly on species of three genera, *Sulfolobus*, *Thermoproteus* and *Pyrococcus*. *Pyrococcus* uses a modified form of the EM pathway, *Thermoproteus* uses a mixture of modified forms of both the EM and ED pathway, while *Sulfolobus* uses a modified version of the ED pathway (154). Comparisons of the metabolisms and properties of individual enzymes in these organisms and in other archaea will be very useful in understanding diversity of archaeal physiology. A tremendous resource for such comparison is the genome sequences of eighteen archaea (Table 1.2) which are currently available through NCBI (www.ncbi.nlm.nih.gov/PMGifs/Genomes/micr.html)

The Metabolism of Peptides by *P. furiosus*

P. furiosus is one of the best studied of the hyperthermophilic archaea and is sometimes considered the '*E. coli*' of the hyperthermophilic world. Like most of the heterotrophic archaea *P. furiosus* can grow on peptides as a carbon source, but it then requires the presence of S^o (43). This is also true for its close relatives, *P. horikoshii* and *P. abyssi* (40, 49). There is little information on how peptides and amino acids are metabolized intracellularly in the archaea. Most research has been done with *Pyrococcus* and *Thermococcus* species and a metabolic pathway has been proposed (see Figure 1.2; (2)). In the first step, amino acids are deaminated by the appropriate transaminase and the glutamate dehydrogenase cycle to yield 2-ketoacids and ammonia. Subsequently the 2-ketoacids are converted by several distinct ferredoxin-linked 2-ketoacid oxidoreductases

to the corresponding acyl-CoA. 2-Ketoacid ferredoxin oxidoreductases (KORs) include IOR which is specific for aromatic 2-ketoacids (112), VOR which is specific for branched chain 2-ketoacids (58), KGOR which is specific for 2-ketoglutarate only (111), and POR which also functions in glucose metabolism and mainly utilizes pyruvate (12). All four enzymes are closely related in sequence and contain similar motifs (158). The genome sequence of *P. furiosus* contains additional homologs of the KOR family but their function is unknown (110). The acyl-CoA derivatives produced by the KORs are converted to the corresponding organic acid by the combined action of two reversible ADP-dependent acetyl-CoA synthetases (Figure 1.3) (113).

The Metabolism of Glucose by *P. furiosus*

P. furiosus is also able grow on a variety of carbohydrates, including starch, maltose and cellobiose but not glucose, in both the presence and absence of S^o, producing acetate, CO_2 and H_2 (or H_2S in the presence of S^o) as major end products (43). The first reports on *P. furiosus* glucose metabolism indicated the existence of a non-phosphorylated ED type pathway (117, 149). However, based on ^{13}C-labeling and enzyme studies, a modified EM pathway was later proposed (80). Modifications of the *P. furiosus* EM pathway were subsequently found to include two ADP-dependent sugar kinases, glucokinase and phosphofructokinase (Figure 1.4; (80, 82, 176). In addition, the classical glycolytic enzymes glyceraldehyde-3-phosphate dehydrogenase (GAPDH) and phosphoglycerate kinase (PGK) are replaced by one enzyme, glyceraldehyde-3-phosphate ferredoxin oxidoreductase (GAPOR (116). This is a novel tungsten and iron-sulfur cluster containing enzyme that catalyzes the direct phosphate-independent conversion of glyceraldehyde-3-phosphate (GAP) to 3-phosphoglycerate with ferredoxin as the electron

acceptor rather than NAD(P). It has also been proposed that this enzyme is a central point of regulation in the glycolytic pathway of *P. furiosus* (178). Omitting the ATP generating steps from GAP to 3-phosphoglycerate reduces the overall substrate level ATP yield of the *P. furiosus* glycolysis to zero. ATP is generated when pyruvate is converted to acetate. In all acetate-forming archaea, the conversion from pyruvate to acetate involves two enzymes (Figure 1.4). The first enzyme, pyruvate ferredoxin oxidoreductase (POR) catalyzes the oxidative decarboxylation to acetyl-CoA with ferredoxin as an electron donor and the second enzyme, an ADP forming acetyl-CoA synthetase (ACS), couples acetate formation to the substrate level phosphorylation of ADP to ATP (113, 150). These two enzymes form a connection between glucose and peptide metabolism as depicted in Figure 1.3. The ACS enzyme is unique to the domain of archaea. In bacteria, this reaction is normally accomplished by two enzymes, phosphate acetyltransferase and acetate kinase (154), two enzymes that have been found thus far only found in the archaea in acetate-utilizing *Methanosarcina* species (97, 104).

The Metabolism of Glucose by *Thermoproteus* and *Sulfolobus*

Thermoproteus tenax

Thermoproteus (Tt) tenax is a strict anaerobic archaeon isolated from hot spring in Iceland and has an optimal growth temperature of 88 ºC (196). It is capable of growing both chemolithoautotrophically on H_2, CO_2 and S^o as well as heterotrophically on carbohydrates like glucose, starch and amylose using S^o as and electron acceptor. ^{13}C-labeling studies demonstrated that sugar metabolism involves a modified EM pathway as well as a modified ED pathway (with fluxes of approximately 85% and 15%, respectively (160). Its EM type pathway is different from the *P. furiosus* version in that it contains an

ATP (rather than ADP)-dependent glucokinase and a pyrophosphate (rather than ADP)-dependent phosphofructokinase (164, 165). The conversion of glyceraldehyde-3-P proceeds through a irreversible phosphate-independent GAPDH (GAPN) with NAD as an electron acceptor, analogous to the *P. furiosus* reaction except that ferredoxin is not utilized as it is in the GAPOR enzyme (22). *Tt. tenax* also contains a canonical GAPDH but this enzyme is mainly expressed during autotrophic growth and likely functions solely in gluconeogenesis (23). Surprisingly, unlike the analogous *P. furiosus* GAPOR enzyme, GAPN does not appear to be transcriptional regulated (23). However the GAPN enzyme is allosterically regulated by several metabolites. NADPH, NADP, NADH and ATP reduce its affinity for its cosubstrate, NAD, while glucose-1-P, AMP, fructose-6-P, ADP, fructose-1-P and ribose-5-P increase the affinity for NAD. The ED type pathway in *Tt. tenax* is similar to the one found in *Sulfolobus* (see below) and the first enzyme in this pathway, glucose dehydrogenase, has been characterized (166). The rationale for the presence of two glycolytic pathways in *Tt. tenax* is a mystery. *Tt. tenax* uses an oxidative TCA cycle to completely oxidize its growth substrate to CO_2 and is strictly dependent on S^o to do so (164). How *Tt. tenax* couples the reoxidation of ferredoxin and NADH to the reduction of S^o is completely unknown, but presumably energy is conserved in this process as *Tt. tenax* can grow autotrophically using H_2 and S^o as an energy source.

Sulfolobus

Sulfolobus species are generally aerobes (microaerophiles) and most of them grow at low pH (1-5) optimally between 70 and 80°C and are considered thermoacidophiles (147, 171). They can grow heterotrophically on peptides or a variety of carbohydrates including glucose and some are autotrophic gaining energy by the oxidation of various sulfur-containing compounds such as thiosulfates (154). Glucose degradation has mainly

been examined in two species, *Sulfolobus (Sl) solfataricus* and *Sl acidophilum* and in both it proceeds through a modified version of the ED pathway as depicted in Figure 1.5 (160). This pathway is different from the standard ED pathway in that the upper half does not require phosphorylation since 2-phosphoglycerate is formed by a unique glycerate kinase (31, 32). Under aerobic conditions, pyruvate is completely degraded to CO_2 through the TCA cycle. This modified or non-phosphorylated ED pathway is also thought to operate in less thermophilic (Topt ~ 60°C) archaeon, *Thermoplasma (Tp) acidophilum* (31). The NAD(P)H that is generated in the glycolysis and the TCA cycle is reoxidized by a relatively simple respiratory pathway involving two quinol oxidases (148). However, only an incomplete NADH dehydrogenase complex was identified in the genome sequence of *Sl. solfataricus* rendering the precise mechanism of the respiratory chain unknown (161).

The Metabolism of Poly- and Oligosaccharides by *P. furiosus*

A large number of archaeal species have been identified that can growth on a variety of α- and β- linked polysaccharides as well as on monosaccharides (83). Within the family of Thermococcales, the main carbohydrates used are starch and glycogen. From a biotechnological standpoint there is much interest in enzymes able to degrade starch at elevated temperatures since many industrial processes are performed at high temperatures (100). Starch is a polymer composed of a-1,4 linked glucose units with a-1,6 linked branches. From *P. furiosus* several starch degrading enzymes have been described, including an intracellular amylase (PF0272, (94), an extracellular amylase (PF0477, (76) and an amylopullulanase (PF1935, (37). Amylases cleave the a-1,4 bonds in starch releasing oligomaltosaccharides while amylopullulanases can cleave both a-1,4

and a-1,6 bonds and thus debranch the starch molecule. The starch-degrading enzymes are very well characterized with respect to their biochemical properties, however, very little is known about their physiological role in the metabolism of *P. furiosus*. The amylases of this organism were first thought not to be dependent on the presence of Ca ions for stability, however, it has been shown that the amylopullulanase contains tightly bound Ca and the extracellular amylase contains both Ca and Zn (102, 145, 146)}. In order to degrade maltooligosaccharides including maltose, *P. furiosus* presumably uses an intracellular a-glucosidase. However the identity of this enzyme is still unclear. An enzyme with this activity was isolated, but was not identified in the genome sequence (29).

So far only a few studies have addressed how these oligosaccharides are transported in to an archaeal cell. A high affinity ABC-type maltose/trehalose transport system has been extensively studied in the hyperthermophile *Thermococcus (Tc) litoralis* (192, 193). The transport unit, depicted in Figure 1.6, consists of four proteins; an extracellular membrane anchored maltose binding protein (MalE), two membrane-spanning permease proteins (MalF and G) and an ATP-binding protein (MalK) (193). Interestingly, the genes encoding these proteins are clustered together and potentially consist of the following three transcriptional units (Figure 1.6); MalE (PF1739), MalF, G and a putative trehalose synthase (PF1740-1742), and the MalK encoding gene, which is potentially co-transcribed with a transcriptional regulator (PF1743 and 1744). It was demonstrated that PF1743 codes for a transcriptional suppressor acting on the Mal cluster. Upon binding to its ligand, maltose, and to a lesser extent, trehalose, this suppression is released, thus allowing expression of the Mal cluster (99). The function of PF1742, which is annotated as trehalose synthase, has yet to be elucidated but a role in

maltose metabolism seems logical. Other than that, the Mal cluster appears to be a functional maltose transport/utilization unit. It was suggested that *P. furiosus* might have acquired the Mal cluster from *Tc. litoralis* through a transposon-mediated horizontal transfer event (36). A 16 kb DNA region, including the Mal cluster and flanked by transposons, is almost identical in *P. furiosus* and *Tc. litoralis*. Its presence in *P. furiosus* likely gives the organism the ability to utilize maltose as a carbon source (36). Moreover, it was shown that MalF, G and K could be expressed in *E. coli* as a functional unit despite the difference in growth temperature and membrane composition (51).

P. furiosus and *Tc. litoralis* contain a second Mal cluster (II), in addition to the one described above. This Mal II cluster is similar (at the amino acid level) to Mal I and contains homologs of MalE (PF1938), F (PF1937), G (PF1936) and K (1933), although instead of a trehalose synthase mal II contains the amylopullulanase (PF1935) mentioned above (37) as well as an unknown ORF. The crystal structure of the Mal II E protein from *P. furiosus* has been determined in the presence of maltose and surprisingly maltotriose was bound, indicating that this transporter might act on maltooligosaccharides (probably generated by the amylopullulanase) rather than the disaccharide maltose (42). This Mal II cluster has been identified in *Tc. litoralis* (NCBI genbank entry AB054186) but does not indicate a ‘recent’ history of horizontal transfer due to the lack of sequence similarity on nucleotide level. This Mal II cluster might be involved in the transport of maltooligosaccharides during growth on starch.

Besides a-linked sugars, *P. furiosus* has also been reported to grow on the ß-(1,4) linked sugar cellobiose as well as higher oligomer forms (up to 6 glucose units; (81)). These are potential breakdown products of cellulose and a ß-glucosidase (PF0073) able to hydrolyze cellobiose was identified (78, 186). However, cellulose itself does not seem to

serve as a carbon source. *P. furiosus* is also able to utilize additional ß-(1,3) and ß-(1,4) linked sugars such as laminarin, ß-glycan and lichenan, and subsequently a ß-1,3-endoglucanase (PF0076) capable of hydrolyzing these three substrates was identified (52, 78). The endoglucanase was found in an operon with two alcohol dehydrogenases (PF0074 and 0075) and this operon appeared to share a promoter domain with the gene coding for the above mentioned ß-glucosidase (187). Moreover the ß-glucosidase also hydrolyses ß-(1,3) oligoglucosides and they are presumably the products of endoglucanase activity (34). Recently a high affinity ABC-type transport system specific for both ß-(1,3) and (1,4) oligoglucosides was described in *P. furiosus* and it appeared that the genes encoding it (PF1357-1361) cluster together in a fashion analogous to that of the maltose/trehalose transport cluster (91). The genome sequence of *P. furiosus* contains three additional uncharacterized ABC transporter clusters with similar organization and these are PF0191-0194; PF0357-0361; PF1408-1412.

The Metabolism of Hydrogen and Sulfur in *P. furiosus*.

P. furiosus appears to utilize hydrogenases and an unknown sulfur reduction system for the disposal of reducing equivalents. Hydrogenases catalyze the interconversion of molecular hydrogen and protons, normally in a reversible manner. Based upon sequence homology and active site geometry, three classes of hydrogenases are recognized: iron-only (Fe), nickel-iron (Ni-Fe) and metal free hydrogenases (184). Fe-only hydrogenases are mainly found in anaerobic bacteria and some primitive anaerobic eukaryotes, for example, in the genera *Clostridia*, *Thermotoga* and *Trichomonas* (27, 77, 179) but so far they have not been identified in the domain of archaea. On the other hand, Ni-Fe hydrogenases are found in archaea as well as in bacteria. The metal free

hydrogenases are currently only found in methanogens (197). Both Fe only and Ni-Fe hydrogenases are complex metalloenzymes, containing both a unique catalytic center and several iron sulfur clusters ([Fe-S]) and they require a set of accessory proteins for maturation (184). Crystal structures are available for both the Fe and Ni-Fe enzymes (125, 185). One of the most remarkable features of both types of hydrogenase is the presence of CO and CN ligands coordinated to iron in their active sites (124, 127). For *E. coli* it was shown that the CO and CN ligands are likely derived from carbamoyl phosphate and thus linking hydrogenase maturation to amino acid metabolism (16, 121). It is striking that the enzymatic conversion involving the simplest of chemical compounds, molecular hydrogen, requires such complex enzymes.

P. furiosus contains two cytosolic, NADPH linked Ni-Fe hydrogenases (HyhI and II) and one membrane bound, ferredoxin linked Ni-Fe hydrogenase (105, 144). Both cytosolic hydrogenases consist of four different subunits ($\alpha\beta\gamma\delta$) and contain 6 [FeS] clusters, 1 NiFe site and 1 FAD (105). Both enzymes can reversible couple H_2 oxidation to the reduction of NADP or the artificial carrier methyl viologen, as well as reduce S^o with H_2 or NADPH. Hydrogenase II is approximately an order of magnitude less active than hydrogenase I (105). It was first proposed that hydrogenase I (or so-called sulfhydrogenase) had a novel dual function in the disposal of electrons by reducing protons as well as S^o using NADPH as the electron carrier (108). The discovery of a complex membrane bound hydrogenase (MBH) that could couple ferredoxin oxidation to the formation of H_2 made the pathway of electron transfer thermodynamically more feasible. It was shown that the H_2 production activity of MBH was more than an order of magnitude higher than that of the cytosolic hydrogenases leading to the proposal that MBH is responsible for the major path of ferredoxin reoxidation (Figure 1.7) (144, 167).

The MBH appears to be encoded by a 14 gene operon and interestingly three of these ORFs are homologous to components of the proton translocating NADH dehydrogenase complex from *E. coli* (144). The MBH is indeed able to generate a proton motive force during the reoxidation of ferredoxin coupled to the reduction of protons and represents the simplest form of respiration (Figure 1.7; (143)). It is likely that the reduced ferredoxin that is produced during glucose metabolism is oxidized via the MBH. No NAD(P)H need be formed in this reaction (Figure 1.4) and so the function(s) of the cytosolic hydrogenases remain unknown. When it was shown that both cytosolic and membrane bound hydrogenase activity as well as the expression of hydrogenase genes were down-regulated in S^o containing cultures, involvement of the hydrogenases in S^o metabolism became unlikely and the presence of an unknown S^o reducing mechanism was proposed (1, 159).

Besides the cytoplasmic hydrogenases, one other enzyme has been shown to possess S^o reduction activity *in vitro* and this is termed ferredoxin NADPH oxidoreductase (FNOR). This enzyme can transfer electrons between ferredoxin and NAD(P) and it can reduce S^o with NADPH as electron donor (106). FNOR is a two subunit protein (53 kDa and ß: 31 kDa) and both subunits show homology to other proteins in the genome with presumably unrelated functions. For example, the alpha subunit shows homology to glutamate synthase and the beta subunit shows homology to the gamma subunit of the cytoplasmic hydrogenases. Indeed the latter might be responsible for the S^o reductase activity of the two enzymes (53). FNOR has an interesting content of cofactors in that it contains a [2Fe-2S] cluster (in the a-subunit) and a [3Fe-4S] and a [4Fe-4S] cluster (in the ß-subunit) cluster and each subunit does contain flavin in the form of FAD (53). Because of its biochemical properties the physiological

role of FNOR is more likely to be the electron transfer from ferredoxin to NADP (106). From the genome sequence it appears that a close homolog of FNOR (tentatively called FNOR II) might be present as there are two ORFs (PF1910 and 1911) that show high homology to the FNOR I alpha and beta subunit respectively (92% and 62%) (53, 159). FNOR might be widespread among anaerobes because several potential FNOR encoding ORFs (homologous to *P. furiosus* FNOR) can be identified based in genome sequences. Potential homologs are present in many prokaryotes including, *P. horikoshii*, *P. abyssi*, *Thermotoga maritima*, *Thermoanaerobacter tengcongensis*, *Methanosarcina (Ms) mazei* and *Ms. acetivorans* (126). Moreover, the presence of FNOR in various organisms that do not metabolize S° also suggests that the enzyme is not likely to be involved in S^o reduction.

Tungsten-Containing Enzymes in *P. furiosus*

Tungsten (W) and molybdenum (Mo) are chemically similar elements. They have about the same ionic and atomic radii, as well as oxidation states. It has been known for many years that tungsten can replace molybdenum in Mo-containing enzymes but this typically leads to inactive W-analogs (86). Mo-enzymes have been found in most of the organisms, including archaea and higher eukaryotes, studied thus far (62, 63). The observation that tungsten has a functional role in biology was made several decades ago (103). In the last 20 years, several W-enzymes have been described and all of them are from prokaryotes (136). Several W-enzymes have been described from hyperthermophilic archaea, in particularly *P. furiosus*, and the obligatory preference of W-enzymes over Mo-enzymes is considered a novel feature of the hyperthermophilic archaea (74). To date four different W-enzymes have been purified from *P. furiosus*. They are aldehyde ferredoxin

oxidoreductase (AOR, (117)), formaldehyde ferredoxin oxidoreductase (FOR, (138)), glyceraldehyde-3-P ferredoxin oxidoreductase (GAPOR, (116)) and a W-enzyme homologous to AOR tentatively called WOR4 for tungsten oxidoreductase type 4 (135). AOR was the first tungsten enzyme purified from *P. furiosus* and it catalyzes the oxidation of a wide range of aldehydes using either methyl viologen (MV), benzyl viologen (BV) or ferredoxin (117) as the electron acceptor. Interestingly, the enzyme has the highest affinity for aldehydes that are derived from amino acids (Table 1.3). It has been shown that in vitro acetaldehyde is formed during catalysis by POR in a CoA dependent matter, as a side product of the oxidative decarboxylation of pyruvate (107). It is likely that other KOR enzymes also display this side reaction, thus providing a possible clue for the generation of aldehydes during growth of *P. furiosus* on both peptides and carbohydrates. AOR is proposed to convert these potentially harmful aldehydes to their corresponding carboxylic acid, however, one ATP is lost by this reaction because the only substrate level ATP is generated at the level of the ACS enzymes (Figure 1.2). The discovery that the membrane bound hydrogenase can generate a proton motive force upon formation of hydrogen and reoxidation of ferredoxin, produced by AOR, means that some ATP is still gained by the AOR pathway via ferredoxin oxidation (143).

The crystal structure of AOR showed that it exists as a homodimer of 67 kDa subunits bridged by a single iron on the dimer interphase (28). The active site tungsten is coordinated by two pterin cofactors, a nonplanar three ring structure with dithiolene, hydroxyl and a phosphate group. The tungsten is clamped within the two dithiolene groups from both pterins (28). A [4Fe-4S] cluster is positioned near the active site tungsten-pterin site and is presumably involved in the electron transfer to ferredoxin. So far, tungsten-containing AOR enzymes have been only characterized from the

hyperthermophiles *P. furiosus* and *Thermococcus strain* ES1 (57, 117). However a sequence entry in the NCBI database (AJ318790) has been made for a tungsten-containing AOR in *Eubacterium(Eb) acidaminophilum* (114).

A second distinct type of aldehyde-oxidizing, tungsten-containing enzyme was first isolated from *Tc. litoralis* and later also from *P. furiosus* (115, 138). It was named formaldehyde ferredoxin oxidoreductase for its ability to oxidize short chain aldehydes (C1-C3). However its true physiological substrate is not known because the K_m values of the tested substrates is relatively high (Table 1.3). Only glutaric dialdehyde displays a K_m value less than 1 mM, which might indicate that semi- or dialdhydes function as substrate in vivo (138). The crystal structure of FOR has been determined and it showed a striking similarity to that of AOR structure with regard to the active site tungsten, dipterin and [4Fe-4S] cluster (64). The main difference between the two is that FOR is a homotetramer and forms a ring-like structure and does not have a bridging iron on the subunit interface. The only W-enzyme in *P. furiosus* with a well-defined physiological role is glyceraldehydes-3-P ferredoxin oxidoreductase (GAPOR). This enzyme specifically oxidizes glyceraldehydes-3-P for which it has a high affinity and this enzyme functions in glycolysis as described above (116).

The W-enzymes in *P. furiosus* display a high sequence similarity on the amino acid level. For example, AOR and FOR have about 40% sequence similarity and both these sequences are about 23%similar to that of GAPOR. In addition to their overall homology, these enzymes contain conserved domains, which are likely to be involved in coordinating the [4Fe-4S] and the pterin cofactors (128, 137, 178). Based on sequence homology, two genes encoding two more members of the AOR family enzymes were identified in the *P. furiosus* genome sequence, and these were termed WOR4 and WOR5.

Based on predicted size and the presence of tungsten, WOR4 was purified and was indeed a tungsten-containing protein (135) However, WOR4 did not have any aldehyde oxidation activity and no indication of potential substrates could be demonstrated.

With the booming availability of complete sequences of microbial genomes, searching for distribution of genes or gene families has become a valuable tool in understanding gene function. Table 1.4 gives the results of homology searches of *P. furiosus* AOR, FOR and GAPOR (4). It is clear that homologs of AOR are not restricted to hyperthermophilic archaea, as several mesophiles including bacteria such as *E. coli* contain potential homologs. Those are listed in Table 1.4 are all of similar length (around 600 residues) and do contain putative iron sulfur cluster and pterin coordinating motifs. It is not surprising to find tungsten-containing enzymes under the bacterial domain as the first W-enzyme was isolated from *Clostridium thermoaceticum* (194) and this organism and related species are likely to contain additional W-enzymes such as AOR. Moreover, in *Eb. acidaminophilum,* AOR activity has been demonstrated as well as a tungsten uptake system (114). The presence of AOR-like enzymes in a mesophile (with a developed genetic system) might provide the means to resolve the physiological function of AOR in these organisms as well as in hyperthermophilic archaea. For example *E. coli* possess an AOR homolog but whether this enzyme contains tungsten and oxidizes aldehydes is unclear, especially considering that at least five different molybdenum-containing enzymes are present in this organism (62). Recently, the first molybdenum-containing protein was characterized from a hyperthermophile: the nitrate reductase of the archaeon *Pyrobaculum (Pb) aerophilum*. The genome sequence of *Pb. aerophilum* indicates that it contains several AOR type enzymes and its growth is dependent on both molybdenum and tungsten. These data suggest that this organism contains both W and

Mo- enzymes and can readily distinguish between the two metals (3, 45). Interestingly, the genomes of the acidophiles *Sl. solfataricus* and *Sl. tokodaii,* do not contain any homologs of the AOR family. This is consistent with the description of a molybdenum-containing aldehyde oxidizing enzyme for *Sl. acidocaldarius* and the strict molybdenum dependence of its growth on glucose (79).

Transcription in Archaea

The archaeal transcription machinery closely resembles that of the eukaryotes rather than bacteria. Evidence for this similarity came to light with the discovery of transcription factors in the Euryarchaeote *Methanococcus vanniellii* and the Crenarchaeote *Sulfolobus sp.* B12 (47, 70) An element analogous to the eukaryal TATA box could be identified +/- 25 bp upstream of the transcription start (131). Subsequently two essential archaeal transcription factors were identified, the TATA box binding protein (TBP) and transcription factor IIB (TFB) as well as a eukaryote type RNA polymerase (11). The similarity of the archaeal and eukaryal transcription machinery was further demonstrated by the finding that the homologous human and yeast TBP proteins could functionally replace the archaeal TBP in a cell-free transcription system (189). The archaeal transcription factors are highly conserved throughout all archaea and can be easily identified in genome sequences (60). The archaeal promoter sequence consists of three elements; the transcription start (+1), the TATA box (-25) and the transcription factor B recognition element (BRE, -31). In the process of basal transcription initiation, TBP binds to the TATA box and TFB interacts with both the BRE element and TBP, and determines the correct orientation for binding of the RNA polymerase (60). Promoter element consensus sequences for several archaeal species have been determined and four

groups have been recognized. These are in methanogens, halophiles, Crenarchaeota (mainly *Sulfolobus*) and Euryarchaeota (60, 168). Although all four groups have their own consensus promoter the overall consensus of the TATA box is represented by a stretch of AT-rich nucleotides between –30 and –23 nucleotides from the transcription start and the BRE element is represented by an A-rich stretch directly preceding the TATA box (-36 through –31) (60, 169). The consensus TATA box for *P. furiosus*, based on genes with an experimental determined transcription start, consist of –30(NTTWWWWA)-23 and for the BRE element it is –36(RAAAAN)-31 (R=A or G, W=A or T) (60); van der Oost, J., personal communication). Despite known consensus sequences, identifying the promoter of an uncharacterized ORF is difficult because promoters vary and many AT-rich stretches can be found at random. In order to correctly map a promoter the transcription start site has to be determined. A cell-free transcription system has been described for *P. furiosus* and has been shown to generate RNA with the same transcription start as in vivo mRNA (59, 178, 187).

Analysis of archaeal genome sequences has revealed that archaea contain mainly bacterial type transcription regulators despite the close relationship of the basal transcription factors with their eukaryal counterparts (92). A particular family of regulators, represented by the leucine response protein (LRP), has been the focus of regulatory studies in both *P. furiosus* and *Sulfolobus*. It was shown that, in both organisms, LRP homologs could bind to their own promoters and suppress transcription in vitro (20, 118). LRP regulators were initially identified in *E. coli* and comprise a complex global regulation mechanism of largely unknown function (71). It has been proposed that *P. furiosus* contains a novel heat shock mechanism, distinct from either bacterial or eukaryal response (183). A transcriptional regulator (Phr) of heat shock

response was described, which was shown to bind to its own promoter region as well as to the promoter of the heat shock responsive proteins AAA^+ ATPase and a small heat shock protein (95, 183). Binding of Phr to its target promoter prevents efficient recruitment of the transcription machinery, which is released upon heat shock from 95 to 103 °C (183). Clearly, the transcription analysis of archaeal systems is still in its infancy. The development of global transcript analysis techniques such as DNA microarrays is expected to have a large impact on the understanding of archaeal regulation, especially when combined with other studies involving environmental challenges such as heat shock.

DNA Microarray Technology

DNA microarrays have become a very powerful molecular tool to study global gene expression since its first application in yeast (96, 152). It is a high-through-put technique closely related to the more familiar technique of dot-blotting, however, the era of genome sequencing has unleashed the global regulation application of DNA microarrays. Historically, techniques such as Southern and Northern blotting utilized a single labeled oligonucleotide or polynucleotide probe in the liquid phase. This is hybridized to a complex mixture of DNA or RNA attached to a solid support, either separated on a gel or as a single spot. In Northern blotting the relative abundance of a particular transcript can be determined and information is also obtained about the size of the transcript if the RNA is separated in a gel. In a DNA microarray experiment, the same principles are used but they are modified in several important ways. In an array experiment, gene-specific probes, such as oligos, PCR products, library clones, etc., are attached to a solid support in a coordinated matrix format (array). The solid support may be a nylon membrane, a coated

microscope slide or a chip. The complex target is randomly labeled and is free in solution, essentially the reverse of a Northern or Southern blot. After hybridization and washing the level of hybridization signal of each spotted probe is measured individually, which should correlated to the relative amount of a particular message (target) present.

Membrane-Based Arrays

The simplest and cheapest way of executing an array experiment is with the use of nylon membranes and microtiter plates with probes in the form of PCR products of library clones. These probes can be arrayed by hand using a 96/384 pin stamp for a relatively small number of probes (156). When large numbers of probes (representing genes) are involved a more sophisticated approach with a robot such as the Qbot (Genetix, Hampshire, UK) is preferred. Hybridization with radioactively-labeled complex targets, for example, cDNA samples is performed with the same equipment used in standard Southern or Northern blotting as long as a digital signal is obtained. Two or more sets of cDNA derived from different conditions can be probed using the same membrane (after stripping). Signals can be balanced and normalized using constitutive expressed genes and control spots. Many membrane arrays (mostly eukaryotic systems) are available commercially from companies like Clontech and Research Genetics.

Glass Slide Microarrays

Using glass as a solid support has a number of advantages: low fluorescence, non-porosity, rigidity and the possibility of several chemical surface modifications. The surface of the glass slide is commonly coated with either poly-L-lysine or aminosilane in order to bind nucleic acid. Glass microarrays were first produced in the Brown laboratory

at Stanford University (152). Arrays are printed either with quilted pins or inkjet-like devices using a XYZ-axis robot (Figure 1.8). Probe solutions are transferred in nl quantities from either 96- or 384-well plates to the glass slides in a precise pattern. The probes are covalently bound to the surface using UV-light which is comparable to crosslinking DNA to a nylon membrane. Hybridization to glass slides is normally performed with two channels using two fluorescent labels such as CY3 (excitation 550 nm, emission 570 nm) and CY5 (excitation 649 nm, emission 670 nm). The label is incorporated into cDNA by the reverse transcriptase (RT) reaction carried out in the presence of fluorescently-labeled nucleotides. In most microarray experiments, differential hybridization is performed by labeling one cDNA pool with CY3 (reference), using RNA derived from one growth condition, and a second cDNA pool with CY5 (variable) from another growth condition. Both cDNA pools are mixed and hybridized to one slide. Signal intensities for each dye are obtained separately using a laser confocal scanner. Because both channels are read from the same slide signal intensities can be balanced between both channels in such a way that the overall signal intensities are similar. Using two channels for one slide, two growth conditions can be analyzed and regulation is presented as relative expression changes.

Affymetrix DNA Chips

Instead of printing probes on a solid support the Affymetrix photolithography technology allows the controlled synthesis of oligonucleotide probes on a chip (www.Affymetrix.com; Figure 1.8). As many as 500,000 unique oligos can be synthesized simultaneously on a 1.28 x 1.28 cm quartz window. The key feature of this technique is the synthesis of multiple oligos complementary to different sections of a

target RNA. In addition mismatch oligos are synthesized and serve as negative controls. Because the intensity of a particular target is calculated from multiple probes the signal to noise ratio is the strong point of this technique. Affymetrix chips are normally hybridized with biotin-labeled cDNA obtained from one growth condition, and for each growth condition a new chip has to be used. After hybridization the biotin label is fluorescently stained with streptavidin-phycoerythin and intensities for each of the features are obtained with a confocal laser scanner. Multiple data sets are balanced and normalized to obtain relative transcription levels between different conditions. The Affymetrix system is probably the most powerful microarray technique available. However the drawbacks of this system are the high cost, the requirement that all the chips have to be made by the Affymetrix company, and the limited selection of chips that are available although custom arrays are offered.

The Use of DNA Microarrays to Study *P. furiosus*

Eukaryotes such as yeast and human have been the main focus of DNA microarray studies mainly because of the ease of isolating mRNA (via the polyA tails) and because extensive cDNA libraries are available (48, 109). In prokaryotes, on the other hand, microarray based studies are a very recent development and working with prokaryotic RNA is quite cumbersome. Although microarray analyses have now been published for 16 prokaryote organisms, most of these studies were published only within the last two years (Table 1.5). At the time my research was initiated relatively little was known about the practical aspects of conducting microarray analysis with prokaryotes, and the technique had not been applied to archaea. In fact, my study using a targeted gene set of *P. furiosus* was the first such application (119; see below) and the first complete

genome DNA microarray analysis of an archaeon, *Halobacterium* NRC-1, was not published until 2002 (8)

The genome sequence forms the basis of the microarray technique. The genome sequence of *P. furiosus* was made available to us by Dr. R. Weiss, University of Utah, and Dr. F. Robb, University of Maryland, before it was released in 1998 (http://comb5-156.umbi.umd.edu/genemate/). Initial array experiments were done in collaboration with Dr. J. Zhou, Oak Ridge National Laboratory, who provided training and access to the equipment. Subsequently a targeted array was constructed at the University of Georgia with 271 selected ORFs, including those coding for many key metabolic enzymes. This provided the necessary experience in obtaining, managing and interpreting the data. The 271 ORF array was used to compare *P. furiosus* cultures grown in the presence and absence of S^o (Chapter 4). These results were published (159) and they represent the first microarray analysis of a hyperthermophile, as well as an archaeon. The study was extended to a whole genome microarray contained probes for all 2065 annotated ORFs (http://comb5-156.umbi.umd.edu/genemate/). In addition to these ORFs, 121 small putative ORFs not annotated in the genome were also analyzed (Eckman et al. unpublished results; Gerwe et al., unpublished results). PCR primers were initially designed to yield probes which covered the entire ORF and these primers were used to generated probes for all 2186 (2065 + 121) ORFs in *P. furiosus*. All handling and PCR-amplifications were done in 96- or 384-well plates. The initial amplification yielded products for 2060 ORFs as judged by gel electrophoresis. In order to amplify the remaining 126 ORFs, many of which were larger than 2 kb, internal primers were designed to yield products of about 1 kb. After 2 rounds of PCR, products for all *P. furiosus* ORFs were obtained. Amplified DNA was purified and concentrated to obtain

about 10 µl probe solution (100-500 µg/ml) in 50% (v/v) DMSO/water. Addition of DMSO to the spotting solution denatures the DNA and prevents evaporation of the sample during array printing. Before proceeding to the printing step, all PCR products were transferred to 384-well plates.

For the production of DNA microarrays, the Omnigrid (Genemachines, San Carlos, CA) robotic slide printer was used in the Applied Genetic Technology Center (AGTEC) at the University of Georgia. DNA probes were spotted on aminosilane (positively charged) coated slides (Sigma, St Louis, MO; PerkinElmer, Boston, MA; Asper, Tartu, Estonia) and crosslinked to the slides using UV irradiation. Microarrays are divided into subarrays, with each subarray containing the spots produced by each of the printing pins. Subarrays are within 4.5 x 4.5 mm squares, equivalent to the well to well distance in a 384-wel plate (the printing source) and the pin to pin distance in the print head. The distance between pins is fixed but the distance between spot can be freely adjusted. The distance between spots was set to 225 µm and the spot diameter was approximately 150 µm, leaving sufficient space between the spots. These dimensions gave a maximum of 361 spots per subarray. A 2 x 4 pin configuration was used, yielding up to 2888 spots, more than enough to cover all probes representing the entire genome of *P. furiosus*. To minimize data loss, for example, by irregularities on the array, the ORF set was printed in duplicate. Using this configuration it was possible to print the complete *P. furiosus* genome in duplicate within a 1.8 x 1.8 cm area.

Generally, in microarray analysis the targets (mRNA) in the sample are fluorescently-labeled with dyes such as CY3 and CY5 (Amersham, Piscataway, NJ). To label the total RNA pool from a sample, RNA is reverse transcribed into cDNA in the presence of fluorescently-tagged nucleotides. In most microarray experiments, differential

hybridization is carried out with a cDNA pool labeled with CY3 (reference) derived from one growth condition and a second cDNA pool labeled with CY5 (variable) from another growth condition. Microarrays with two dyes give rise to two black and white pictures and the scanner normally creates electronic (tif) files as output. An overlay of these pictures is most easily visualized by assigning colors to each of them and traditionally this is green for the condition 1 and red for the condition 2, as depicted in Figure 1.9. Yellow is produced if both "colors" are mixed in similar amounts and this represents no significant change in the expression of that particular ORF. If an ORF is differentially expressed it either is represented by a green color (higher expression in condition 1) or a red color (higher expression in condition 2; see Figure 1.9).

However, the results presented in this thesis show that microarray analyses can be taken to the next level by the use of more than two dyes in one experiment. Molecular Probes Inc. offers ARES DNA labeling kits that cover 10 different fluorphores. Four of these dyes are compatible with the laser and filter setting of the confocal laser scanner (Scanarray 5000, PerkinElmer, Boston, MA) and can be used together with little overlap of their excitation/emission spectra. They are: Alexa 488 (ex. 488 nm/em. 520 nm), Alexa 546 (ex. 546 nm/em. 570 nm), Alexa 594 (ex. 594 nm/em. 615 nm) and Alexa 647 (ex. 647 nm/em. 670 nm). Using all four dyes, four labeled cDNA pools (each with a different dye) can be mixed and hybridized to the same slide. Microarray experiments using four dyes generate four picture files and because of the three primary color limitation (red, green and blue) it is only possible to present the data of three conditions in a multicolor overlay (Figure 1.10). The actual data analysis is performed by obtaining relative fluorescence intensities for each of the spot using image analysis software such as Gleams (Nutec, Houston, TX). The average intensity of the pixels within a spot is determined,

and this is corrected for background by using pixels surrounding the spot. The relative expression levels between cDNA derived from different growth conditions are calculated as a ratio of background subtracted intensities. In order to calculate averages and standard deviation between slides the ratios are converted to a linear $\log_2$ scale. After performing microarray experiments with at least two independent RNA samples from each of the conditions and comparing each of the 4 possible combinations twice, average $\log_2$ ratios and standard deviation are obtained. It should be pointed out that some of the results using the four dye approach presented herein were used in advertisements by the manufacturer of the dyes (Molecular Probes) in their advertisements (Science vol. 298, no 5591 p. 59 and vol. 298 no 5601 p. 2131).

In order to perform microarray experiments and supporting analysis such as enzyme assays, it is important to grow consistent and reproducible cell cultures for RNA isolation, to produce cell-free extracts, carry out metabolite analysis, etc. In order to grow *P. furiosus* under 'defined' conditions a custom 20 liter fermentor was constructed. In Chapter 3 results are described for growth studies of *P. furiosus* under various conditions and the activity of twenty-one enzymes are measured in cell-free extracts. These cultures were used to isolate RNA for the microarray studies described in Chapters 4 and 5. In Chapter 5 the first results of a full genome array of a hyperthermophile is presented, in which the effect of two carbon sources, peptides and maltose (both in the presence of S^o) is analyzed. It is shown that the analysis of microarray results combined with sequence comparisons and biochemical data are a tremendous resource and can be used to give dramatic insights into the metabolism and physiology of *P. furiosus*. The following chapter (2) presents an analysis of several members of the 2-ketoacid ferredoxin oxidoreductase family. These carry out key reactions in the metabolism of both

carbohydrates and peptides. The results are described on both the biochemical level as well as the genome level and are utilized in subsequent chapters to support some of the microarray data.

Table 1.1. Metabolic diversity of (hyper)thermophiles

Organism	Substrates	e-acceptors	products	pathway
Thermococcales				EM
Pyrococcus furiosus	pep, cbh	S^o, H^+	Org. acids, CO_2, H_2, H_2S	
Pyrococcus abyssi	pep	S^o, H^+	Org. acids, CO_2, H_2, H_2S	
Pyrococcus horikoshii	pep	S^o, H^+	Org. acids, CO_2, H_2, H_2S	
Thermococcus stetteri	pep, cbh	S^o, H^+	Org. acids, CO_2, H_2, H_2S	
Thermococcus celer	pep	S^o, H^+	Org. acids, CO_2, H_2, H_2S	
Thermococcus litoralis	pep, cbh	S^o, H^+	Org. acids, CO_2, H_2, H_2S	
Desusulfurococcales				EM
Desulfurococcus amylolyticus	pep, cbh	S^o, H^+	Org. acids, CO_2, H_2, H_2S	
Desulfurococcus mucosus	pep	S^o, H^+	Org. acids, CO_2, H_2, H_2S	
Desulfurococcus mobiles	pep	S^o, H^+	Org. acids, CO_2, H_2, H_2S	
Staphylothermus marinus	pep	S^o	Org. acids, CO_2, H_2S	
Pyrodictiales				
Pyrodictium abyssi	pep, cbh	S^o, H^+	Org. acids, CO_2, H_2, H_2S	
Pyrodictium occultum	H_2	S^o, $S_2O_3^{2-}$	H_2S	
Hyperthermus butylicus	pep	S^o, H^+	Org. acids, CO_2, H_2, H_2S	
Thermoproteales				EM/ED
Thermoproteu tenaxs	pep, cbh, H_2, formate, ethanol			
Thermofilum pendens	pep	S^o	CO_2, H_2S	
Thermodiscus maritimus	Pep, H_2	S^o	CO_2, H_2S	
Pyrobaculum organotrophum	pep	S^o	CO_2, H_2S	
Pyrobaculum islandicum	Pep, H_2	S^o	CO_2, H_2S	
Pyrobaculum aerophilum	pep, acetate, H_2, formate	NO_3^-, NO_2^-, O_2	CO_2, N_2	

Archaeoglobales				EM
Archaeoglobus fulgidus	pep, cbh, H_2, formate	SO_4^{2-} ,$S_2O_3^{2-}$	Org. acids, CO_2, H_2S	
Sulfolobales				ED
Sulfolobus solfataricus	pep, cbh	O_2	CO_2	
Sulfolobus acidocaldarius	pep, cbh	O_2	CO_2	
Acidianus brierleyi	pep, Sº, FeS	O_2	CO_2, H_2S	
Metallospaera sedula	pep, Sº, FeS	O_2	CO_2, H_2S	
Methanobacteria				?
Methanothermobacter thermautotrophicus	H_2	CO_2	CH_4	
Methanopyri				
Methanopyrus kandleri	H_2	CO_2	CH_4	
Methanococcales				EM
Methanocaldococcus jannaschii	H_2	CO_2	CH_4	
Methanothermaceae				
Methanothermus fervidus	H_2	CO_2	CH_4	
Methanothermus sociabilis	H_2	CO_2	CH_4	

Table modified from (83) and (154).
.

Table 1.2. Available archaeal genomes.

Organism	Genome size	Date of completion
Aeropyrum pernix	1669695 bp	Jul 5 2001
Archaeoglobus fulgidus	2178400 bp	Dec 17 1997
Halobacterium sp. NRC-1	2014239 bp	Oct 31 2001
Methanococcus jannaschii	1664970 bp	Aug 23 1996 rev. Sep 10 2001
Methanopyrus kandleri AV19	1694969 bp	Feb 4 2002
Methanosarcina acetivorans str. C2A	5751492 bp	Apr 3 2002
Methanosarcina mazei	4096345 bp	May 17 2002
Methanothermobacter thermautotrophicus str. Delta H	1751377 bp	Sep 19 2001
Pyrobaculum aerophilum	2222430 bp	Jan 16 2002
Pyrococcus abyssi	1765118 bp	Feb 13 2002
Pyrococcus furiosus DSM	1908256 bp	Feb 12 2002
Pyrococcus horikoshii	1738505 bp	Feb 14 2002
Sulfolobus solfataricus	2992245 bp	Oct 3 2001
Sulfolobus tokodaii	2694765 bp	Sep 15 2001
Thermoplasma acidophilum	1564906 bp	Oct 12 2001
Thermoplasma volcanium	1584804 bp	Mar 22 2001
Ferroplasma acidarmanus	1933093 bp	Aug 21 2002
Methanosarcina barkeri	5133054 bp	Sep 17 2002
Unfinished genomes		
Haloarcula marismortui		
Halobacterium salinarium		
Methanococcus maripaludis		
Methanogenium frigidum		

Source: www.ncbi.nlm.nih.gov/PMGifs/Genomes/micr.html

Table 1.3. Substrate specificity of aldehyde Fd oxidoreductase (AOR) and formaldehyde Fd oxidoreductase (FOR), apparent K_m (mM).

Substrate	AOR	FOR
Formaldehyde	1.42	25.0
Acetaldehyde	0.02	60.0
Propionaldehyde	0.15	62.0
Crotonaldehyde	0.14	ND
Benzaldehyde	0.06	ND
Isovaleraldehyde	0.03	ND
Phenylacetaldehyde	0.08	ND
Phenylpropionaldehyde	NA	15.0
Indoleacetaldehyde	0.05	25.0
Succinic semialdehyde	NA	8.0
Glutaric dialdehyde	NA	0.8

ND not detectable, NA not determined, data taken from (136).

Table 1.4. Distribution of Aldehyde Fd oxidoreductase homologs* in available microbial genome sequences.

Organism	ORF number(s)
Archaea	
Aeropyrum pernix	0266
Archaeoglobus fulgidus	0023, 0077, 0340, 2281
Methanosarcina acetivorans	1714, 2962, 3989
Methanosarcina mazei	0921, 2645, 3326
Methanococcus jannaschii	1183
Methanococcus maripuludis	Contig31 - 7434-9272
Pyrobaculum aerophilum	0622, 1029, 2052, 3427
Pyrococcus abyssi	0647, 0798, 1315, 2085, 2330,
Pyrococcus horikoshii	0028, 0457, 0891, 1019, 1274
Pyrococcus furiosus	0346, 0464, 1203, 1480, 1961
Thermoplasma volcanium	0795, 1239
Thermoplasma acidophilum	0810, 0834, 1142
Bacteria	
Clostridium acetobutylicum	2018
Desulfitobacterium hafniense	3018
Desulfovibrio desulfuricans	0761, 1055
Eubacterium acidaminophilum	AJ318790.1
Escherichia coli K12	1673
Escherichia coli O157:H7	2701
Geobacter metallireducens	0033, 0655, 0948, 3157
Magnetospirillum magnetotacticum	8013

* Homologs are identified based on the presence of conserved domains potentially involved in the binding of cofactors and the overall protein length of about 600 residues.

Table 1.5. Prokaryotes which are subjected to whole genome microarray studies.

Organism	Subject of study	Reference
Bacillus subtilus	Anaerobic/aerobic	(195)
Escherichia coli	Host integration factor	(7)
Pseudomonas syringae	Pathogenicity factor	(46)
Helicobacter pylori	Acid exposure	(6)
Mycobacterium tuberculosis	Drug response	(190)
Shewanella oneidensis	Electron transport regulator	(10)
Pasteurella multocida	Iron limitation	(122)
Streptomcoccus pneumoniae	Quorum sensing	(33)
Staphylococcus aurus	Virulence factors	(38)
Streptomyces coelicolor	Antibiotic biosynthesis	(65)
Erwinia chrysanthemi	Virulence	(120)
Salmonella enterica	Virulence	(30)
Synechocystis sp strain PCC 6803	High light exposure	(61)
Borrelia burgelorferi	Virulence	(132)
Halobacterium NRC-1	Phototrophic mutants	(8)
Pseudomonas aeruginosa	Regulators of mucoidy	(44)
Pyrococcus furiosus	Peptide/carbohydrate	(157)

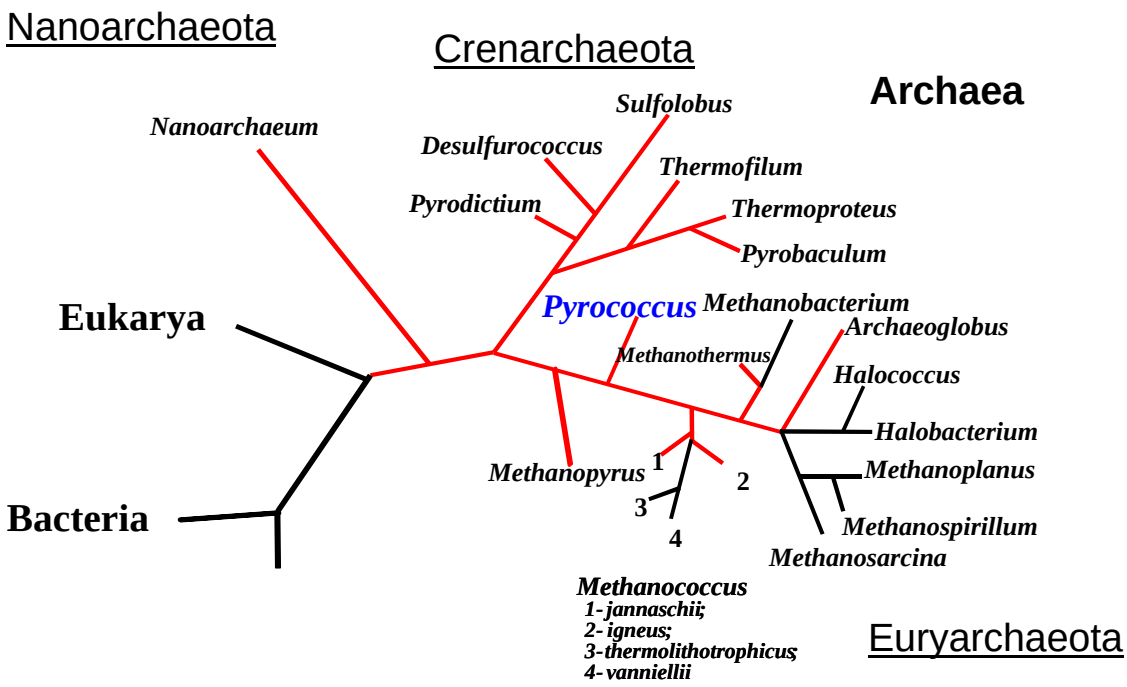

Figure 1.1. Hyperthermophiles (in red) within the universal phylogenetic tree. The genus *Pyrococcus* is shown in blue (redrawn and modified from (14)).

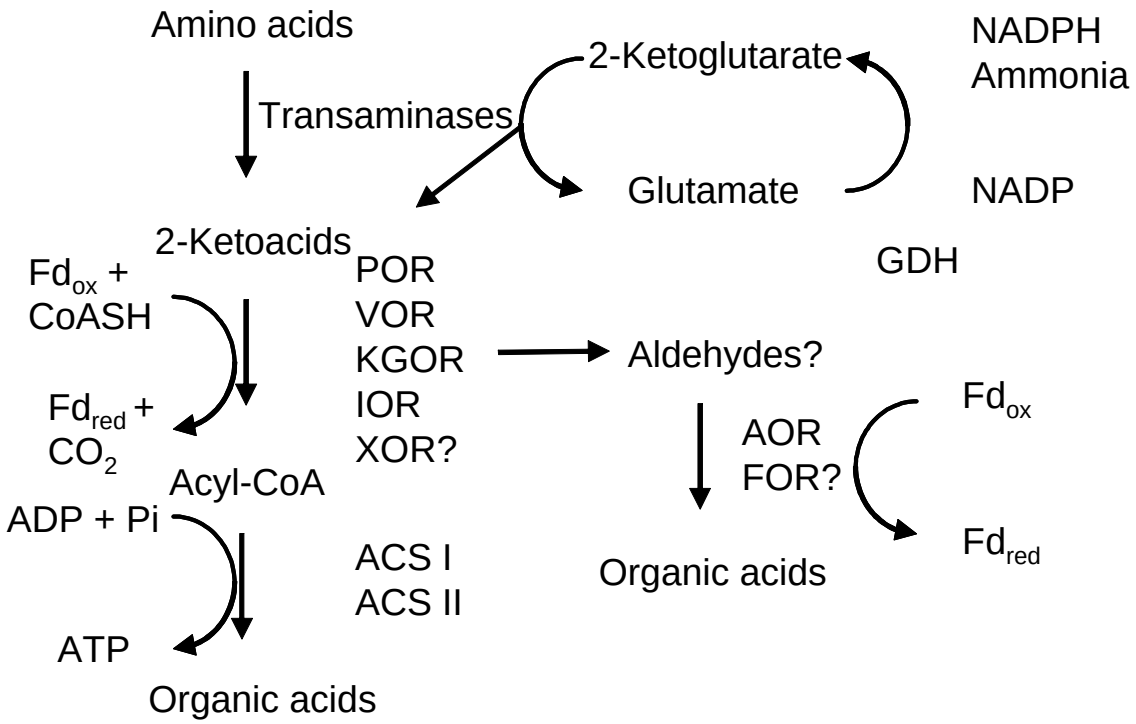

Figure 1.2. Proposed pathway of amino acid metabolism and the involvement of aldehyde ferredoxin oxidoreductase (AOR) and formaldehyde ferredoxin oxidoreductase (FOR) in *P. furiosus*. The abbreviations are: GDH, glutamate dehydrogenase; POR, pyruvate ferredoxin oxidoreductase;, VOR, isovalerate ferredoxin oxidoreductase; KGOR, 2-ketoglutarate ferredoxin oxidoreductase; IOR, indolepyruvate ferredoxin oxidoreductase; XOR, 2-ketoacid ferredoxin oxidoreductase; Fd, ferredoxin (red, reduced, ox, oxidized); and ACS I and II, acetyl-CoA synthetase I and II.

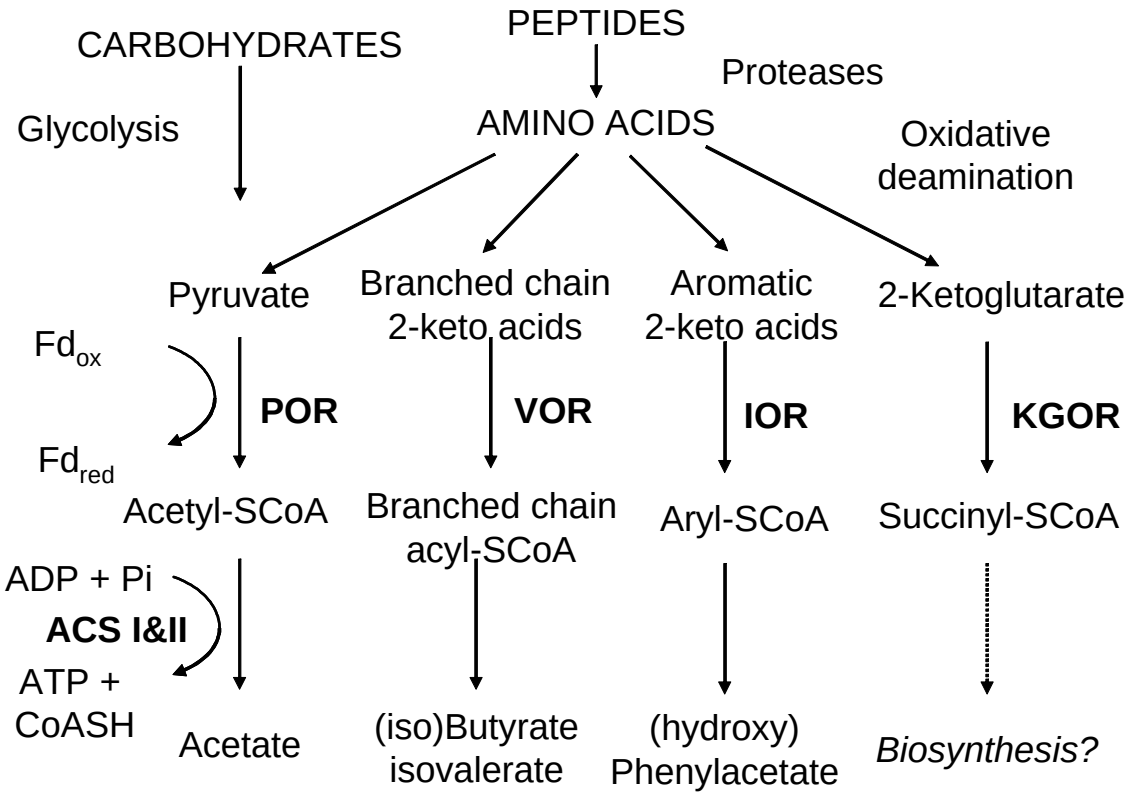

Figure 1.3. Schematic representation of the proposed involvement of 2-ketoacid ferredoxin oxidoreductases and acetyl-CoA synthetases in the fermentation of amino acids by *P. furiosus* (redrawn and modified from (2)). The abbreviations are: POR; pyruvate ferredoxin oxidoreductase; VOR; 2-ketoisovalerate ferredoxin oxidoreductase; IOR; indolepyruvate ferredoxin oxidoreductase; KGOR; 2-ketoglutarate ferredoxin oxidoreductase; ACS; acetyl-CoA synthetase; Fd; ferredoxin; and CoASH; coenzyme A.

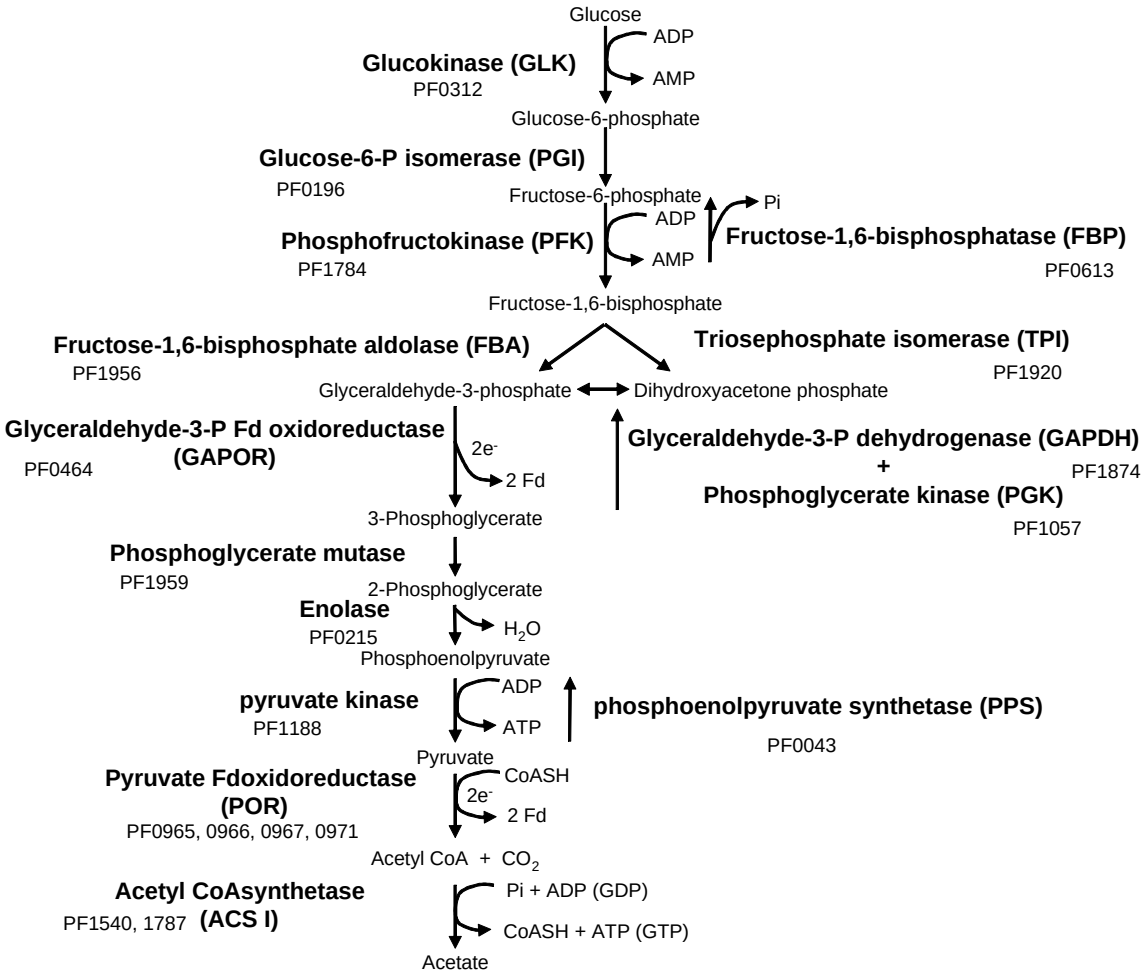

Figure 1.4. Schematic representation of the Embden-Meyerhof pathway and pyruvate metabolism in *P. furiosus*. The 'PF' numbers refer to the gene designations in the annotated genome sequence.

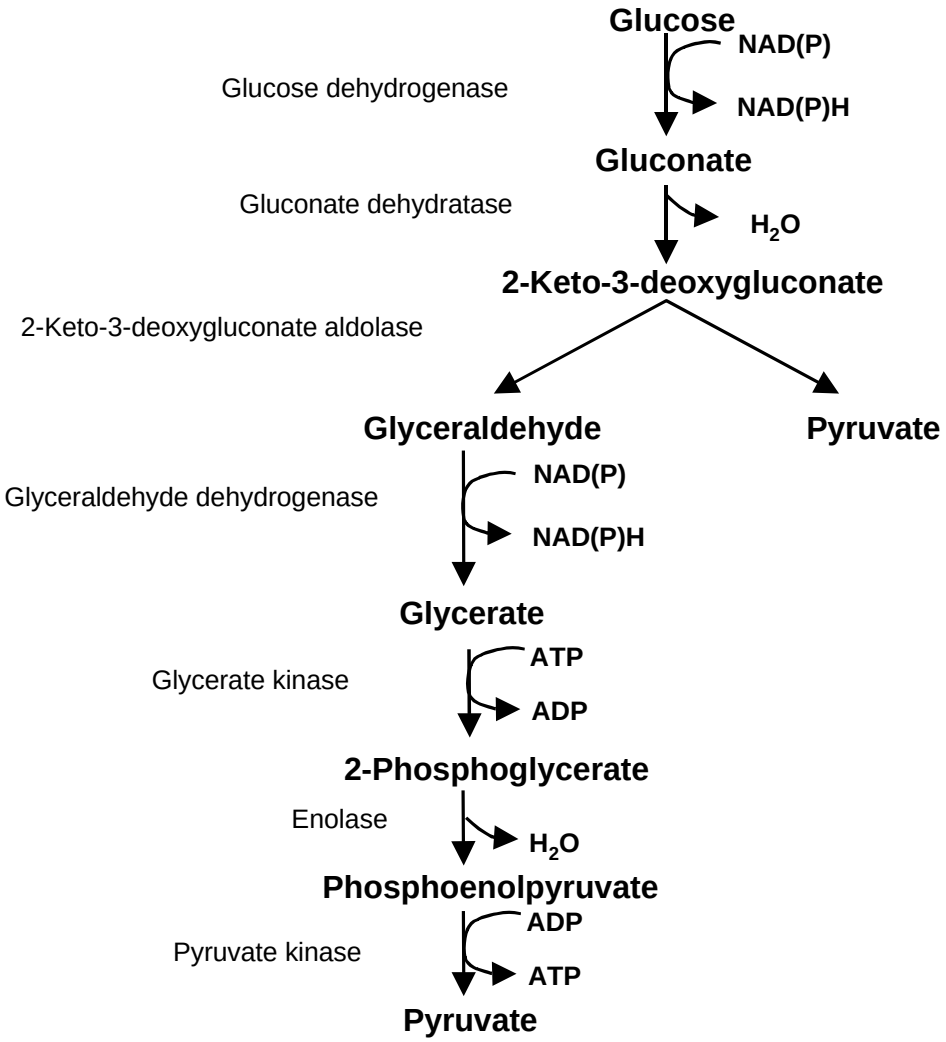

Figure 1.5. Modified Entner-Doudoroff pathway proposed in the aerobic hyperthermophile *Sulfolobus* and the thermophile *Thermoplasma acidophilum* (redrawn and modified from (154)).

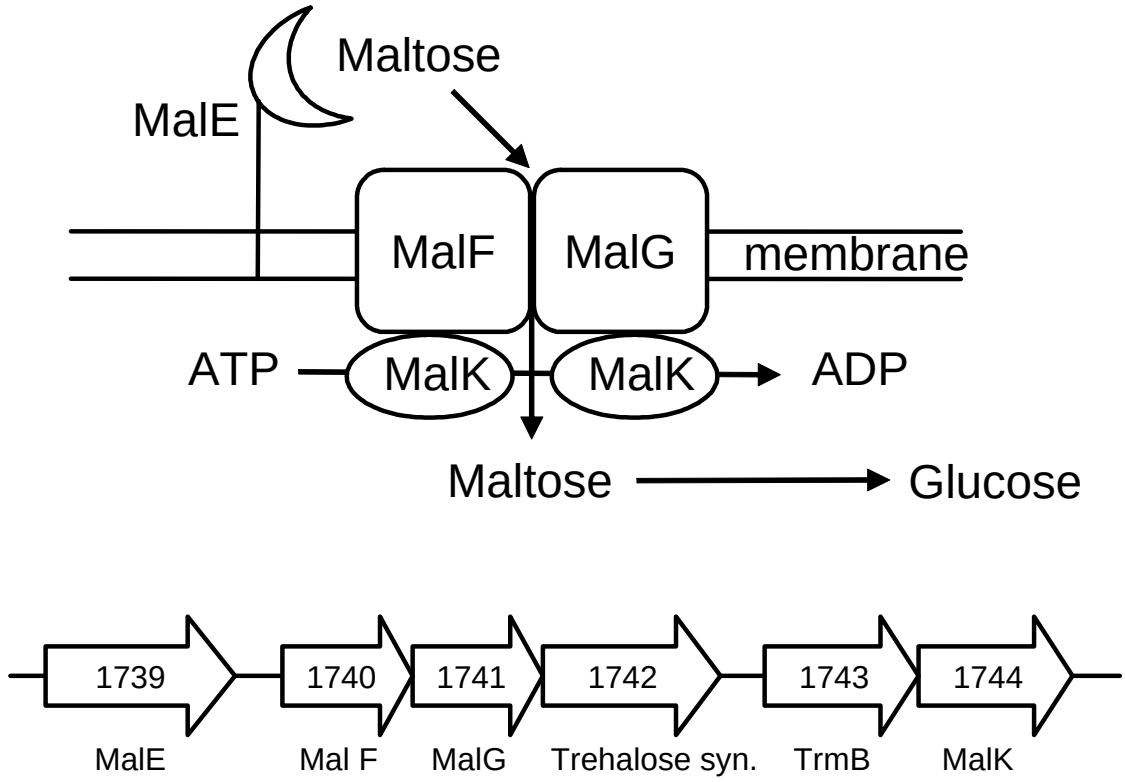

Figure 1.6. Proposed pathway for maltose uptake in *Thermococcus litoralis* (modified from (193)). The abbreviations are: MalE, maltose/trehalose binding protein; MalF, MalG, and MalK, components of the maltose/trehalose ABC transport system; trehalose syn, trehalose synthase homolog; and TrmB, transcriptional regulator of mal operon.

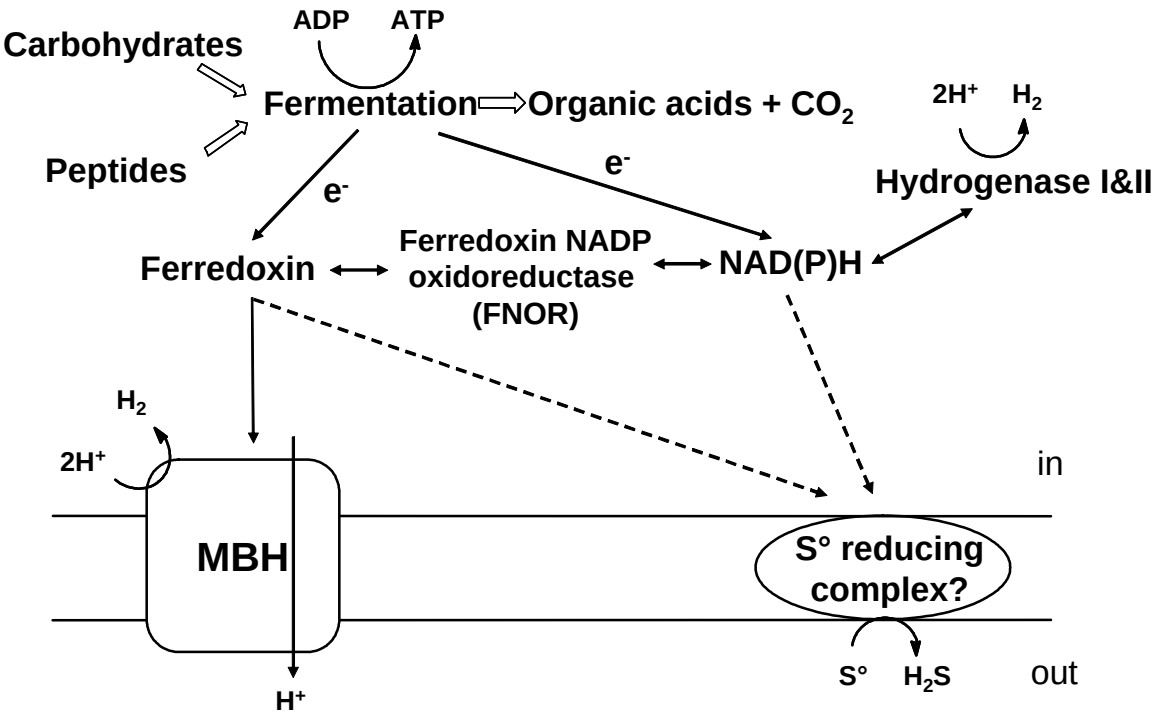

Figure 1.7. Proposed pathway for electron flow during the fermentation of carbohydrates and peptides in *P. furiosus*. MBH represents the membrane bound hydrogenase.

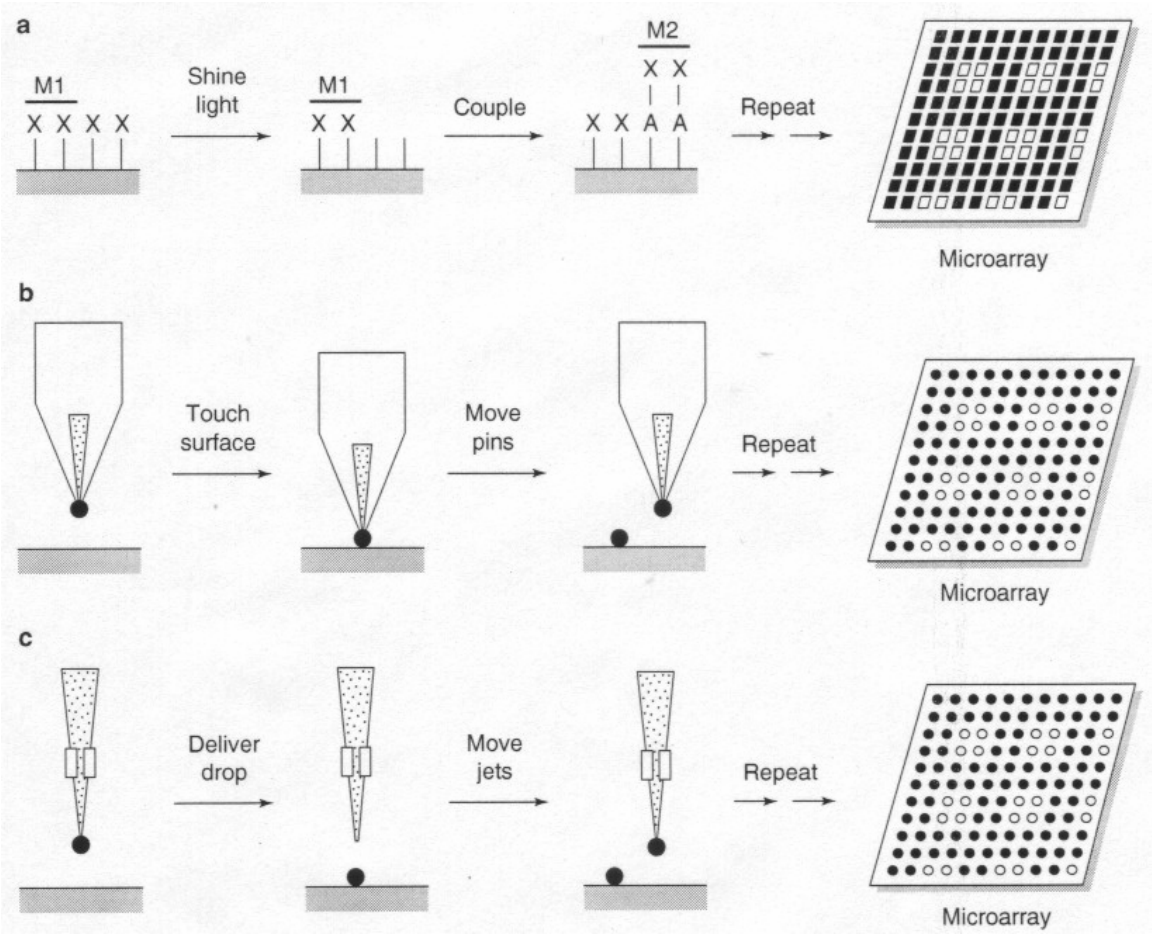

Figure 1.8. Microarray technologies. Three approaches to microarray manufacturing are depicted (taken from (153)). a) Photolithopgraphy, b) Mechanical microspotting, c) Ink jet printing. X, photo-labile protecting group, M1 and 2 photomask 1 and 2.

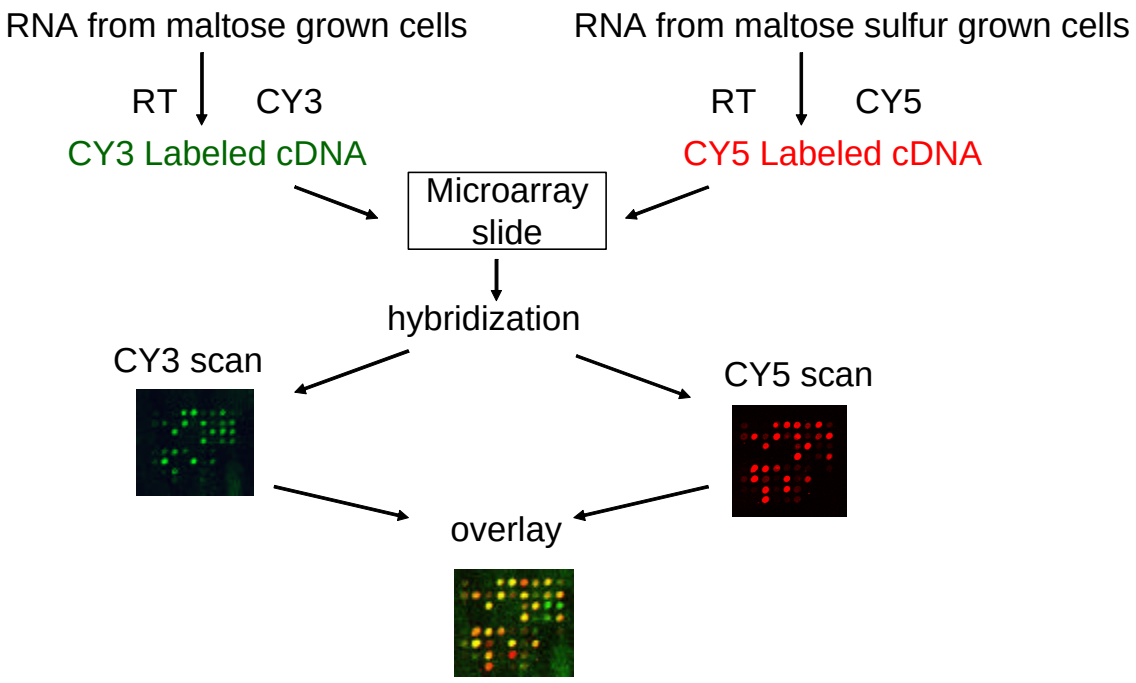

Figure 1.9. Schematical representation of the hybridization procedure for two dye microarrays and the presentation of a false two color overlay. RT represents the reverse transcription reaction.

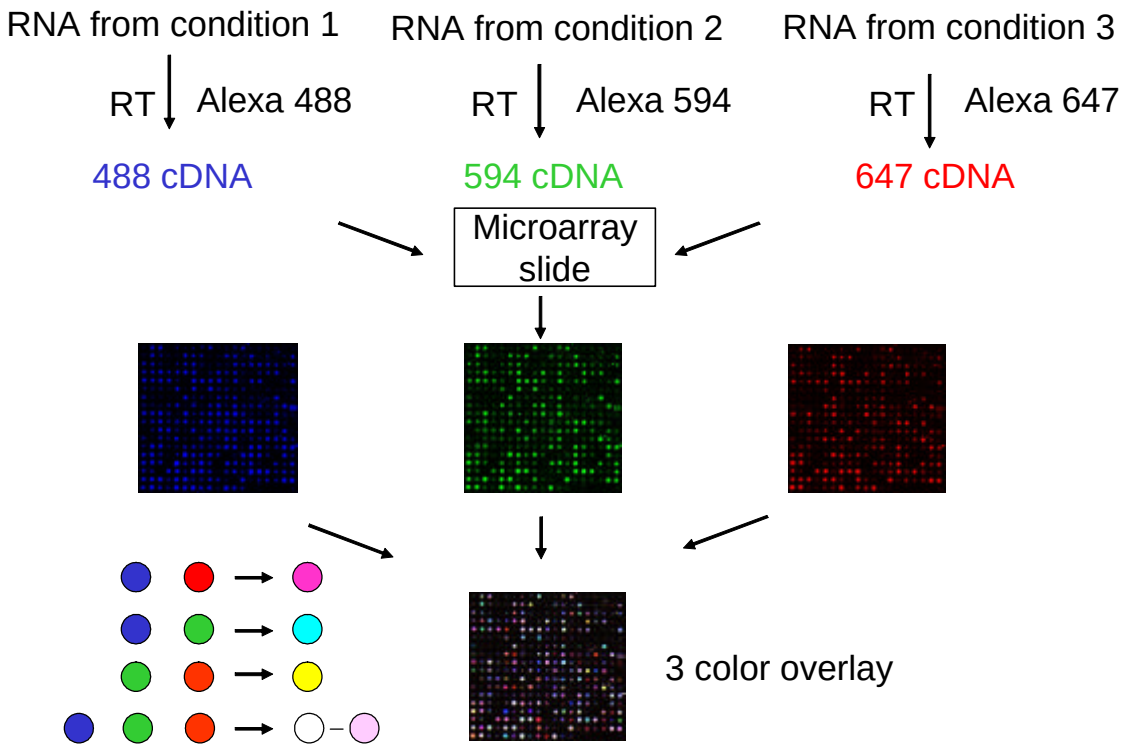

Figure 1.10. Schematical representation of the hybridization procedure for multi dye microarrays and the presentation of a false three color overlay. In three color overlays, the following colors can be observed; blue and red yields purple, blue and green yields aqua, green and red yields yellow and blue, green and red yields white (but can appear pinkish depending

CHAPTER 2

2-KETO ACID OXIDOREDUCTASE FROM *Pyrococcus furiosus* AND *Thermococcus litoralis*[1]

[1]Schut, G.J., A.L. Menon, and M.W.W. Adams. 2001. *Methods in Enzymology*. 331:144-158.

Reprinted here with permission of the publisher

INTRODUCTION

In most aerobic organisms the oxidative decarboxylation of pyruvate to acetyl CoA is catalyzed by a large NAD-dependent pyruvate dehydrogenase complex. On the other hand, the same reaction in anaerobic organisms is catalyzed by a reversible, ferredoxin-dependent, pyruvate oxidoreductase (POR). PORs have been purified from archaea, bacteria, and anaerobic eukaryotic protists. The majority of bacterial and eukaryotic PORs are homodimers with subunits of about 120 kDa [1,2,3,4], while a POR comprised of two subunits (86 and 42 kDa) that form heterotetramers ($\alpha_2\beta_2$) have been purified from the extremely halophilic archaeon *Halobacterium halobium*[5]. Most archaeal PORs, however, contain four subunits ($\alpha\beta\gamma\delta$; 45, 32, 25 and 13 kDa) and are octamers ($\alpha_2\beta_2\gamma_2\delta_2$) of approximately 240 kDa. These include PORs from the fermentative hyperthermophiles, *Pyrococcus furiosus* and *Thermococcus litoralis*[6,7], from the sulfate-reducing hyperthermophile *Archaeoglobus fulgidus*[8], and a number of methanogic archaea including both mesophiles and thermophiles[9,10,11]. However, heterotetrameric PORs are not unique to archaea nor to the hyperthermophiles. They are also present in hyperthermophilic bacterium, *Thermotoga maritima*[12] and in the mesophilic bacterium, *Helicobacter pylori*[13]. Amino acid sequence comparisons have shown that the one and two subunit PORs represent a mosaic of the four "ancestral" subunits found in the enzymes in the hyperthermophilic archaea[14]. The structure of the single subunit enzyme from the mesophilic bacterium, *Desulfovibrio africanus*, has been

reported[15]. The mechanism of pyruvate oxidation is distinct from that of the pyruvate dehydrogenase complex[16,17].

A number of organisms, mostly archaea, are known to contain at least three 2-keto acid oxidoreductases (KORs) in addition to POR, and these are able to utilize substrates other than pyruvate. The enzymes are indolepyruvate ferredoxin oxidoreductase (IOR)[18], 2-ketoisovalerate ferredoxin oxidoreductase (VOR)[19] and 2-ketoglutarate ferredoxin oxidoreductase (KGOR)[20]. They preferentially use as substrates the transaminated forms of aromatic amino acids, branched chain amino acids, and glutamate, respectively. All three enzymes have been found so far only in archaea, which include hyperthermophilic heterotrophs such as *Pyrococcus* sp.[14] and in methanogens such as *Methanobacterium thermoautotrophicum*[11]. Sequence analysis indicates that the four types of oxidoreductases, POR, VOR, KGOR and IOR, are closely related. VOR and KGOR, like POR, contain four different subunits while IOR represents a two-subunit gene mosaic of four "ancestral" subunits. The genes encoding POR and VOR of *P. furiosus* have been cloned and sequenced and it was shown that the two enzymes share the same γ subunit encoded by a single gene[7]. In addition to the genes encoding POR, the genome of hyperthermophilic bacterium *T. maritima*[21,22] contains a number of unknown KOR homologs although IOR and VOR activities are not detectable in cell-free extracts[14].

In hyperthermophilic, fermentative archaea such as *Pyrococcus* sp., POR is a key enzyme in the sugar fermentation pathway. It converts the pyruvate produced by

glycolysis into acetyl CoA, which is converted to acetate with the conservation of energy in the form of ATP by acetyl CoA synthetase[23,24]. Similarly, VOR and IOR, in addition to POR, are thought to convert the deaminated forms of most amino acids to their corresponding acyl- or aryl-CoA derivative. These are also used as sources of energy with the concomitant production of the corresponding acid (see Figure 2.1)[14, 18, 19]. KGOR appears to function in biosynthesis rather than peptide catabolism[20]. Herein we describe the purification of POR, VOR and IOR from *P. furiosus* and KGOR from *T. litoralis* and some of the molecular and catalytic properties of this enzyme family.

ASSAYS FOR 2-KETO ACID OXIDOREDUCTASE

KORs catalyze the oxidative decarboxylation of 2-keto acids according to Eqn. 1.

$$R.CO.COOH + CoASH \rightarrow R.CO.SCoA + CO_2 + 2H^+ + 2e^- \quad (1)$$

Inside the cell the electrons from this reversible reaction are transferred to the low potential redox protein ferredoxin and are ultimately disposed as H_2, H_2S or as an organic compound[14]. Under assay conditions the artificial electron mediator methyl viologen (MV) replaces ferredoxin. The rate of 2-keto acid reduction is proportional to the reduction of MV and this is measured by the appearance of blue color at 578 nm. Strictly anaerobic conditions must be maintained during the assay as reduced MV is instantly

oxidized by oxygen and the enzymes themselves are irreversibly inactivated by oxygen (see below).

Reagents. The following stock solutions are prepared in 50 mM N-(2-hydroxyethyl) piperazine-N'-3-propanesulfonic acid (EPPS), buffer, pH 8.4 containing 2 mM $MgCl_2$.

Sodium dithionite (DT), 100 mM

MV, 100 mM (100X)

Thiamine pyrophosphate (TPP), 160 mM (400X)

Coenzyme A (CoASH), 40 mM (400X)

Substrates: sodium pyruvate, 500 mM (100X, for POR), sodium 2-ketoisovalerate, 500 mM (100X, for VOR), sodium 2-ketoglutarate, 500 mM (100X, for KGOR), and sodium indolepyruvate, 125 mM (50X, for IOR). Indole pyruvate is made as a 125 mM solution in ethanol due to its limited solubility. EPPS buffer is prepared from a 1.0 M stock solution. The buffer is degassed thoroughly on a vacuum manifold and flushed with Ar. Appropriate amounts of all dry chemicals are weighed out in powder form and degassed in empty 8 ml serum-stoppered vials before EPPS is added by syringe under Ar.

Procedure. The activities of IOR, VOR and KGOR, but not POR, are considerable enhanced by the presence of TPP and this is routinely included in the standard assay mixture. The assay solution is prepared by transferring 2 ml of 50 mM EPPS buffer (pH, 8.4) containing $MgCl_2$ (2 mM) into an anaerobic, serum-stoppered cuvette under Ar. After the addition of 20 µl of MV, 5 µl of TPP and 5 µl of CoASH stock solutions, the cuvette is incubated for 3 mins at 80°C in a spectrophotometer equipped with a thermostatic cuvette holder and a thermoinsulated cell compartment. The final

concentration of reagents in the standard assay mixture are methyl viologen (1 mM), $MgCl_2$ (2 mM), TPP (0.4 mM), CoA-SH (0.1 mM), and the appropriate 2-keto acid (5 mM), except for indole acetate (2.5 mM). To ensure that the cuvette is anaerobic, a few µl of DT are added. A light blue color of reduced MV should be apparent and this should remain after gently shaking the cuvette. If the solution turns colorless, then the cuvette is not anaerobic and a fresh reaction mixture should be prepared. The enzyme sample is then added, followed immediately by the appropriate 2-keto acid to initiate the reaction. The reaction is measured as an increase in absorbance at 578 nm at 80°C. Activities are calculated by converting the change in absorbance to µmoles MV reduced using a molar absorbance coefficient of 9,700 $M^{-1}cm^{-1}$. Protein concentrations are routinely estimated using the Bradford assay[25]. Results are expressed as units (U) per mg of protein, where 1 unit equals the amount of enzyme required to reduce 2 µmoles of MV/min, which is the equivalent of 1 µmole of 2-keto acid oxidized/min.

PURIFICATION OF POR AND VOR FROM *P. furiosus*

POR and VOR are routinely purified from the same batch of *P. furiosus* cells in this laboratory. In fact, they can be purified along with several other oxidoreductase-type enzymes and redox proteins[26]. The oxidation of pyruvate can be used as a specific assay for POR and the oxidation of 2-ketoisovalerate is specific for VOR since neither enzyme oxidizes the other substrate to any significant extent. In the published purification procedures[6,19] the two enzymes co-elute after the application of a cell-free extract to a

DEAE-Sepharose column and are separated from each other by a second chromatography step using Hydroxyapatite. The two proteins are then purified separately, although the same columns are used for each. This protocol has now been modified to take advantage of the similarities in the properties of POR and VOR. As described below, in the modified procedure the two proteins are copurified through three chromatography steps (ion-exchange, hydrophobic interaction and gel filtration) and are not separated until the final purification step (Hydroxyapatite). Both enzymes are oxygen-sensitive and must be purified under strictly anaerobic, reducing conditions[26].

P. furiosus (DSM 3638) is obtained from the Deutsche Sammlung von Mikroorganismen, Germany. It is routinely grown at 90°C in a 600-liter fermentor with maltose as the carbon source as described previously[26,27]. POR and VOR are routinely purified from 300 g (wet weight) of cells at 23°C under strictly anaerobic conditions. The procedures to prepare the cell-free extract and to carry out the first chromatography step are described elsewhere in this volume[26]. In brief, cells are thawed in (1 g per 3 ml) 50 mM Tris-HCl pH 8.0 containing 2 mM sodium dithionite, 2 mM dithiothreitol and 0.5 µg/ml DNase I. After incubation at 37°C for 1 hr and centrifugation at 30,000 x g for 1 hr, the cell-free extract loaded onto a column (10 x 20 cm) of DEAE-Sepharose FF (Pharmacia Biotech) equilibrated with 50 mM Tris-HCl containing 2 mM sodium dithionite and 2 mM dithiothreitol (buffer A). The extract is diluted three-fold with the buffer as it is loaded. The bound proteins are eluted with a linear gradient (15 liters) from 0 to 0.5 M NaCl in buffer A and 125 ml fractions are collected. POR and VOR elute as overlapping peaks as 170 - 260 mM NaCl is applied to the column.

Q-Sepharose Chromatography. Fractions containing POR and VOR activities are diluted 3-fold with buffer A and loaded onto a column (5 x 20 cm) of Q-Sepharose Fast Flow (Pharmacia-Biotech). After washing with two column volumes of buffer A, a 2.3 liter linear gradient from 0 to 0.5 M NaCl in buffer A is applied at a flow rate of 10 ml/min and fractions of 100 ml are collected. POR and VOR coelute from the column as between 200 and 300 mM NaCl is applied.

Phenyl-Sepharose Chromatography. The POR- and VOR-containing fractions from the previous column are diluted with an equal volume of buffer B (buffer A containing 10%, v/v, glycerol) containing 2.0 M ammonium sulfate (pH 8.0) and applied directly to a column (3.5 x 10 cm) of Phenyl Sepharose (High Performance, Pharmacia-Biotech) equilibrated with buffer B containing 1.0 M ammonium sulfate (pH 8.0) at a flow rate of 6 ml/min. The column is washed with buffer B containing 1.0 M ammonium sulfate (pH 8.0). POR and VOR do not bind to the column under these conditions and are present in the pass-through fractions (50 ml each). These are combined (300 ml) and concentrated anaerobically to approximately 12 ml using an ultrafilter fitted with a YM-100 membrane (Amicon, Bedford, MA).

Superdex 200 Chromatography. The concentrated sample is directly applied to a column (3.5 x 60 cm) of Superdex 200 (Pharmacia Biotech) equilibrated with buffer C (buffer A containing 200 mM KCl). The column is run at a flow rate of 1.5 ml/min and 15 ml fractions are collected.

Hydroxyapatite Chromatography. Fractions containing VOR and POR are directly applied on to a column (2.6 x 9 cm) of ceramic Hydroxyapatite (American International Chemicals) equilibrated with buffer C. After washing with three column volumes of buffer C at a flow rate of 3 ml/min, the bound proteins are eluted with a 1000 ml linear gradient from 0 to 200 mM potassium-phosphate in buffer C and 25 ml fractions are collected. This column separates POR from VOR, with POR eluting from 20 mM to 45 mM phosphate and VOR from 50 mM to 70 mM phosphate. Fractions containing pure POR or VOR, as determined by SDS-gel electrophoresis, are combined and concentrated, and washed with buffer A by ultrafiltration using an Amicon PM30 membrane to protein concentration of approximately 15 mg/ml and 5 mg/ml, respectively. The concentrated samples are stored as pellets in liquid nitrogen. The yield of POR and VOR are approximately 220 mg and 30 mg, respectively.

PURIFICATION OF IOR FROM *P. furiosus*

IOR can be purified from the same batch of cells used to purify VOR and POR from *P. furiosus* as described above. IOR activity begins to elute as 150 mM NaCl from the DEAE Sepharose Fast Flow column, before POR and VOR. There is some overlap of activities but this is clearly evident by the activity assays. Indolepyruvate, which is used as the substrate for IOR, cannot be used by either POR or VOR. Like these enzymes, IOR is oxygen-sensitive and has to be purified under strictly anaerobic and reducing conditions[18].

Hydroxyapatite Chromatography. Fractions (100 ml) from the DEAE Sepharose column with IOR activity above 1.5 units/mg are combined (600 ml) and loaded directly onto a column (8 x 30 cm) of Hydroxyapatite (High Resolution, Boehring Diagnostics) equilibrated with buffer A. The adsorbed proteins are eluted with a gradient (1.2 liter) from 0 to 200 mM potassium phosphate in the same buffer at a flow rate at 3 ml/min. IOR activity elutes as 170 - 200 mM phosphate is applied.

Superdex 200 Chromatography. Fractions (50 ml) with IOR activity above 2.5 units/mg are combined (200 ml) and concentrated to approximately 25 ml by ultrafiltration (Amicon PM-30). The concentrated sample of IOR is applied to a column (6 x 60 cm) of Superdex 200 (Pharmacia LKB, NJ) equilibrated at 5 ml/min with buffer A containing 200 mM NaCl.

Phenyl-Sepharose Chromatography. Fractions (25 ml) with IOR activity above 9 units/mg are combined (200 ml), diluted with an equal volume of buffer A containing 2.0 M ammonium sulfate and are applied to a column (3.5 x 10 cm) of Phenyl Sepharose (Pharmacia Biotech) previously equilibrated with buffer A containing 1.0 M ammonium sulfate at 2 ml/min. The adsorbed protein is eluted with a 2 liter decreasing gradient from 1.0 to 0 M ammonium sulfate. IOR activity is detected in the eluent as 300 mM ammonium sulfate is applied. Fractions (15 ml) with IOR activity above 30 units/mg are separately analyzed by SDS-gel electrophoresis. Those judged pure are combined (75 ml), concentrated by ultrafiltration to approximately 8 mg/ml. The yield is approximately 100 mg with a specific activity of 38 U/mg.

PURIFICATION OF KGOR FROM *T. litoralis*

P. furiosus contains KGOR activity[20] but it is very unstable and we have been unable to purify it. The activity is lost after one or two column chromatography steps. For unknown reasons, KGOR from *T. litoralis* is much more stable and the activity of the enzyme is maintained even after multiple chromatography steps[20]. The stability of KGOR from *T. litoralis* is increased by the presence of glycerol (10%, v/v) and dithiothreitol (DTT, 2 mM) and this is added to all buffers used in the purification. Sodium dithionite is also included to maintain anaerobic conditions.

T. litoralis (DSM 5473) is obtained from the Deutsche Sammlung von Mikroorganismen, Germany[28]. It is grown at 85°C in a 600-liter fermentor in the same medium that is used to grow *P. furiosus*[26,27] except that maltose is omitted and the NaCl concentration is increased to 3·8% (w/v). The pH of the medium was maintained at 5·5 at 85°C and the cells were harvested at the end of the log phase (A_{600} = 0·5). Cells were immediately frozen in liquid N_2 and stored at -80° C. Cell yields were typically ~ 1 kg (wet weight). The procedures to prepare the cell-free extract of *T. litoralis* and to carry out the first chromatography step using DEAE Sepharose (Pharmacia Biotech) are the same as those described for *P. furiosus*[26]. The exception is that the column is eluted using a 9 liter linear gradient from 0 to 500 mM NaCl in buffer D (50 mM Tris-HCl, pH 8.0, containing 2 mM sodium dithionite, 2 mM dithiothreitol and 10%, v/v, glycerol). KGOR activity elutes as 280 - 312 mM NaCl is applied to the column.

Hydroxyapatite Chromatography. Fractions with KGOR activity above 0.6 units/mg are combined (600 ml) and loaded directly onto a column (5 x 10 cm) of Hydroxyapatite (High Resolution, Boehring Diagnostics) equilibrated with buffer B. The absorbed protein is eluted with a 1.2 liter gradient from 0 to 200 mM potassium phosphate in the same buffer at a flow rate at 3 ml/min. Fractions of 50 ml are collected and KGOR activity elutes as 0.10 - 0.14 M phosphate is applied.

Hydrophobic Interaction Chromatography.

Fractions with KGOR activity above 1.0 unit/mg are combined (250 ml), diluted with an equal volume of buffer containing ammonium sulfate (2.0 M),and applied to a column (3.5 x 10 cm) of Phenyl Sepharose (Pharmacia LKB, Piscataway, NJ) previously equilibrated with buffer B containing ammonium sulfate (1.0 M) at 6 ml/min. The adsorbed proteins are eluted with a 720 ml gradient from 1.0 to 0 ammonium sulfate. KGOR activity is detected in the eluent as 134 mM ammonium sulfate is applied.

Superdex 200 Chromatography. Fractions with KGOR activity above 6.0 units/mg are combined (120 ml) and concentrated to approximately 10 ml by ultrafiltration using a PM-30 membrane (Amicon). The concentrated KGOR sample is applied to a column (6 x 60 cm) of Superdex 200 (Pharmacia LKB, NJ) equilibrated at 3 ml/min with buffer B containing 200 mM NaCl.

Q-Sepharose Chromatography. Fractions (20 ml) with KGOR activity above 14 units/mg are combined (80 ml) and loaded onto a column (1.6 x 10 cm) of Q Sepharose High Performance (Pharmacia Biotech) previously equilibrated with buffer B. Using a

500 ml gradient from 0 - 500 mM NaCl in buffer B, KGOR activity elutes at 288 mM NaCl. Fractions (10 ml) with KGOR activity above 20 units/mg are separately analyzed by non-denaturing and SDS gel electrophoresis. Those judged pure are combined (40 ml) and concentrated by ultrafiltration to approximately 13 mg/ml, and are stored at -80°C. The yield is about 40 mg of protein with a specific activity of 22 U/mg.

MOLECULAR PROPERTIES OF POR, IOR, VOR AND KGOR

The physical properties of the four types of KORs (POR, VOR, KGOR and IOR) so far known to be present in the heterotrophic, hyperthermophilic archaea are summarized in Table 2.1. These enzymes have been purified from *P. furiosus*, *T. litoralis* or both and VOR has also been purified from *Pyrococcus* sp. ES-4 and *Thermococcus* sp. ES-1[19]. All of the KORs appear to be composed of two "catalytic units". In the case of POR, VOR and KGOR, this unit (120 kDa) is made up of four distinct subunits ($\alpha\beta\gamma\delta$) with approximate masses of 43, 35, 23 and 12 kDa. In contrast, the IOR "catalytic unit" is smaller (~ 90 kDa) and consists of only two subunits ($\alpha'\beta'$) of 66 and 23 kDa (reviewed in ref. 14). All the KORs characterized so far have been found to contain TPP and iron-sulfur clusters. The TPP contents reported are variable and are typically less than 1 mol per catalytic unit. With KGOR, VOR and IOR, the cofactor is easily lost during purification and TPP must be added to the enzyme assay mixtures to maximal activity. With POR the presence of TPP does not enhance activity so this enzyme appears to have a more tightly-bound cofactor. All of the KORs are sensitive to inactivation by oxygen, presumably due to damage of their iron-sulfur clusters.

The genes encoding POR and VOR subunits of *P. furiosus* are adjacent and most likely divided into three operons[7]. The γ subunits of the two enzymes are encoded by a single gene, and the sequences of the genes encoding δαβ from VOR are very similar to the corresponding genes from POR. Sequence comparisons indicates that all four types of oxidoreductases are closely related, where IOR probably represents a two subunit gene mosaic of the four subunits found in the other enzymes. The genes encoding VOR and IOR can be located in the *P. furiosus* genome[29] using the reported N-terminal amino acid sequences. The genome has ORFs that appear to correspond to a fifth member of the KOR family in *P. furiosus*, which is tentively called XOR. Its genes are located immediately downstream from the genes encoding KGOR. These two enzymes share the same gene for the δ-subunit in the same manner as POR and VOR share a singly γ-subunit[30]. The function of this putative fifth KOR is as yet unknown. The five KOR sequences form a paralogous gene family, indicative of gene duplication and rearrangements of the four "ancestral" genes during evolution to give rise to KORs with different substrate specificites[30]. An overview of the five KOR sequences with respect to their subunit composition and shared subunits is given in Figure 2.2.

Sequence analysis of the four subunits (domains) of the hyperthermophilic KORs shows that the δ-subunit contains two conserved ferredoxin-type [4Fe-4S] cluster binding motifs, while the β-subunit contains a conserved TPP-binding domain as well as four conserved cysteine residues, which could presumably bind a third [4Fe4S] cluster[7,14]. The presence of two [4Fe-4S] clusters in the δ-subunit has been confirmed by expressing in *E. coli* the gene encoding the δ-subunit of *P. furiosus* POR[31]. The reconstituted δ-

subunit is monomeric and contains 8 Fe atoms per mole. Its electron paramagnetic resonance (EPR) properties indicate the presence of two, spin-spin interacting $[4Fe\text{-}4S]^{1+}$ clusters. The recombinant δ-subunit acts as a functional redox carrier with properties very similar to those of 4Fe-ferredoxins, and it was proposed that the δ-subunit directly evolved from these redox proteins[31]. When the EPR properties of the recombinant δ-subunit are compared with those of the reduced holoenzyme, it is evident that the latter contains a third $[4Fe\text{-}4S]^{1+}$ cluster in addition to the two within the δ-subunit. This third cluster probably resides within the β-subunit domain, based on the sequence analysis of these enzymes. The proposed pathway of electron flow from the oxidation of the 2-ketoacid to ferredoxin, the external electron acceptor, is shown in Figure 2.3. The genes encoding the two subunits of IOR from P. *kodakaraensis* KOD1 have been expressed in *E. coli* and after a heat treatment step exhibit detectable activity[32].

CATALYTIC PROPERTIES OF POR, IOR, VOR AND KGOR

The four KORs purified from *P. furiosus* and *T. litoralis* are identified on the basis of their abilities to oxidatively decarboxylate different 2-keto acids into their CoA derivatives, namely pyruvate (POR), indolepyruvate (IOR), 2-ketoglutarate (KGOR) and 2-ketoisovalerate (VOR). The substrate specificities of the four enzymes are summarized in Table 2.2. POR is only reactive towards acyl keto acids and shows highest activity with pyruvate, its physiological substrate. VOR and IOR utilize a much broader range of substrates. VOR preferentially utilizes 2-keto acid derivatives of branched chain amino acids, while IOR uses the transaminated forms of aromatic amino acids. In contrast,

KGOR is very specific for 2-ketoglutarate, a substrate not used by any of the other enzymes, which it converts to succinyl-CoA. Thus, in combination, the four enzymes could function to activate 2-keto acids derived from most common amino acids found *in vivo*. The CoA derivatives serve as sources of energy via the two acetyl CoA synthetase enzymes (ACS I and II) which generate the organic acids and ATP (see Figure 2.1). Both isoenzymes use the CoA derivatives generated by POR and VOR, but only ACS II uses indoleacetyl CoA, the product of the IOR reactions. Neither isoenzyme utilizes succinyl CoA, and this may be used for biosynthesis possibly via a modified TCA cycle[33]. POR and VOR are the dominant KORs in *P. furiosus,* with specific activities in cell-free extracts of about 10 and 2 units/mg, respectively. The specific activities of IOR and KGOR are about 10-fold lower that that of VOR. These data can be used to give a reasonable estimate of the relative amounts of these proteins within the cells, since the specific activities of the purified enzymes are comparable (20 and 50 U/mg). The four enzymes vary in their affinities for CoASH (K_m= 17 - 110 µM) and for ferredoxin, the physiological electron carrier (K_m= 8 - 94 µM, see Table 2.3). The physiological significance of these differences, if any, is not known. None of the enzymes are able to couple 2-keto acid oxidation to the reduction of NAD or NADP, which is consistent with ferredoxin being the physiological electron acceptor.

In addition to the oxidative decarboxylation of pyruvate to produce acetyl CoA, POR from *P. furiosus* has been shown to catalyze the decarboxylation of pyruvate to generate acetaldehyde in a CoA-dependent reaction[34]. The apparent K_m values for CoASH (0.11 mM) and pyruvate (1.1 mM) in the non-oxidative decarboxylation reaction are very similar to those determined previously for pyruvate oxidation. The other three

KORs probable also catalyze this reaction and it has been proposed that this reaction is of some significance because it generates aldehydes from the transaminated forms of amino acids[33]. However, this has yet to be confirmed by *in vivo* analyses.

ACKNOWLEDGMENT

This research was supported by grants from the Department of Energy.

REFERENCES

1. R. C. Wahl, and W. H. Orme-Johnson, *J. Biol. Chem.* **262,** 10489 (1987).

2. B. Meinecke, J. Bertram, and G. Gottschalk, *Arch. Microbiol.* **152,** 244 (1989).

3. E. Brostedt, and S. Nordlund, *Biochem J.*. **279,** 155 (1991).

4. L. Pieulle, B. Guigliarelli, M. Asso, F. Dole, A. Bernadac, and E. C. Hatchikian, *Biochim. Biophys. Acta* **1250,** 49 (1995).

5. L. Kerscher, and D. Oesterhelt, *Eur. J. Biochem.* **116,** 595 (1981).

6. J. M. Blamey, and M. W. W. Adams, *Biochim. Biophys. Acta* **1161,** 19 (1993).

7. A. Kletzin, and M. W. W. Adams, *J. Bacteriol.* **178,** 248 (1996).

8. J. Kunow, D. Linder, and R. K. Thauer, *Arch. Microbiol*. **163,** 21 (1995).

9. A. K. Bock, J. Kunow, J. Glasemacher, and P. Schönheit, *Eur. J. Biochem.* **237,** 35 (1996).

10. C. J. Bult, O. White, G. J. Olsen, L. Zhou, R. D. Fleischmann, G. G. Sutton, J. A. Blake, L. M. FitzGerald, R. A. Clayton, J. D. Gocayne, A. R. Kerlavage, B. A. Dougherty, J. F. Tomb, M. D. Adams, C. I. Reich, R. Overbeek, E. F. Kirkness, K. G. Weinstock, J. M Merrick, A. Glodek, J. L. Scott, N. S. M. Geoghagen, J. C. Venter, *Science* **273,** 1058 (1996).

11. A. Tersteegen, D. Linder, R. K. Thauer, and R. Hedderich, *Eur. J. Biochem.* **244,** 862 (1997).

12. J. M. Blamey, and M. W. W. Adams, *Biochemistry* **33,** 1000 (1994).

13. N. J. Hughes, P. A. Chalk, C. L.Clayton, and D. J. Kelly, *J. Bacteriol.* **177,** 3953 (1995).

14. M. W. W. Adams and A. Kletzin, *Adv. Prot. Chem.* **48,** 101 (1996).

15. E. Chabriere, M. H. Charon, A. Volbeda, L. Pieulle, E. C. Hatchikian and J. C. Fontecilla-Camps, *Nat. Struct. Biol.* **6,** 182 (1999).

16. L. Kerscher, L. and D. Oesterhelt, *Eur. J. Biochem.* **116,** 595 (1981).

17. S. Menon and S. W. Ragsdale, *Biochemistry* **36,** 8484 (1997).

18. X. Mai, and M. W. W. Adams, *J. Biol. Chem.* **269,** 16726 (1994).

19. J. Heider, X. Mai, and M. W. W. Adams, *J. Bacteriol*. **178,** 780 (1996).

20. X. Mai, and M. W. W. Adams, *J. Bacteriol*. **178,** 5890 (1996).

21. K. E. Nelson, R. A. Clayton, S. R. Gill, M. L. Gwinn, R. J. Dodson, D. H. Haft, E. K. Hickey, J. D. Peterson, W. C. Nelson, K. A. Ketchum, L. McDonald, T. R. Utterback, J. A. Malek, K. D. Linher, M. M. Garrett, A. M. Stewart, M. D. Cotton, M. S. Pratt, C. A. Phillips, D. Richardson, J. Heidelberg, G. G. Sutton, R. D. Fleischmann, J. A. Eisen, O. White, S. L. Salzberg, H. O. Smith, J. C. Venter, and C. M. Fraser, *Nature* **399,** 323 (1999).

22. K. E. Nelson, (The genome of *Thermotoga maritima*), this volume, A, (2000).

23. X. Mai, and M. W. W. Adams, *J. Bacteriol*. **178,** 5897 (1996).

24. A. Hutchins, X. Mai and M. W. W. Adams, (Acetyl CoA synthetases I and II from *Pyrococcus furiosus*), this volume, B (2000).

25. M. M. Bradford, *Anal. Biochem*. **72,** 248 (1976)

26. M. F. J. M. Verhagen, A. L. Menon, G. J. Schut, and M. W. W. Adams, (Large scale cultivation and purification of hyperthermophilic enzymes) this volume, A (2000).

27. F. O. Bryant and M. W. W. Adams, *J. Biol. Chem*. **264,** 5070 (1989).

28. A. Neuner, H. W. Jannasch, S. Belkin, and K. O. Stetter, *Arch. Microbiol.* **153,** 205 (1990).

29. F. T. Robb (The genome of *Pyrococcus furiosus*), this volume, A (2000).

30. D. L. Meader, R. B. Weiss, D. M. Dunn, J. L. Cherry, J. M. González, J. DiRuggiero, and F. T. Robb, *Genetics* **152,** 1299 (1999).

31. A. L. Menon, H. Hendrix, A. Hutchins, M. F. J. M. Verhagen and M. W. W. Adams, *Biochemistry* **37,** 12838 (1998).

32. M. A. Siddiqui, S. Fujiwara, M. Takagi, and T. Imanaka, *FEBS Lett.* 434, 372 (1998).

33. Q. Zhang, T. Iwasaki, T. Wakagi, and T. Oshima, *J. Biochem.* **120,** 587 (1996).

34. K. Ma, A. Hutchins, S. S. Sung, and M. W. W. Adams, *Proc. Natl. Acad. Sci. USA* **94,** 9608 (1997).

Table 2.1. Molecular properties of 2-keto acid oxidoreductases from hyperthermophilic archaea.

Enzyme[a]	Quaternary Structure	Molecular weight	
		Biochemical [b]	Calculated[c]
POR	$\alpha_2\beta_2\gamma_2\delta_2$	47, 31, 24, 13	44, 36, 20, 12
VOR	$\alpha_2\beta_2\gamma_2\delta_2$	47, 34, 23, 13	44, 35, 20, 12
IOR	$\alpha'_2\beta'_2$	66, 23	71, 24
KGOR	$\alpha_2\beta_2\gamma_2\delta_2$	43, 29, 24, 10	44, 31, 18, 10
XOR[d]	nd[e]	nd[e]	43, 31, 20, 10

[a]POR, IOR and XOR are from *P. furiosus* and KGOR and VOR are from *T. litoralis* . Biochemical data are taken from Ref. 14.
[b]Based on SDS-gel electrophoresis.
[c]Calculated from the genome sequence[29]. Genes were identified based on the N-terminal amino acid sequences of the subunits.
[d]XOR is a putative 2-keto acid oxidoreductase in *P. furiosus*. The genes proposed to encode it were identified in the genome databse by sequence simlilarity to the other 2-keto acid reductases.
[e]Not determined.

Table 2.2. Substrate specificities of 2-keto acid oxidoreductases from hyperthermophilic archaea.

	Specific activity (K_m) [a]			
Substrate	Pf POR	Tl VOR	Pf IOR	Tl KGOR
Pyruvate	21 (460)	4	0	0
2-Ketoisovalerate	0	47 (90)	0	0
Phenylpyruvate	0	9	87	0
2-Ketoglutarate	0	0	0	22 (250)
p-Hydroxyphenylpyruvate	0	13	70	0
Indolepyruvate	0	7	38 (250)	0
Keto-γ-methylthiobutyrate	0	10	26	0
2-Ketoisocaproate	5	31	15	0
2-Ketobutyrate	11	35	0	0
Phenylglyoxylate	0	13	0	0

[a] Specific activity is expressed as unit/mg. The apparent K_m value (in μM) is given in parenthesis where known. Data are taken from Refs. 6, 18, 19 and 20.

Table 2.3. Cofactor affinities of 2-keto acid oxidoreductases of hyperthermophilic archaea.

	Apparent K_m (μM)[a]			
Substrate	Pf POR	Tl VOR	Pf IOR	Tl KGOR
CoASH	110	50	17	40
Ferredoxin	94	17	48	8

[a]POR and IOR are from *P. furiosus* (Pf) and KGOR and VOR are from *T. litoralis* (Tl). The biochemical data are taken from Refs. 6, 18, 19 and 20.

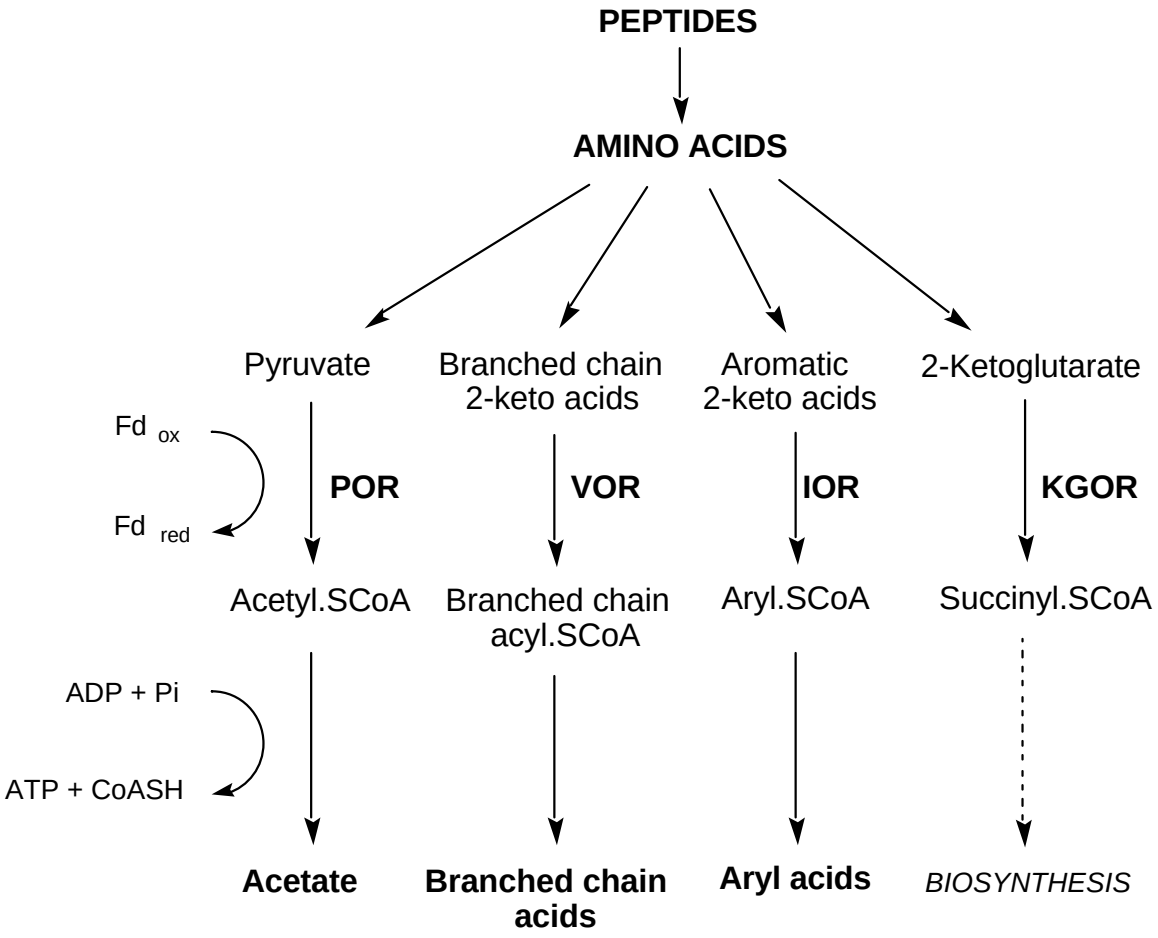

Figure 2.1. Proposed pathway of peptide metabolism in fermentative hyperthermophilic archaea. The abbreviations used are: Fd_{ox}; oxidized ferredoxin; Fd_{red}, reduced ferredoxin; POR, pyruvate oxidoreductase; VOR, 2-ketoisovalerate oxidoreductase; KGOR, 2-ketoglutarate oxidoreductase; IOR, indolepyruvate oxidoreductase; CoA, coenzyme A. Data taken from M. W. W. Adams and A. Kletzin, *Adv. Prot. Chem.* **48,** 101 (1996)

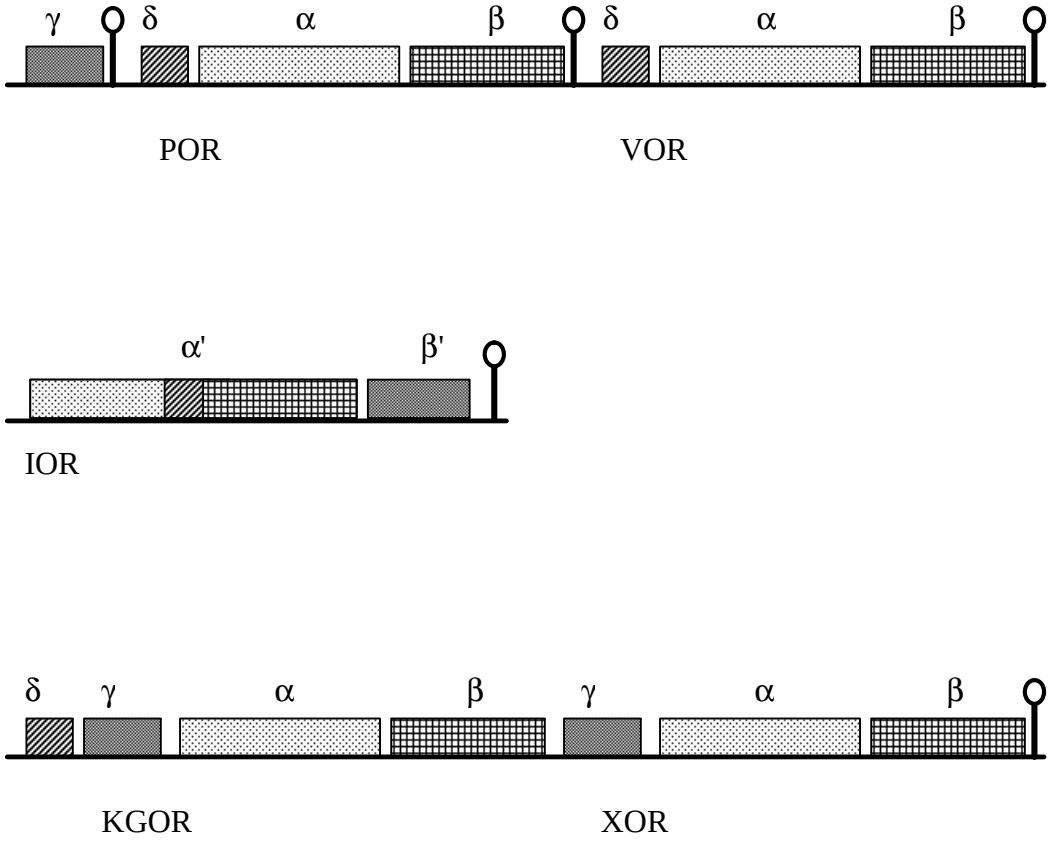

Figure 2.2. Comparison of the subunit and domain structures of the paralogous KOR gene family from *P. furiosus*. Homologous domains are indicated with the same shading. Putative transcription stop sites are indicated by a ball on stick. Data taken from A. Kletzin, and M. W. W. Adams, *J. Bacteriol.* **178,** 248 (1996), F. T. Robb (The genome of *Pyrococcus furiosus*), this volume, A (2000) and D. L. Meader, R. B. Weiss, D. M. Dunn, J. L. Cherry, J. M. González, J. DiRuggiero, and F. T. Robb, Genetics **152,** 1299 (1999).

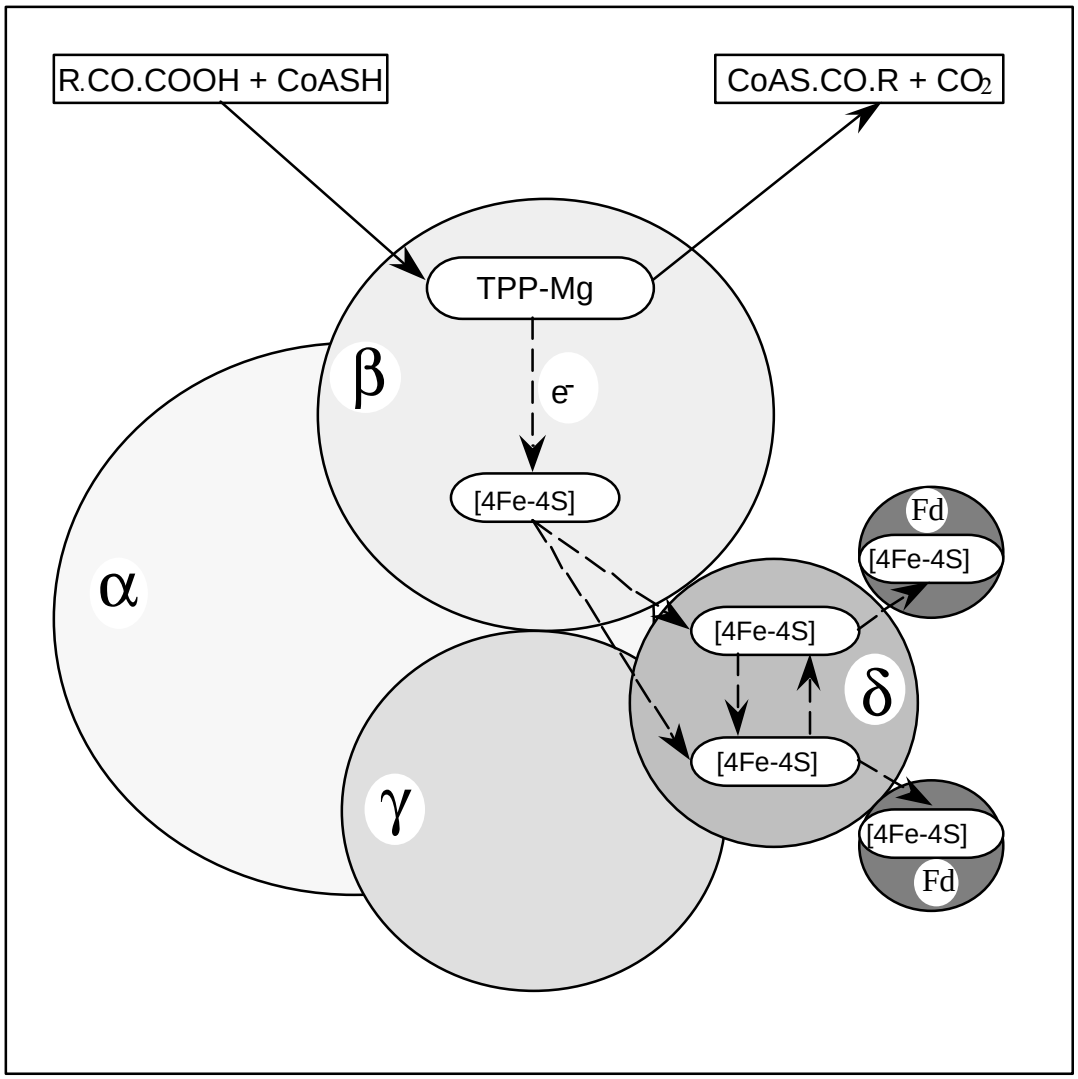

Figure 2.3. Schematic diagram of the four subunit KOR and the proposed pathway of electron flow. Ferredoxin is the electron acceptor and is represented as Fd. The other abbreviations are: TPP, thiamine pyrophosphate; CoA, coenzyme A, [4Fe-4S], iron sulfur cluster. It is assumed that each δ-subunit, which can transfer two electrons, interacts with two molecules of ferredoxin, which is a one electron carrier. Data taken from M. W. W. Adams and A. Kletzin, *Adv. Prot. Chem.* **48,** 101 (1996)

.

CHAPTER 3

DNA MICROARRAY ANALYSIS OF THE HYPERTHERMOPHILIC ARCHAEON *Pyrococcus furiosus*: EVIDENCE FOR A NEW TYPE OF SULFUR-REDUCING ENZYME COMPLEX[1]

[1]Gerrit J. Schut, J. Zhou, and M.W.W. Adams. 2001. *Journal of Bacteriology*. 183:7027-7036.

Reprinted here with permission of the publisher.

ABSTRACT

DNA microarrays were constructed using 271 ORFs from the genome of the archaeon *Pyrococcus furiosus*. They were used to investigate the effects of elemental sulfur (S°) on the levels of gene expression in cells grown at 95°C using maltose as the carbon source. The ORFs included those that are proposed to encode proteins mainly involved in the pathways of sugar and peptide catabolism, in the metabolism of metals, and in the biosynthesis of various cofactors, amino acids and nucleotides. The expression of 21 ORFs decreased by more than 5-fold when cells were grown with S° and of these 18 encode subunits associated with three different hydrogenase systems. The remaining three ORFs encode homologs of ornithine carbamoyltransferase and HypF, both of which appear to be involved in hydrogenase biosynthesis, as well as a conserved hypothetical protein. The expression of two previously uncharacterized ORFs increased by more than 25-fold when cells were grown with S°. Their products, termed SipA and SipB (for sulfur-induced proteins), are proposed to be part of a novel S°-reducing, membrane-associated, iron-sulfur cluster-containing complex. Two other previously uncharacterized ORFs encoding a putative flavoprotein and a second FeS protein were up-regulated more than 6-fold in S°-grown cells, and these are also thought be involved in S° reduction. Four ORFs that encode homologs of proteins involved in amino acid metabolism were similarly up-regulated in S°-grown cells, consistent with the fact that growth on peptides is a S°-dependent process. An ORF encoding a homolog of the eukaryotic ribosomal RNA processing protein, fibrillarin, was also up-regulated 6-fold in the presence of S°, although the reason for this is as yet unknown. Of the 20 S°-independent ORFs that are the most highly expressed (at more than 20-times the detection limit), 12 of them

represent enzymes purified from *P. furiosus*, but none of the products of the 34 S°-independent ORFs that are not expressed above the detection limit have been characterized. These results represent the first derived from the application of DNA microarrays to either an archaeon or a hyperthermophile.

INTRODUCTION

Hyperthermophiles are microorganisms that grow optimally at temperatures of 80°C and above, and most are classified as archaea (66). They are a rather diverse group with respect to their metabolic capabilities but many of them utilize peptides as a carbon source and reduce elemental sulfur (S°) to H_2S (67). Of these, the majority are obligately proteolytic and show little if any growth unless S° is added to the growth medium. The exceptions include some species of *Pyrococcus* that metabolize poly- and oligosaccharides as well as peptides (3, 4, 15). For example, *P. furiosus* grows on a disaccharide (maltose) to high cell densities in the absence of S° and produces H_2 as an end product rather than H_2S. On the other hand, *P. furiosus* requires S° in the growth medium when it utilizes peptides as a carbon source (1). A comparison of the activities of some key metabolic enzymes in cells grown either on peptides (with S°) or on maltose (with and without S°) provided the first evidence for a highly regulated fermentative-based metabolism in *P. furiosus*, with S° or its metabolites playing a key regulatory role (1). The molecular mechanism by which S° achieves this control is not known.

The pathways by which *P. furiosus* metabolizes peptides and carbohydrates are reasonably well established. The organism contains a modified Embden-Meyerhof pathway in which hexokinase and phosphofructokinase are ADP- rather than ATP-dependent (29, 69). In addition, the expected glyceraldehyde-3-phosphate dehydrogenase and phophoglycerate kinase are replaced by a single phosphate-independent enzyme, glyceraldehyde-3-phosphate ferredoxin oxidoreductase (GAPOR; (42)), which is regulated at the transcriptional level (70). The pyruvate produced by this pathway is converted to the end product acetate in two steps involving pyruvate ferredoxin

oxidoreductase (POR; (5)) and acetyl-CoA synthetases I and II (40, 62), with the concomitant production of ATP from ADP and phosphate. The oxidative steps in the pathway of acetate production from glucose therefore involve two ferredoxin-dependent enzymes (GAPOR and POR), and a similar mechanism is present during peptide catabolism by *P. furiosus.* The organism contains, in addition to POR, three other, ferredoxin-dependent, 2-keto acid oxidoreductases, and these convert transaminated amino acids into their corresponding CoA derivatives (5, 19, 39), which are then transformed to their corresponding organic acids by the two acetyl-CoA synthetases with concomitant ATP synthesis (40).

How *P. furiosus* and related species couple the oxidation of the reduced ferredoxin generated by the catabolic pathways to the reduction of S° is not known. The organism contains three different hydrogenases: two cytoplasmic, NAD(P)H-dependent enzymes, and one as part of a membrane-bound complex (9, 38, 60). The cytoplasmic hydrogenases were thought to play a role in S° reduction as they can reduce S° *in vitro* (37), but this appears not to be the case as the total hydrogenase activity of S°-grown cells is dramatically lower than that of cells grown without S° (1). The mechanism by which S° affects hydrogenase activity is not understood. Moreover, the nature of the enzyme system that reduces S° remains unknown. In mesophilic organisms, the only S°-reducing enzyme that has been well-characterized is the trimeric, membrane-bound, molybdenum (Mo)-containing, polysulfide reductase of the mesophilic bacterium, *Wolinella succinogenes* (32), but the genome of *P. furiosus* (55) does not contain ORFs that would encode a homolog of the mesophilic enzyme. Moreover, *P. furiosus* is not known to utilize Mo but contains at least three enzymes that utilize the analogous element tungsten (W; (27)), suggesting perhaps a role for W in S° reduction.

The ability of *P. furiosus* to grow well both with and without S°, together with the availability of its complete genome sequence, provide an opportunity to investigate S° metabolism by expression analysis using DNA microarrays. In fact, the genus *Pyrococcus* is unique in that complete genome sequences are available from three species; *P. horikoshii*, *P. abyssi* and *P. furiosus* (28, 51, 55). While DNA microarrays (61) have revolutionized functional genomics in eukaryotic systems, e.g., (14, 57, 64), there have been far fewer applications with prokaryotes. Studies initially focused on pathogens (11, 17, 59, 68, 75) and more recently have included *Escherichia coli* (2, 30, 54, 74, 80), *Bacillus subtilus* (77, 79) and a cyanobacterium (21)**.** As yet there have been no reports of using this technique with either a hyperthermophile or an archaeon. The genome of *P. furiosus* contains about 2,200 ORFs with more than 50% of unknown function. As a prelude to a complete genomic analysis, herein we focus on 271 ORFs that encode proteins that are proposed to be involved in the primary metabolic pathways, energy conservation and metal metabolism. The results indicate that S° or its metabolites play a major regulatory role at the transciptional level and that S° reduction appears to be accomplished by a new type of enzyme system involving the products of previously uncharacterized ORFs.

MATERIALS AND METHODS

Primer Design and PCR. Gene sequences were obtained from the *P. furiosus* genome site (http://comb5-156.umbi.umd.edu/) (55). Of the 275 ORFs that were examined in this study, 87 of them are listed in Tables 3.1-3.4. A complete list of the 275 ORFs is available at http://adams.bmb.uga.edu/pubs/sup228.pdf. Primers were designed for the

ORFs using the Primer 3 program (Whitehead Institute MIT) and were purchased from Stanford University and from MWG biotech (High Point, NC). For the initial round of PCR the primer pairs were designed to give products corresponding to the complete ORFs and this yielded products for 249 of them as verified using gel electrophoresis. The remaining 42 primer pairs were designed to yield a product of about 1 kb (unless the target ORF was smaller). Of these only 4 ORFs did not yield suitable PCR products and these were not pursued further. PCR products were purified with a Strataprep 96 PCR purification kit (Stratagene, La Jolla, CA) and eluted in 33% (v/v) DMSO. They were spotted in duplicate on aminosilane coated slides (Sigma, St Louis, MO) in four subarrays using a robotic slide printer (Omnigrid, Genemachines, San Carlos, CA). The slides were processed as previously described (8).

Growth of *P. furiosus* and RNA preparation. *P. furiosus* was grown in batch mode in a 20 liter custom fermentor at 95°C using maltose as the primary carbon source and was harvested in mid-log phase (1). The only variable was the presence or absence of S°. The cells that were used to prepare RNA for the microarray analyses were from experiments that have been described previously (1). In that case, activity assays were determined for more than 20 enzymes involved in the primary metabolic pathways using cytoplasmic and membrane fractions, and these results are referred to below. Samples (2000 ml) of the same cultures were cooled on ice and total RNA was extracted using acid phenol extraction (72). No significant contamination of the RNA with genomic DNA could be detected by Northern blot hybridization or preliminary microarray experiments (data not shown) and so a DNase treatment was not used.

Preparation of cDNA and Hybridization Conditions. Fluorescently labeled cDNA was prepared with the ARES DNA labeling kit (Molecular Probes, Eugene, OR). In brief, 15 µg of total RNA was reversed transcribed in a total volume of 20 µl using Stratascript RT (Stratagene, La Jolla, CA) in the presence of 1 mM dA, C, GTP, 0.3 mM dTTP, 0.5 mM aminoallyl dUTP and 1 µg random 9-mers (Stratgene, La Jolla, CA) according to the manufacturer's instructions. After a 1.5 h incubation at 42 °C, RNA was destroyed by the addition of 0.1 N NaOH followed by a 10 min incubation at 70 °C. After neutralization with 0.1 N HCl, amine-modified cDNA was purified using a QIAquick PCR purification kit (Qiagen, Valencia, CA) except that the wash buffer was replaced with 75% (v/v) ethanol and the cDNA was eluted with 45 µl of distilled water and dried under vacuum. The amine modified cDNA was labeled with Alexa 488 or Alexa 594 dyes (Molecular Probes, Eugene, OR) according to the manufacturer's instructions. Alexa 546 was used as third dye for the triple-labeling experiments. The labeled cDNA was purified with the Qiagen kit as described above and was dried under vacuum. Differentially labeled (Alexa 488 and 594) cDNA derived from *P. furiosus* cells grown in the presence and absence of S° were pooled and hybridized to the microarrays. The labeled cDNA was dissolved in 20 µl hybridization buffer (Sigma, St Louis, MO) and hybridization was performed under a coverslip at 65 °C in a humidity chamber (Arrayit, Sunnyville, CA) for between 10 and 15 h. The slides were then washed twice for 5 min in each of 2xSSC/0.1% SDS and 0.2xSSC/0.1% SDS, rinsed in distilled water and blown dry with compressed air. The intensities of the Alexa 488 and 594 dyes were measured using a Scan Array 5000 spectrometer (Packard, Meriden, CT) with the appropriate laser and filter settings and analyzed using Quantarray (Packard, Meriden, CT).

Data analysis. To compute signal intensities for each ORF, the areas surrounding each spot were taken as the background and 17 control spots, where only spotting buffer was printed, were included on the 384 spot array. The control spots were corrected for local background and the average was used to correct the signals from each ORF after their background correction. The relative amounts of the transcripts (with and without S°) are presented in a linear fashion by converting all ratios to a $\log_2$ function. For the two different growth conditions tested, a negative value below -2.3 represents a more than 5-fold down-regulation of expression from a given ORF by S° and this corresponds to a green color in a false color overlay. Conversely, a positive value above 2.3 represents a more than 5-fold up-regulation and corresponds to a red color in a false color overlay. ORFs that display $\log_2$ values between approximately -1 and 1 are minimally affected by S° and show a yellow color on the overlay. The detection limit of fluorescent signals was set arbitrary to 1000 intensity units (see Fig. 3.1) and such spots are not visible on the false overlay. Only ORFs that display intensities more than twice the detection limit are considered valid. Conversion of intensity ratios enables the data to be presented as a $\log_2$ value with a standard deviation. This represents an average of 6 hybridization experiments using cDNA derived from 5 different cultures of *P. furiosus*, two grown with S° and three grown without**.** In preliminary experiments we did not observe any significance difference in the quality of the data between different Alexa dyes (Molecular Probes) nor when the Alexa dyes were replaced with CY3 and CY5 (Amersham, Piscataway, NJ), dyes that are more usually used as fluorescent labels (12). The advantage of the Alexa dyes is that labeling with three dyes is possible using the lasers and filters available in the Scanarray 5000 (Packard, Meriden, CT). Statistical significance of the

observed fluorescence signal ratios was obtained by a paired t-test analysis using the statistical software JMP 4 (SAS institute, Cary, NC).

RESULTS AND DISCUSSION

Selection of ORFs. Of the approximately 2,200 ORFs in the *P. furiosus* genome (55), 271 were selected for microarray analysis. The targets were putative genes involved in the primary metabolic pathways of carbon, nitrogen and energy metabolism, and those that are, or might be, related to the metabolism of S° and H_2. They included ORFs that are proposed to encode various enzymes and proteins involved in the pathways of sugar and peptide catabolism, utilization of metals (such as Fe, Ni, W and Mo), in the biosynthesis of cofactors, amino acids, lipids, polyamines, ribosomes, nucleotides together with putative chaperonins, ATP-ases and transcriptional regulators. Unless otherwise indicated, each ORF is referred to by its end nucleotide number and by its current annotation, which is based on homology searches (depicted in brackets, see Table 3.1; (55)). It is specifically noted in Tables 3.1-3.4 where there are experimental data derived using *P. furiosus* to support the ORF assignment (given without brackets and with a reference, see Table 3.1).

Experimental Protocols and Data Analysis. The efficacy of the microarray experiment using mRNA derived from *P. furiosus* cells is shown in Fig. 3.1. Fig. 3.1A shows data using differentially labeled cDNA samples of RNA prepared from the same batch of cells, grown with maltose in the absence of S°, and hybridized to the same microarray. The intensity of the fluorescence signals varied over a range of more than 10^3, consistent with

what has been reported with other organisms (26, 34, 46, 79). Those ORFs with intensities below approximately 2000 (Fig. 3.1A) are considered below the detection limit and it cannot be concluded that these ORFs are expressed to a significant degree. From Fig 3.1A it is clear that ORFs that give rise to low intensity signals show a high deviation because of background fluorescence, whereas the data derived from ORFs that give high signal intensities lie near or on the diagonal.

As shown in Fig. 3.1B, S° and/or its metabolites clearly have a dramatic effect on the expression of many of the 271 ORFs that were examined. It was previously shown that the presence of S° in the growth medium affects the activities of several metabolic enzymes (1). The microarray data indicate that this regulation is primarily at the transciptional level. In the following, we focus on ORFs whose expression appears to be strongly regulated by S°, where the signal intensity changes by at least 5-fold (shown by the upper and lower diagonal lines in Fig. 3.1B). The standard deviations ($\log_2$ intensity ratios) for almost all of these ORFs are less than 2 and they are differentially regulated with at least a 95% confidence level as determined using a paired t-test analysis ($p > 0.95$). However, there are three exceptions. These are ORFs 1419794 ([formate dehydrogenase alpha chain]), 156299 ([3-isopropyl malate dehydrogenase]) and 438413 ([phosphoribosylglycinamide formyltransferase]) whose $\log_2$ intensities showed deviations above 2 ($p < 0.90$). For these ORFs a large variation in the ratios was obtained using the same growth condition (maltose without S°). This was verified when cDNA samples from three independently-grown cultures were separately labeled with Alexa 488, 546 or 594 dyes and all three cDNAs were hybridized to the same slide. Only these three (of 271) ORFs showed distinct false colors indicating differential expression in one

of the three samples. The reasons for this are not clear but these ORFs appear not to be regulated by S° and are not considered further.

ORFs strongly down-regulated by S°. The expression of 21 of the 271 ORFs examined decreased by more than a factor of 5 when RNA was derived from cells grown with S° (Fig. 3.1B) and these are listed in Table 3.1. Of these, 18 ORFs encode subunits associated with the three different hydrogenase systems that have been characterized from *P. furiosus*. These include those encoding six of the eight subunits of the two cytoplasmic hydrogenases (I and II, (38, 50)), whose expression decrease between 6 and 14-fold in the presence of S° (Table 3.1). Expression of the other two ORFs (encoding the α- and γ-subunits of hydrogenase I) decrease by 2.2-4.8-fold. These data are in accord with the report that the presence of S° in the medium decreased the total hydrogenase activity of the cytoplasmic fraction by approximately 16-fold (1). Since the specific activity of hydrogenase I is about 10-fold higher that of hydrogenase II in in vitro assays, it was not possible to determine from the activity analyses if hydrogenase II activity was regulated by S°. However, the microarray data clearly show that both hydrogenases are strongly regulated. Moreover, S° regulates the expression of the genes encoding the cytoplasmic hydrogenases in a negative fashion, rather than S° (or its metabolites) having some inhibitory effect on activity. Obviously, these hydrogenases are unlikely to play a role in S° reduction, as originally suggested (37).

It was previously shown that the activity of the membrane-bound hydrogenase of *P. furiosus* decreases by almost 30-fold when cells are grown in the presence of S° (1). After solubilization and purification from cells grown in the absence of S°, the enzyme contained two subunits (Mbh11, Mbh12) and, based on their N-terminal sequences, the

genes encoding them were proposed to be part of a 14 ORF operon (Mbh1-14: (60)). All but one (Mbh7) of the 14 ORFs were included on the DNA microarray. As shown in Table 3.1, the expression of all but one of them decreased by more than 5-fold in the presence of S° (the remainder, Mbh9, decreased by 4.2-fold). These data confirm that the 14 ORFs do indeed constitute an operon and that its products are involved in the metabolism of H_2. The average fluorescence intensities associated with the 13 ORFs of the membrane-bound hydrogenase operon are shown in Fig. 3.2, along with the values for the eight subunits that encode the two cytoplasmic hydrogenases. The ORFs are depicted according to their order in their respective operons. All show a similar pattern in that they are down-regulated to close to the detection limit (see Fig. 3.1B) in the presence of S°, consistent with barely detectable hydrogenase activities in cell-free extracts (1). The apparent exception is the ORF encoding the α-subunit of hydrogenase I. Although this ORF is expressed at about five times the detection limit, the results show that it is regulated by S° as determined by the paired t-test analysis ($p > 0.98$). However, the 3' end of this ORF (ORF 867811) overlaps by two nucleotides with the 3' end of an ORF (ORF 867808) on the opposing strand. If the untranslated 3' end of ORF 867811 mRNA extends far enough into the complementary strand of *hyhA*, this could give rise to a 'false signal' due to cross hybridization. ORF 867811 encodes a putative ABC transporter (ATP binding protein) and was not included on the microarray. The interference of overlapping mRNAs in microarray analyses has been reported (30) although it has not been systematically analyzed with any genome. With the 18 hydrogenase-related ORFs (Fig. 3.2), there is considerable variation in the absolute signal intensities but this appears to arise to some extent from the differences in ORF sizes, several of which are less than 500 bps.

Hence, of the 21 of the 271 ORFs that are strongly down-regulated (> 5-fold) in the presence of S°, 18 represent structural genes for the three hydrogenases. Of the other three S°-responsive ORFs, one (ORF 577932) showed an almost 40-fold decrease in expression, the largest of any of the down-regulated ORFs (Table 3.1). ORF 577932 is annotated as *hypF* and shows 37% sequence identity to its closest homolog, HypF from the aerobic bacterium *Ralstonia eutrophicus* (76). HypF is thought to be involved in biosynthesis of the metal site of NiFe-hydrogenases. There is only one gene of this type in *P. furiosus* so it appears that, as in *E. coli* (25), one HypF protein is involved in the maturation of three different hydrogenases (two cytoplasmic and one membrane-bound). As a processing enzyme one would expect HypF to be present at low intracellular concentrations, and why its gene appears to be so strongly regulated by S° is not clear at this point. *P. furiosus* contains homologs of several other genes that are involved in hydrogenase maturation and metal insertion in mesophilic bacteria. These include *hycI* (ORF 637303) and *hypACDE* (ORFs 636092, 566869, 567973 and 626147: a version of *hypB* appears not to be present in the *P. furiosus* genome). These ORFs were also included on the microarray. The expression of the *hyp* genes, which are all expressed at significant levels (1.5 – 9.6 times the detection limit; see Fig. 3.1B) decreased by 2-3 fold when S° was added but expression of *hycI* was below the detection limit under both conditions.

One of the two remaining ORFs that are strongly down-regulated by S° (Table 3.1) may also be related to hydrogenase biosynthesis. This is ORF 615154 which encodes ornithine carbamoyltransferase (OTCase). This enzyme has been purified from *P. furiosus*, its gene has been cloned and expressed, and its crystal structure is available (36, 71). OTC-ase catalyzes the transfer of a carbamoyl group from carbamoyl phosphate to

ornithine generating citrulline in the arginine biosynthetic pathway. The potential link between OTC-ase and the hydrogenases stems from the recent proposal that the source of the C1 (CO and CN) ligands to the metals at the active site of hydrogenases is the carbamoyl group of carbamoyl phosphate (48). In view of the regulation of both OTC-ase and hydrogenase expression by S° in *P. furiosus*, we speculate that citrulline is the precursor of the carbamoyl group for the synthesis of the active sites of the three hydrogenases in this organism. Citrulline may well be preferred to carbamoyl phosphate because of the high thermal lability of the latter compound (35). One would expect citrulline also to be needed for arginine biosynthesis even in the presence of S°, and this appears to be the case, since OTC-ase is expressed at close to three-times the detection level in S°-grown cells.

The remaining ORF that is strongly down-regulated by S° is ORF 51760, and this is annotated as a conserved hypothetical protein (Table 3.1). It is adjacent to the gene (ORF 49183) encoding PEP synthetase, a gluconeogenic enzyme recently purified from *P. furiosus* (24); see below), and an ORF (ORF 53135) encoding a conserved hypothetical protein, neither of which showed significant (less than 2-fold) changes in expression according to the microarray data. The function of the S°-responsive ORF 51760 is therefore unclear at present.

ORFs strongly up-regulated by S°. Of the 271 ORFs examined, the expression of 12 of them was strongly up-regulated (more than 5-fold) when S° was present in the growth medium (Table 3.2). In contrast to the ORFs that were down-regulated by S°, all of the up-regulated ORFs represent putative proteins since none of their products have been characterized from *P. furiosus*. Moreover, the two most strongly-regulated ORFs,

1871822 and 1872873, which are up-regulated more than 25-fold, are next to each other on the genome. The products of these two ORFs show no sequence similarity to any known protein. Nevertheless, they will be referred to as SipA (1871822) and SipB (1872873) for 'sulfur-induced protein' as expression of their genes clearly responds to S° or its metabolites. Both genes are also very tightly regulated, as there appears to be little or no expression from them when cells are grown in the absence of S° (their signal intensities are less than the detection limit).

What is now termed *sipA* was included in the list of ORFs for microarray analysis because its product had been previously identified (from the N-terminal sequence) after gel electrophoresis of *P. furiosus* extracts. The protein was present in washed, membrane preparations of cells grown with S° but was not detected in cells grown without S° (23). SipA is a 19 kDa protein that contains a single Cys residue. Although it is strongly associated with the membrane, sequence analyses do not reveal any transmembrane helix motifs (23). What we now term *sipB* is currently annotated as a 'putative polyferredoxin' and it contains Cys motifs that could coordinate two [4Fe-4S] clusters. However, the closest homolog (25% sequence identity) to this putative 15 kDa protein is actually the δ-subunit of the *P. furiosus* enzyme 2-ketoisovalerate ferredoxin oxidoreductase (VOR, see below), a protein that also contains two [4Fe-4S] centers (see (41)). Interestingly, although *sipA* and *sipB* are side by side, they are transcribed in opposite directions. Figure 3.3 shows a detailed analysis of putative transcriptional and ribosomal binding sites for *sipA* and *sipB* and these strongly suggest that both genes are expressed from a shared promoter domain, as previously shown for the genes encoding β-glucosidase and alcohol dehydrogenase of *P. furiosus* (73). Homologs of *sipA* and *sipB* are present in the genomes of the S°-reducing *Pyrococcus* species, *P. abyssi* (PAB1692 and PAB0578) and

P. horikoshii (PH1227 and PH0982) but their genes are not arranged back to back like they are in *P. furiosus* and SipB is much larger (by ~15 kDa) in these other two species. In *P. furiosus*, this SipB 15 kDa extension is encoded by a separate ORF (1873389) that is adjacent to *sipB* (see Fig 3.3). The product of ORF 1873389 shows no significant sequence similarity to any characterized protein. This ORF was included in the microarray analyses but it is not expressed above the detection limit when cells were grown with or without S° (Table 3.4). This difference in genome arrangement amongst the *Pyrococcus* species might be related to the ability of *P. furiosus*, but not *P. abyssi* and *P. horikoshii*, to grow in the absence of S°.

Considering the tight regulation of *sipA* and *sipB* by S° and the likely electron transfer ability of SipB, it seems reasonable to suggest that SipA and SipB form part of a membrane-associated complex that directly reduces S° to H_2S. Two of the other ORFs listed in Table 3.2 that are strongly up-regulated by S°, ORFs 1131551 and 102519, may also be directly involved in S° reduction as both show sequence similarity to the disulfide oxidoreductase family of enzymes. ORF 1131551 is annotated as NADH oxidase (*noxA-2*) and would encode a 49 kDa cytoplasmic protein that shows significant sequence similarity to NADH peroxidase, a flavoprotein with an active site cysteine (65). ORF 102519 is predicted to encode a 26 kDa cytoplasmic protein that contains four Cys residues (as two -CxxC- motifs). Both ORFs are expressed at near the detection limit in the absence of S° but increase to the 'highly-expressed' category (more than 10-fold the detection limit, see below) in S°-grown cells, and neither appears to be part of an operon. Homologs of both ORFs are also present in *P. abyssi* (PAB0936 and PAB2245) and *P. horikoshii* (PH0572 and PH0178).

Two of the other S°-induced proteins that might be related to S° metabolism are ORF 1805557, which is annotated as a conserved hypothetical protein, and ORF 1352727, which is annotated as a NADH dehydrogenase (Table 3.2). The expression of ORF 1805557 changes from below the detection limit to twice the detection limit when cells are grown with S°. This ORF would encode a 27 kDa cytoplasmic protein where the N-terminal part has high sequence similarity to ATP/GTP-binding proteins (13), while the C-terminal half contains six Cys residues including a CxxCxxxC motif. ORF 1352727 is part of a putative operon containing 13 ORFs, most of which have homology to membrane-bound NADH dehydrogenases. Hagen and coworkers suggested that this operon encodes a (fourth) hydrogenase system in *P. furiosus* (63), but this seems unlikely in view of the up-regulation of ORF 1352727 by S° and the corresponding dramatic decrease in membrane-associated hydrogenase activity (1). Moreover, two other ORFs (1350388 and 1359534) in this putative operon were included in the microarray analysis and these are also up-regulated by S° (3 and 4-fold, data not shown). It is tempting to postulate that ORFs 1805557 and 1352727 (and possibly other ORFs in the putative operon) are involved in nucleotide binding and electron transfer during S° reduction, although further evidence is obviously required to substantiate this.

Four of the remaining six ORFs that are up-regulated more than five-fold by S° (Table 3.2) appear to encode proteins that are involved in amino acid metabolism. These are annotated as an oligopeptide permease (ORF 204761), acetolactate synthase (which is involved in the biosynthesis of branched chain amino acids; ORF 900019), and as subunits of aspartokinase (ORF 1008251) and tryptophan synthase (ORF 1487371)**.** Although all are putative proteins at present, these data support the relationship between S° and amino acid metabolism that was recently established by growth studies of *P.*

furiosus, in which it was shown that peptides can only serve as the primary carbon source if S° is present (1). All four of these ORFs are expressed at significant levels in the absence of S° (more than twice the detection limit), but all four fall into the highly-expressed category (more that 10-fold the detection limit, see below) in S°-grown cells. Of the other two up-regulated ORFs in Table 3.2, one is annotated as the thermosome (ORF 1825269). This protein is highly conserved in archaea and is a type II chaperonin, a class that also includes the eukaryotic TCP-1(CCT) proteins (7). The thermosome is expressed at about twice the detection limit in the absence of S°, although why its expression should increase about 7-fold in the presence of S° is not clear.

The other S°-responsive ORF in Table 3.2 is annotated as a fibrillarin-like protein (ORF 62257). It shows more than 50% sequence identity to a key eukaryotic nucleolar protein that associates with small nucleolar RNAs (snoRNAs) directing 2'-O-ribose methylation of the rRNA. Homologs of fibrillarin and some its associated proteins, such as Nop56/58, as well as snoRNAs, have only recently been identified in archaea although their function in these organisms is not clear (16, 33, 44, 45, 47). In *P. furiosus*, the ORF encoding the fibrillarin homolog is directly adjacent to a homolog of Nop56/58 (ORF 66216). The microarray data indicate that these ORFs are expressed at twice and six-times the detection limit, respectively, in the absence of S°, but their expression increases a further 6- and 3-fold, respectively, when S° is present. Indeed, the microarray experiment included two copies of the ORF encoding the fibrillarin homolog and both gave remarkably similar results using RNA from cells grown with (intensity of 22,237 ± 1074, see Fig. 3.1B) and without S° (3590 ± 185). *P. furiosus* also contains five homologs of a family of RNA m^5C methyl transferases (53) and four were included in the microarray analysis (ORFs 1191037; 674979; 179810; 1197174). All of them are

annotated as a nucleolar NOL1-NOP2-sun family protein but none appear to be regulated by S°. Thus, it is not obvious why S° should cause the genes encoding homologs of eukaryotic nucleolar rRNA processing proteins to be expressed at such high levels. Fibrillarin is also found in archaea that do not metabolize S° such as methanogens (20), so this protein must have a more general role, but one that is associated with S° metabolism, at least in *P. furiosus*.

Sulfur independent ORFs. In the preceding discussion we have considered all 33 of the 271 ORFs that show more than a 5-fold change in expression when cells are grown in the presence of S°. In addition to these 33, there are 84 ORFs that show between a 2 and 5-fold response to S° (data not shown). At this point further comment on the nature and function of these ORFs seems premature as there are no obvious trends and corroborating experimental data are required. That leaves 154 of the 271 ORFs remaining that show little if any response to S° (less than 2-fold) and these can be separated into three groups. They are a) 20 ORFs that appear to be the most highly expressed, where the transcripts are at more than 10-times the detection level (> 20,000 intensity units, see Fig. 3.1B), b) 34 ORFs that appear to be poorly expressed, if at all, where the transcripts are below the detection level (< 2,000 intensity units), and c) 100 ORFs that appear to be moderately expressed (2,000 - 20,000 intensity units). It should be noted that relative signal intensities do not necessarily correlate with the degrees of expression of different ORFs because intensity depends on many factors, including PCR product size and efficiencies of labeling and hybridization. However, the following shows that there may be some merit in this general assumption.

As discussed above, it was anticipated that S° reduction by *P. furiosus* would involve Mo- or W-containing proteins, analogous to the situation in mesophilic S°-reducers. For example, the polysulfide (sulfur) reductase of the mesophilic bacterium, *Wolinella succinogenes* is a molybdoenzyme (32). Consequently, the microarray for *P. furiosus* included numerous ORFs involved in the metabolism of these metals, as well as putative molybdo- and tungstoenyzmes. In fact, the genome contains two ORFs (1175771 and 1419794) that show sequence similarity to members of the ubiquitous molybdenum-containing family of enzymes (22). However, both ORFs are expressed either below or close to the detection limit and show no response to the presence of S° (data not shown). In addition, *P. furiosus* appears to contain five distinct tungstoenzymes. Three of them have been purified and characterized (abbreviated AOR, GAPOR and FOR, encoded by ORFs 356987, 478142 and 1145403, respectively) and two are putative (WOR4 and WOR5, encoded by ORFs 1812948 and 1385199, respectively; see (58)). FOR, GAPOR and AOR are in the highly expressed category (above 10-fold detection limit, see Table 3.3), while WOR4 and WOR5 are moderately expressed and are only slightly up-regulated in the presence of S° (data not shown). Similarly, *P. furiosus* contains several ORFs that would encode homologs of proteins involved in the biosynthesis of pterin (designated *moa, mob* and *moe,* see (52)), the cofactor that binds the Mo and W in molybdo- and tungstoenzymes. None of these ORFs showed any significant changes in expression when cells were grown with S°, with the exception of ORF 1805557, discussed above. In light of these data, it is concluded that S° reduction in *P. furiosus* does not involve Mo-, W- or pterin-containing proteins, or at least those that can be identified by sequence similarity to known proteins of this type.

Some comment is also necessary on the nature of the proteins encoded by the ORFs that are designated as either poorly or highly-expressed. For example, the ORF with the highest intensity on the microarray (~ 23-times the detection limit) encodes phosphoenolpyruvate synthase (*ppsA*). This enzyme was recently purified from *P. furiosus* and was shown to be present at extremely high cellular concentrations (24), consistent with the highly-expressed connotation. In fact, of the 20 ORFs that show the highest intensities on the microarray (more than 10-times the detection limit, see Table 3.3), 12 of them encode proteins that have been purified from *P. furiosus.* The biochemical data therefore supports the notion that, in general, these ORFs encode proteins that are indeed present at relatively high cellular concentrations, and that signal intensity is a reasonable measure of this. Further evidence for this qualitative relationship comes from the 34 ORFs that are in the poorly-expressed category, as none of the proteins that they are proposed to encode have been characterized from *P. furiosus*, see Table 3.4 (although one, encoding a putative phosphoglycerate kinase, has been cloned and expressed from the related organism, *P.* woesei; (10)). Of the 100 (of 271) ORFs that are in the moderately-expressed category, the products of 12 of them have been characterized (data not shown).

Four of the highly-expressed ORFs listed in Table 3.3 encode the two α- and the two β-subunits of two closely-related, heterotetrameric enzymes, pyruvate ferredoxin oxidoreductase (POR, (6) and 2-ketoisovalerate ferredoxin oxidoreductase (VOR, (19). Both of these enzymes have been purified from *P. furiosus.* The genes encoding them form three adjacent operons, in which the third is a common gene encoding their γ subunits (31). The gene arrangement and their transcript intensities in cells with and without S° are shown in Fig. 3.4. Although the 2-fold difference in expression of *porG* is

statistically significant ($p > 0.95$), S° does not dramatically affect the expression of POR and accordingly the specific activity of POR is comparable in the two cell types (1). Moreover, while the apparent amounts of the mRNA species encoding the two α- and the two β-subunits are consistent with the high cellular concentrations of the enzymes (1, 6, 19), this is not true for the other subunits and particular for the ORF encoding the δ-subunit of VOR, which is barely above the detection limit. How these three operons are regulated such that they produce two functional enzymes at high cellular concentrations and with a common subunit is not clear from the transcript levels measured using the DNA microarray. Thus, while there may be some overall relationship between transcript intensities on the microarray slide and cellular concentration, that encoding the δ-subunit of VOR is a notable exception. On the other hand, the biochemical and electrophoretic data strongly support the dramatic down-regulation of the expression of the three hydrogenases by S°, and the dramatic up-regulation of at least one of the 'conserved hypothetical' ORFs (*sipA*) that are now proposed to form a new type of S°-responsive complex. Further analyses of this type are now required to determine the nature of this complex, whether it is directly involved in S° reduction, and the nature of the effector molecule that mediates the S° response.

ACKNOWLEDGEMENTS

This research was funded by grants to MWWA from the National Institutes of Health (GM 60329), the National Science Foundation (MCB 9904624, MCB 9809060, and BES-0004257) and the Department of Energy (FG05-95ER20175 and contract 992732401 with Argonne National Laboratory), and to JZ from the Department of Energy

under the Microbial Genome Program and the Natural and Accelerated Bioremediation Research Program of the Office of Biological and Environmental Research. Oak Ridge National Laboratory is managed by the University of Tennessee-Battelle LLC for the Department of Energy under contract DE-AC05-00OR22725. We thank Gary Li, Scott Lee and Marc Sudman for their help in preparing the microarray slides, F. Robb and R. Weiss for making the *P. furiosus* sequence available prior to publication, and Frank E. Jenney, Jr., Angeli Lal Menon, James F. Holden, Eleanor Green and Rajat Sapra for many helpful discussions.

REFERENCES

1. **Adams, M. W. W., J. F. Holden, A. L. Menon, G. J. Schut, A. M. Grunden, C. Hou, A. M. Hutchins, F. E. Jenney, Jr., C. Kim, K. Ma, G. Pan, R. Roy, R. Sapra, S. V. Story, and M. F. Verhagen.** 2001. Key role for sulfur in peptide metabolism and in regulation of three hydrogenases in the hyperthermophilic archaeon *Pyrococcus furiosus*. J. Bacteriol. **183:**716-724.

2. **Arfin, S. M., A. D. Long, E. T. Ito, L. Tolleri, M. M. Riehle, E. S. Paegle, and G. W. Hatfield.** 2000. Global gene expression profiling in *Escherichia coli* K12. The effects of integration host factor. J. Biol. Chem. **275:**29672-29684.

3. **Barbier, G., A. Godfroy, J. R. Meunier, J. Querellou, M. A. Cambon, F. Lesongeur, P. A. Grimont, and G. Raguenes.** 1999. *Pyrococcus glycovorans* sp. nov., a hyperthermophilic archaeon isolated from the East Pacific Rise. Int. J. Syst. Bacteriol. **49 Pt 4:**1829-1837.

4. **Blamey, J., M. Chiong, C. Lopez, and E. Smith.** 1999. Optimization of the growth conditions of the extremely thermophilic microorganisms *Thermococcus celer* and *Pyrococcus woesei*. J. Microbiol. Methods **38:**169-175.

5. **Blamey, J. M., and M. W. W. Adams.** 1994. Characterization of an ancestral type of pyruvate ferredoxin oxidoreductase from the hyperthermophilic bacterium, *Thermotoga maritima*. Biochemistry **33:**1000-1007.

6. **Blamey, J. M., and M. W. W. Adams.** 1993. Purification and characterization of pyruvate ferredoxin oxidoreductase from the hyperthermophilic archaeon *Pyrococcus furiosus*. Biochim. Biophys. Acta **1161:**19-27.

7. **Bosch, G., W. Baumeister, and L. O. Essen.** 2000. Crystal structure of the beta-apical domain of the thermosome reveals structural plasticity in the protrusion region. J. Mol. Biol. **301:**19-25.

8. **Brown, P. O., and D. Botstein.** 1999. Exploring the new world of the genome with DNA microarrays. Nat. Genet. **21:**33-37.

9. **Bryant, F. O., and M. W. W. Adams.** 1989. Characterization of hydrogenase from the hyperthermophilic archaebacterium, *Pyrococcus furiosus*. J. Biol. Chem. **264:**5070-5079.

10. **Crowhurst, G., J. McHarg, and J. A. Littlechild.** 2001. Phosphoglycerate kinases from bacteria and archaea. Methods Enzymol. **331:**90-104.

11. **de Saizieu, A., U. Certa, J. Warrington, C. Gray, W. Keck, and J. Mous.** 1998. Bacterial transcript imaging by hybridization of total RNA to oligonucleotide arrays. Nat. Biotechnol. **16:**45-48.

12. **Duggan, D. J., M. Bittner, Y. Chen, P. Meltzer, and J. M. Trent.** 1999. Expression profiling using cDNA microarrays. Nat. Genet. **21:**10-14.

13. **Eaves, D. J., T. Palmer, and D. H. Boxer.** 1997. The product of the molybdenum cofactor gene mobB of *Escherichia coli* is a GTP-binding protein. Eur. J. Biochem. **246:**690-697.

14. **Edman, C. F., P. Mehta, R. Press, C. A. Spargo, G. T. Walker, and M. Nerenberg.** 2000. Pathogen analysis and genetic predisposition testing using microelectronic arrays and isothermal amplification. J. Investig. Med. **48:**93-101.

15. **Fiala, G., and K. O. Stetter.** 1986. *Pyrococcus furiosus* sp. nov. represents a novel genus of marine heterotrophic archaebacteria growing optimally at 100 °C. Arch. Microbiol. **145:**56-61.

16. **Gaspin, C., J. Cavaille, G. Erauso, and J. P. Bachellerie.** 2000. Archaeal homologs of eukaryotic methylation guide small nucleolar RNAs: lessons from the *Pyrococcus* genomes. J. Mol. Biol. **297:**895-906.

17. **Gingeras, T. R., G. Ghandour, E. Wang, A. Berno, P. M. Small, F. Drobniewski, D. Alland, E. Desmond, M. Holodniy, and J. Drenkow.** 1998. Simultaneous genotyping and species identification using hybridization pattern recognition analysis of generic *Mycobacterium* DNA arrays. Genome Res. **8:**435-448.

18. **Halio, S. B., I. I. Blumentals, S. A. Short, B. M. Merrill, and R. M. Kelly.** 1996. Sequence, expression in *Escherichia coli*, and analysis of the gene encoding a novel intracellular protease (PfpI) from the hyperthermophilic archaeon *Pyrococcus furiosus*. J. Bacteriol. **178:**2605-2612.

19. **Heider, J., X. Mai, and M. W. W. Adams.** 1996. Characterization of 2-ketoisovalerate ferredoxin oxidoreductase, a new and reversible coenzyme A-dependent enzyme involved in peptide fermentation by hyperthermophilic archaea. J. Bacteriol. **178:**780-787.

20. **Hickey, A. J., A. J. Macario, and E. Conway de Macario.** 2000. Identification of genes in the genome of the archaeon *Methanosarcina mazeii* that code for homologs of nuclear eukaryotic molecules involved in RNA processing. Gene **253:**77-85.

21. **Hihara, Y., A. Kamei, M. Kanehisa, A. Kaplan, and M. Ikeuchi.** 2001. DNA microarray analysis of cyanobacterial gene expression during acclimation to high light. Plant Cell **13:**793-806.

22. **Hille, R.** 1996. The mononuclear molybdenum enzymes. Chem. Rev. **96:**2757-2816.

23. **Holden, J. F., F.L., Poole, S. L. Tollaksen, C. S. Giometti, H. Lim, J. R. Yates, and M. W. W. Adams.** 2001. Identification of membrane proteins in the hyperthermophilic archaeon *Pyrococcus furiosus* using proteomics and prediction programs. Comp. Funct. Genomics **in press**.

24. **Hutchins, A. M., J. F. Holden, and M. W. Adams.** 2001. Phosphoenolpyruvate synthetase from the hyperthermophilic archaeon *Pyrococcus furiosus*. J. Bacteriol. **183:**709-715.

25. **Jacobi, A., R. Rossmann, and A. Bock.** 1992. The hyp operon gene products are required for the maturation of catalytically active hydrogenase isoenzymes in *Escherichia coli*. Arch. Microbiol. **158:**444-451.

26. **Jia, M. H., R. A. Larossa, J. M. Lee, A. Rafalski, E. Derose, G. Gonye, and Z. Xue.** 2000. Global expression profiling of yeast treated with an inhibitor of amino acid biosynthesis, sulfometuron methyl. Physiol. Genomics **3:**83-92.

27. **Johnson, M. K., D. C. Rees, and M. W. W. Adams.** 1996. Tungstoenzymes. Chem. Rev. **96:**2817-2839.

28. **Kawarabayasi, Y., M. Sawada, H. Horikawa, Y. Haikawa, Y. Hino, S. Yamamoto, M. Sekine, S. Baba, H. Kosugi, A. Hosoyama, Y. Nagai, M. Sakai, K. Ogura, R. Otsuka, H. Nakazawa, M. Takamiya, Y. Ohfuku, T. Funahashi, T. Tanaka, Y. Kudoh, J. Yamazaki, N. Kushida, A. Oguchi, K. Aoki, and H. Kikuchi.** 1998. Complete sequence and gene organization of the genome of a hyper-thermophilic archaebacterium, *Pyrococcus horikoshii* OT3 (supplement). DNA Res. **5:**147-155.

29. **Kengen, S. W., J. E. Tuininga, F. A. de Bok, A. J. Stams, and W. M. de Vos.** 1995. Purification and characterization of a novel ADP-dependent glucokinase from the hyperthermophilic archaeon *Pyrococcus furiosus*. J. Biol. Chem. **270:**30453-30457.

30. **Khodursky, A. B., B. J. Peter, N. R. Cozzarelli, D. Botstein, P. O. Brown, and C. Yanofsky.** 2000. DNA microarray analysis of gene expression in response to physiological and genetic changes that affect tryptophan metabolism in *Escherichia coli*. Proc. Natl. Acad. Sci. USA **97:**12170-12175.

31. **Kletzin, A., and M. W. W. Adams.** 1996. Molecular and phylogenetic characterization of pyruvate and 2-ketoisovalerate ferredoxin oxidoreductases from *Pyrococcus furiosus* and pyruvate ferredoxin oxidoreductase from *Thermotoga maritima*. J. Bacteriol. **178:**248-257.

32. **Krafft, T., R. Gross, and A. Kroger.** 1995. The function of *Wolinella succinogenes psr* genes in electron transport with polysulphide as the terminal electron acceptor. Eur. J. Biochem. **230:**601-606.

33. **Lafontaine, D. L., and D. Tollervey.** 1998. Birth of the snoRNPs: the evolution of the modification-guide snoRNAs. Trends Biochem. Sci. **23:**383-388.

34. **Lee, H., G. H. Greeley, and E. W. Englander.** 2001. Age-associated changes in gene expression patterns in the duodenum and colon of rats. Mech. Ageing Dev. **122:**355-371.

35. **Legrain, C., V. Stalon, J. P. Noullez, A. Mercenier, J. P. Simon, K. Broman, and J. M. Wiame.** 1977. Structure and function of ornithine carbamoyltransferases. Eur. J. Biochem. **80:**401-409.

36. **Legrain, C., V. Villeret, M. Roovers, D. Gigot, O. Dideberg, A. Pierard, and N. Glansdorff.** 1997. Biochemical characterisation of ornithine carbamoyltransferase from *Pyrococcus furiosus*. Eur. J. Biochem. **247:**1046-1055.

37. **Ma, K., R. N. Schicho, R. M. Kelly, and M. W. W. Adams.** 1993. Hydrogenase of the hyperthermophile *Pyrococcus furiosus* is an elemental sulfur reductase or sulfhydrogenase: evidence for a sulfur-reducing hydrogenase ancestor. Proc. Natl. Acad. Sci. USA **90:**5341-5344.

38. **Ma, K., R. Weiss, and M. W. W. Adams.** 2000. Characterization of hydrogenase II from the hyperthermophilic archaeon *Pyrococcus furiosus* and assessment of its role in sulfur reduction. J. Bacteriol. **182:**1864-1871.

39. **Mai, X., and M. W. W. Adams.** 1994. Indolepyruvate ferredoxin oxidoreductase from the hyperthermophilic archaeon *Pyrococcus furiosus*. A new enzyme involved in peptide fermentation. J. Biol. Chem. **269:**16726-16732.

40. **Mai, X. H., and M. W. W. Adams.** 1996. Purification and characterization of two reversible and ADP-dependent acetyl coenzyme-A synthetases from the hyperthermophilic archaeon *Pyrococcus furiosus*. J. Bacteriol. **178:**5897-5903.

41. **Menon, A. L., H. Hendrix, A. Hutchins, M. F. J. M. Verhagen, and M. W. W. Adams.** 1998. The delta-subunit of pyruvate ferredoxin oxidoreductase from *Pyrococcus furiosus* is a redox-active, iron-sulfur protein: evidence for an ancestral relationship with 8Fe-type ferredoxins. Biochemistry **37:**12838-12846.

42. **Mukund, S., and M. W. W. Adams.** 1995. Glyceraldehyde-3-phosphate ferredoxin oxidoreductase, a novel tungsten-containing enzyme with a potential glycolytic role in the hyperthermophilic archaeon *Pyrococcus furiosus*. J. Biol. Chem. **270:**8389-8392.

43. **Mukund, S., and M. W. W. Adams.** 1991. The novel tungsten-iron-sulfur protein of the hyperthermophilic archaebacterium, *Pyrococcus furiosus*, is an aldehyde ferredoxin oxidoreductase. Evidence for its participation in a unique glycolytic pathway. J. Biol. Chem. **266:**14208-14216.

44. **Newman, D. R., J. F. Kuhn, G. M. Shanab, and E. S. Maxwell.** 2000. Box C/D snoRNA-associated proteins: two pairs of evolutionarily ancient proteins and possible links to replication and transcription. RNA **6:**861-879.

45. **Noon, K. R., E. Bruenger, and J. A. McCloskey.** 1998. Posttranscriptional modifications in 16S and 23S rRNAs of the archaeal hyperthermophile *Sulfolobus solfataricus*. J. Bacteriol. **180:**2883-2888.

46. **Oh, M. K., and J. C. Liao.** 2000. Gene expression profiling by DNA microarrays and metabolic fluxes in *Escherichia coli*. Biotechnol. Prog. **16:**278-286.

47. **Omer, A. D., T. M. Lowe, A. G. Russell, H. Ebhardt, S. R. Eddy, and P. P. Dennis.** 2000. Homologs of small nucleolar RNAs in Archaea. Science **288:**517-522.

48. **Paschos, A., R. S. Glass, and A. Bock.** 2001. Carbamoyl phosphate requirement for synthesis of the active center of [NiFe]-hydrogenases. FEBS Lett. **488:**9-12.

49. **Peak, M. J., J. G. Peak, F. J. Stevens, J. Blamey, X. Mai, Z. H. Zhou, and M. W. W. Adams.** 1994. The hyperthermophilic glycolytic enzyme enolase in the archaeon, *Pyrococcus furiousus* - comparison with mesophilic enolases. Arch. Biochem. Biophys. **313:**280-286.

50. **Pedroni, P., A. Della Volpe, G. Galli, G. M. Mura, C. Pratesi, and G. Grandi.** 1995. Characterization of the locus encoding the [Ni-Fe] sulfhydrogenase from the archaeon *Pyrococcus furiosus*: evidence for a relationship to bacterial sulfite reductases. Microbiology **141:**449-458.

51. **Prieur, D., P. Forterre, J.-C. Thierry, and J. Dietrich.** 1999. Complete genome sequence of *Pyrococcus abyssi*. http://www.genoscope.cns.fr/Pab/.

52. **Rajagopalan, K. V.** 1997. Biosynthesis and processing of the molybdenum cofactors. Biochem. Soc. Trans. **25:**757-761.

53. **Reid, R., P. J. Greene, and D. V. Santi.** 1999. Exposition of a family of RNA m(5)C methyltransferases from searching genomic and proteomic sequences. Nucleic Acids Res. **27:**3138-3145.

54. **Richmond, C. S., J. D. Glasner, R. Mau, H. Jin, and F. R. Blattner.** 1999. Genome-wide expression profiling in *Escherichia coli* K-12. Nucleic Acids Res. **27:**3821-3835.

55. **Robb, F. T., D. L. Maeder, J. R. Brown, J. DiRuggiero, M. D. Stump, R. K. Yeh, R. B. Weiss, and D. M. Dunn.** 2001. Genomic sequence of hyperthermophile, *Pyrococcus furiosus*: implications for physiology and enzymology. Methods Enzymol. **330:**134-157.

56. **Robb, F. T., J. B. Park, and M. W. W. Adams.** 1992. Characterization of an extremely thermostable glutamate dehydrogenase - a key enzyme in the primary metabolism of the hyperthermophilic archaebacterium, *Pyrococcus furiosus*. Biochim. Biophys. Acta **1120:**267-272.

57. **Ross, D. T., U. Scherf, M. B. Eisen, C. M. Perou, C. Rees, P. Spellman, V. Iyer, S. S. Jeffrey, M. Van de Rijn, M. Waltham, A. Pergamenschikov, J. C. Lee, D. Lashkari, D. Shalon, T. G. Myers, J. N. Weinstein, D. Botstein, and P. O. Brown.** 2000. Systematic variation in gene expression patterns in human cancer cell lines. Nat. Genet. **24:**227-235.

58. **Roy, R., A. L. Menon, and M. W. Adams.** 2001. Aldehyde oxidoreductases from *Pyrococcus furiosus*. Methods Enzymol. **331:**132-144.

59. **Salama, N., K. Guillemin, T. K. McDaniel, G. Sherlock, L. Tompkins, and S. Falkow.** 2000. A whole-genome microarray reveals genetic diversity among *Helicobacter pylori* strains. Proc. Natl. Acad. Sci. USA **97:**14668-14673.

60. **Sapra, R., M. F. Verhagen, and M. W. W. Adams.** 2000. Purification and characterization of a membrane-bound hydrogenase from the hyperthermophilic archaeon *Pyrococcus furiosus*. J. Bacteriol. **182:**3423-3428.

61. **Schena, M., D. Shalon, R. W. Davis, and P. O. Brown.** 1995. Quantitative monitoring of gene expression patterns with a complementary DNA microarray. Science **270:**467-470.

62. **Schönheit, P., and T. Schäfer.** 1995. Metabolism of hyperthermophiles. World J. Microbiol. Biotech. **11:**26-57.

63. **Silva, P. J., E. C. van den Ban, H. Wassink, H. Haaker, B. de Castro, F. T. Robb, and W. R. Hagen.** 2000. Enzymes of hydrogen metabolism in *Pyrococcus furiosus*. Eur. J. Biochem. **267:**6541-6551.

64. **Staudt, L. M., and P. O. Brown.** 2000. Genomic views of the immune system. Annu. Rev. Immunol. **18:**829-859.

65. **Stehle, T., S. A. Ahmed, A. Claiborne, and G. E. Schulz.** 1991. Structure of NADH peroxidase from *Streptococcus faecalis* 10C1 refined at 2.16 Å resolution. J. Mol. Biol. **221:**1325-1344.

66. **Stetter, K. O.** 1999. Extremophiles and their adaptation to hot environments. FEBS Lett. **452:**22-25.

67. **Stetter, K. O.** 1996. Hyperthermophilic procaryotes. Fems Microbiol. Rev. **18:**149-158.

68. **Talaat, A. M., P. Hunter, and S. A. Johnston.** 2000. Genome-directed primers for selective labeling of bacterial transcripts for DNA microarray analysis. Nat. Biotechnol. **18:**679-682.

69. **Tuininga, J. E., C. H. Verhees, J. van der Oost, S. W. Kengen, A. J. Stams, and W. M. de Vos.** 1999. Molecular and biochemical characterization of the ADP-dependent phosphofructokinase from the hyperthermophilic archaeon *Pyrococcus furiosus*. J. Biol. Chem. **274:**21023-21028.

70. **van der Oost, J., G. Schut, S. W. Kengen, W. R. Hagen, M. Thomm, and W. M. de Vos.** 1998. The ferredoxin-dependent conversion of glyceraldehyde-3-phosphate in the hyperthermophilic archaeon *Pyrococcus furiosus* represents a novel site of glycolytic regulation. J. Biol. Chem. **273:**28149-28154.

71. **Villeret, V., B. Clantin, C. Tricot, C. Legrain, M. Roovers, V. Stalon, N. Glansdorff, and J. Van Beeumen.** 1998. The crystal structure of *Pyrococcus furiosus* ornithine carbamoyltransferase reveals a key role for oligomerization in enzyme stability at extremely high temperatures. Proc. Natl. Acad. Sci. USA **95:**2801-2806.

72. **Voorhorst, W. G., R. I. Eggen, E. J. Luesink, and W. M. de Vos.** 1995. Characterization of the *celB* gene coding for beta-glucosidase from the hyperthermophilic archaeon *Pyrococcus furiosus* and its expression and site-directed mutation in *Escherichia coli*. J. Bacteriol. **177:**7105-7111.

73. **Voorhorst, W. G., Y. Gueguen, A. C. Geerling, G. Schut, I. Dahlke, M. Thomm, J. van der Oost, and W. M. de Vos.** 1999. Transcriptional regulation in the hyperthermophilic archaeon *Pyrococcus furiosus*: coordinated expression of divergently oriented genes in response to beta-linked glucose polymers. J. Bacteriol. **181:**3777-3783.

74. **Wei, Y., J. M. Lee, C. Richmond, F. R. Blattner, J. A. Rafalski, and R. A. LaRossa.** 2001. High-density microarray-mediated gene expression profiling of *Escherichia coli*. J. Bacteriol. **183:**545-556.

75. **Wilson, M., J. DeRisi, H. H. Kristensen, P. Imboden, S. Rane, P. O. Brown, and G. K. Schoolnik.** 1999. Exploring drug-induced alterations in gene expression in *Mycobacterium tuberculosis* by microarray hybridization. Proc. Natl. Acad. Sci. USA **96:**12833-12838.

76. **Wolf, I., T. Buhrke, J. Dernedde, A. Pohlmann, and B. Friedrich.** 1998. Duplication of hyp genes involved in maturation of [NiFe] hydrogenases in A*lcaligenes eutrophus* H16. Arch. Microbiol. **170:**451-459.

77. **Ye, R. W., W. Tao, L. Bedzyk, T. Young, M. Chen, and L. Li.** 2000. Global gene expression profiles of *Bacillus subtilis* grown under anaerobic conditions. J. Bacteriol. **182:**4458-4465.

78. **Yeh, A. P., Y. Hu, F. E. Jenney, Jr., M. W. W. Adams, and D. C. Rees.** 2000. Structures of the superoxide reductase from *Pyrococcus furiosus* in the oxidized and reduced states. Biochemistry **39:**2499-2508.

79. **Yoshida, K., K. Kobayashi, Y. Miwa, C. M. Kang, M. Matsunaga, H. Yamaguchi, S. Tojo, M. Yamamoto, R. Nishi, N. Ogasawara, T. Nakayama, and Y. Fujita.** 2001. Combined transcriptome and proteome analysis as a powerful approach to study genes under glucose repression in *Bacillus subtilis*. Nucleic Acids Res. **29:**683-692.

80. **Zimmer, D. P., E. Soupene, H. L. Lee, V. F. Wendisch, A. B. Khodursky, B. J. Peter, R. A. Bender, and S. Kustu.** 2000. Nitrogen regulatory protein C-controlled genes of *Escherichia coli*: scavenging as a defense against nitrogen limitation. Proc. Natl. Acad. Sci. USA **97:**14674-14679.

Table 3.1. ORFs whose expression is dramatically (> 5-fold) down-regulated by S°.

ORF[a]	ORF description[b]	Mean intensity Ratio ($log_2 \pm SD$)[c]	Change in expression (fold)[c]
577932	[hydrogenase expression/formation regulatory protein, *hypF*]	5.28 ± 0.89	39.0
1337916	membrane bound hydrogenase ORF 1, *mbh1*[d]	4.14 ± 0.80	17.6
1251888	hydrogenase II gamma, *hyhG2* (38)	3.78 ± 1.47	13.7
1338167	membrane bound hydrogenase ORF 2, *mbh2*[d]	3.77 ± 1.29	13.6
1339081	membrane bound hydrogenase ORF 5, *mbh5*[d]	3.68 ± 1.30	12.8
1339520	membrane bound hydrogenase ORF 6, *mbh6*[d]	3.65 ± 0.77	12.6
1253842	hydrogenase II alpha, *hyhL2* (38)	3.57 ± 1.45	11.8
1341399	membrane bound hydrogenase ORF 8 (like *cooM*, *mbh8*)[d]	3.49 ± 0.79	11.2
1338538	membrane bound hydrogenase ORF 3, *mbh3*[d]	3.31 ± 1.66	9.9
1252601	hydrogenase II delta, *hyhS2* (38)	3.25 ± 1.43	9.5
1342770	membrane bound hydrogenase ORF 11, *mbh11*[d]	3.06 ± 1.22	8.3
866528	hydrogenase I delta, *hyhS1* (37)	2.95 ± 0.66	7.7
1345018	membrane bound hydrogenase ORF 13 (like *hydC*, *cooK*, *echB*, *mbh13*)[d]	2.77 ± 0.85	6.8
1345434	membrane bound hydrogenase ORF 14 (like *hycF*, *echF*, *cooX*, *mbh14*)[d]	2.73 ± 1.40	6.6
1344050	membrane bound hydrogenase ORF 12, catalytic NiFe subunit, *mbh12* (60)	2.68 ± 0.59	6.4
864857	hydrogenase I beta, *hyhB1* (37)	2.66 ± 1.08	6.3
1251025	hydrogenase II beta, *hyhB2* (38)	2.65 ± 1.04	6.3
1342256	membrane bound hydrogenase ORF 10, small subunit homolog, *mbh10*[d]	2.59 ± 0.87	6.0
51760	[conserved hypothetical protein]	2.59 ± 1.14	6.0
1338785	membrane bound hydrogenase ORF 4, *mbh4*[d]	2.54 ± 2.16	5.8
615154	ornithine carbamoyltransferase, *argF* (36)	2.43 ± 0.49	5.4

[a]ORF designation is the end nucleotide number (55).

[b]The ORF description is derived either from annotation by homology (given within brackets) or from the indicated reference where there is experimental data to support the ORF assignment specifically in *P. furiosus* (given without brackets).
[c]The intensity ratio is expressed as a $\log_2$ value so that the standard deviation can be given. For ease of comparison between ORFs, the apparent change in the expression level of a given ORF is also indicated.
[d]This work (see text for details).

Table 3.2. ORFs whose expression is dramatically (> 5-fold) up-regulated by S°.

ORF[a]	ORF Description[a]	Intensity Ratio (log_2 ± SD) [a]	Change in expression (-fold)[a]
1871822	[conserved hypothetical protein, *sipA*[b]]	5.94 ± 1.43	61.4
1872873	[putative polyferredoxin, *sipB*[b]]	4.65 ± 1.90	25.1
1487371	[tryptophan synthase, subunit beta, *trpB-1*]	2.98 ± 0.69	7.9
1805557	[conserved hypothetical protein]	2.93 ± 1.29	7.6
1008251	[aspartokinase II alpha subunit]	2.92 ± 0.89	7.6
1131551	[NADH oxidase, *noxA-2*]	2.88 ± 0.39	7.4
1825269	[thermosome, single subunit]	2.83 ± 1.69	7.1
900019	[acetolacetate synthase]	2.78 ± 1.02	6.9
65527	[fibrillarin-like pre-rRNA processing protein]	2.70 ± 0.80	6.5
204761	[oligopeptide transport system permease protein]	2.68 ± 0.45	6.4
102519	[glutaredoxin-like protein]	2.61 ± 1.72	6.1
1352206	[NADH dehydrogenase subunit]	2.59 ± 0.59	6.0

[a]See Table 3.1 for details.
[b]See text for details.

Table 3.3. Highly-expressed S°-independent ORFs.

ORF[a]	Description[b]
49183	phosphoenolpyruvate synthetase, *ppsA* (24)
143318	[conserved hypothetical protein]
232621	enolase (2-phosphoglycerate dehydratase) (49)
236793	[hexulose-6-phosphate synthase]
358419	aldehyde ferredoxin oxidoreductase, *aor* (43)
478142	glyceraldehyde-3-phosphate ferredoxin oxidoreductase, *gor* (42)
683389	[methylmalonyl-CoA decarboxylase, subunit alpha, *mmdA*]
720985	[alkyl hydroperoxide reductase subunit C]
925374	pyruvate ferredoxin oxidoreductase beta, *porB* (6)
926380	pyruvate ferredoxin oxidoreductase alpha, *porA* (6)
927947	2-ketoisovalerate ferredoxin oxidoreductase beta, *vorB* (19)
928888	2-ketoisovalerate ferredoxin oxidoreductase subunit alpha, *vorA* (19)
1145403	formaldehyde ferredoxin oxidoreductase, *for* (58)
1208774	[LSU ribosomal protein L10]
1210188	superoxide reductase, *sor* (78)
1210814	[rubrerythrin]
1425928	[ethylene-inducible protein homolog]
1493675	glutamate dehydrogenase, *gdh* (56)
1599202	intracellular protease, *pfpI* (18)
1619038	[putative trehalose synthase]

[a]ORFs displaying average fluorescent intensities >20,000 (see Fig. 3.1B).
[b]See Table 3.1 for details

Table 3.4. Poorly-expressed S°-independent ORFs

ORF[a]	Description[b]
53135	[conserved hypothetical protein]
349245	[flagella-related protein D, putative]
350457	[conserved hypothetical protein]
350944	[flagellin B2 precursor]
351748	[flagellin B2 precursor]
373060	[ABC transporter, OppBC family]
379218	[beta-galactosidase precursor]
488057	[DNA mismatch repair protein, *MutS*]
562899	[molybdopterin converting factor, subunit 1, *moaD*]
575520	[NADH oxidase, *noxA-4*/nitrite reductase]
637268	[molybdopterin-guanine dinucleotide biosynthesis protein, *mobA*]
637303	[hydrogenase maturation protease, *hycI*]
722839	[conserved hypothetical protein]
738742	[conserved hypothetical protein]
743892	[putative proline depeptidase]
834030	[conserved hypothetical protein]
838710	[conserved hypothetical protein]
880926	[ferric enterobactin transport ATP-binding protein homolog]
881669	[iron (III) ABC transporter, permease protein, *hemU-1*]
882732	[iron (III) ABC transporter ATP-binding protein, *hemV-2*]
962748	[alkaline phosphatase IV precursor]
1012695	[phosphoglycerate kinase]
1138558	[transcriptional regulator (FurR family)
1158892	[dissimilatory sulfate adenylyl transferase]
1165967	[4-aminobutyrate aminotransferase]
1197174	[putative nucleolar protein II, Nol1-Nop2-sun family]
1208389	[conserved hypothetical protein]
1417217	[sugar-binding transport ATP-binding protein]

1647980	[2-keto acid:ferredoxin oxidoreductase subunit alpha]
1668574	[sarcosine oxidase, alpha subunit, *SoxA*]
1669077	[putative polyferredoxin, *muhB*]
1711295	[molybdenum cofactor biosynthesis protein, *moaC*]
1873595	[nitrogen reductase, N-terminus]
1873914	[ferredoxin-family protein]

[a]ORFs displaying average fluorescent intensities below 2,000 (see Fig. 3.1B).
[b]See Table 3.1 for details.

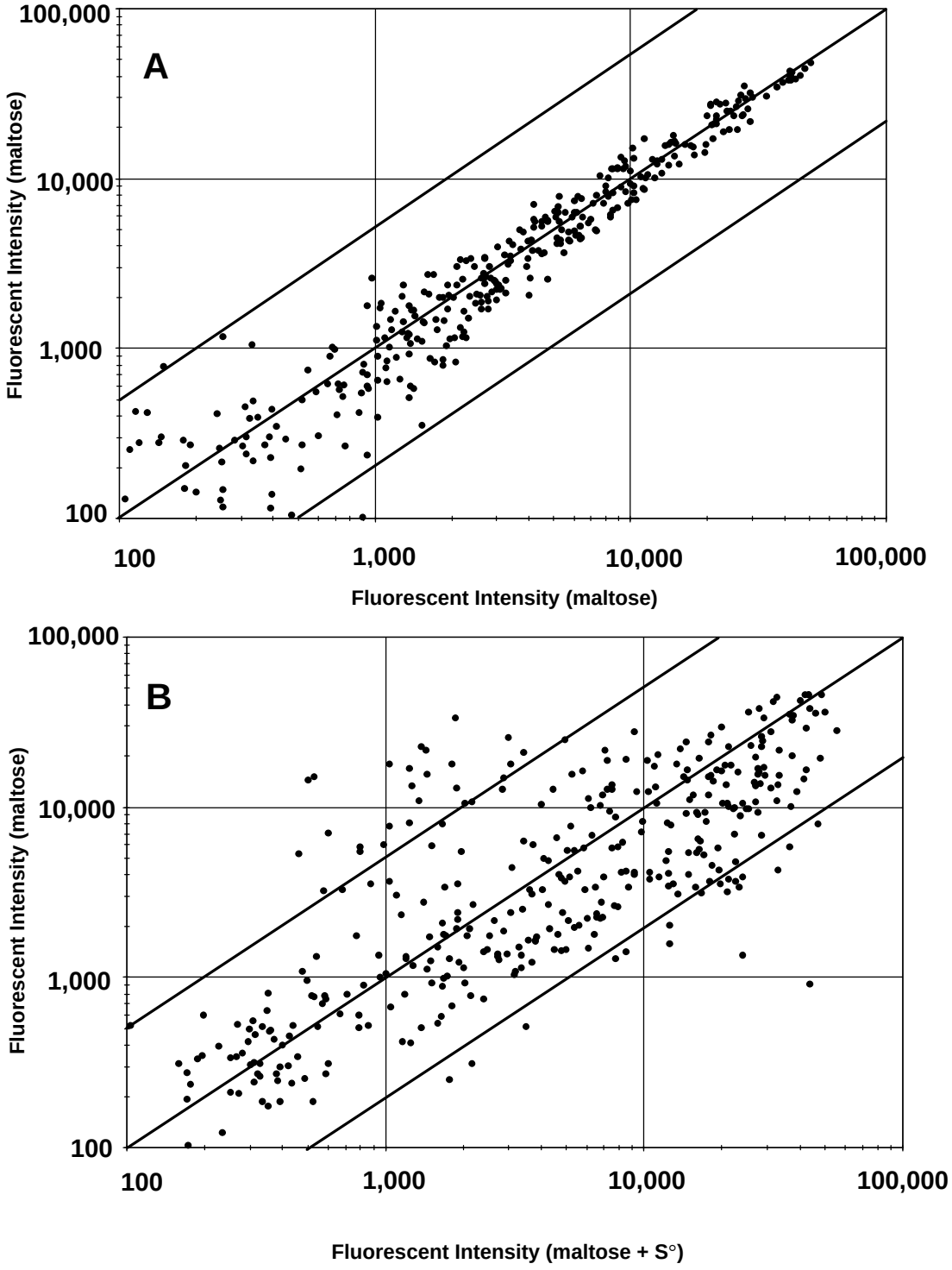

Figure 3.1. Fluorescence intensities of DNA microarrays**.** A) cDNA vs cDNA derived from the same cultures of cells grown on maltose (no S°). B) cDNA vs cDNA derived from cells grown on maltose with and without S°. The upper and lower diagonal lines indicate 5-fold changes in the signal intensities. See text for details.

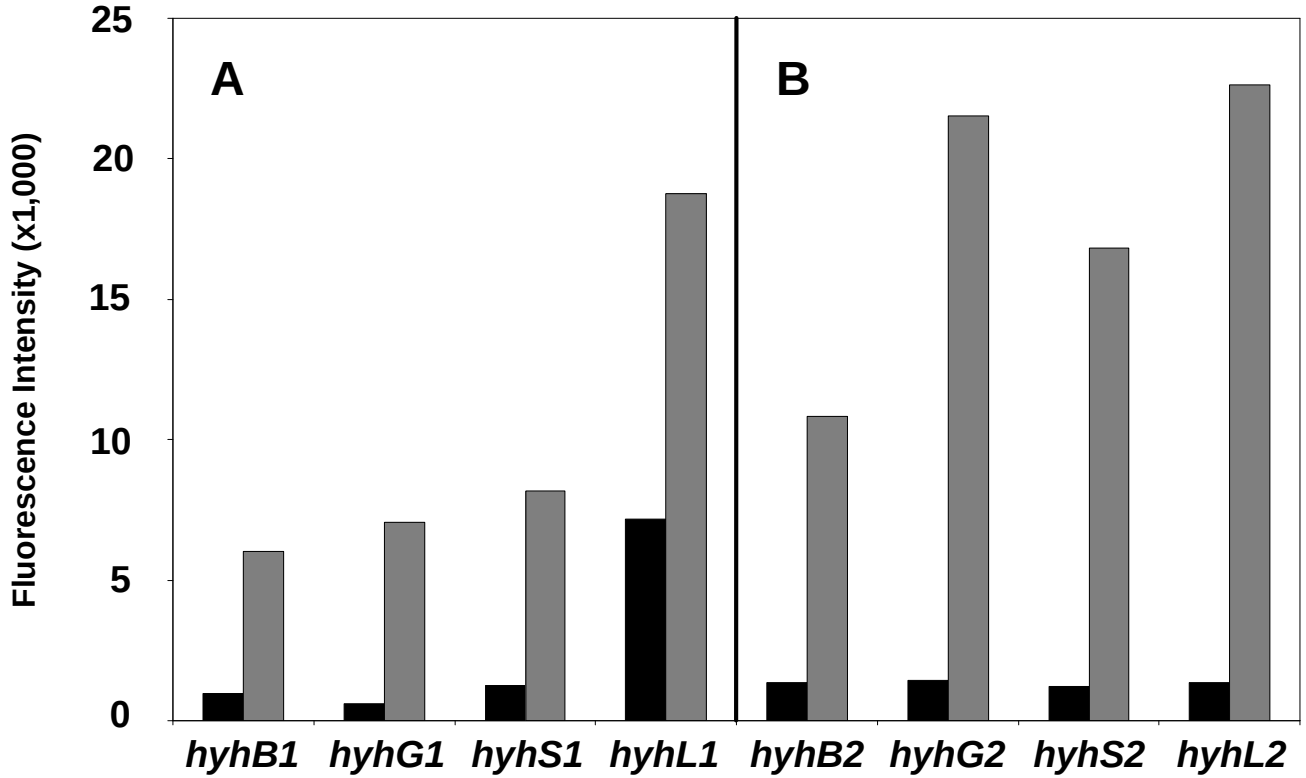

Figure 3.2. Expression of ORFs encoding hydrogenase-related subunits with and without S°. The ORFs encoding the subunits of the cytoplasmic hydrogenase I (A), cytoplasmic hydrogenase II (B) and the membrane-bound hydrogenase (C) are arranged according to their positions in their respective operons. These are plotted against signal intensities for cDNA obtained from cells grown with (solid bars) or without (shaded bars) S°. The results with all subunits have a confidence level of at least 96% ($p > 0.98$ for the cytoplasmic hydrogenases and $p > 0.96$ for the membrane-bound enzyme).

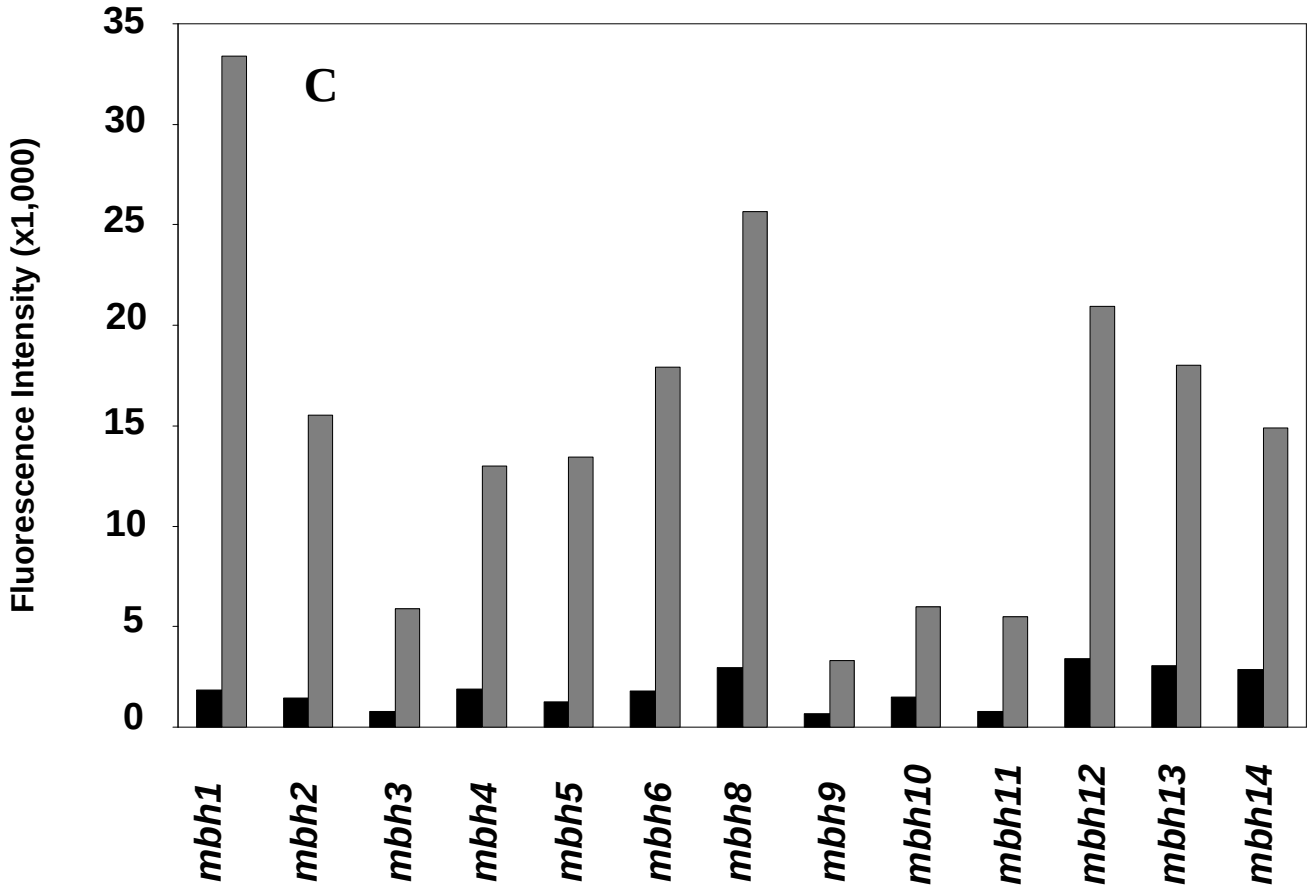

Figure 3.2. cont'd. Expression of ORFs encoding hydrogenase-related subunits with and without S°. The ORFs encoding the subunits of the cytoplasmic hydrogenase I (A), cytoplasmic hydrogenase II (B) and the membrane-bound hydrogenase (C) are arranged according to their positions in their respective operons. These are plotted against signal intensities for cDNA obtained from cells grown with (solid bars) or without (shaded bars) S°. The results with all subunits have a confidence level of at least 96% ($p > 0.98$ for the cytoplasmic hydrogenases and $p > 0.96$ for the membrane-bound enzyme).

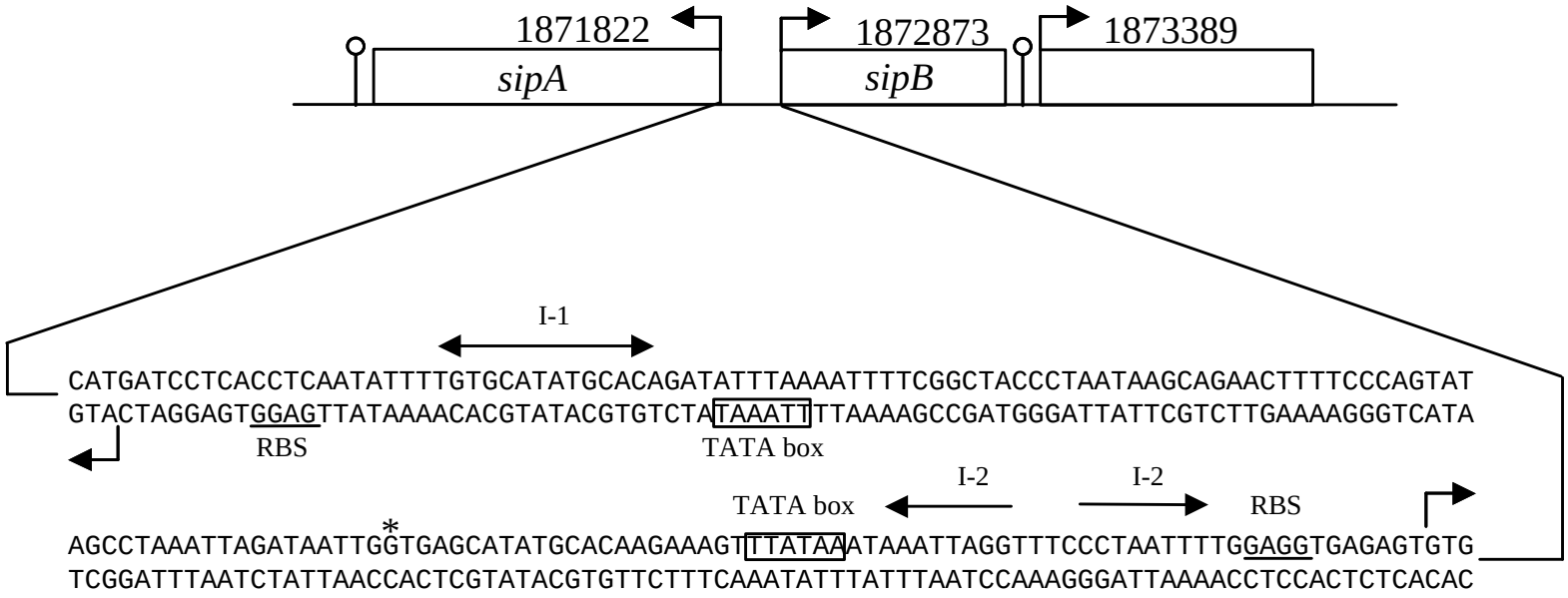

Figure 3.3. Genome organization of *sip*A and *sip*B. The back to back ORFs coding for SipA (179 amino acids) and SipB (115 amino acids) are shown with the indicated directions for transcription. Putative transcription stop sites are indicated with a ball on stick and putative translational start sites are indicated with right-angled arrows. The putative start sites are preceded with possible ribosomal binding sites (underlined) and TATA boxes (boxed). The start site for *sip*B shown here is not the same as that given in the genome annotation (which is indicated with an asterisk: (55)). Both *sip*A and *sip*B contain an inverted repeat (I-1 and I-2) directly next to the proposed TATA boxes. The position of the ORF (1873389) encoding the SipB extension (142 amino acids) is indicated.

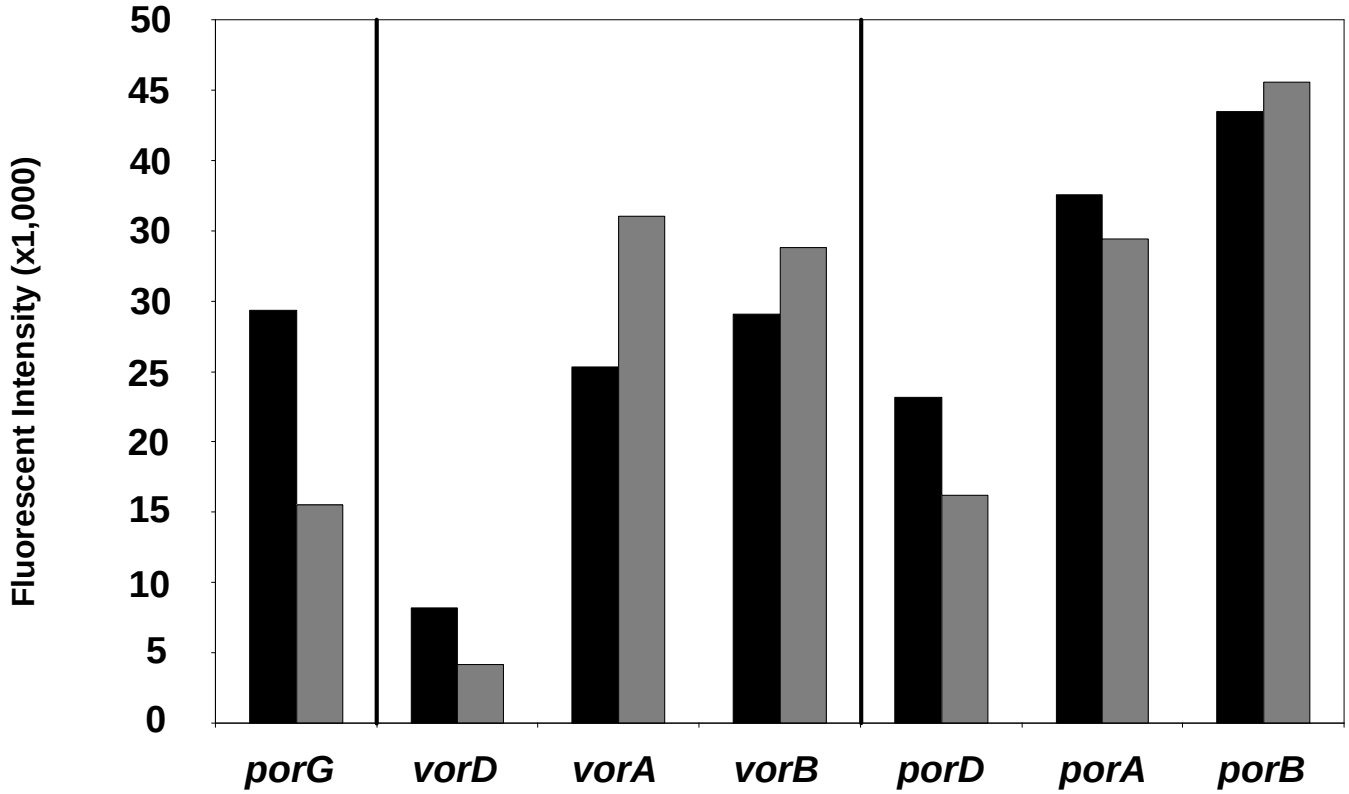

Figure 3.4. Expression of the ORFs encoding pyruvate ferredoxin oxidoreductase (POR) and 2-ketoisovalerate ferredoxin oxidoreductase (VOR) with and without S°. The genes (A, B and D) encoding the α-, β- and δ-subunits of POR and of VOR are arranged according to their positions in their respective operons, along with the gene (G) encoding the γ-subunit which is shared between the two enzymes (31). For each ORF, the signal intensities are indicated for cDNA obtained from cells grown with (solid bars) and without (shaded bars) S°.

CHAPTER 4

WHOLE GENOME DNA MICROARRAY OF A HYPERTHERMOPHILE AND AN ARCHAEON: *Pyrococcus furiosus* GROWN ON CARBOHYDRATES OR PEPTIDES[1]

[1]Schut, G.J., S. Brehm, S. Datta, and M.W.W. Adams.
Accepted *Journal of Bacteriology*, 03/21/03

ABSTRACT

The first complete genome DNA microarray was constructed for a hyperthermophile or a non-halophilic archaeon using the 2065 ORFs that have been annotated in the genome of *Pyrococcus furiosus* (T_{opt} 100°C). This was used to determine relative transcript levels in cells grown at 95 °C using either peptides or a carbohydrate (maltose) as the primary carbon source. Approximately 20% (398/2065) of the ORFs did not appear to be significantly expressed under either growth condition. Of the remaining 1,667 ORFs, the expression of 126 of them (8%) differed by more than 5-fold between the two cultures (p-value <0.05, from 16 data points for each ORF), and 82 of the 126 (65%) appear to be part of operons, indicating massive coordinate regulation. Of the 27 operons that are regulated, five or them encode (conserved) hypothetical proteins. A total of 18 operons are up-regulated (>5-fold) in maltose-grown cells, including those responsible for maltose transport and for the biosynthesis of twelve amino acids, of ornithine and of citric acid cycle intermediate. A total of 9 operons are up-regulated (> 5-fold) in peptide-grown cells, including those encoding enzymes involved in the production of acyl and aryl acids and 2-keto acids, which are used for energy conservation. Analyses of the spent growth media confirmed the production of branched chain and aromatic acids during growth on peptides. In addition, six non-linked enzymes in the pathways of sugar metabolism were regulated more than 5-fold, three in maltose-grown cells that are unique to the unusual glycolytic pathway, and three in peptide-grown cells that are unique to gluconeogenesis. The catalytic activities of sixteen metabolic enzymes whose expression appeared to be highly-regulated in the two cell types correlated very well with the microarray data. The degree of coordinate regulation

revealed by the microarray data was unanticipated and shows that *P. furiosus* can readily adapt to a change in its primary carbon source.

INTRODUCTION

Hyperthermophiles are microorganisms that grow optimally at temperatures of 80°C and above (54). Most are classified as archaea and many utilize peptides as a carbon source and reduce elemental sulfur (S°) to H_2S (54). Some, including several species of *Pyrococcus* and *Thermococcus*, are able to metabolize poly- and oligosaccharides as well as peptides (5, 6, 16). Herein we focus on the primary carbon metabolism of one of the best studied of all hyperthermophiles, *Pyrococcus furiosus.* This organism was isolated from a shallow marine volcanic vent and grows optimally near 100°C using either peptides or carbohydrates as its carbon and energy sources (16).

Prior studies of the primary pathways for carbon metabolism by *P. furiosus* have yielded several surprises. In particular, it contains a modified Embden-Meyerhof (EM) pathway with two ADP- rather than ATP-dependent kinases, glucokinase and phosphofructokinase (26, 56). In addition, the expected glyceraldehydes-3-phosphate dehydrogenase and the phosphoglycerate kinase are replaced by a single enzyme (GAPOR) that catalyzes the direct oxidation of glyceraldehydes-3-phosphate to 3-phosphoglycerate using ferredoxin as an electron acceptor (36). The pyruvate produced by glycolysis is oxidized to acetyl-CoA by another ferredoxin-linked enzyme, pyruvate ferredoxin oxidoreductase (POR), and ATP is formed by substrate level phosphorylation by another novel enzyme, acetyl-CoA synthetase I (33). Reduced ferredoxin is oxidized either by a respiratory-type membrane bound hydrogenase complex that both translocates and reduces protons, or by an as yet uncharacterized S^o-reducing system (45, 46). The biosynthesis of amino acids from glycolytic intermediates is assumed to occur by the

conventional pathways found in mesophilic bacteria but this has not been investigated to any extent.

On the other hand, during growth of *P. furiosus* on peptides, carbon is channeled to sugars by what appears to be a slightly modified version of the classical gluconeogenic pathway. This does contain the expected GAPDH and PGK, even though they do not function in glycolysis (47, 59), but the enzyme that catalyzes the hydrolysis of fructose-1,6-bisphosphate is not defined and two candidates have been proposed (40, 60). Energy is conserved during amino acid catabolism via the acyl and aryl CoAs that are generated by transamination and oxidation of the 2-ketoacids by a family of ferredoxin-dependent, 2-ketoacid oxidoreductases. These utilize 2-ketoglutarate (KGOR), aromatic (IOR) or branched chain 2-ketoacids (VOR). The CoA derivatives are converted to organic acids by ACS I and its isoenzyme, ACS II, with concomitant generation of ATP (33).

How the pathways of sugar and amino acid metabolism are regulated in *P. furiosus* and related organisms is largely unknown. Studies of the expression of some individual genes have indicated that glucose-6-phosphate isomerase and GAPOR are the key regulation points in glycolysis (59, 61) while fructose-1,6-bisphosphate aldolase (FBA) serves the same role in the gluconeogenic pathway (52). A preliminary study *P. furiosus* grown either on maltose or peptides with and without S° provided the first evidence for a significant regulatory role for both S° and the carbon source, based on the activities of several key metabolic enzymes (1). Herein we have extended this analysis by using the same cells to determine whole genome transcriptional profiles using DNA microarrays.

The application of whole genome DNA microarrays (48) have revolutionized functional genomics in eukaryotic systems, e.g., (43), but there have been far fewer analyses using prokaryotes. In the last two years, studies on 14 species have been reported, including with *Bacillus subtilus* (66), *Escherichia coli* (38), a cyanobacterium (20) and an extreme halophile (4). However, complete genome analyses have yet to be applied to either a non-halophilic member of the archaeal domain, or to a thermophilic or hyperthermophilic organism. Indeed, for such organisms results from only one partial genome array (271 ORFs) have been reported and this study focused on the effects of S° on the metabolism of *P. furiosus* (50). Herein we describe transcriptional analysis using all of the 2,065 ORFs that have been annotated in the complete genome of *P. furiosus* (42). The results reveal massive coordinate regulation in response to a change in the primary carbon source, a conclusion validated to a large extent by enzymatic and metabolic product analyses.

MATERIALS AND METHODS

Array design and RNA preparation. Primers were designed for the 2065 ORFs in the *P. furiosus* genome (http://comb5-156.umbi.umd.edu/genemate/) using Array Designer (Premier Biosoft International, Palo Alto, CA) and custom scripts (Poole, F., personal communication). Specific 50-mer oligonucleotides were designed for PF1327, PF1852 and PF1910 in addition to the full length probes as these ORFs have highly similar sequences. All primers were purchased from MWG Biotech (High Point, NC). PCR products were generated for 1949 complete ORFs and for the remainder primers were designed to give products of about 1 kb (unless the target ORF was smaller). Products

were obtained for all ORFs. These were purified with a 96 PCR purification kit (Telechem, Sunnyvale, CA), eluted in 50% (v/v) DMSO, and spotted in duplicate on aminosilane coated slides (Perkin Elmer, Boston, MA; Asper, Tartu, Estonia) in sixteen subarrays using a robotic slide printer (Omnigrid, Genemachines, San Carlos, CA). The slides were processed as previously described (10).

P. furiosus (DSM 3638) was grown in batch mode in a 20 liter custom fermentor at 95°C in the presence of S° using either peptides (hydrolyzed casein) or maltose as the primary carbon source (1). The cells that were used to prepare RNA for the microarray analyses were from experiments that have been described previously (1). In that case, activity assays were determined for more than twenty enzymes involved in the primary metabolic pathways using cytoplasmic and membrane fractions, and these results are referred to below. Samples (2000 ml) of the same cultures were removed towards the end of log phase growth, cooled on ice, and total RNA was extracted using acid phenol extraction (62).

Preparation of cDNA and Hybridization Conditions. cDNA was prepared as described previously (50) except that it was labeled with the Alexa dye 488, 546, 594 or 647 (Molecular Probes, Eugene, OR) according to the manufacturer's instructions. Differentially-labeled cDNA derived from *P. furiosus* cells grown in the presence of peptides or maltose were pooled and hybridized to the microarrays using a Genetac hybridization station (Genomic Solutions, Ann harbor, MI) for between 10 and 15 h. The slides were then washed automatically for 20 sec in each of 2xSSC/0.1% Tween-20, 0.2xSSC/0.1% Tween-20, 0.2xSSC and finally rinsed in distilled water and blown dry with compressed air. Fluorescence intensities of each of the four dyes were measured

using a Scan Array 5000 slide reader (Perkin Elmer, Boston, MA) with the appropriate laser and filter settings.

Data analysis. Spots were identified and quantitated using the Gleams software package (Nutec, Houston, TX). The relative amounts of the transcripts are presented in a linear fashion by converting all ratios to a $\log_2$ function. The detection limit of fluorescent signals was set arbitrary to 1,000 intensity units and such spots are not visible on the false overlay. Only ORFs that display intensities more than twice the detection limit (2,000 arbitrary units) are considered valid. All $\log_2$ values have a standard deviation that represents an average of four hybridization experiments in duplicate using cDNA derived from four different cultures of *P. furiosus*, two grown on peptides and two grown on maltose. The results for each ORF therefore consisted of thirty-two expression values, sixteen each for peptide and maltose. Individual t-test procedures were conducted to identify the significantly differentially-expressed ORFs and Holm's step down p-value adjustment procedure was performed (21) to give modified p-values.

Enzyme assays. Cell-free extracts used for all assays were prepared as described earlier (1). Isocitrate dehydrogenase activity was measured at 85 °C by the formation of NADPH by the previously described method (53) except that 50 mM EPPS, pH 7.5, was used as the buffer. Amylase activity was measured by the release of remazolbrillant blue (41). A 0.6% (w/v) suspension of starch azure (Sigma, St Louis, MO) was washed in 50 mM EPPS, pH 7.5, containing 40 mM NaCl at 95 °C for 2 minutes. The insoluble substrate was recovered by centrifugation and resuspended at 0.6% (w/v) in the same buffer. Cell-free extracts were incubated with the substrate suspension at 85 °C with continuous

mixing. Product release was measured at 595 nm (41). Acetolactate synthase was measured by incubating cell-free extracts in EPPS buffer, pH 7.5, in the presence of 50 mM pyruvate, 1 mM TPP and 10 µM FAD at 85 °C. Formation of acetolactate was determined as described previously (65). GAPDH activity was measured by following NADPH production as described previously (51). Carbamoyl-phosphate synthetase (CPS) and carbamate kinase (CK) activites were estimated by measuring carbamoyl phosphate indirectly using the ornithine transcarbamoylase pathway in cell-free extracts to produce citrulline (30). The reaction mixture used to measure both enzyme activities contained 50 mM EPPS, pH 8.0, 8 mM L-ornithine, 20 mM ATP, 0.4 mg/mL urease (Sigma, St Louis, MO) and 100 mM sodium bicarbonate. The N source for the CK and CPS assays were 200 mM ammonium chloride and 2.5 mM glutamine, respectively. The reaction (500 µl) was incubated at 60 °C for 30 min and was stopped by the addition of 5 µl of concentrated sulfuric acid. Citrulline was determined as described previously (7).

Determination of organic acids. Samples of media (1 ml) were removed from growing cultures of *P. furiosus* at various points in the growth phase and cells were collected by centrifugation. The supernatant fractions were extracted three times with an equal volume of ether and converted to their potassium salts by adding 1 M KOH to pH 8 and lyophilized. To obtain derivatives of the organic acids, the dried samples were suspended in 2 ml acetonitrile containing α,*p*-dibromoacetophenone with 18-crown-6 ether as catalyst to yield UV-absorbing compounds as described previously (14). The adducts of the common organic acids were separated by HPLC (Alliance 2690, Waters, Milford, MA) using a C18 column (150 x 3.9 mm) with a linear gradient of 45 - 75% (v/v) methanol in water. The adducts were detected with a photodiode array detector (Waters,

Milford, MA) at 260 nm. The identity of the organic acids was determined from standards and verified with electron spray mass spectrometry at the MS facility of the University of Georgia.

RESULTS AND DISCUSSION

Experimental Protocols and Data Analysis. A total of 2065 ORFs are annotated in the genome sequence of *P. furiosus* (http://comb5-156.umbi.umd.edu/genemate/). Approximately 50% of these are designated as (conserved) hypothetical and show no similarity to characterized ORFs in other genomes (42). Each of the 2065 ORFs was cloned by PCR amplification and was arrayed onto glass slides. The arrays were used to assess differential gene expression in *P. furiosus* cells grown in the presence of S° using either peptides (hydrolyzed casein) or the disaccharide maltose as the primary carbon source. Results were obtained from RNA samples that were prepared from four different *P. furiosus* cultures, two grown independently on each carbon source. All possible hybridization combinations were performed twice in duplicate using the four sources of RNA, giving rise to 16 data points for each of the 2065 ORFs.

The efficacy of the microarray experiment is shown by using RNA samples derived from two different cultures of *P. furiosus* cells grown independently under the same set of conditions. These were differentially labeled and hybridized to the same slide. Fig. 4.1A shows the two sets of signal intensities using cells grown on peptides. Intensities vary over a $>10^3$ range, and ORFs with intensities less than 2000 arbitrary units (or twice the detection limit, see Fig. 4.1A) are considered not to be significantly expressed. As expected, low intensity signals show a high standard deviation because of

background fluorescence, but otherwise the data points from the majority of the ORFs lie close to the diagonal. As indicated by the multiple lines, more then a 5-fold difference in signal intensity (outer lines in Fig. 4.1A) is readily discerned, while a 2-fold change is generally within experimental error.

As shown in Fig. 4.1B, a change in the primary carbon source from peptides to maltose has has a dramatic effect on gene expression when viewed on a genome-wide basis (c.f., Fig. 4.1A). In the following, we focus on ORFs whose expression appears to be strongly regulated by the presence of peptides or maltose such that the signal intensity changes by at least 5-fold (shown by the upper and lower diagonal lines in Fig. 4.1B) and are statistically different (p-value <0.05). Approximately 80% (1666/2065) of the ORFs are significantly expressed under one or both growth condition (intensity more than two-fold detection limit). Of these, the expression of 125 (7.5%) are up-regulated by more than 5-fold (p-value <0.05, from 16 data points for each ORF) in either maltose- (80 in total) or peptide-grown (45) cells and these are listed in Tables 4.1 and 4.2, respectively. The remaining ORFs can be sub-divided into those that appear to be up-regulated between 2 and 5-fold by maltose (46 in total) or peptides (99) and those that are not significantly regulated (1396) under either condition, in addition to those that are not expressed (399). Information on the ORFs not listed in Tables 4.1 and 4.2 are available as supplementary information (http://adams.bmb.uga.edu/pubs/sup238.pdf).

Coordinate regulation of ORF expression. The ORFs that are up-regulated more than 5-fold are listed in Tables 4.1 and 4.2 in the order that they are found in the genome. Those that are adjacent to each other with intergenic distances of less than 30 nucleotides are assumed to be coordinately-regulated and to be part of the same operon. Remarkably,

of the 125 ORFs that are up-regulated, 82 (65%) are part of a total of 27 different operons, 18 affected by maltose and 9 by peptides. That these are operons is supported by the short intergenic distances (compared with >30 nucleotides for the genome in general), and by the proposed (annotated) functions of the ORFs, which in most of the operons are clearly closely-related. The notable exceptions are 5 of the 27 operons that encode only (conserved) hypothetical proteins and so their functions cannot be assessed.

The power of the microarray approach is demonstrated by the fact that the operons that are up-regulated more than 5-fold by maltose include those that are responsible for maltose transport and for the biosynthesis of twelve amino acids (Glu, Arg, Leu, Val, Ile, Ser, Thr, Met, His, Phe, Trp and Try), for ornithine and for citric acid cycle intermediates (Table 4.1). Conversely, operons that are up-regulated in peptide-grown cells include those encoding enzymes involved in the production of acyl and aryl acids and 2-ketoacids from amino acids (Table 4.2). These data obviously demonstrate a massive biosynthesis of amino acids during growth on maltose**,** and support the proposed pathways for the catabolism of peptide-derived amino acids via transamination and formation of energy-yielding CoA-derivatives (1, 33, 49). Moreover, as shown in Fig. 4.2, analyses of the growth media that were used to obtain the cells that provided the RNA for the microarrays show that a mixture of organic acids, including isovalerate, butyrate, isobutyrate and phenylacetate, are produced during growth on peptides, whereas acetate is the major product during growth on maltose. These results support a dramatic switch in regulation in response to a change in the primary carbon source. In the following, we consider the biochemical consequences of the coordinately-regulated pathways that are indicated by the microarray analyses.

Biosynthesis of amino acids in maltose-grown cells. Not only are many of the ORFs involved in amino acid biosynthesis in *P. furiosus* arranged in operons, but those specific for aromatic amino acids, histidine, ornithine and branched chain amino acids are clustered together in a 51 kb segment (PF1657-1715). As shown in Fig. 4.3, the majority of the ORFs in this region are up-regulated in maltose-grown cells. In fact, those that are not, encode proteins involved in ribose transport or are (conserved) hypothetical ORFs. The activity of one of the enzymes (PF0935) involved in branched chain amino acid biosynthesis, acetolactate synthase, increased 40-fold in maltose-grown cells (Table 4.3), in agreement with the measured 17-fold increase in transcript level (Table 4.1). Carbon for amino acid biosynthesis during growth on maltose appears to be made available in part via three TCA cycle enzymes, citrate synthase, aconitase and isocitrate dehydrogenase (PF0201-0203). These presumably supply 2-ketoglutarate for glutamate synthesis and are arranged in an operon that is up-regulated more than 5-fold in maltose-grown cultures (Table 4.1). The activity of isocitrate dehydrogenase is more than 2-fold higher in maltose-grown cells (Table 4.3). In agreement with a biosynthetic role for these enzymes, the closely related-species *P. horikoshii* and *P. abyss*i, which do not utilize carbohydrates, lack homologs of these three ORFs (2, 23).

The microarray data also shed light on the controversial issue of carbamate metabolism in *P. furiosus*. Previously, it was proposed that *P. furiosus* possesses a novel carbamate kinase (CK, PF0676) that synthesizes carbamoyl phosphate for arginine and pyrimidine biosynthesis (13, 57), rather than its usual physiological role of using carbamoyl phosphate to synthesize ATP. However, the expression of PF0676 is up-regulated (5.7-fold) in peptide-grown cells (Table 4.2), which is more consistent with the latter energy-conserving role in amino acid catabolism. Moreover, CK is proposed to

form a physiological complex with ornithine carbamoyltransferase (OTCase, PF0594; (34)) but this is not significantly regulated by peptides (<2-fold). In addition, *P. furiosus* contains two ORFs (PF1713 and PF1714) that are annotated as (a heterodimeric) carbamoyl phosphate synthetase (CPS). These two ORFs are up-regulated (8.0 and 2.3-fold) in maltose-grown cells, consistent with a role for the enzyme in the biosynthesis of arginine. Further evidence for a traditional role for CK in *P. furiosus* is its presence in the proteolytic, non-saccharolytic archaea *P. abyssi* and *P. horikoshii*, organisms that do not possess a CPS homolog (2).

New information is also provided by the array data on glutamate metabolism in *P. furiosus.* For example, the TCA cycle enzymes (PF0201-PF0203) that are up-regulated during growth on maltose are adjacent to an operon of three ORFs (PF0204-PF0206), all of which are also up-regulated by about an order of magnitude. PF0205 is annotated as the large subunit of an NAD-dependent glutamate synthase (GltS), an enzyme that catalyzes the reductive transfer of the amine group of glutamine to 2-ketoglutarate forming glutamate. However, all three ORFs appear to encode a heterotrimeric, ferredoxin-linked glutamate synthase that is equivalent to the large single subunit enzymes found in cyanobacteria (37). This enzyme usually functions in concert with a glutamine synthetase, which forms glutamine from glutamate and ammonia in an ATP-dependent reaction. Accordingly, the putative glutamine synthetase (PF0450) in *P. furiosus* is up-regulated on maltose by almost 20-fold (Table 4.1). Interestingly, *P. abyssi* and *P. horikoshii* do not possess ORFs corresponding to PF0204-0206, consistent with their inability to utilize maltose. *P. furiosus* also contains a homolog (PF1852) of a novel type of glutamate synthase that has been characterized from another *Pyrococcus* species (KOD1; (24)). This catalyzes the synthesis of glutamate from ammonia and 2-

ketoglutarate in an NADPH-dependent reaction. In *P. furiosus*, expression of PF1852 is up-regulated 6-fold in maltose-grown cells, consistent with a role for the enzyme in amino acid biosynthesis.

Transport of carbon growth substrates. The genome sequence of *P. furiosus* contains several ORFs that are annotated as peptide transporters of one type or another (PF0191-0194; 0357-0361; 0999-1001; 1408-1412). However, none of them are up-regulated in peptide-grown cells suggesting that peptides can be also utilized as a carbon source when *P. furiosus* is grown in a maltose-containing medium. In fact, the low concentrations of organic acids (other than acetate) found in the growth media of maltose-grown cells (Fig. 4.2) are consistent with this notion. On the other hand, for maltose uptake, there are two operons that show high sequence similarity to the ORFs in the maltose/trehalose transporter (Mal) operon of the hyperthermophile *Thermococcus litoralis* (64). Both operons are up-regulated more than 5-fold in maltose-grown *P. furiosus* cells (Table 4.2). This transport cluster is not found in the genomes of the non-saccharolytic *P. horikoshii* and *P. abyssi* (http://www.genoscope.cns.fr/Pab/, (29)). The Mal cluster in *T. litoralis* encodes a maltose binding protein (MalE), two transmembrane proteins (MalF and G) and an ATPase subunit (MalK) (64), together with a maltose-specific transcriptional regulator, TrmB, and an ORF annotated as a trehalose synthase (29). An almost exact copy (even on the nucleotide level) of the Mal cluster in *T. litoralis* is present in *P. furiosus* (Fig. 4.3) and this is thought to have arisen by horizontal gene transfer between the two organisms (11). The microarray data indicate that the Mal (I) cluster in *P. furiosus* is divided into three transcriptional units, MalE, MalFG/(trehalose synthase), and TrmB/MalK (Fig. 4.3). The finding of significant amounts of the MalE and (TrmB -

MalK) transcripts in maltose-grown *P. furiosus* cells (Fig. 4.3) is in agreement with the report that the MalK and MalE proteins can be detected in *T. litoralis* cells grown in the absence of maltose (17) and that TrmB represses the synthesis of the MalEFG/(trehalose synthase) cluster (29). However, although *P. furiosus* converts maltose into glucose (64), no obvious candidate for an α-glucosidase has been identified in the genome. A protein with α-glucosidase activity was purified from *P. furiosus* but sequence information was not obtained (9). A likely candidate for at least one maltose-utilizing enzyme is the putative trehalose synthase, which contains glucanotransferase motifs, present in the Mal I cluster.

Interestingly, the second maltose transporter (Mal II) cluster in *P. furiosus* (PF1938-1933) is also up-regulated in maltose-grown cells and is organized in a similar fashion to Mal I with three transcription units, except that the ORF adjacent to MalG is annotated as an amylopullulanase (12) rather than as a trehalose synthase (Fig. 4.3). The two Mal clusters are probably induced by maltose and/or maltooligosaccharides and their gene products presumably work together to metabolize these sugars as well as others derived from starch. In fact, the expression of an α-amylase (PF0272: (27)) is up-regulated 26-fold in maltose-grown cultures, consistent with the high α-amylase activity measured in such cells (Table 4.3). However, peptide-grown cells still contain significant α-amylase activity (Table 4.3). This is assumed to arise from the product of PF0477, which is also annotated as an α-amylases (25) and is up-regulated 5.3-fold in peptide-grown cells (Table 4.2). This enzyme is not present in the genome of *P. horikoshii* nor *P. abyssi* (2) and presumably generates oligosaccharides that then induce the complete saccharolytic pathways when polysaccharides become available during peptide-dependent growth.

Glucose metabolism. Unlike ORFs that encode some of the enzymes involved with maltose metabolism, ORFs encoding glycolytic and gluconeogenic enzymes are unlinked in the genome. Their relative transcript levels under the two growth conditions are shown in Table 4.4. Three of them that are unique to the glycolytic pathway, glucose-6-phosphate isomerase (PGI), ADP phophofructokinase (PFK), and glyceraldehyde-3-phosphate ferredoxin oxidoreductase (GAPOR), are strongly up-regulated in maltose-grown cells. This was previously shown for PGI and GAPOR (59, 61), and the increase in the transcript level of GAPOR is in agreement with the measured increase in enzyme activity (Table 4.3). Interestingly, glucokinase, which is thought to have arisen from PFK by gene duplication (56), is not regulated and significant amounts of the transcript are found in peptide-grown cells (Table 4.4). Conversely, three enzymes unique to gluconeogenesis, fructose-1,6-bisphosphatase (FBPase), phosphoglycerate kinase PGK) and glyceraldehydes-3-phosphate dehydrogenase (GAPDH) are all up-regulated in peptide-grown cells (Table 4.4). The increase in the transcript level of GAPDH in peptide-grown cells is in agreement with the observed increase in enzyme activity (Table 4.3). FBPase (PF0613) is up-regulated 15-fold in peptide-grown cells and this corresponds to the FBPase proposed by Imanka and coworkers (40). The other FBPase candidate (PF2014**,** (60)) is not significantly regulated and is therefore unlikely to play a gluconeogenic role. Fructose-1,6-bisphosphate aldolase (FBA) was reported to be up-regulated in maltose-grown cells relative to those grown on pyruvate (52) but such regulation is not observed here in peptide-grown cells (Table 4.4).

One would not expect the remaining thirteen ORFs that encode glycolytic and gluconeogenic enzymes to be regulated and this is the case (Table 4.4), with one notable exception. Triosephosphate isomerase is apparently up-regulated almost 5-fold in

maltose-grown cells for reasons that are not clear at present. Both pyruvate kinase and its gluconeogenic counterpart, phosphoenolpyruvate synthetase (PPS), are each expressed at comparable levels under the two types of growth condition (Table 4.4), and this was confirmed for PPS with activity measurements (Table 4.3). PPS is one of the most abundant enzymes in *P. furiosus* although the function of the enzyme in maltose-gown cells is not obvious (22, 44). Two other highly expressed enzymes involved in glucose catabolism are pyruvate ferredoxin oxidoreductase (POR) and acetyl CoA synthetase (ACS I). Like PPS, both the array data (Table 4.4) and activity measurements (Table 4.3) do not indicate significant regulation of either enzyme. This is expected since POR and ACS I also play key roles in energy conservation in peptide metabolism using amino acid-derived pyruvate.

Amino acid catabolism. The first step in the utilization of amino acids in peptide-grown cells is thought to involve transamination (49) and, accordingly, several transaminases are up-regulated. They include one yet to be characterized (PF1253, 6.1-fold) and two that have been purified, PF0121 (4.5-fold; (3)) and PF1497 (2.5-fold; (63)). These transamination reactions produce various 2-ketoacids as well as glutamate from 2-ketoglutarate. Glutamate dehydrogenase (GDH) serves to regenerate the 2-ketoglutarate, and the expression of its gene also increases significantly (4.4-fold) in peptide-grown cells (see Supplemental Material). The 2-ketoacids are oxidized by four distinct 2-ketoacid ferredoxin oxidoreductases (KORs) that have been characterized from *P. furiosus* (49). Two of them, which are specific for 2-ketoglutarate (KGOR, PF1767-1770) and for 2-ketoacids derived from aromatic amino acids (IOR, PF0533-0534), are up-regulated in peptide-grown cultures (Table 4.2). The other two, which utilize pyruvate

(POR) and 2-ketoacids derived from the branched-chain amino acids (VOR), are expressed at high levels in peptide-grown as well as in maltose-grown cells. This is expected for POR as it also uses pyruvate produced from glycolysis during growth on maltose, but the function of VOR in maltose-grown cells is unclear. In any event, the activities of VOR, IOR, KGOR and POR in cell-free extracts correspond well with the expression levels determined by the array analyses (Table 4.3). However, KGOR has been purified (49) and it is comprised of four different subunits, (PF1767-PF1770), but the KGOR operon contains three additional ORFs, and these encode homologs of the KGOR subunits (PF1771-1773). All three ORFs are co-regulated with the four ORFs of KGOR in peptide-grown cells and presumably encode a fifth member of the KOR family with as yet unknown substrate specificity (Table 4.2).

The CoA derivatives generated by the KORs are used to conserve energy by ACS I and ACS II. These enzymes have both been purified and they utilize acyl- and aryl-CoAs, respectively. Although ACS I (PF1540, PF1787) is not dramatically regulated by the carbon source, the expression of the alpha subunit (PF0532) of ACS II increases more than 5-fold in peptide-grown cells although the expression of its beta subunit (PF1837) is unaffected, as is its activity in cell-free extracts (Table 4.3). Rationalizing such data is not trivial as the genome contains three more homologs of the alpha subunit of ACS II (PF0233, PF1085 and PF1838), none of which are significantly regulated and their corresponding beta subunits cannot be identified. Clearly, the nature and role of the ACS family of enzymes is complex and more biochemical analyses are needed to complement the array data.

During amino acid catabolism, reductant is generated both as reduced ferredoxin from the KORs and as NAD(P)H from GDH. These are interconverted by ferredoxin

NAD(P) oxidoreductase (FNOR), an enzyme previously characterized from *P. furiosus* (31). Surprisingly, the expression of the two subunits of FNOR (PF1327, PF1328) are both down-regulated more than 5-fold in peptide-grown cells (Table 4.1), yet FNOR activity is largely unaffected (Table 4.2). However, the genome contains two ORFs (PF1901, PF1911) that appear to be close homologs of the two FNOR subunits and their expression increase by more than an order of magnitude in peptide-grown cells, presumably in a compensatory fashion (Table 4.2). It therefore seems reasonable to conclude that the interconversion of NAD(P)H and ferredoxin is catalyzed by two distinct FNORs (I and II), the expression of which is dependent upon the carbon source. FNOR was also referred to as sulfide dehydrogenase because of its ability to reduce S° *in vitro* (31). Indeed, PF1901 and PF1911 have been referred to by Hagen and coworkers as subunits (SudXY) of a second sulfide dehydrogenase based on sequence analyses (18). However, S° metabolism in *P. furiosus* involves a novel system unrelated to the two FNOR enzymes (50) and the designation SudXY is inappropriate for the subunits of what is referred to here as FNOR II (Table 4.2).

Finally, the microarray data also provide intriguing information on one other class of enzyme, hydrogenase. Previous studies have shown both the expression and the activities of the two cytoplasmic and one membrane-bound hydrogenase of *P. furiosus* dramatically decrease in maltose-grown cultures when S° is present (1, 50). To our surprise, however, transcript levels of the four subunits of hydrogenase I all increase by about an order of magnitude in peptide-grown cultures (in the presence of S°, see Table 4.2), even though the hydrogenase activity in the cell-free extracts remained very low (1). In fact, the expression of the hydrogenase maturation protein HypF (PF0559) is also up-regulated 5-fold in peptide-grown cells so lack of this protein should not prevent

formation of active hydrogenase I (Table 4.2). On the other hand, as expected, transcripts for the four subunits of hydrogenase II could not be detected in peptide-grown cells and no significant up-regulation of the membrane-bound hydrogenase was observed. It is not clear why hydrogenase I appears to be up-regulated in peptide-grown cells, especially without a corresponding increase in activity, and this phenomenon is currently under study.

ACKNOWLEDGEMENTS

This research was funded by grants from the National Institutes of Health (GM 60329), the National Science Foundation (MCB 0129841, MCB 9904624 and BES-0004257) and the Department of Energy (FG05-95ER20175). We thank, Frank E. Jenney, Jr., Angeli Lal Menon, James F. Holden, Eleanor Green and Rajat Sapra for many helpful discussions, Farris Poole for bioinformatic analyses, Patrick Lynch for assistance with the acid analyses, and Frank T. Robb for providing access to preliminary information from the *P. furiosus* genome sequencing project.

REFERENCES

1. **Adams, M. W. W., J. F. Holden, A. L. Menon, G. J. Schut, A. M. Grunden, C. Hou, A. M. Hutchins, F. E. Jenney, Jr., C. Kim, K. Ma, G. Pan, R. Roy, R. Sapra, S. V. Story, and M. F. Verhagen.** 2001. Key role for sulfur in peptide metabolism and in regulation of three hydrogenases in the hyperthermophilic archaeon *Pyrococcus furiosus*. J. Bacteriol. **183:**716-24.

2. **Altschul, S. F., T. L. Madden, A. A. Schaffer, J. Zhang, Z. Zhang, W. Miller, and D. J. Lipman.** 1997. Gapped BLAST and PSI-BLAST: a new generation of protein database search programs. Nucleic. Acids Res. **25:**3389-402.

3. **Andreotti, G., M. V. Cubellis, G. Nitti, G. Sannia, X. Mai, M. W. Adams, and G. Marino.** 1995. An extremely thermostable aromatic aminotransferase from the hyperthermophilic archaeon *Pyrococcus furiosus*. Biochim. Biophys. Acta **1247:**90-6.

4. **Baliga, N. S., M. Pan, Y. A. Goo, E. C. Yi, D. R. Goodlett, K. Dimitrov, P. Shannon, R. Aebersold, W. V. Ng, and L. Hood.** 2002. Coordinate regulation of energy transduction modules in *Halobacterium sp.* analyzed by a global systems approach. Proc. Natl. Acad. Sci.U S A.

5. **Barbier, G., A. Godfroy, J. R. Meunier, J. Querellou, M. A. Cambon, F. Lesongeur, P. A. Grimont, and G. Raguenes.** 1999. *Pyrococcus glycovorans* sp. nov., a hyperthermophilic archaeon isolated from the East Pacific Rise. Int. J. Syst. Bacteriol. **49 Pt 4:**1829-37.

6. **Blamey, J., M. Chiong, C. Lopez, and E. Smith.** 1999. Optimization of the growth conditions of the extremely thermophilic microorganisms *Thermococcus celer* and *Pyrococcus woesei*. J. Microbiol. Methods **38:**169-75.

7. **Boyde, T. R., and M. Rahmatullah.** 1980. Optimization of conditions for the colorimetric determination of citrulline, using diacetyl monoxime. Anal. Biochem. **107:**424-31.

8. **Bryant, F. O., and M. W. W. Adams.** 1989. Characterization of hydrogenase from the hyperthermophilic archaebacterium, *Pyrococcus furiosus*. J. Biol. Chem. **264:**5070-9.

9. **Costantino, H. R., S. H. Brown, and R. M. Kelly.** 1990. Purification and characterization of an alpha-glucosidase from a hyperthermophilic archaebacterium, *Pyrococcus furiosus*, exhibiting a temperature optimum of 105 to 115 degrees C. J. Bacteriol. **172:**3654-60.

10. **de Saizieu, A., C. Gardes, N. Flint, C. Wagner, M. Kamber, T. J. Mitchell, W. Keck, K. E. Amrein, and R. Lange.** 2000. Microarray-based identification of a

novel *Streptococcus pneumoniae* regulon controlled by an autoinduced peptide. J. Bacteriol. **182:**4696-703.

11. **Diruggiero, J., D. Dunn, D. L. Maeder, R. Holley-Shanks, J. Chatard, R. Horlacher, F. T. Robb, W. Boos, and R. B. Weiss.** 2000. Evidence of recent lateral gene transfer among hyperthermophilic archaea. Mol. Microbiol. **38:**684-93.

12. **Dong, G., C. Vieille, and J. G. Zeikus.** 1997. Cloning, sequencing, and expression of the gene encoding amylopullulanase from *Pyrococcus furiosus* and biochemical characterization of the recombinant enzyme. Appl. Environ. Microbiol. **63:**3577-84.

13. **Durbecq, V., C. Legrain, M. Roovers, A. Pierard, and N. Glansdorff.** 1997. The carbamate kinase-like carbamoyl phosphate synthetase of the hyperthermophilic archaeon *Pyrococcus furiosus*, a missing link in the evolution of carbamoyl phosphate biosynthesis. Proc. Natl. Acad. Sci.U S A **94:**12803-8.

14. **Durst, H. D., M. Milano, E. J. Kikta, Jr., S. A. Connelly, and E. Grushka.** 1975. Phenacyl esters of fatty acids via crown ether catalysts for enhanced ultraviolet detection in liquid chromatography. Anal. Chem. **47:**1797-1801.

15. **Evdokimov, A. G., D. E. Anderson, K. M. Routzahn, and D. S. Waugh.** 2001. Structural basis for oligosaccharide recognition by *Pyrococcus furiosus* maltodextrin-binding protein. J. Mol. Biol. **305:**891-904.

16. **Fiala, G., and K. O. Stetter.** 1986. *Pyrococcus furiosus* sp-nov represents a novel genus of marine heterotrophic archaebacteria growing optimally at 100-degrees C. Arch. Microbiol. **145:**56-61.

17. **Greller, G., R. Horlacher, J. DiRuggiero, and W. Boos.** 1999. Molecular and biochemical analysis of MalK, the ATP-hydrolyzing subunit of the trehalose/maltose transport system of the hyperthermophilic archaeon *Thermococcus litoralis*. J. Biol. Chem. **274:**20259-64.

18. **Hagen, W. R., P. J. Silva, M. A. Amorim, P. L. Hagedoorn, H. Wassink, H. Haaker, and F. T. Robb.** 2000. Novel structure and redox chemistry of the prosthetic groups of the iron-sulfur flavoprotein sulfide dehydrogenase from *Pyrococcus furiosus*; evidence for a [2Fe-2S] cluster with Asp(Cys)3 ligands. J. Biol. Inorg. Chem. **5:**527-34.

19. **Hansen, T., M. Oehlmann, and P. Schonheit.** 2001. Novel type of glucose-6-phosphate isomerase in the hyperthermophilic archaeon *Pyrococcus furiosus*. J. Bacteriol. **183:**3428-35.

20. **Hihara, Y., A. Kamei, M. Kanehisa, A. Kaplan, and M. Ikeuchi.** 2001. DNA microarray analysis of cyanobacterial gene expression during acclimation to high light. Plant Cell **13:**793-806.

21. **Holm, S.** 1979. A simple sequentially rejective multiple test procedure. Scand. J. Statist. **6:**65-70.

22. **Hutchins, A. M., J. F. Holden, and M. W. W. Adams.** 2001. Phosphoenolpyruvate synthetase from the hyperthermophilic archaeon *Pyrococcus furiosus*. J. Bacteriol. **183:**709-15.

23. **Huynen, M. A., T. Dandekar, and P. Bork.** 1999. Variation and evolution of the citric-acid cycle: a genomic perspective. Trends Microbiol. **7:**281-91.

24. **Jongsareejit, B., R. N. Rahman, S. Fujiwara, and T. Imanaka.** 1997. Gene cloning, sequencing and enzymatic properties of glutamate synthase from the hyperthermophilic archaeon *Pyrococcus* sp. KOD1. Mol. Gen. Genet. **254:**635-42.

25. **Jorgensen, S., C. E. Vorgias, and G. Antranikian.** 1997. Cloning, sequencing, characterization, and expression of an extracellular alpha-amylase from the hyperthermophilic archaeon *Pyrococcus furiosus* in *Escherichia coli* and *Bacillus subtilis*. J. Biol. Chem. **272:**16335-42.

26. **Kengen, S. W., J. E. Tuininga, F. A. de Bok, A. J. Stams, and W. M. de Vos.** 1995. Purification and characterization of a novel ADP-dependent glucokinase from the hyperthermophilic archaeon *Pyrococcus furiosus*. J. Biol. Chem. **270:**30453-7.

27. **Laderman, K. A., K. Asada, T. Uemori, H. Mukai, Y. Taguchi, I. Kato, and C. B. Anfinsen.** 1993. Alpha-amylase from the hyperthermophilic archaebacterium *Pyrococcus furiosus*. Cloning and sequencing of the gene and expression in *Escherichia coli*. J. Biol. Chem. **268:**24402-7.

28. **Laderman, K. A., B. R. Davis, H. C. Krutzsch, M. S. Lewis, Y. V. Griko, P. L. Privalov, and C. B. Anfinsen.** 1993. The purification and characterization of an extremely thermostable alpha-amylase from the hyperthermophilic archaebacterium *Pyrococcus furiosus*. J. Biol. Chem. **268:**24394-401.

29. **Lee, S. J., A. Engelmann, R. Horlacher, Q. Qu, G. Vierke, C. Hebbeln, M. Thomm, and W. Boos.** 2002. TrmB, a sugar-specific transcriptional regulator of the trehalose/maltose ABC transporter from the hyperthermophilic archaeon *Thermococcus litoralis*. J. Biol. Chem.

30. **Legrain, C., V. Villeret, M. Roovers, C. Tricot, B. Clantin, J. Van Beeumen, V. Stalon, and N. Glansdorff.** 2001. Ornithine carbamoyltransferase from *Pyrococcus furiosus*. Methods Enzymol. **331:**227-35.

31. **Ma, K., and M. W. W. Adams.** 2001. Ferredoxin NADP oxidoreductase from *Pyrococcus furiosus*. Methods Enzymol. **334:**40-5.

32. **Ma, K., and M. W. W. Adams.** 1994. Sulfide dehydrogenase from the hyperthermophilic archaeon P*yrococcus furiosus*: a new multifunctional enzyme involved in the reduction of elemental sulfur. J. Bacteriol. **176:**6509-17.

33. **Mai, X., and M. W. W. Adams.** 1996. Purification and characterization of two reversible and ADP-dependent acetyl coenzyme A synthetases from the hyperthermophilic archaeon *Pyrococcus furiosus*. J. Bacteriol. **178:**5897-903.

34. **Massant, J., P. Verstreken, V. Durbecq, A. Kholti, C. Legrain, S. Beeckmans, P. Cornelis, and N. Glansdorff.** 2002. Metabolic channeling of carbamoyl phosphate, a thermolabile intermediate: evidence for physical interaction between carbamate kinase-like carbamoyl-phosphate synthetase and ornithine carbamoyltransferase from the hyperthermophile *Pyrococcus furiosus*. J. Biol. Chem. **277:**18517-22.

35. **Muir, J. M., R. J. Russell, D. W. Hough, and M. J. Danson.** 1995. Citrate synthase from the hyperthermophilic Archaeon, *Pyrococcus furiosus*. Protein Eng. **8:**583-92.

36. **Mukund, S., and M. W. W. Adams.** 1995. Glyceraldehyde-3-phosphate ferredoxin oxidoreductase, a novel tungsten-containing enzyme with a potential glycolytic role in the hyperthermophilic archaeon *Pyrococcus furiosus*. J. Biol. Chem. **270:**8389-92.

37. **Navarro, F., E. Martin-Figueroa, P. Candau, and F. J. Florencio.** 2000. Ferredoxin-dependent iron-sulfur flavoprotein glutamate synthase (GlsF) from the Cyanobacterium *Synechocystis* sp. PCC 6803: expression and assembly in *Escherichia coli*. Arch. Biochem. Biophys. **379:**267-76.

38. **Oh, M. K., and J. C. Liao.** 2000. Gene expression profiling by DNA microarrays and metabolic fluxes in *Escherichia coli*. Biotechnol Prog **16:**278-86.

39. **Peak, M. J., J. G. Peak, F. J. Stevens, J. Blamey, X. Mai, Z. H. Zhou, and M. W. W. Adams.** 1994. The hyperthermophilic glycolytic enzyme enolase in the archaeon, *Pyrococcus furiosus*: comparison with mesophilic enolases. Arch. Biochem. Biophys. **313:**280-6.

40. **Rashid, N., H. Imanaka, T. Kanai, T. Fukui, H. Atomi, and T. Imanaka.** 2002. A novel candidate for the true fructose-1,6-bisphosphatase in archaea. J. Biol. Chem. **277:**30649-55.

41. **Rinderknecht, H., E. P. Marbach, C. R. Carmack, C. Conteas, and M. C. Geokas.** 1971. Clinical evaluation of an a-amylase assay with insoluble starch labeled with Remazolbrilliant Blue (amylopectin-azure). Clin. Biochem. **4:**162-74.

42. **Robb, F. T., D. L. Maeder, J. R. Brown, J. DiRuggiero, M. D. Stump, R. K. Yeh, R. B. Weiss, and D. M. Dunn.** 2001. Genomic sequence of

hyperthermophile, *Pyrococcus furiosus*: implications for physiology and enzymology. Methods Enzymol. **330:**134-57.

43. **Ross, D. T., U. Scherf, M. B. Eisen, C. M. Perou, C. Rees, P. Spellman, V. Iyer, S. S. Jeffrey, M. Van de Rijn, M. Waltham, A. Pergamenschikov, J. C. Lee, D. Lashkari, D. Shalon, T. G. Myers, J. N. Weinstein, D. Botstein, and P. O. Brown.** 2000. Systematic variation in gene expression patterns in human cancer cell lines. Nat. Genet. **24:**227-35.

44. **Sakuraba, H., E. Utsumi, C. Kujo, and T. Ohshima.** 1999. An AMP-dependent (ATP-forming) kinase in the hyperthermophilic archaeon *Pyrococcus furiosus*: characterization and novel physiological role. Arch. Biochem. Biophys. **364:**125-8.

45. **Sapra, R., K. Bagramyan, and M. W. W. Adams.** The simplest respiratory system, proton reduction coupled to proton translocation. Submitted.

46. **Sapra, R., M. F. Verhagen, and M. W. W. Adams.** 2000. Purification and characterization of a membrane-bound hydrogenase from the hyperthermophilic archaeon *Pyrococcus furiosus*. J. Bacteriol. **182:**3423-8.

47. **Schafer, T., and P. Schonheit.** 1993. Gluconeogenesis from pyruvate in the hyperthermophilic archaeon *Pyrococcus furiosus* - involvement of reactions of the Embden-Meyerhof pathway. Arch. Microbiol. **159:**354-363.

48. **Schena, M., D. Shalon, R. W. Davis, and P. O. Brown.** 1995. Quantitative monitoring of gene-expression patterns with a complementary-DNA microarray. Science **270:**467-470.

49. **Schut, G. J., A. L. Menon, and M. W. W. Adams.** 2001. 2-ketoacid oxidoreductases from *Pyrococcus furiosus* and *Thermococcus litoralis*. Methods Enzymol. **331:**144-58.

50. **Schut, G. J., J. Zhou, and M. W. W. Adams.** 2001. DNA microarray analysis of the hyperthermophilic archaeon *Pyrococcus furiosus*: evidence for a new type of sulfur-reducing enzyme complex. J. Bacteriol. **183:**7027-36.

51. **Selig, M., K. B. Xavier, H. Santos, and P. Schonheit.** 1997. Comparative analysis of Embden-Meyerhof and Entner-Doudoroff glycolytic pathways in hyperthermophilic archaea and the bacterium *Thermotoga*. Arch. Microbiol. **167:**217-32.

52. **Siebers, B., H. Brinkmann, C. Dorr, B. Tjaden, H. Lilie, J. van der Oost, and C. H. Verhees.** 2001. Archaeal fructose-1,6-bisphosphate aldolases constitute a new family of archaeal type class I aldolase. J. Biol. Chem. **276:**28710-8.

53. **Steen, I. H., D. Madern, M. Karlstrom, T. Lien, R. Ladenstein, and N. K. Birkeland.** 2001. Comparison of isocitrate dehydrogenase from three

hyperthermophiles reveals differences in thermostability, cofactor specificity, oligomeric state, and phylogenetic affiliation. J. Biol. Chem. **276:**43924-31.

54. **Stetter, K. O.** 1999. Extremophiles and their adaptation to hot environments. FEBS Lett. **452:**22-5.

55. **Tsunasawa, S., S. Nakura, T. Tanigawa, and I. Kato.** 1998. Pyrrolidone carboxyl peptidase from the hyperthermophilic Archaeon *Pyrococcus furiosus*: cloning and overexpression in *Escherichia coli* of the gene, and its application to protein sequence analysis. J. Biochem. (Tokyo) **124:**778-83.

56. **Tuininga, J. E., C. H. Verhees, J. van der Oost, S. W. Kengen, A. J. Stams, and W. M. de Vos.** 1999. Molecular and biochemical characterization of the ADP-dependent phosphofructokinase from the hyperthermophilic archaeon *Pyrococcus furiosus*. J. Biol. Chem. **274:**21023-8.

57. **Uriarte, M., A. Marina, S. Ramon-Maiques, I. Fita, and V. Rubio.** 1999. The carbamoyl-phosphate synthetase of *Pyrococcus furiosus* is enzymologically and structurally a carbamate kinase. J. Biol. Chem. **274:**16295-303.

58. **van der Oost, J., M. A. Huynen, and C. H. Verhees.** 2002. Molecular characterization of phosphoglycerate mutase in archaea. FEMS Microbiol. Lett. **212:**111-20.

59. **van der Oost, J., G. Schut, S. W. Kengen, W. R. Hagen, M. Thomm, and W. M. de Vos.** 1998. The ferredoxin-dependent conversion of glyceraldehyde-3-phosphate in the hyperthermophilic archaeon *Pyrococcus furiosus* represents a novel site of glycolytic regulation. J. Biol. Chem. **273:**28149-54.

60. **Verhees, C. H., J. Akerboom, E. Schiltz, W. M. de Vos, and J. van der Oost.** 2002. Molecular and biochemical characterization of a distinct type of fructose-1,6-bisphosphatase from *Pyrococcus furiosus*. J. Bacteriol. **184:**3401-5.

61. **Verhees, C. H., M. A. Huynen, D. E. Ward, E. Schiltz, W. M. de Vos, and J. van der Oost.** 2001. The phosphoglucose isomerase from the hyperthermophilic archaeon *Pyrococcus furiosus* is a unique glycolytic enzyme that belongs to the cupin superfamily. J. Biol. Chem. **276:**40926-32.

62. **Voorhorst, W. G., R. I. Eggen, E. J. Luesink, and W. M. de Vos.** 1995. Characterization of the *cel*B gene coding for beta-glucosidase from the hyperthermophilic archaeon *Pyrococcus furiosus* and its expression and site-directed mutation in *Escherichia coli*. J. Bacteriol. **177:**7105-11.

63. **Ward, D. E., S. W. Kengen, J. van Der Oost, and W. M. de Vos.** 2000. Purification and characterization of the alanine aminotransferase from the hyperthermophilic Archaeon *Pyrococcus furiosus* and its role in alanine production. J. Bacteriol. **182:**2559-66.

64. **Xavier, K. B., R. Peist, M. Kossmann, W. Boos, and H. Santos.** 1999. Maltose metabolism in the hyperthermophilic archaeon *Thermococcus litoralis*: purification and characterization of key enzymes. J. Bacteriol. **181:**3358-67.

65. **Xing, R. Y., and W. B. Whitman.** 1987. Sulfometuron methyl-sensitive and -resistant acetolactate synthases of the archaebacteria *Methanococcus* spp. J. Bacteriol. **169:**4486-92.

66. **Ye, R. W., W. Tao, L. Bedzyk, T. Young, M. Chen, and L. Li.** 2000. Global gene expression profiles of *Bacillus subtilis* grown under anaerobic conditions. J. Bacteriol. **182:**4458-65.

Table 4.1: ORFs whose expression is dramatically up-regulated in maltose-grown cells and their potential operon arrangement.

ORF number	Description [a]	Mean intensity ratio (log_2±SD [b])	Change in expression (fold) [c]
PF0101	[Conserved hypothetical protein]	4.4±2.5	21.1
TCA cycle			
PF0201	[Aconitase]	2.4±0.5	5.3
PF0202	Isocitrate dehydrogenase (53)	2.4±0.5	5.3
PF0203	Citrate synthase (35)	4.1±1.2	17.1
[Glutamate biosynthesis]			
PF0204	[Conserved hypothetical protein]	4.3±0.7	19.7
PF0205	[Glutamate synthase, alpha]	3.8±0.9	13.9
PF0206	[Conserved hypothetical protein]	3.2±0.9	9.2
[Arginine biosynthesis]			
PF0207	[Argininosuccinate synthase]	2.8±1.4	7.0
PF0208	[Argininosuccinate lyase]	2.4±1.6	5.3
PF0209	[Ribosomal protein s6 modification protein]	1.6±0.7	3.0
PF0272	Alpha-amylase (27, 28)	4.7±1.7	26.0
PF0371	[Putative transporter]	3.1±1.2	8.6
PF0428	[Partial alanyl-tRNA synthetase]	2.7±0.9	6.5
PF0429	[Putative proline permease]	2.9±0.8	7.5
PF0450	[Glutamine synthetase I]	4.3±0.7	19.7
PF0464	Glyceraldehydes-3-P Fd oxidoreductase (36)	2.5±0.5	5.8
PF0514	[Alanine glycine permease]	2.4±0.8	5.3
PF0651	[Conserved hypothetical protein]	2.4±0.7	5.3
[Unknown]			
PF0881	[ABC transporter]	3.1±0.7	8.6

PF0882	[Hypothetical protein]	3.6±0.7	12.1
PF0883	[Conserved hypothetical protein]	2.2±1.0	4.6
PF0884	[Conserved hypothetical protein]	3.6±0.6	12.1

[Branched amino acid biosynthesis]

PF0935	[Acetolactate synthase]	4.1±0.4	17.1
PF0936	[Ketol-acid reductoisomerase]	5.0±2.5	32.0
PF0937	[2-Isopropylmalate synthase]	2.7±0.5	6.5
PF0938	[3-Isopropylmalate dehydratase, large]	2.6±0.3	6.1
PF0939	[3-Isopropylmalate dehydratase, small]	2.3±0.6	4.9
PF0940	[3-Isopropylmalate dehydrogenase]	2.6±0.4	6.1
PF0941	[Alpha-isopropylmalate synthase]	2.3±0.4	4.9
PF0942	[Dihydroxy-acid dehydratase]	2.5±0.5	5.7
PF0962	[Hypothetical protein]	2.4±0.6	5.3
PF1025	[Conserved hypothetical protein]	2.5±0.7	5.7

[Serine/threonine biosynthesis]

PF1052	[Probable aspartokinase]	4.7±1.1	26.0
PF1053	[Aspartokinase II, alpha]	5.6±2.0	48.5
PF1054	[Homoserine kinase]	5.0±2.3	32.0
PF1055	[Threonine synthase]	4.8±1.6	27.9
PF1056	[Aspartate-semialdehyde dehydrogenase]	4.0±1.0	16.0
PF1104	[Homoserine dehydrogenase]	3.0±0.5	8.0

[Unknown]

PF1109	[Hypothetical protein]	3.4±0.7	10.6
PF1110	[Hypothetical protein]	2.2±0.8	4.6

[Unknown]

PF1129	[Conserved hypothetical protein]	2.2±0.2	4.5
PF1130	[Conserved hypothetical protein]	2.5±0.3	5.5

[Methionine biosynthesis]

PF1266	[Cystathionine gamma-lyase]	4.6±1.4	24.3
PF1267	[Conserved hypothetical protein]	4.4±1.7	21.1
PF1268	[Conserved hypothetical protein]	5.5±16	45.3
PF1269	[Methionine synthase]	4.4±1.5	21.1
Ferredoxin:NADPH oxidoreductase I			
PF1327	Fd NADPH oxidoreductase, alpha (32)	2.5±0.7	5.7
PF1328	Fd NADPH oxidoreductase, beta (32)	2.5±0.6	5.7
[Unknown]			
PF1536	[Conserved hypothetical protein]	2.1±0.6	4.3
PF1537	[Conserved hypothetical protein]	1.9±0.7	3.7
PF1538	[N-ethylammeline chlorohydrolase]	3.2±06	9.2
PF1592	[Tryptophan synthase, beta]	3.6±0.5	12.1
[Histidine biosynthesis]			
PF1657	[Histidyl-tRNA synthetase]	3.4±0.5	10.6
PF1658	[ATP phosphoribosyltransferase]	3.5±2.1	11.3
PF1659	[Histidinol dehydrogenase]	2.8±0.5	7.0
PF1661	[Glutamine amidotransferase]	2.0±0.4	4.0
PF1662	[HisA]	2.4±1.0	5.3
PF1663	[Imidazoleglycerol-phosphate synthase]	2.8±0.4	7.0
PF1665	[histidinol-phosphate aminotransferase]	2.0±0.9	4.0
PF1670	[Alkaline serine protease]	3.0±0.4	8.0
[Branched amino acid biosynthesis]			
PF1678	[2-Isopropylmalate synthase]	5.4±1.5	42.2
PF1679	[3-Isopropylmalate dehydratase, large]	5.0±1.4	32.0
PF1680	[3-Isopropylmalate dehydratase, small]	3.0±0.6	16.0
[Ornithine biosynthesis]			
PF1682	[Ribosomal protein s6 modification protein]	3.5±0.6	11.3
PF1683	[N-acetyl-γ-glutamyl-phosphate reductase]	3.8±1.0	13.9

PF1684	[Acetylglutamate kinase]	3.1±0.6	8.6
PF1685	[Acetylornithine aminotransferase]	2.4±0.5	5.3
PF1686	[Acetylornithine deacetylase]	2.9±2.5	7.5

[Aromatic amino acid biosynthesis]

PF1687	[Conserved hypothetical protein]	2.1±1.0	4.3
PF1688	[Transketolase N-terminal section]	3.3±0.8	9.8
PF1689	[Transketolase C-terminal section]	2.1±0.6	4.3
PF1690	[2-Dehydro-3-deoxyphosphoheptonate aldolase]	3.1±0.5	8.6
PF1692	[3-Dehydroquinate dehydratase]	2.7±0.4	6.5
PF1693	[Shikimate 5-dehydrogenase]	4.1±2.3	17.1
PF1694	[Archaeal shikimate kinase]	2.7±0.5	6.5

[Aromatic amino acid biosynthesis]

PF1699	[3-Phosphoshikimate 1-carboxyvinyltransferase]	2.3±0.9	4.9
PF1700	[Chorismate synthase]	2.0±0.3	4.0
PF1701	[Chorismate mutase]	2.9±2.1	7.5
PF1702	[Aspartate aminotransferase]	4.1±0.5	17.1
PF1703	[Prephenate dehydrogenase]	3.9±0.7	14.9
PF1706	[Tryptophan synthase, subunit beta]	2.1±0.5	4.3
PF1708	[Anthranilate synthase component II]	2.1±1.0	4.3
PF1709	[Anthranilate synthase component I]	2.7±1.4	6.5
PF1710	[Anthranilate phosphoribosyltransferase]	2.9±1.0	7.5
PF1711	[Indoleglycerol phosphate synthase]	4.1±0.7	17.1
PF1713	[Carbamoyl-phosphate synthase, small]	3.0±1.1	8.0
PF1739	[Trehalose/maltose binding protein]	2.6±0.6	6.1

[Maltose transport]

PF1740	[Trehalose/maltose transport protein]	3.6±0.7	12.1
PF1741	[Trehalose/maltose transport protein]	3.4±0.5	10.6

PF1742	[Trehalose synthase]	3.4±0.8	10.6
PF1784	ADP-Phosphofructokinase (56)	2.5±0.5	5.8
PF1852	[Glutamate synthase, small]	2.6±0.5	6.1
PF1870	[Hypothetical protein]	4.0±1.7	16.0
[Maltose transport]			
PF1935	Amylopullulanase (12)	2.3±0.8	4.9
PF1936	[Sugar transport protein]	2.4±0.7	5.3
PF1937	[Sugar transport protein]	2.6±0.8	6.1
PF1938	Maltotriose binding protein (15)	2.1±0.3	4.3
PF1951	[Partial asparaginyl-tRNA synthetase]	4.2±1.1	18.4
PF1975	[Conserved hypothetical protein]	4.5±1.9	22.6

[a]The ORF description is derived either from the annotation (http://comb5-156.umbi.umd.edu/genemate: given within brackets), or from the indicated reference where there is experimental data to support the ORF assignment specifically in *P. furiosus* (given without brackets). Potential operons are indicated by shaded boxes where the intergenic distances are less than 30 nt.

[b]The intensity ratio is expressed as a $\log_2$ value so that the standard deviation can be given. For comparison between ORFs, the apparent change in the expression level is also indicated. ORFs are listed that are more than 5-fold regulated or that are potentially part of an operon with > 5-fold regulated ORFs but themselves are regulated by at least 3-fold.

Table 4.2. ORFs whose expression is dramatically up-regulated in peptide-grown cells and their potential operon arrangement.

ORF number	Description[a]	Mean intensity ratio (log_2±SD)[a]	Change in expression (-fold)[a]
PF0289	[Phosphoenolpyruvate carboxykinase]	-2.9±0.5	7.5
Aminopeptidase			
PF0366	[Conserved hypothetical protein]	-1.9±0.5	3.7
PF0368	[Conserved hypothetical protein]	-1.8±0.3	3.5
PF0369	Deblocking aminopeptidase (55)	-1.8±0.9	3.5
PF0370	[Phosphoglycerate dehydrogenase]	-2.6±0.4	6.1
PF0477	Alpha amylase (25)	-2.4±0.5	5.3
[Cobalt metabolism]			
PF0528	[Cobalt transport ATP-binding protein]	-2.4±0.7	5.3
PF0529	[Conserved hypothetical protein]	-2.1±0.8	4.3
PF0530	[Conserved hypothetical protein]	-1.6±1.1	3.0
PF0531	[Cobalamin biosynthesis protein]	-2.2±0.8	4.6
Aryl 2-ketoacid metabolism			
PF0532	Acetyl-CoA synthetase II alpha (33)	-2.8±0.9	7.0
PF0533	Indolepyruvate Fd oxidoreductase alpha (49)	-2.2±0.6	4.6
PF0559	[Hydrogenase regulatory protein]	-2.4±0.9	5.3
PF0612	[Conserved hypothetical protein]	-2.8±1.1	7.0
PF0613	Fructose-1,6-bisphosphatase (40)	-3.9±0.7	15.5
PF0676	Carbamate kinase (57)	-2.5±0.8	5.6
PF0689	[Conserved hypothetical protein]	-2.5±1.7	5.6
PF0692	[Prismane]	-3.0±0.8	8.0
Hydrogenase I			

PF0891	Hydrogenase I beta (8)	-3.2±0.7	9.2
PF0892	Hydrogenase I gamma (8)	-3.7±0.8	13.0
PF0893	Hydrogenase I delta (8)	-3.4±0.8	10.6
PF0894	Hydrogenase I alpha (8)	-3.0±0.5	8.0
PF0913	[Conserved hypothetical protein]	-3.0±0.9	8.0
PF0915	[Conserved hypothetical protein]	-2.7±2.2	6.5
[Acetyl-CoA synthetase]			
PF0972	[Acyl carrier protein synthase]	-2.4±0.5	5.3
PF0973	[Acetyl CoA synthase]	-2.3±0.9	4.9
PF0974	[Conserved hypothetical protein]	-2.2±0.6	4.6
PF1057	[Phophoglycerate kinase]	-2.9±1.2	7.3
[Amino acid metabolism]			
PF1245	[d-Nopaline dehydrogenase]	-2.4±1.1	5.1
PF1246	[Sarcosine oxidase, beta]	-2.3±0.7	4.9
PF1253	[Aspartate transaminase]	-2.6±0.7	6.1
PF1341	[Aminomethyltransferase]	-2.9±0.3	7.5
2-keto acid ferredoxin oxidoreductases			
PF1767	2-Ketoglutarate Fd oxidoreductase, delta (49)	-2.9±0.5	7.5
PF1768	2-Ketoglutarate Fd oxidoreductase alpha (49)	-3.2±0.5	9.2
PF1769	2-Ketoglutarate Fd oxidoreductase beta (49)	-2.5±0.9	5.6
PF1770	2-Ketoglutarate Fd oxidoreductase gamma (49)	-3.0±1.0	8.0
PF1771	[2-Ketoacid Fd oxidoreductase, alpha]	-2.7±0.4	6.5
PF1772	[2-Ketoacid Fd oxidoreductase, beta]	-2.4±0.6	5.3
PF1773	[2-Ketoacid Fd oxidoreductase, gamma]	-2.5±0.6	5.6
PF1874	[Glyceraldehyde-3-P dehydrogenase]	-3.2±0.8	9.3
[Ferredoxin:NADPH oxidoreductase II]			

PF1910	[Fd NADPH oxidoreductase II]	-4.1±0.8	17.1
PF1911	[Fd NADPH oxidoreductase II]	-3.8±0.7	13.9
[Unknown]			
PF2001	[Conserved hypothetical protein]	-3.6±1.1	12.2
PF2002	[Sucrose transport protein]	-3.4±0.9	10.6
PF2047	[l-Asparaginase]	-2.4±1.0	5.3

[a]See Table 4.1 for details

Table 4.3. Activities and expression levels of key metabolic enzymes.

Enzyme[a]	Peptides (U/mg)[d]	Maltose (U/mg)[d]	Ratio (-fold) [d]	Peptides (signal intensity)[e]	Maltose (signal intensity)[e]	Ratio (-fold)[f]
Acetolactate synthase[b]	0.0001 ± 0.0001	0.004 ± 0.001	+40	1685	28160	+17.1
Isocitrate dehydrogenase[b]	0.06 ± 0.03	0.15 ± 0.08	+2.5	4921	24940	+5.1
GAPDH[b]	0.07 ± 0.02	0.01 ± 0.004	-7.0	21051	1967	-9.3
Amylase[b]	4.9 ± 1.7	26.1 ± 8.7	+5.3	1874	30126	+26.0
Carbamate kinase[b]	0.07 ± 0.02	0.06 ± 0.03	-1.2	19579	3152	-5.7
Carbamoyl phosphate synthetase[b]	0.01 ± 0.007	0.02 ± 0.009	+2.0	8382	21041	+2.3
GAPOR[c]	0.42 ± 0.38	2.25 ± 0.85	+5.4	4340	24580	+5.8
GDH[c]	5.70 ± 0.67	0.73 ± 0.20	-7.8	54613	12807	-4.4
POR[c]	4.95 ± 1.60	4.89 ± 0.87	1.0	46512	29744	-1.5
KGOR[c]	0.44 ± 0.02	0.20 ± 0.03	-2.2	24841	2654	-9.4
IOR[c]	0.25 ± 0.09	0.02 ± 0.01	-12.5	33474	7281	-4.7
VOR[c]	1.80 ± 0.61	0.79 ± 0.08	-2.3	33699	24435	-1.4
ACS I[c]	0.35 ± 0.12	0.15 ± 0.01	-2.3	34988	28575	-1.2
ACS II[c]	0.08 ± 0.02	0.08 ± 0.04	1.0	32985	4536	-6.8
PPS[c]	1.59 ± 0.09	1.02 ± 0.55	-1.6	54969	45403	-1.2
H_2ase I+II[c]	0.39 ± 0.06	0.16 ± 0.10	-2.4	37936	5102	-7.8

[a]Abbreviations: GAPDH, glyceraldehydes-3-phosphate dehydrogenase; GAPOR, glyceraldehyde-3-ferredoxin (Fd) oxidoreductase; GDH, glutamate dehydrogenase; POR, pyruvate Fd oxidoreductase; KGOR, 2-ketoglutarate Fd oxidoreductase; IOR, indolepyruvate: Fd oxidoreductase; VOR, 2-ketoisovalerate Fd oxidoreductase; ACS, acetyl-CoA synthetase; PPS, phosphoenolpyruvate synthetase; H_2ase I+II, hydrogenase I and hydrogenase II.

[b]This study.

[c]Taken from ref. (1)

[d]Units are defined as µmole product formed per min per mg of protein. The ratio indicates if they increase (+) or decrease (-) in maltose-grown cells compared to peptide-grown cells.

[e]Average values from eight hybridization experiments carried out in duplicate. Only values for the alpha subunits are given for heteromeric proteins.

[f]The -fold regulation indicates if expression is up- (+) or down (-) regulated in maltose-grown cells and is calculated from the average $\log_2$ values (see Tables 5.1 and 5.2).

Table 4.4. Relative expression of genes involved in glucose catabolism and synthesis.

ORF number[a]	Description[a]	Mean intensity ratio (log_2 ±SD) [ab]	Relative expression (maltose/ peptide x 1000)[c]
Glycolysis			
PF0312	ADP-glucokinase (26)	1.1±0.5	27/13
PF0196	Glucose-6-P isomerase (19)8)	**+2.3±0.4**	17/4
PF1784	ADP-phosphofructokinase (56)	**+2.5±0.5**	27/5
PF0464	Glyceraldehydes-3-P Fd oxidoreductase (36)	**+2.5±0.5**	25/4
PF1188	[Pyruvate kinase]	-0.6±0.6	4/6
Glycolysis and gluconeogenesis			
PF1956	Fructose-1,6-bisphosphate aldolase (52)	0.3±0.5	25/23
PF1959	Phosphoglycerate mutase (58)	1.7±0.4	28/8
PF0215	Enolase (39)	1.3±0.6	25/11
PF0971	Pyruvate Fd oxidoreductase gamma (49)	0.1±0.3	32/29
PF0967	Pyruvate Fd oxidoreductase delta (49)	-0.7±0.5	26/41
PF0966	Pyruvate Fd oxidoreductase alpha (49)	-0.7±0.3	29/46
PF0965	Pyruvate Fd oxidoreductase beta (49)	-0.5±0.3	31/45
PF1540	Acetyl-CoA synthetase alpha (33)	-0.3±0.4	29/35
PF1787	Acetyl-CoA synthetase beta (33)	-0.6±0.3	21/32
PF1920	[Triose phosphate isomerase]	+2.2±0.6	21/4
Gluconeogenesis			
PF0043	Phosphoenolpyruvate synthetase (22)1)	0.2±0.8	34/31
PF0613	Fructose-1,6-bisphosphatase (40)	**-3.9±0.7**	3/36
PF1874	[Glyceraldehydes-3-P dehydrogenase]	**-3.2±0.8**	2/21
PF1057	[Phosphoglycerate kinase]	**-2.9±1.2**	1/8

[a]See Table 4.1 for details.
[b]ORFs that are significantly up (+) or down (-) regulated in the presence of maltose are indicated in bold (p-values <0.05).
[c]Relative expression is signal intensity in peptide-grown cells/signal intensity in maltose-grown cells divided by 1,000 for each ORFs (16 data points).

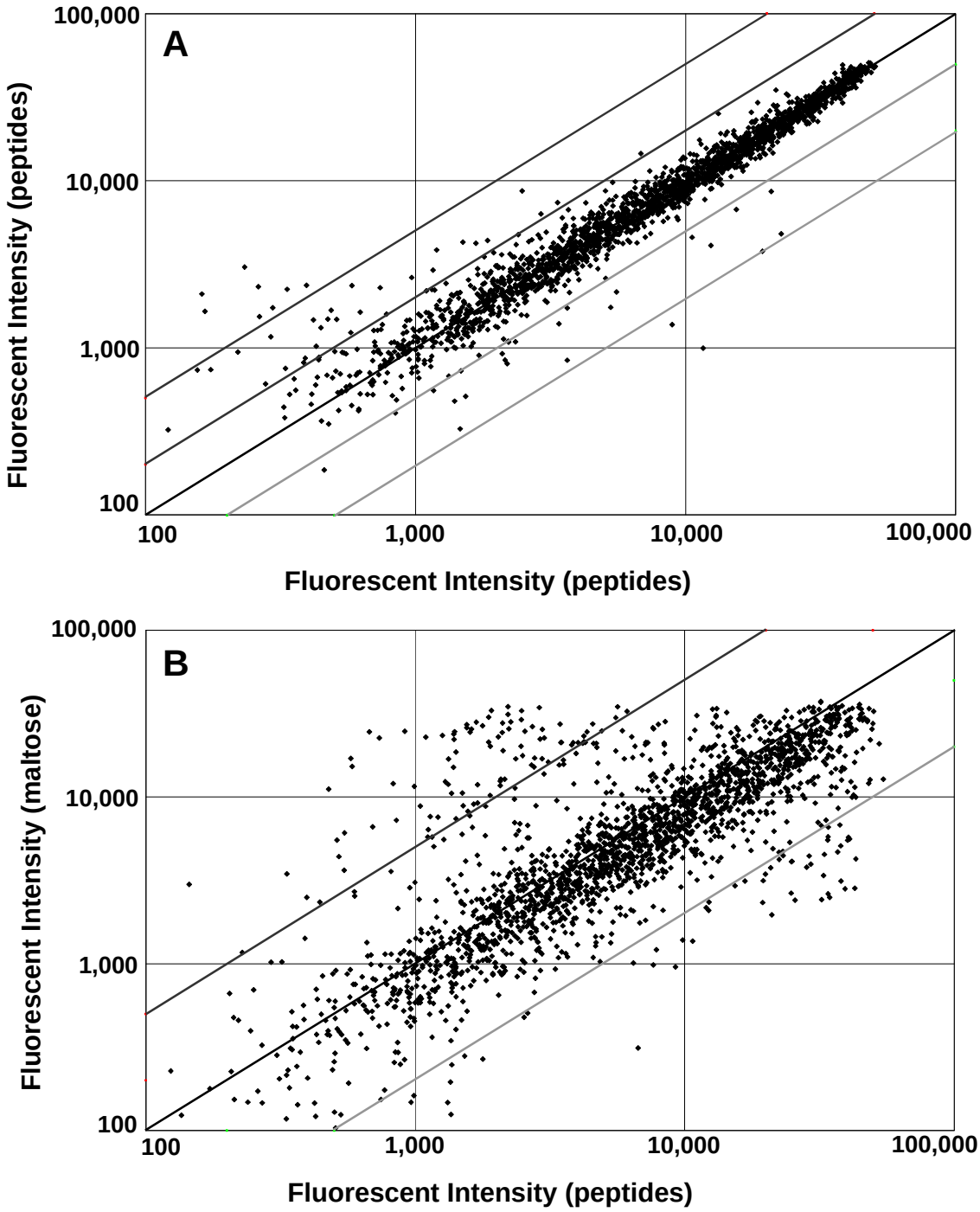

Figure 4.1. Fluorescence intensities of DNA microarrays. A) cDNA vs cDNA derived from two independent cultures of cells grown with peptides as the carbon source. B) cDNA vs cDNA derived from two independent cultures of cells grown with peptides or maltose as the carbon source. In A), the upper and lower diagonal line pairs indicate 2-fold and 5-fold changes in the signal intensities, respectively, while only the lines indicating 5-fold changes are given in B). See text for details.

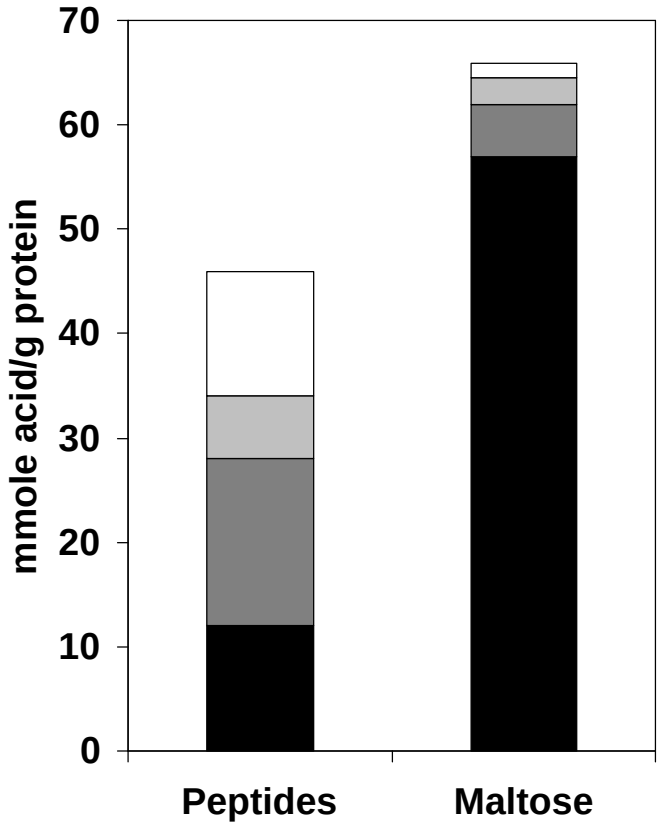

Figure 4.2. Organic acid production by *P. furiosus.* Spent media of cells grown using either peptides or maltose as the carbon source were analyzed for acetate (black), isovalerate (dark gray), (iso)butyrate (light gray) and phenylacetate (white).

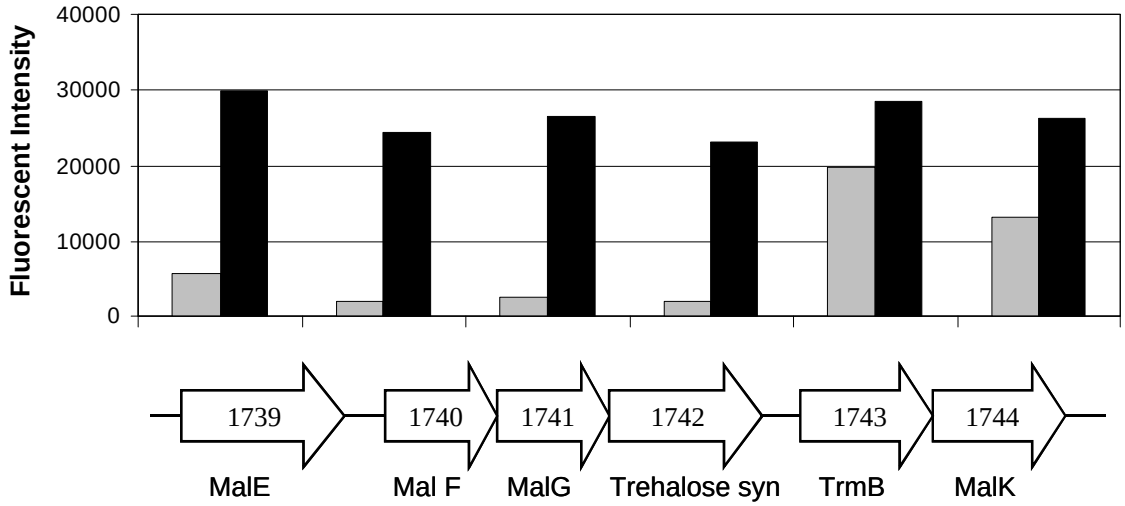

Figure 4.3. Expression of ORFs of the Mal I operon in the presence of peptides or maltose. The six ORFs encoding the subunits of the maltose transporter I are arranged according to their genome positions. The relative signal intensities for cDNA obtained from cells grown on peptides (gray bars) or maltose (solid bars) are indicated (actual values with SD are given in Table 4.2).

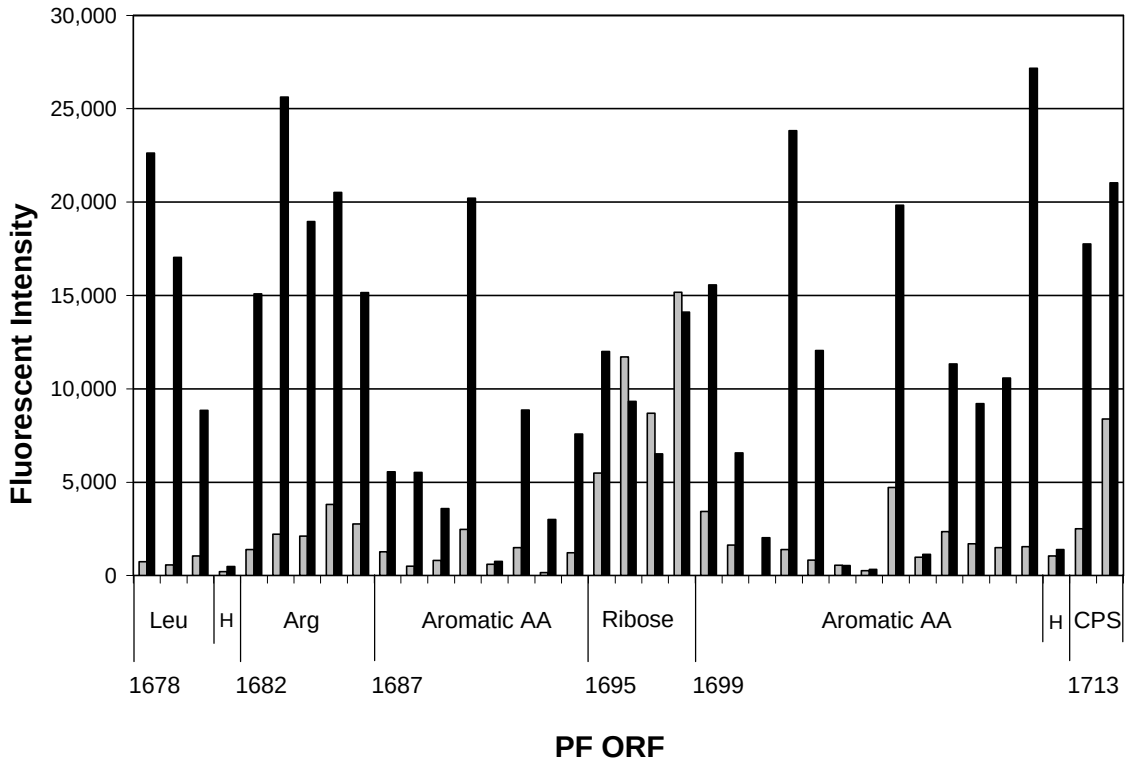

Figure 4.4. Expression and genome organization of PF1678 to PF1714. The ORFs encoding the subunits of homologs to enzymes involved in the biosynthesis of leucine (Leu), arginine (Arg), aromatic amino acids and carbamoyl phosphate (CPS), in the transport of ribose (Ribose), and hypothetical (H) ORFs, are indicated. The relative signal intensities are displayed for cDNA obtained from cells grown on peptides (gray bars) or maltose (solid bars).

CHAPTER 5

DISCUSSION AND CONCLUSIONS

Within the last decade the availability of whole genome sequences has revolutionized the study of prokaryote metabolism. At the beginning of 2003 the genome sequences of 103 prokaryotes were publicly available and 16 of these were from archaea (www.ncbi.nlm.nih.gov/PMgifs/Genomes/micr.html). With of the availability of these sequences, DNA microarray analysis has become, in just the last two year or so, a method to study prokaryote physiology. A big advantage with the prokaryote systems is the relatively small genome size. With space for 20,000 or more elements on a DNA microarray, the entire genome of even the largest prokaryote can be analyzed multiple times on one slide, in contrast to the situation with eukaryotes such as human. A limitation to interpreting the results microarray analysis is the lack of complete annotation in genome sequences. Even in an extremely well studied organisms such as *E. coli* less than two-thirds of the genome is so-called known (13). In *P. furiosus* about half of the ORFs in the genome have been annotated but only few of them have been described in the literature.

In chapter 2, the 2-ketoacid ferredoxin oxidoreductase enzyme family of *P. furiosus* is described at the biochemical as well as the molecular level and such information is of great assistance in interpreting microarray results. The result of DNA microarray analyses is beginning to revolutionize our understanding of the physiology of *P. furiosus*. In chapters 3 and 4, the three hydrogenases of *P. furiosus* were studied with respect to their regulation and their involvement in the bioenergetics and the pathways of electron flow in this organism. Initially, a novel dual function was proposed for the

cytosolic hydrogenases in which they reduce both protons as well as S° (105, 108). With the finding that the expression of the genes of all three hydrogenases are down-regulated in a S°-containing medium, a role in S° metabolism for any of these enzymes is unlikely and thus an unknown S°-reducing system must be present. Two previously uncharacterized ORFs were highly up-regulated in S°-containing media, and these were tentatively named SipA and SipB (for S° induced protein). These might participate in S° reduction although biochemical data has yet to be obtained to confirm the nature of the S° reducing system in *P. furiosus* and the role, if any, of the Sip proteins. Chapter 4 describes the results obtained using a directed DNA microarray (271 ORFs) to investigate S°-metabolism in *P. furiosus*. It represents the first such study in an archaeon or hyperthermophile.

Chapter 5 describes the results of a study in which the expression of the ORFs in the entire *P. furious* genome was determined in cells grown on peptides and on maltose. The amount of data generated with DNA microarrays is overwhelming and choices have to be made in presenting such data. For example, the ORFs of greatest significance are those for which additional information is available such as biochemical characterization in *P. furiosus* or related species. In the case of comparing of cells grown on peptide and maltose, regulation was observed in five major types of proteins, those involved in degrading amino acids, hydrolyzing starch, transport, amino acid biosynthesis and in glycolysis. One of the best understood transport systems in hyperthermophilic archaea is the maltose transporter of *Thermococcus (Tc) litoralis*. This maltose transporter consists of a maltose binding protein (MalE), two transmembrane proteins (MalF and G), an uncharacterized ORF annotated as trehalose synthase, a transcriptional regulator (TrmB) and an ATPase subunit (MalK). The corresponding maltose transporter in *P. furiosus* is

almost identical to that of *Tc. litoralis* and is thought to have arisen by horizontal transfer (36). In *P. furiosus* the elements for the transporter are clustered together and potentially form three transcript units (Figure 5.1). This cluster is highly regulated by its substrate maltose and Figure 5.1 shows the expression pattern of ORFs PF1739-1744 coding for the transporter. PF1743 and 1744 are clearly expressed in the absence of maltose. PF1743 codes for TrmB, a transcriptional maltose-sensitive repressor of MalE which presumably also regulates the other two transcript units (99). It was demonstrated that in the absence of maltose TrmB interferes with the transcription of *mal*E, and only low levels of transcripts were formed compared to the control without TrmB (99). Interestingly low transcript levels of *mal*E were also observed in the microarray data. It will be very interesting to see what effect TrmB has on the other two transcript units in an in vitro transcription experiment to complement the microarray data.

The genome sequence of *P. furiosus* revealed that in the region from PF1657 to PF1715 there are several ORFs that potentially code for enzymes involved in the biosynthesis of histidine, ornithine, arginine, branched amino acids and aromatic amino acids. About 80% of the ORFs in this region are potentially involved in amino acid biosynthesis, and the expression of most of them is up-regulated in the maltose-containing medium. *P. furiosus* is probably able to synthesize all amino acids and this allows it to grow well on carbohydrates (www.genome.ad.jp/kegg/kegg2.html). In contrast, *P. horikoshii* and *P. abyssi* lack several of the ORFs coding for several key enzymes of amino acid biosynthesis, such as histidine and arginine, and this may account for why they do not grow solely on carbohydrates (98).

Sugar Metabolism in *P. furiosus*

With most bacteria the identity of their glycolytic enzymes is obvious in searches of their genome sequences (www.genome.ad.jp/kegg/kegg2.html). However analysis of the *P. furiosus* genome sequence does not automatically yield obvious candidates for all of the ORFs coding for glycolytic enzymes. Biochemical and molecular studies have shown that six out of the nine glycolytic enzymes are encoded by novel genes, even though some of them perform the 'normal' reaction. All six of the novel enzymes have been characterized on a biochemical level, and the other three can be easily identified based on sequence homology, therefore, all ORFs encoding glycolytic enzymes can be accounted for in *P. furiosus*. Interestingly none of these enzymes in the *P. furiosus* pathway are reported to be allosterically regulated. Microarray results show that the mechanism of regulation for *P. furiosus* is mainly at the transcriptional level. Figure 5.2 illustrates the control points in the glycolytic and glyconeogenic pathways. Four glycolytic enzymes are strongly up-regulated during growth on maltose (PGI, PFK, GAPOR and TPI), while three gluconeogenic enzymes are strongly up-regulated in the peptides grown cultures (GAPDH, PFK and FBP). It seems that the latter three enzymes are the major regulation points for the switch between gluconeogenesis and glycolysis. In contrast, the glycolytic pathway in *E. coli* does not seem to be very strongly regulated at the transcriptional level when comparing acetate and glucose grown cells (119).

Regulation of the glycolytic pathway in the Crenarchaote *Thermoproteus (Tt) tenax* has been studied extensively. For example, the GAPN (non-phosphorylating GAPDH) and GAPDH enzymes are differentially regulated between glycolysis and gluconeogenesis. GAPN catalyzes essentially the same reaction as GAPOR in *P. furiosus* except that NAD is the electron acceptor. GAPN is mainly expressed when carbohydrates

are the major carbon source while GAPDH functions in gluconeogenesis when cells are grown autotrophically (23, 24). The difference is that GAPN is not transcriptionally regulated but instead its activity is inhibited by NADPH, NADP, NADH, and ATP and positively regulated by glucose-1-P, AMP, fructose-6-P, ADP, fructose-1-P and ribose-5-P (22). Apparently, allosteric regulation does exist for some of the glycolytic enzymes in the hyperthermophilic archaea. On the other hand, the GAPDH enzyme of *Tt. proteus* is regulated at the transcription level rather than allosterically, and in this sense it resembles the *P. furiosus* enzyme (24). Pyruvate kinase (PK) enzyme is another example of a regulatory difference between the two organisms. In *Tt. Tenax*, PK is transcriptionally regulated but this is not the case in *P. furiosus* (155). Searches of the available archaeal genome sequences indicate that the glycolytic enzymes of *P. furiosus* are not universally conserved within the archaea although none of them appear to utilize a 'normal' EM pathway for their glycolysis. Several version of a modified EM pathway exist and these include ADP-, pyrophosphate-, and ATP-dependent sugar kinases, and phosphate-independent GAPDH and GAPOR (Figure 5.3).

ORFs involved in glycolysis, gluconeogenesis and pyruvate metabolism in *P. furiosus* were used to search the genome sequences of archaea with an emphasis on those of the hyperthermophiles. Table 5.1 summarizes the results and shows homologs of the various glycolytic enzymes (EM-pathway) in the various organisms. Those containing an ED pathway are included because both EM and ED pathways overlap in the lower half at the level of triosephosphates and organisms that utilize an ED type pathway often use the EM type pathway for gluconeogensis (154). In the following the glycolytic enzymes are examined one by one to determine what general conclusions can be made about the distribution of these archaeal enzymes.

ADP-Dependent Glucokinase

The ADP-dependent kinase (ADP-GLK) of *P. furisosus* is not related to the classical bacterial glucokinase or to the eukaryal hexokinase but instead is part of a unique family that includes ADP-dependent phosphofructokinases (82, 87, 176). ADP-GLK is also found in other *Pyrococcus* and *Thermococcus* species (87). Homologs of ADP-GLK can also be found in the genome sequence of the two *Methanosarcina* species (4), although for *M. mazei* ADP-glucokinase activity could not be detected in a cell-free extract (182). In *Methanocaldococcus (Mc) jannaschii*, a novel bifuntional sugar kinase has been found that is capable of carrying out both glucokinase and phosphofructokinase reactions with ADP as the phosphate donor (141). Consequently no separate phosphofructokinase has been identified in the *Mc. jannaschii* genome sequence. The activity of ADP-GLK has been measured in extracts of *Archaeoglobus (Ag) fulgidus* strain 7324, (93) but the genome sequence of a closely related strain (VC16) does not contain a homolog to either *P. furiosus* glucokinase or classical bacterial glucokinase (Table 5.1). Rather than ADP-GLK, homologs of ATP-dependent GLK are found among other archaea (Figure 5.3), including *Thermoplasma (Tp) volcanium*, *Tp. acidophilum*, *Aeropyrum (Ap) pernix*, and *Pyrobaculum (Pb) aerophylum* (www.genome.ad.jp/kegg/kegg2.html). For the two *Thermoplasma* species, a GLK homolog is not expected because these organisms appear to utilize a modified ED pathway for sugar degradation (26). So far the ATP-GLK has been biochemically characterized only from *Ap. pernix* (55).

Phosphoglucose Isomerase

The gene encoding phosphoglucose isomerase (PGI) has been cloned and characterized from *P. furiosus* (54, 181). This is the first PGI gene to be described for any archaeon, and it appears to be unrelated to its bacterial and eukaryal counterparts. Instead it belongs

to the so-called cupin superfamily of enzymes related to sugar metabolism (181). This type of PGI seems to be restricted to the *Pyrococcus* and *Methanosarcina* species (and probably *Thermococcus*). The ORF encoding PGI in *P. furiosus* apparently overlaps 25 nt with an adjacent ORF (PF0196). This suggests that both ORFs are co-transcribed however it was demonstrated by Northern blotting that PGI is monocistronic (181), a conclusion supported by microarray analysis (157). *Mc. jannashii* contains a homolog of the classical PGI gene (www.genome.ad.jp/kegg/kegg2.html). This is also the case for the archaea *Sl. solfataricus, Sl. tokodaii, Tp. volcanium, Tp. acidophilum, Pb. aerophilum* and *Ap. pernix*, all of which show highest similarity to the PGI gene of the bacterium *Aquifex (Af) aeolicus* (AA0750; (35)). Other archaea such as *Mp. kandleri*, *Mt. thermoautotrophicus* and *Ag. fulgidus* lack clear homologs to PGI.

Phosphofructokinase

The phosphofructokinase (PFK) in *P. furiosus* is a novel ADP-dependent enzyme that does not show homology to the classical ATP-dependent enzyme found in bacteria and eukarya (80, 87, 176). Interestingly, this enzyme is homologous to the ADP-glucokinase, indicating that they evolved by gene-duplication (176). This suggestion is supported by the finding that *Mc. jannaschii* contains a bifunctional ADP-dependent sugar kinase catalyzing both PFK and GLK reactions (141). Why these sugar kinases are ADP rather than ATP dependent is unclear but they are not restricted to hyperthermophiles. For example, the two sequenced *Methanosarcina* species contain homologs of both ADP-PFK and GLK, and ADP-PFK activity has been measured in extracts of the mesophile *Ms. mazei* (182). In both *Ms. acetivorans* and *Ms. mazei*, the PFK-coding ORFs cluster together with a potential GLK-coding ORF, indicating that these organisms might have separate PFK and GLK enzymes, in contrast to the situation in *Mc. jannaschii*. The

genome sequences of hyperthermophiles also contain homologs of conventional ATP-dependent sugar kinases such as those found in *Pb. aerophilum* and *Ap. pernix* (Figure 5.3). The PFK of *Ap. pernix* has been characterized and represents the first classical ATP-dependent PFK to be characterized from a hyperthermophile, an enzyme that is apparently not allosterically regulated (56). A third type of PFK exists in *Tt. tenax*. This enzyme is pyrophosphate (PPi)-dependent and is also found among some bacteria and eukaryotes (165). *Ag. fulgidus* seems not to contain any homolog of PFK, although for strain 7423, a ADP-dependent PFK activity has been measured in cell extracts (93).

Fructose-1,6-bisphosphate Aldolase

The reversible aldol cleavage in *P. furiosus* is performed by yet another new class of enzyme. *P. furiosus* fructose-1,6-bisphosphate aldolase (FBA) sequence shows signatures typical of class I aldolases but distinct enough to propose an archaeal class I aldolase (163). FBA is not involved in the irreversible ED type pathway, and consequently is not found in the *Thermoplasma* species. However, both *Sl. solfataricus* and *Sl. tokodaii* contain a FBA homolog, that is probably involved in gluconeogenesis (154). The absence of a candidate for FBA in *Pb. aerophilum* is puzzling, and it seems to be the only glycolytic enzyme missing in this organism (Table 5.1).

Triose Phosphate Isomerase

Table 5.1 shows that all sequenced archaea do have an obvious triose phosphate isomerase (TPI) homolog, indicating that TPI does not display extensive variation unlike some of the other glycolytic enzymes. This enzyme catalyzes a reversible reaction and does not take part in the ED pathway (regular or modified) but seems to be required for those organisms harboring an ED-type pathway apparently in order to perform gluconeogenesis. It has previously been noticed that the TPI of hyperthermophiles is

smaller (about 225 amino acids) than the TPI found in mesophiles such as *E. coli* (~ 255 amina acids; (88)). The structure of the enzyme from the hyperthermophile *P. woesei* has been determined and compared to the mesophilic homolog, is a more compact protein with several amino acid residues missing throughout the protein sequence (188). Interestingly, all archaea possess this smaller version of TPI (around 225 amino acids) while eukaryotes and bacteria, as well as the hyperthermophilic bacterium *Af. aeolicus*, contain the larger version (~ 250 amino acids).

Glyceraldehyde-3-phosphate Ferredoxin Oxidoreductase

Glyceraldehyde-3-phosphate ferredoxin oxidoreductase (GAPOR) is a novel tungsten-containing enzyme responsible for the direct conversion of glyceraldehyde-3-phosphate into 3-phosphoglycerate in a phosphate-independent manner (116). GAPOR is part of a family of tungsten-containing enzymes termed the AOR-type. Three of the five AOR-family members have been biochemically characterized, and each catalyzes the ferredoxin-dependent oxidation of aldehydes (137). From the crystal structure of one of these enzymes, aldehyde ferredoxin oxidoreductase (AOR), it has been shown that the tungsten is coordinated by two pterin ligands and that the protein contains a [4Fe-4S] cluster (28). The pterin ligands and the iron-sulfur cluster are coordinated by conserved amino acid residues. Based on sequence alignments, a typical GAPOR signature in the [4Fe-4S] cluster-coordinating residues was observed (CGEPCPXXC), while the other AOR family members contain a less conserved signature (CXXCXXXC; Oost (178)). Using this conserved signature, potential homologs to GAPOR can be found in *P. horikoshii*, *P. abyssi*, *Pb. aerophilum* and *Mc. jannaschii*. GAPOR Activity was measured in cell extracts of *Mc. jannaschii* (Schut and Oost, unpublished results), *Ag. fulgidus* strain 7423 (93), *Desulfurococcus amylolyticus* and *Tc. litoralis* (160).

Instead of GAPOR *Tt. tenax* contains an irreversible phosphate independent enzyme (GAPN) that converts GAP to 3-phosphoglycerate using NAD as the electron acceptor (22), and the same enzyme has also been proposed to be present in *Ap. pernix* (Figure 5.3; (55)).

Phosphoglycerate Mutase

Phosphoglycerate mutase (PGM) was the final glycolytic enzyme to be characterized in the glycolytic pathway of *P. furiosus*. This enzyme is responsible for interconverting 3-phosphoglycerate and 2-phosphoglycerate, and has been characterized from *P. furiosus* as well as *Mc. jannaschii* (50, 177). The archaeal enzyme is distantly related to bacterial PGMs and has been placed in it own family (177). PGM was the last 'missing-link' of the *P. furiosus* glycolytic pathway, and had been a subject of discussion since the organism was first described (43). This new family of PGM is present in all archaea whose genome has been sequenced (Table 5.1).

Enolase

The enolase of *P. furiosus* has been characterized and shows high similarity to enolases from various sources (123). Enolases can be identified in all archaeal genomes and represent the canonical type. They appear to be highly conserved throughout the three domains and have been helpful in constructing phylogenetic relations (175).

Pyruvate Kinase

As expected the final step in the glycolytic pathway of *P. furiosus* is carried out by the pyruvate kinase (PK). Although homologs of the PK are present in many of the archaeal genome sequences it seems to be missing in the autotrophs *Mp. kandleri*, *Mt. thermoautotrophicus* and strangely also in *Ag. fulgidus*. Interestingly, all three of these organisms also lack homologs of GLK, GPI, and PFK (Table 5.1). It is possible that

methanogens that are able to synthesize glycogen as a storage material (90) contain homologs of enzymes involved in the EM version of glycolysis and gluconeogenesis, in order that they can both synthesize and degrade this storage material. Another storage material, 2,3-cyclopyrophosphoglycerate, was detected in *Methanobacterium* species (174). *M. thermoautotrophicus* lacks obvious candidates for GLK, PFK and PK, which is puzzling because a pathway for glucose metabolism was proposed in this organism (41).

Glyceraldehyde-3-Phosphate Dehydrogenase and Phosphoglycerate Kinase

In *P. furiosus*, the glyceraldehyde-3-phosphate dehydrogenase (GAPDH) and phosphoglycerate kinase PGK enzymes are thought to function solely in gluconeogenesis (178). Archaeal GAPDH enzymes tend to have a dual cofactor specificity and have comparable activity with NAD and NADP, while bacterial and eukaryal enzymes are normally specific for NAD (24). The GAPDH and PGK homologs can be easily identified in all the archaeal genome sequences, even in those which use an ED-type glycolytic pathway. The GAPDH and PGK enzymes in all of these organisms probably function in gluconeogenesis when heterotrophic species grow on peptides as a carbon source or when autotrophic species utilized CO_2 (154).

Phosphoenolpyruvate Synthetase

PK normally catalyzes an irreversible reaction in the glycolytic direction and does not function in PEP formation. In gluconeogenesis, this step is usually performed by phosphoenolpyruvate synthetase (PPS). The *P. furiosus* enzyme was characterized and its catalytic properties were consistent with a function in gluconeogenesis (72). Surprisingly, relatively large amounts of this enzyme can be purified from cells grown with maltose and peptides as the carbon sources (72). In addition, high transcript levels are found in carbohydrate-grown cells (133). It had been suggested that the *P. furiosus* PPS might play

a novel glycolytic role, synthesizing ATP from PEP and AMP (140), but kinetic data do not support such a conclusion (72). Homologs of the *P. furiosus* enzyme can be found among all the archaea listed in Table 5.1. It will be interesting to see if these homologs are also constitutively expressed at high levels like that of *P. furiosus*.

Fructose-1,6-bisphosphatase

A classical version of the gluconeogenic enzyme, fructose-1,6-bisphosphatase (FBP), is not present in *P. furiosus* or in any of the sequenced archaeal genomes except in that of the mesophilic extreme halophile *Halobaceterium spp* (www.genome.ad.jp/kegg/kegg2.html). In *Mc. Jannaschii*, an enzyme with a dual activity, inositol-1-monophosphatase and FBP, was described (170), and homologs of this enzyme are found in several (but not all) archaea including *P. furiosus* (Table 5.1). The homolog in *P. furisosus* (PF2014) has its properties similar to those of the *Mc. jannaschii* enzyme and it was proposed to be involved in gluconeogenesis (180). Surprisingly, the ORF encoding FBP appears to be in an operon with a hypothetical membrane protein and an endonuclease for stalled replication forks (89), neither of which have any obvious relationship to gluconeogensis. At the same time, another study reported an alternative candidate for FBP in *Thermococcus (Tc) kodakaraensis* KOD1 (129). In contrast to PF2014, this enzyme is specific for fructose-1,6-bisphosphate. Homologs of this FBP can be found in most of the sequenced archaea, including *P. furiosus,* but it seems to be lacking in the *Methanosarcina* species (Tabel 6.1). So far only two bacteria possess homologs of this ‘archaeal’ type FBP, the hyperthermophile *Af aeolicus* (AQ1790) and the moderate thermophile *Thermoanaerobacter tengcongensis* (TTE0285). The *Tc. kodakaraensis* enzyme might represent the true FBP in archaea because the transcriptional regulation in *P. furiosus* and *Tc. kodakaraensis* of this ORF indicates a

function solely in gluconeogenesis (129, 157). Consistent with this, the inositol-1-monophosphatase/FBP in *P. furiosus* shows no regulation at the transcript level in peptide- and maltose-grown cell and is thus unlikely to be involved in gluconeogenesis (157, 180). Intriguingly, *Methanosarcina* species only contain a homolog of the inositol-1-monophosphatase/FBP enzyme, and it is adjacent to GAPDH, indicating that this protein might indeed have a gluconeogenic role and function as a FBP in at least some of these organisms but not *P. furiosus*.

Pyruvate Ferredoxin Oxidoreductase

In most aerobic organisms the NAD(P)-dependent pyruvate dehydrogenase (PDH) complex carries out the oxidative decarboxylation of pyruvate to acetyl-CoA. On the other hand, in anaerobic organisms, this reaction is performed by a ferredoxin-linked pyruvate oxidoreductase (POR). PORs have been purified from bacteria, eukarya and archaea (12, 21, 134). Most archaeal PORs contain four subunits (aß?d) and form octamers of approximately 240 kDa. They include the PORs from the hyperthermophilic archaea *P. furiosus*, *Tc. litoralis* and the hyperthermophilic bacterium *Thermotoga maritima* (85). Homologs of the four ORFs encoding the *P. furiosus* enzyme can be found in all but one of the archaea listed in Table 5.1. The exception is *Ap. pernix*, which is an obligate aerobe and presumably contains PDH. It is probably not capable of acetate production (139), although the presence of POR homologs in the other aerobic organisms listed in Table 5.1 indicates that they may be capable of acetate production. Interestingly, all of the aerobic archaea whose genome sequences are known (Sso, Sto, Tac, Tvo, Pae and Ape, see Table 5.1) also possess PDH, the aerobic analog of POR, (75, 84). All the methanogens listed also contain a POR homolog and it has been shown that some species

can take up acetate and incorporate this into cell carbon presumably by a reversal of the POR reaction (18, 162, 173).

ADP-Dependent Acetyl-CoA Synthetase

In archaea the conversion of acetyl-CoA to acetate is catalyzed by a novel ADP-dependent enzyme acetyl-CoA synthetase (ADP-ACS; (150)). This should not be confused with two unrelated enzymes. These are AMP-dependent acetyl-CoA synthetase (AMP-ACS) that is responsible for the acetate uptake in methanogens such as *Methanobacterium*, or with the acetyl-CoA synthase (or CO dehydrogenase) involved in CO_2 fixation in methanogens and acetogens (101, 151). Besides its presence in all acetate-forming archaea, ADP-ACS can also be found in eukarytic protists such as *Entamoeba histolytica* and *Giardia lamblia* in which it is also involved in carbohydrate fermentation (130, 142). In contrast, all acetate-forming bacteria use the two canonical enzymes phosphate acetyltransferase and acetate kinase for acetate formation and ATP generation (17, 154). The ADP-ACS enzyme from *P. furiosus* was characterized and represents a major energy conservation point in the both peptide and carbohydrate metabolism (113). From Table 5.1 it is clear that the ADP-ACS is widespread among the archaea. It seems to be absent from *Ap. pernix* which also lacks POR homologs. The other (micro)aerobic archaea *Pb. aerophilum*, *Tp. volcanium*, *Tp. acidophilum*, *Sl. solfataricus* and *Sl. tokodaii* do possess an ADP-ACS homolog, and in addition they also possess a AMP-ACS homolog (www.genome.ad.jp/kegg/kegg2.html). These organisms might be able to both produce and utilize acetate depending on the growth conditions. For the halophilic archaea, *Halococcus saccharolyticus* and *Haloferax volcanii*, it was shown that these organisms produce acetate from glucose using an ADP-ACS during exponential growth and this is reabsorbed during the stationary phase using an AMP-ACS (19). In

addition, in some acetoclastic methanogens, acetate can be activated with AMP-ACS while others such as *Methanosarcina* species use the canonical acetate kinase and phosphate acetyltransferase (73). Interestingly, all the methanogens with known genome sequences contain an ADP-ACS in addition to the enzymes for activation of acetate (and perhaps other organic acids). It is possible that these methanogens can produce acetate from intracellular storage materials under H_2 deprivation, and can take up organic acids from the medium and channel this into cell carbon (151, 173).

Applications of Four Dye DNA Microarrays

With a working protocol for microarray analysis of *P. furiosus* now demonstrated, it will be possible to monitor whole genome expression for a wide range of growth conditions. Even though the amount of data generated already is overwhelming, this is actually the beginning of the microarray analysis in archaea. The development of a four dye microarray system is seen as a significant development as it enables simultaneous comparisons of four different growth conditions. This is particularly powerful when applied to time course experiments, in which the culture is modified at time zero and samples are taken at subsequent time points. For example, a preliminary experiment was performed in which *P. furiosus* was grown on a peptide medium and maltose was added to the medium in mid log phase (time zero). RNA samples were taken at time zero and at 30, 60 and 120 min after maltose addition. This type of experiment is different from the steady-state comparison described in Chapter 5. Instead of comparing two different batch cultures, this is a kinetic experiment in which the carbon source of a culture is changed from peptides to peptides plus maltose. Essentially the effect that maltose has on a peptide grown culture, is followed over time with respect to global expression levels. The

dynamic nature of the global transcript changes over time is illustrated by scatterplots in Figure 5.4. At 30 min, relatively few ORFs are differentially regulated, at 60 min this marginally increases but at 120 min a large change in the global expression levels is apparent (Figure 5.4).

The microarray data obtained from the time course mainly follows two expression patterns, ORFs are either directly regulated (negatively of positively) after addition of maltose and stay regulated or ORFs are more slowly regulated (negatively or positively) and reach a constant level at 120 min. No ORFs were observed whose transcriptional regulation (negatively or positively) was maximal at 30 or 60 min compared to 0 min and 120 min. Table 5.2 shows that only about half of the ORFs that are more than 4-fold regulated in the steady-state peptide versus maltose comparison are also regulated by the addition of maltose to a peptide grown culture. Although the time course experiment is executed differently from the steady-state comparison, valuable information is still obtained to supplement the steady-state peptide versus maltose comparison. Tables 5.3 and 6.4 present those ORFs whose regulation is strongly affected at all the time points of the kinetic experiment as well as the steady-state comparison. What is clear from such data is that upon a change in carbon supply; *P. furiosus* takes about two generation times to completely response.

The two ferredoxin NADP oxidoreductases (FNOR I and II) in *P. furiosus* that were discussed in Chapter 5 provide an example of how useful information can be obtained from kinetic DNA microarray experiments. The ORFs coding for the putative FNOR II enzyme are rapidly down regulated by maltose indicating that it has a specific role in peptide metabolism. FNOR I was proposed to have a role in maltose (carbohydrate) metabolism (Chapter 5) but there was no evidence of this in the peptides

to maltose switch. The DNA microarray analysis has revealed several surprises about this intriguing enzyme pair although further biochemical analysis has to be carried out in order to understand their physiological functions. Another example is the expression of the maltose transport (Mal I) cluster which, as expected, is rapidly up-regulated in the presence of maltose presumably due to the release of the repression by its transcriptional regulator TrmB (99). Glyceraldehydes-3-P dehydrogenase (GAPDH) and fructose-1,6-bisphosphatase (FBPase) seem to be the major regulation points of the gluconeogenic pathway of *P. furiosus* and these ORFs are down-regulated very rapidly after the addition of maltose by an unknown metabolite (Table 5.2). Interestingly, their counterparts in glycolysis, glyceraldehydes-3-P ferredoxin oxidoreductase (GAPOR) and phosphofructokinase (PFK), appear to function as the major control points in this pathway (Table 5.3). It is unlikely that maltose directly affects the regulation of all of these enzymes and more likely candidates are glucose or glucose-6-P.

Although the peptide to maltose shift represents a pilot experiment, it demonstrates that such studies provide valuable data and considerably extend as well as complement the results from steady-state, batch-type experiments described in Chapter 5. Moreover, the kinetic-type experimental approach is particular well suited to investigate the effects of various stresses on global gene expression, such as heat and cold shock, oxidation stress and nutrient limitation, e.g. iron, and such studies are currently underway.

Table 5.1. Distribution of enzymes of the EM type pathway in archaea.

Enzyme/organism[a,b]	Pfu	Pho	Pab	Mja	Mac	Mma	Mka	Mth	Sso	Sto	Tac	Tvo	Pae	Afu	Ape
Glucokinase	0312	0589	0967	1604	3562	0472	-	-	-	-	0825[c]	3591[c]	3437[c]	-	2091[c]
Glucose-6-P isomerase	0196	1956	1199	1605[f]	0821	1968	-	-	2281[d]	2245[d]	1419[d]	1438[d]	1610[d]	-	0768[d]
Phosphofructokinase	1784	1645	2013	1604	3562	0473	-	-	-	-	-	-	0835[e]	-	0012[e]
Fructose-1,6-bis-P aldolase	1956	0082	0049	0400	0439	1627	1409	579	3226	2350	-	-	-	0108	0011
Triose-P isomerase	1920	1884	1208	1528	4607	1278	1664	1041	2592	2030	0313	1287	1501	1304	1538
Glyceraldehydes-3-P Fd oxidoreductase	0464	0457	1315	1185	-	-	-	-	-	-		-	1029	-	-
Phosphoglycerate mutase	1959	0037	2318	1612	0132	1418	1193	1591	0417	1357	0413	1158	2326	1751	1616
Enolase	0215	1942	1126	0232	1672	2836	1647	43	0913	1212	0882	0981	0812	1132	2458
Pyruvate kinase	1188	0570	1441	0108	3890	0715	-	-	0981	1617	0896	1020	0819	-	0489
Fructose-1,6-bisphosphatase	0613	0759	1515	0299	-	-	0954	1686	0286	0318	1428	1445	0944	1442	1109
Glyceraldehydes-3-P dehydrogenase	1874	1830	0257	0267 1146	1018 3345	2782	618	1009	0528	1356	1103	0458	1740	1732	0171

Table 5.1. cont'd. Distribution of enzymes of the EM type pathway in archaea.

Phosphoglycerate kinase	1057	1218	1679	0641	2669	0485	1662	1042	0527	1357	1075	0530	1742	1146	0173
Phosphoenolpyruvate synthetase	0043	0092	0057	0542	2667	2723	0252	1118	0883	1235	0886*	0976*	2423	0710	0650
Inositol-1-mono phosphatase/FBP	2014	1897	0189	0109	3344	2783	-	1871	2418	0547	-	-	-	2372	-
Pathway	Mod EM	Mod EM	Mod EM	Mod EM[g]	Mod EM[g]	Mod EM[g]	?	?	NonP ED	NonP ED	NonP ED	NonP ED	?	?	Mod EM[g]

[a] Abbreviations: Pfu, *Pyrococcus furiosus*, Pho, *Pyrococcus horikoshii*, Pab, *Pyrococcus abyssi*, Mja, *Methanocaldococcus jannaschii*, Mac, *Methanosarcina acetivorans*, Mma, *Methanosarcina mazei*, Mka, *Methanopyrus kandleri*, Mth, *Methanothermobacter thermoautotrophicus*, Sso, *Sulfolobus solfataricus*, Sto, *Sulfolobus tokodaii*, Tac, *Themoplasma acidophilum*, Tvo, *Thermoplasma volcanium*, Pae, *Pyrobaculum aerophilum*, Afu, *Archaeoglobus fulgidus*, Ape, *Aeropyrum pernix.*
[b] Potential homologs are indicated with ORF numbers.
[c] Homologs are based on the GLK of *Ap. Pernix* (52).
[d] Homologs are based on the PGI gene annotated in the *Pb. aerophilum* genome (42).
[e] Homologs are based on the PFK pf *Ap. pernix* (53).
[f] Mc. jannaschii contains a canonical PGI (www.genome.ad.jp/kegg/kegg2.html)
[g] Indicates a modified EM pathway but different from *P. furisosus*.

Table 5.2: Number of ORFs that were more than 4-fold regulated by the addition of maltose to a peptide grown culture at different time intervals.

Time (min)	Down-regulated[a]	Up-regulated[a]
30	11 (6)	12 (10)
60	14 (7)	23 (18)
120	33 (15)	92 (34)

[a] The number of ORFs which are also more than 4-fold regulated in the steady state comparison (Chapter 5) is given within brackets.

Table 5.3. ORFs whose expression is rapidly down-regulated by the addition of maltose to a peptide grown culture and are also down-regulated in the steady-state comparison (Chapter 5)[a].

ORF number[b]	Description[c]	Intensity ratios (log_2)[d]		
		30 min	60 min	10 min
PF0121	Aromatic aminotransferase (5)	-3.10	-3.18	-2.22
PF0289	[Phosphoenolpyruvate carboxykinase]	-1.70	-1.73	-2.10
PF0529	[Conserved hypothetical protein]	-1.04	-1.06	-2.12
PF0613	[Fructose-1,6-bisphosphatase]	-3.80	-4.46	-4.65
PF0845	[2-Keto acid:ferredoxin oxidoreductase subunitalpha]	-1.66	-1.98	-2.63
PF0846	[Conserved hypothetical protein]	-1.81	-1.93	-2.65
PF0893	Hydrogenase I delta (25)	-1.17	-1.58	-2.22
PF1341	[Aminomethyltransferase]	-1.70	-2.29	-3.05
PF1602	Glutamate dehydrogenase (39)	-1.59	-1.52	-2.24
PF1874	[Glyceraldehyde-3-phosphate dehydrogenase]	-4.19	-4.23	-3.41
PF1910	[Fd NADPH oxidoreductase II]	-2.04	-1.35	-2.38
PF1911	[Fd NADPH oxidoreductase II]	-2.14	-1.98	-3.07
PF2002	[Sucrose transport protein]	-1.64	-2.36	-3.41

[a] Rapid response includes ORFs which are down-regulated more than 2-fold after 30 minutes and more than 4-fold after 120 minutes.
[b] ORF number corresponding to Genemate (http://comb5-156.umbi.umd.edu/genemate).
[c] The ORF description is derived either from the annotation (http://comb5-156.umbi.umd.edu/genemate: given within brackets), or from the indicated reference where there is experimental data to support the ORF assignment specifically in *P. furiosus* (given without brackets).
[d] The intensity ratio is expressed as log_2 and represent an average of duplicated spots derived from one array hybridization. RNA sample were taken 30, 60 and 120 minutes after the addition of maltose.

Table 5.4. ORFs whose expression is rapidly up-regulated by the addition of maltose to a peptide grown culture and are also up-regulated in the steady-state comparison (Chapter 5)[a].

ORF number	Description	Intensity ratios (log_2)		
		30 min	60 min	120 min
PF0272	Alpha-amylase (94)	3.46	3.56	2.98
PF0450	[Glutamine synthetase]	1.69	2.14	2.26
PF0464	Glyceraldehyde-3-phosphate:ferredoxinoxidoreductase (116)	1.60	1.71	2.09
PF1025	[Conserved hypothetical protein]	2.11	2.02	2.57
PF1053	[Aspartokinase II alpha subunit]	1.33	2.84	3.60
PF1109	[Hypothetical protein]	2.39	2.74	3.14
PF1538	[n-Ethylammeline chlorohydrolase]	1.91	2.33	2.31
PF1739	[Trehalose/maltose binding protein]	2.68	2.88	2.11
PF1740	[Trehalose/maltose transport inner membraneprotein]	2.86	3.28	3.59
PF1741	[Trehalose/maltose transport inner membraneprotein]	2.12	2.35	1.92
PF1742	[Putative trehalose synthase]	2.84	3.27	3.40
PF1784	ADP-dependent phosphofructokinase (176)	2.52	2.13	2.48
PF1852	[Glutamate synthase subunit D]	2.12	3.17	3.70
PF1975	[Conserved hypothetical protein]	1.79	3.19	3.34

[a] Immediate affect was defined as both more than 2-fold up-regulated after 30 minutes and more than 4-fold after 120 minutes. See Table 5.2 for other definitions.

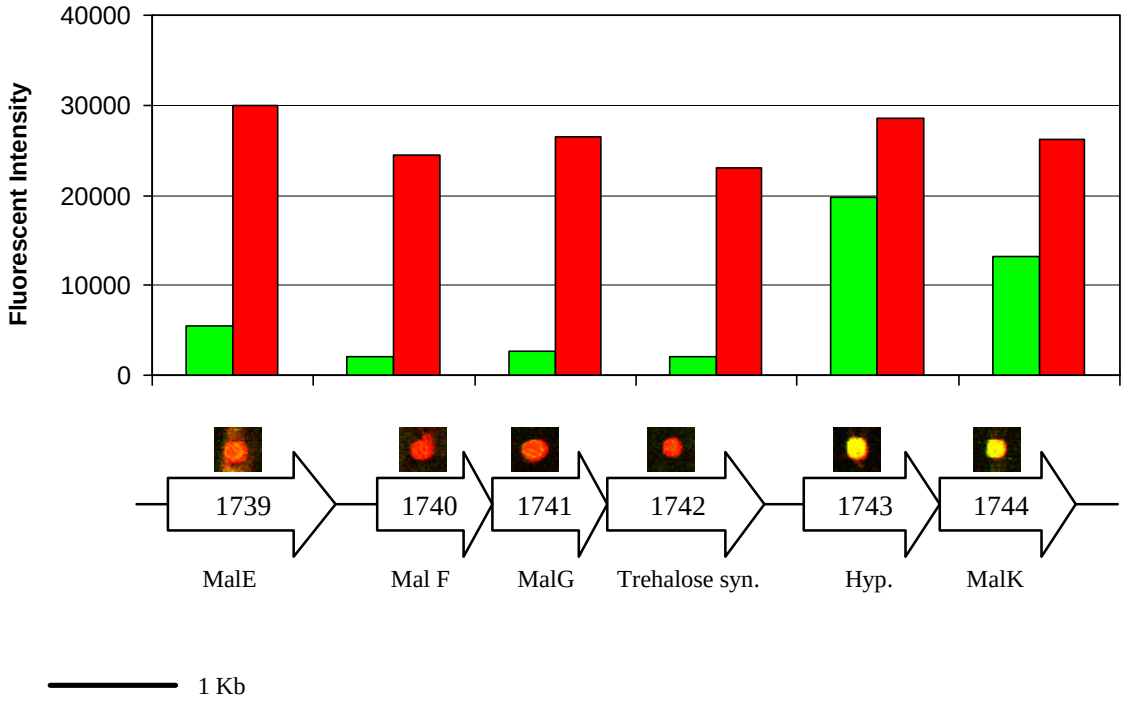

Figure 5.1. Expression levels of the ORFs encoding for the Mal I cluster in the presence of peptides or maltose. The six ORFs are arranged according to their genome position. The relative signal intensities for the cDNA obtained from cells grown on peptides (green bars) or maltose (red bars) are indicated. The false two color overlay of each spot is depicted above the appropriate ORF. A green, red or yellow color means that the ORF is mainly expressed in the peptide grown culture in maltose grown cultures or under both conditions, respectively.

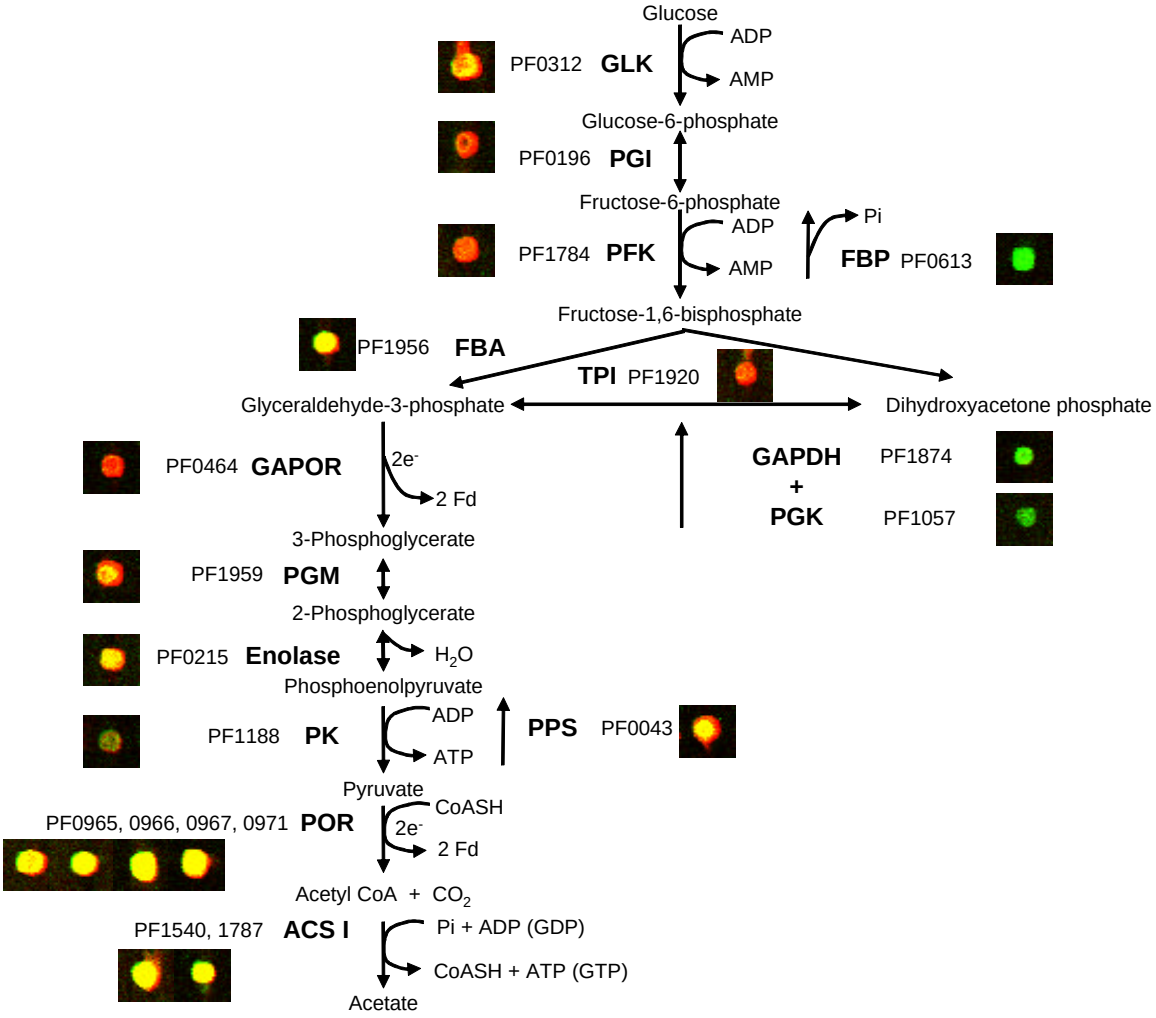

Figure 5.2. Schematic representation of the modified Embden-Meyerhof pathway and pyruvate metabolism in *P. furiosus*. Enzymes and corresponding ORF numbers are indicated. The abbreviations used are as follows: GLK, glucokinase, PGI, glucose-6-P isomerase, PFK, phosphofructokinase, FBP, fructose-1,6-P bisphosphatase, FBA, fructose-1,6-bis-P aldolase, TPI, triosephosphate isomerase, GAPOR, glyceraldehydes-3-P Fd oxidoreductase, GAPDH, glyceraldehydes-3-P dehydrogenase, PGK, phosphoglycerate kinase, PGM, phosphoglycerate mutase, PK, pyruvate kinase, POR, pyruvate Fd oxidoreductase, ACS, acetyl-CoA synthetase. The false color overlay of each spot representing the ORF coding for the enzymes in the pathway are depicted at their appropriate positions. Spot color scheme is the same as in Figure 5.1.

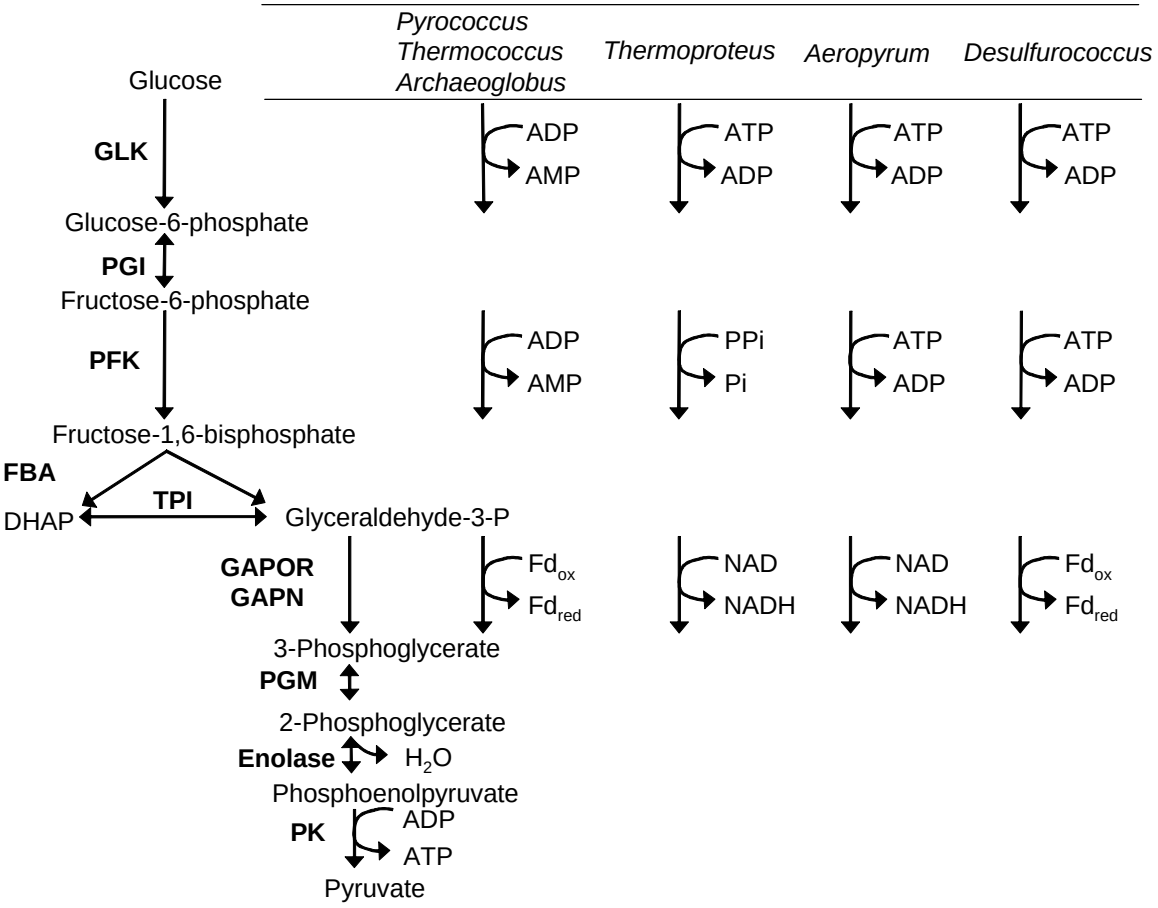

Figure 5.3. Schematic representation of variations in the glucose and pyruvate metabolic pathways of the hyperthermophilic archaea *Pyrococcus*, *Thermococcus*, *Archaeoglobus*, *Thermoproteus*, *Aeropyrum* and *Desulfurococcus*. The abbreviation used for the glycolytic enzymes are the same as in Figure 5.2 except for that GAPN is, non-phosphorylating glyceraldehydes-3-P dehydrogenase.

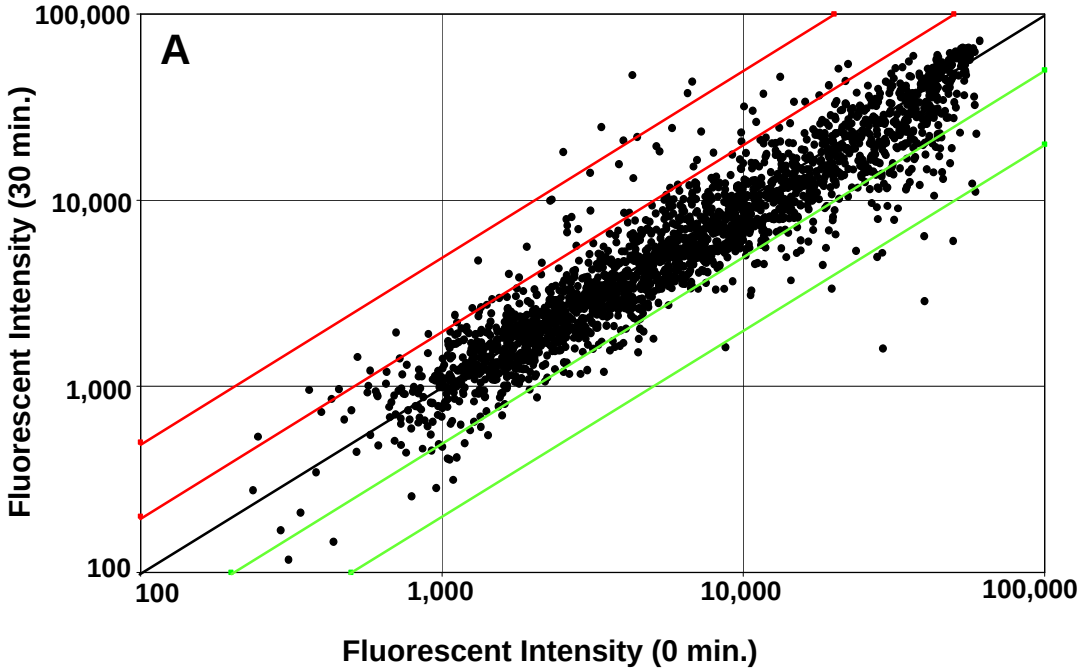

Figure 5.4. Correlation of fluorescence intensities from the DNA microarray analysis representing three time points after the addition of maltose to a culture growing on peptides. A) cDNA vs cDNA derived from a culture grown on peptide and the same culture after exposure to maltose for 30 min. The lower (green) and upper (red) line pairs indicate 2-fold and 5-fold changes in signal intensities, respectively.

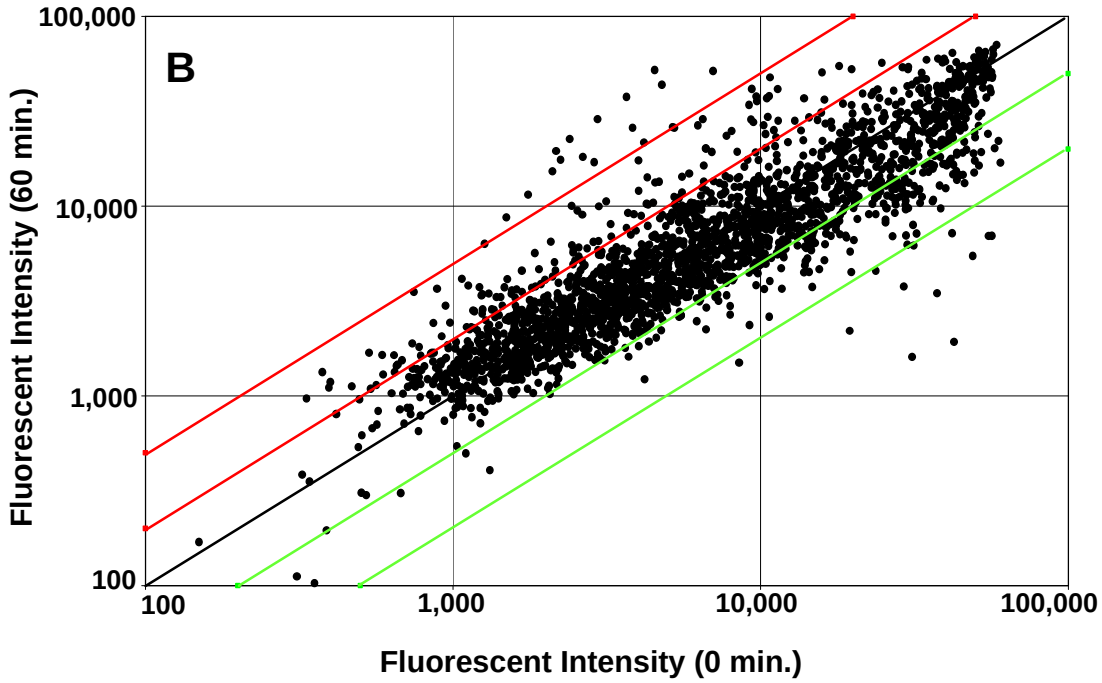

Figure 5.4. cont'd. Correlation of fluorescence intensities from the DNA microarray analysis representing three time points after the addition of maltose to a culture growing on peptides. B) cDNA vs cDNA derived from a culture grown on peptides and the same culture after exposure to maltose for 60 min. The lower (green) and upper (red) line pairs indicate 2-fold and 5-fold changes in signal intensities, respectively.

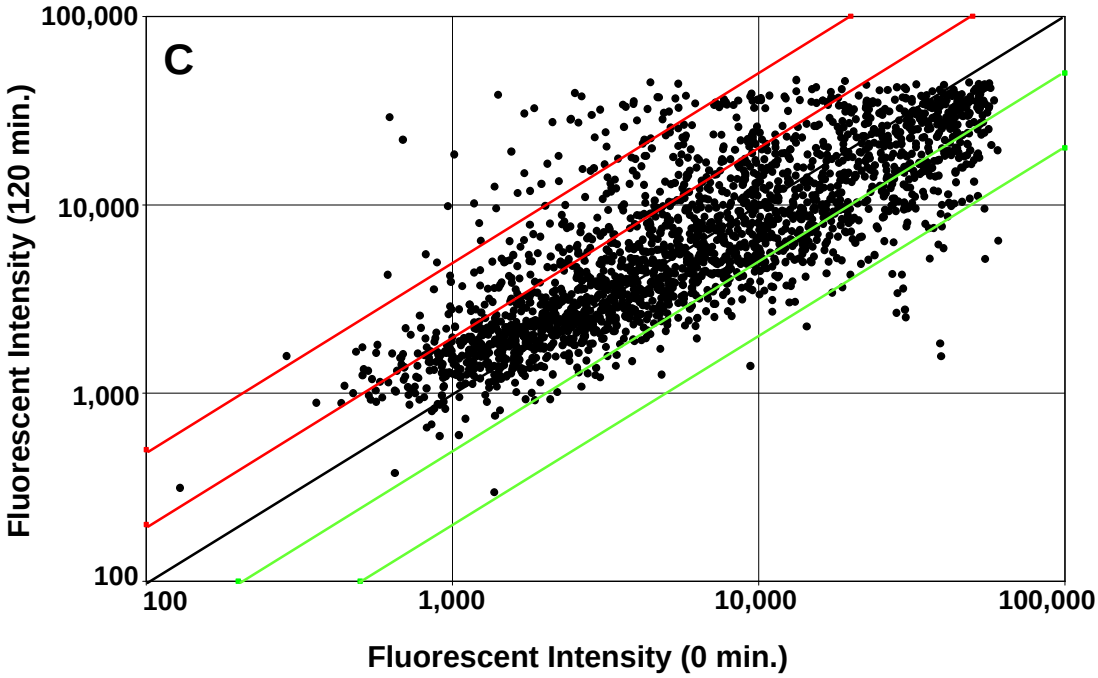

Figure 5.4. cont'd. Correlation of fluorescence intensities from the DNA microarray analysis representing three time points after the addition of maltose to a culture growing on peptides C) cDNA vs cDNA derived from a culture grown on peptides and the same culture after exposure to maltose for 120 min. The lower (green) and upper (red) line pairs indicate 2-fold and 5-fold changes in signal intensities, respectively.

REFERENCES

1. **Adams, M. W. W., J. F. Holden, A. L. Menon, G. J. Schut, A. M. Grunden, C. Hou, A. M. Hutchins, F. E. Jenney, Jr., C. Kim, K. Ma, G. Pan, R. Roy, R. Sapra, S. V. Story, and M. F. Verhagen.** 2001. Key role for sulfur in peptide metabolism and in regulation of three hydrogenases in the hyperthermophilic archaeon *Pyrococcus furiosus*. J. Bacteriol. **183:**716-24.

2. **Adams, M. W. W., and A. Kletzin.** 1996. Oxidoreductase-type enzymes and redox proteins involved in fermentative metabolisms of hyperthermophilic archaea. Adv. Protein Chem. **48:**101-180.

3. **Afshar, S., E. Johnson, S. de Vries, and I. Schroder.** 2001. Properties of a thermostable nitrate reductase from the hyperthermophilic archaeon *Pyrobaculum aerophilum*. J. Bacteriol. **183:**5491-5.

4. **Altschul, S. F., T. L. Madden, A. A. Schaffer, J. Zhang, Z. Zhang, W. Miller, and D. J. Lipman.** 1997. Gapped BLAST and PSI-BLAST: a new generation of protein database search programs. Nucleic. Acids Res. **25:**3389-402.

5. **Andreotti, G., M. V. Cubellis, G. Nitti, G. Sannia, X. Mai, M. W. Adams, and G. Marino.** 1995. An extremely thermostable aromatic aminotransferase from the hyperthermophilic archaeon *Pyrococcus furiosus*. Biochim. Biophys. Acta **1247:**90-6.

6. **Ang, S., C. Z. Lee, K. Peck, M. Sindici, U. Matrubutham, M. A. Gleeson, and J. T. Wang.** 2001. Acid-induced gene expression in *Helicobacter pylori*: study in genomic scale by microarray. Infect. Immun. **69:**1679-86.

7. **Arfin, S. M., A. D. Long, E. T. Ito, L. Tolleri, M. M. Riehle, E. S. Paegle, and G. W. Hatfield.** 2000. Global gene expression profiling in *Escherichia coli* K12. The effects of integration host factor. J. Biol. Chem. **275:**29672-84.

8. **Baliga, N. S., M. Pan, Y. A. Goo, E. C. Yi, D. R. Goodlett, K. Dimitrov, P. Shannon, R. Aebersold, W. V. Ng, and L. Hood.** 2002. Coordinate regulation of energy transduction modules in *Halobacterium sp.* analyzed by a global systems approach. Proc. Natl. Acad. Sci.U S A.

9. **Barns, S. M., C. F. Delwiche, J. D. Palmer, and N. R. Pace.** 1996. Perspectives on archaeal diversity, thermophily and monophyly from environmental rRNA sequences. Proc. Natl. Acad. Sci. U S A **93:**9188-93.

10. **Beliaev, A. S., D. K. Thompson, M. W. Fields, L. Wu, D. P. Lies, K. H. Nealson, and J. Zhou.** 2002. Microarray transcription profiling of a *Shewanella oneidensis* etrA mutant. J. Bacteriol. **184:**4612-6.

11. **Bell, S. D., and S. P. Jackson.** 2001. Mechanism and regulation of transcription in archaea. Curr. Opin. Microbiol. **4:**208-13.

12. **Blamey, J. M., and M. W. W. Adams.** 1993. Purification and characterization of pyruvate ferredoxin oxidoreductase from the hyperthermophilic archaeon *Pyrococcus furiosus*. Biochim. Biophys. Acta **1161:**19-27.

13. **Blattner, F. R., G. Plunkett, 3rd, C. A. Bloch, N. T. Perna, V. Burland, M. Riley, J. Collado-Vides, J. D. Glasner, C. K. Rode, G. F. Mayhew, J. Gregor, N. W. Davis, H. A. Kirkpatrick, M. A. Goeden, D. J. Rose, B. Mau, and Y. Shao.** 1997. The complete genome sequence of *Escherichia coli* K-12. Science **277:**1453-74.

14. **Blochl, E., S. Burggraf, G. Fiala, G. Laurerer, G. Huber, R. Huber, R. Rachel, A. Segerer, K. O. Stetter, and P. Volkl.** 1995. Isolation, Taxonomy and Phylogeny of Hyperthermophilic Microorganisms. World J. Microb. Biot. **11:**9-16.

15. **Blochl, E., R. Rachel, S. Burggraf, D. Hafenbradl, H. W. Jannasch, and K. O. Stetter.** 1997. *Pyrolobus fumarii*, gen. and sp. nov., represents a novel group of archaea, extending the upper temperature limit for life to 113 degrees C. Extremophiles **1:**14-21.

16. **Blokesch, M., and A. Bock.** 2002. Maturation of [NiFe]-hydrogenases in *Escherichia coli*: the HypC cycle. J. Mol. Biol. **324:**287-96.

17. **Bock, A. K., J. Glasemacher, R. Schmidt, and P. Schonheit.** 1999. Purification and characterization of two extremely thermostable enzymes, phosphate acetyltransferase and acetate kinase, from the hyperthermophilic Eubacterium *Thermotoga maritima*. J. Bacteriol. **181:**1861-1867.

18. **Bock, A. K., J. Kunow, J. Glasemacher, and P. Schonheit.** 1996. Catalytic properties, molecular composition and sequence alignments of pyruvate: ferredoxin oxidoreductase from the methanogenic archaeon *Methanosarcina barkeri* (strain Fusaro). Eur. J. Biochem. **237:**35-44.

19. **Brasen, C., and P. Schonheit.** 2001. Mechanisms of acetate formation and acetate activation in halophilic archaea. Arch. Microbiol. **175:**360-368.

20. **Brinkman, A. B., I. Dahlke, J. E. Tuininga, T. Lammers, V. Dumay, E. de Heus, J. H. Lebbink, M. Thomm, W. M. de Vos, and J. van Der Oost.** 2000. An Lrp-like transcriptional regulator from the archaeon *Pyrococcus furiosus* is negatively autoregulated. J. Biol. Chem. **275:**38160-9.

21. **Brostedt, E., and S. Nordlund.** 1991. Purification and partial characterization of a pyruvate oxidoreductase from the photosynthetic bacterium *Rhodospirillum rubrum* grown under nitrogen-fixing conditions. Biochem. J. **279:**155-158.

22. **Brunner, N. A., H. Brinkmann, B. Siebers, and R. Hensel.** 1998. NAD^+-dependent glyceraldehyde-3-phosphate dehydrogenase from *Thermoproteus tenax*. The first identified archaeal member of the aldehyde dehydrogenase superfamily is a glycolytic enzyme with unusual regulatory properties. J. Biol. Chem. **273:**6149-56.

23. **Brunner, N. A., and R. Hensel.** 2001. Nonphosphorylating glyceraldehyde-3-phosphate dehydrogenase from *Thermoproteus tenax*. Methods Enzymol. **331:**117-31.

24. **Brunner, N. A., B. Siebers, and R. Hensel.** 2001. Role of two different glyceraldehyde-3-phosphate dehydrogenases in controlling the reversible Embden-Meyerhof-Parnas pathway in *Thermoproteus tenax*: regulation on protein and transcript level. Extremophiles **5:**101-9.

25. **Bryant, F. O., and M. W. W. Adams.** 1989. Characterization of hydrogenase from the hyperthermophilic archaebacterium, *Pyrococcus furiosus*. J. Biol. Chem. **264:**5070-9.

26. **Budgen, N., and M. J. Danson.** 1986. Metabolism of glucose via a modified Entner-Doudoroff pathway in the thermoacidophilic archaebacterium *Thermoplasma acidophilum*. Febs Lett. **196:**207-210.

27. **Bui, E. T., and P. J. Johnson.** 1996. Identification and characterization of [Fe]-hydrogenases in the hydrogenosome of *Trichomonas vaginalis*. Mol. Biochem. Parasitol. **76:**305-10.

28. **Chan, M. K., S. Mukund, A. Kletzin, M. W. Adams, and D. C. Rees.** 1995. Structure of a hyperthermophilic tungstopterin enzyme, aldehyde ferredoxin oxidoreductase. Science **267:**1463-9.

29. **Chang, S. T., K. N. Parker, M. W. Bauer, and R. M. Kelly.** 2001. alpha-Glucosidase from *Pyrococcus furiosus*. Methods Enzymol. **330:**260-9.

30. **Clements, M. O., S. Eriksson, A. Thompson, S. Lucchini, J. C. Hinton, S. Normark, and M. Rhen.** 2002. Polynucleotide phosphorylase is a global regulator of virulence and persistency in *Salmonella enterica*. Proc. Natl. Acad. Sci. U S A **99:**8784-9.

31. **Danson, M. J.** 1988. Archaebacteria - the comparative enzymology of their central metabolic pathways. Adv. Microb. Physiol. **29:**166-231.

32. **De Rosa, M., A. Gambacorta, B. Nicolaus, P. Giardina, E. Poerio, and V. Buonocore.** 1984. Glucose metabolism in the extreme thermoacidophilic archaebacterium *Sulfolobus solfataricus*. Biochem. J. **224:**407-14.

33. **de Saizieu, A., C. Gardes, N. Flint, C. Wagner, M. Kamber, T. J. Mitchell, W. Keck, K. E. Amrein, and R. Lange.** 2000. Microarray-based identification of a

novel *Streptococcus pneumoniae* regulon controlled by an autoinduced peptide. J. Bacteriol. **182:**4696-703.

34. **de Vos, W. M., S. W. Kengen, W. G. Voorhorst, and J. van der Oost.** 1998. Sugar utilization and its control in hyperthermophiles. Extremophiles **2:**201-5.

35. **Deckert, G., P. V. Warren, T. Gaasterland, W. G. Young, A. L. Lenox, D. E. Graham, R. Overbeek, M. A. Snead, M. Keller, M. Aujay, R. Huber, R. A. Feldman, J. M. Short, G. J. Olsen, and R. V. Swanson.** 1998. The complete genome of the hyperthermophilic bacterium *Aquifex aeolicus*. Nature **392:**353-8.

36. **Diruggiero, J., D. Dunn, D. L. Maeder, R. Holley-Shanks, J. Chatard, R. Horlacher, F. T. Robb, W. Boos, and R. B. Weiss.** 2000. Evidence of recent lateral gene transfer among hyperthermophilic archaea. Mol. Microbiol. **38:**684-93.

37. **Dong, G., C. Vieille, and J. G. Zeikus.** 1997. Cloning, sequencing, and expression of the gene encoding amylopullulanase from *Pyrococcus furiosus* and biochemical characterization of the recombinant enzyme. Appl. Environ. Microbiol. **63:**3577-84.

38. **Dunman, P. M., E. Murphy, S. Haney, D. Palacios, G. Tucker-Kellogg, S. Wu, E. L. Brown, R. J. Zagursky, D. Shlaes, and S. J. Projan.** 2001. Transcription profiling-based identification of *Staphylococcus aureus* genes regulated by the agr and/or sarA loci. J. Bacteriol. **183:**7341-53.

39. **Eggen, R. I., A. C. Geerling, K. Waldkotter, G. Antranikian, and W. M. de Vos.** 1993. The glutamate dehydrogenase-encoding gene of the hyperthermophilic archaeon *Pyrococcus furiosus*: sequence, transcription and analysis of the deduced amino acid sequence. Gene **132:**143-8.

40. **Erauso, G., A. L. Reysenbach, A. Godfroy, J. R. Meunier, B. Crump, F. Partensky, J. A. Baross, V. Marteinsson, G. Barbier, N. R. Pace, and D. Prieur.** 1993. *Pyrococcus abyssi* sp-nov, a new hyperthermophilic archaeon isolated from a deep-sea hydrothermal vent. Arch. Microbiol. **160:**338-349.

41. **Evans, J. N. S., D. P. Raleigh, C. J. Tolman, and M. F. Roberts.** 1986. C-13-Nmr spectroscopy of *Methanobacterium thermoautotrophicum* - carbon fluxes and primary metabolic pathways. J. Biol. Chem. **261:**6323-6331.

42. **Evdokimov, A. G., D. E. Anderson, K. M. Routzahn, and D. S. Waugh.** 2001. Structural basis for oligosaccharide recognition by *Pyrococcus furiosus* maltodextrin-binding protein. J. Mol. Biol. **305:**891-904.

43. **Fiala, G., and K. O. Stetter.** 1986. *Pyrococcus furiosus* sp-nov represents a novel genus of marine heterotrophic archaebacteria growing optimally at 100-degrees C. Arch. Microbiol. **145:**56-61.

44. **Firoved, A. M., and V. Deretic.** 2003. Microarray Analysis of Global Gene Expression in Mucoid *Pseudomonas aeruginosa*. J. Bacteriol. **185:**1071-81.

45. **Fitz-Gibbon, S. T., H. Ladner, U. J. Kim, K. O. Stetter, M. I. Simon, and J. H. Miller.** 2002. Genome sequence of the hyperthermophilic crenarchaeon *Pyrobaculum aerophilum*. Proc. Natl. Acad. Sci.U S A **99:**984-9.

46. **Fouts, D. E., R. B. Abramovitch, J. R. Alfano, A. M. Baldo, C. R. Buell, S. Cartinhour, A. K. Chatterjee, M. D'Ascenzo, M. L. Gwinn, S. G. Lazarowitz, N. C. Lin, G. B. Martin, A. H. Rehm, D. J. Schneider, K. van Dijk, X. Tang, and A. Collmer.** 2002. Genomewide identification of *Pseudomonas syringae* pv. tomato DC3000 promoters controlled by the HrpL alternative sigma factor. Proc. Natl. Acad. Sci.U S A **99:**2275-80.

47. **Frey, G., M. Thomm, B. Brudigam, H. P. Gohl, and W. Hausner.** 1990. An archaebacterial cell-free transcription system. The expression of tRNA genes from *Methanococcus vannielii* is mediated by a transcription factor. Nucleic. Acids. Res. **18:**1361-7.

48. **Futcher, B.** 2000. Microarrays and cell cycle transcription in yeast. Curr. Opin. Cell. Biol. **12:**710-715.

49. **Gonzalez, J. M., Y. Masuchi, F. T. Robb, J. W. Ammerman, D. L. Maeder, M. Yanagibayashi, J. Tamaoka, and C. Kato.** 1998. *Pyrococcus horikoshii* sp. nov., a hyperthermophilic archaeon isolated from a hydrothermal vent at the Okinawa Trough. Extremophiles **2:**123-30.

50. **Graham, D. E., H. M. Xu, and R. H. White.** 2002. A divergent archaeal member of the alkaline phosphatase binuclear metalloenzyme superfamily has phosphoglycerate mutase activity. Febs Lett. **517:**190-194.

51. **Greller, G., R. Riek, and W. Boos.** 2001. Purification and characterization of the heterologously expressed trehalose/maltose ABC transporter complex of the hyperthermophilic archaeon *Thermococcus litoralis*. Eur. J. Biochem. **268:**4011-8.

52. **Gueguen, Y., W. G. Voorhorst, J. van der Oost, and W. M. de Vos.** 1997. Molecular and biochemical characterization of an endo-beta-1,3- glucanase of the hyperthermophilic archaeon *Pyrococcus furiosus*. J. Biol. Chem. **272:**31258-64.

53. **Hagen, W. R., P. J. Silva, M. A. Amorim, P. L. Hagedoorn, H. Wassink, H. Haaker, and F. T. Robb.** 2000. Novel structure and redox chemistry of the prosthetic groups of the iron-sulfur flavoprotein sulfide dehydrogenase from *Pyrococcus furiosus*; evidence for a [2Fe-2S] cluster with Asp(Cys)3 ligands. J. Biol. Inorg. Chem. **5:**527-34.

54. **Hansen, T., M. Oehlmann, and P. Schonheit.** 2001. Novel type of glucose-6-phosphate isomerase in the hyperthermophilic archaeon *Pyrococcus furiosus*. J. Bacteriol. **183:**3428-35.

55. **Hansen, T., B. Reichstein, R. Schmid, and P. Schonheit.** 2002. The first archaeal ATP-dependent glucokinase, from the hyperthermophilic crenarchaeon *Aeropyrum pernix*, represents a monomeric, extremely thermophilic ROK glucokinase with broad hexose specificity. J. Bacteriol. **184:**5955-65.

56. **Hansen, T., and P. Schonheit.** 2001. Sequence, expression, and characterization of the first archaeal ATP-dependent 6-phosphofructokinase, a non-allosteric enzyme related to the phosphofructokinase-B sugar kinase family, from the hyperthermophilic crenarchaeote *Aeropyrum pernix*. Arch. Microbiol. **177:**62-9.

57. **Heider, J., K. Ma, and M. W. Adams.** 1995. Purification, characterization, and metabolic function of tungsten-containing aldehyde ferredoxin oxidoreductase from the hyperthermophilic and proteolytic archaeon *Thermococcus* strain ES-1. J. Bacteriol. **177:**4757-64.

58. **Heider, J., X. Mai, and M. W. Adams.** 1996. Characterization of 2-ketoisovalerate ferredoxin oxidoreductase, a new and reversible coenzyme A-dependent enzyme involved in peptide fermentation by hyperthermophilic archaea. J. Bacteriol. **178:**780-7.

59. **Hethke, C., A. C. Geerling, W. Hausner, W. M. de Vos, and M. Thomm.** 1996. A cell-free transcription system for the hyperthermophilic archaeon *Pyrococcus furiosus*. Nucleic. Acids Res. **24:**2369-76.

60. **Hickey, A. J., E. Conway de Macario, and A. J. Macario.** 2002. Transcription in the archaea: basal factors, regulation, and stress gene expression. Crit. Rev. Biochem. Mol. Biol. **37:**199-258.

61. **Hihara, Y., A. Kamei, M. Kanehisa, A. Kaplan, and M. Ikeuchi.** 2001. DNA microarray analysis of cyanobacterial gene expression during acclimation to high light. Plant Cell **13:**793-806.

62. **Hille, R.** 2002. Molybdenum and tungsten in biology. Trends Biochem. Sci. **27:**360-367.

63. **Hille, R.** 1996. The mononuclear molybdenum enzymes. Chem. Rev. **96:**2757-2816.

64. **Hu, Y., S. Faham, R. Roy, M. W. Adams, and D. C. Rees.** 1999. Formaldehyde ferredoxin oxidoreductase from *Pyrococcus furiosus*: the 1.85 A resolution crystal structure and its mechanistic implications. J. Mol. Biol. **286:**899-914.

65. **Huang, J., C. J. Lih, K. H. Pan, and S. N. Cohen.** 2001. Global analysis of growth phase responsive gene expression and regulation of antibiotic biosynthetic

pathways in *Streptomyces coelicolor* using DNA microarrays. Genes Dev. **15:**3183-92.

66. **Huber, H., M. J. Hohn, R. Rachel, T. Fuchs, V. C. Wimmer, and K. O. Stetter.** 2002. A new phylum of Archaea represented by a nanosized hyperthermophilic symbiont. Nature **417:**63-7.

67. **Huber, R., T. A. Langworthy, H. Konig, M. Thomm, C. R. Woese, U. B. Sleytr, and K. O. Stetter.** 1986. *Thermotoga Maritima* sp-nov represents a new genus of unique extremely thermophilic eubacteria growing up to 90-degrees-C. Arch. Microbiol. **144:**324-333.

68. **Huber, R., and K. O. Stetter.** 2001. Discovery of hyperthermophilic microorganisms. Methods Enzymol. **330:**11-24.

69. **Huber, R., T. Wilharm, D. Huber, A. Trincone, S. Burggraf, H. Konig, R. Rachel, I. Rockinger, H. Fricke, and K. O. Stetter.** 1992. *Aquifex Pyrophilus* gen-nov sp-nov represents a novel group of marine hyperthermophilic hydrogen-oxidizing bacteria. Syst. Appl. Microbiol. **15:**340-351.

70. **Hudepohl, U., W. D. Reiter, and W. Zillig.** 1990. In vitro transcription of two rRNA genes of the archaebacterium *Sulfolobus* sp. B12 indicates a factor requirement for specific initiation. Proc. Natl. Acad. Sci.U S A **87:**5851-5.

71. **Hung, S. P., P. Baldi, and G. W. Hatfield.** 2002. Global gene expression profiling in *Escherichia coli* K12: The effects of Leucine-responsive regulatory protein. J. Biol. Chem.

72. **Hutchins, A. M., J. F. Holden, and M. W. W. Adams.** 2001. Phosphoenolpyruvate synthetase from the hyperthermophilic archaeon *Pyrococcus furiosus*. J. Bacteriol. **183:**709-15.

73. **Jetten, M. S. M., A. J. M. Stams, and A. J. B. Zehnder.** 1992. Methanogenesis from acetate - a comparison of the acetate metabolism in *Methanothrix soehngenii* and *Methanosarcina* Spp. Fems Microbiol. Rev. **88:**181-197.

74. **Johnson, M. K., D. C. Rees, and M. W. W. Adams.** 1996. Tungstoenzymes. Chem. Rev. **96:**2817-2839.

75. **Jolley, K. A., D. G. Maddocks, S. L. Gyles, Z. Mullan, S. L. Tang, M. L. Dyall-Smith, D. W. Hough, and M. J. Danson.** 2000. 2-Oxoacid dehydrogenase multienzyme complexes in the halophilic Archaea? Gene sequences and protein structural predictions. Microbiology **146 (Pt 5):**1061-9.

76. **Jorgensen, S., C. E. Vorgias, and G. Antranikian.** 1997. Cloning, sequencing, characterization, and expression of an extracellular alpha-amylase from the hyperthermophilic archaeon *Pyrococcus furiosus* in *Escherichia coli* and *Bacillus subtilis*. J. Biol. Chem. **272:**16335-42.

77. **Kaji, M., Y. Taniguchi, O. Matsushita, S. Katayama, S. Miyata, S. Morita, and A. Okabe.** 1999. The hydA gene encoding the H_2-evolving hydrogenase of *Clostridium perfringens*: molecular characterization and expression of the gene. FEMS Microbiol. Lett. **181:**329-36.

78. **Kaper, T., C. H. Verhees, J. H. Lebbink, J. F. van Lieshout, L. D. Kluskens, D. E. Ward, S. W. Kengen, M. M. Beerthuyzen, W. M. de Vos, and J. van der Oost.** 2001. Characterization of beta-glycosylhydrolases from *Pyrococcus furiosus*. Methods Enzymol. **330:**329-46.

79. **Kardinahl, S., C. L. Schmidt, T. Hansen, S. Anemuller, A. Petersen, and G. Schafer.** 1999. The strict molybdate-dependence of glucose-degradation by the thermoacidophile *Sulfolobus acidocaldarius* reveals the first crenarchaeotic molybdenum containing enzyme - an aldehyde oxidoreductase. Eur. J. Biochem. **260:**540-548.

80. **Kengen, S. W., F. A. de Bok, N. D. van Loo, C. Dijkema, A. J. Stams, and W. M. de Vos.** 1994. Evidence for the operation of a novel Embden-Meyerhof pathway that involves ADP-dependent kinases during sugar fermentation by *Pyrococcus furiosus*. J. Biol. Chem. **269:**17537-41.

81. **Kengen, S. W., E. J. Luesink, A. J. Stams, and A. J. Zehnder.** 1993. Purification and characterization of an extremely thermostable beta-glucosidase from the hyperthermophilic archaeon *Pyrococcus furiosus*. Eur. J. Biochem. **213:**305-12.

82. **Kengen, S. W., J. E. Tuininga, F. A. de Bok, A. J. Stams, and W. M. de Vos.** 1995. Purification and characterization of a novel ADP-dependent glucokinase from the hyperthermophilic archaeon *Pyrococcus furiosus*. J. Biol. Chem. **270:**30453-7.

83. **Kengen, S. W. M., A. J. M. Stams, and W. M. deVos.** 1996. Sugar metabolism of hyperthermophiles. Fems Microbiol. Rev. **18:**119-137.

84. **Kleiger, G., J. Perry, and D. Eisenberg.** 2001. 3D structure and significance of the GPhiXXG helix packing motif in tetramers of the E1beta subunit of pyruvate dehydrogenase from the archeon *Pyrobaculum aerophilum*. Biochemistry **40:**14484-92.

85. **Kletzin, A., and M. W. Adams.** 1996. Molecular and phylogenetic characterization of pyruvate and 2-ketoisovalerate ferredoxin oxidoreductases from *Pyrococcus furiosus* and pyruvate ferredoxin oxidoreductase from *Thermotoga maritima*. J. Bacteriol. **178:**248-57.

86. **Kletzin, A., and M. W. Adams.** 1996. Tungsten in biological systems. FEMS Microbiol. Rev. **18:**5-63.

87. **Koga, S., I. Yoshioka, H. Sakuraba, M. Takahashi, S. Sakasegawa, S. Shimizu, and T. Ohshima.** 2000. Biochemical characterization, cloning, and sequencing of ADP-dependent (AMP-forming) glucokinase from two hyperthermophilic archaea, *Pyrococcus furiosus* and *Thermococcus litoralis*. J. Biochem. (Tokyo) **128:**1079-85.

88. **Kohlhoff, M., A. Dahm, and R. Hensel.** 1996. Tetrameric triosephosphate isomerase from hyperthermophilic Archaea. FEBS Lett. **383:**245-50.

89. **Komori, K., R. Fujikane, H. Shinagawa, and Y. Ishino.** 2002. Novel endonuclease in Archaea cleaving DNA with various branched structure. Genes Genet. Syst. **77:**227-241.

90. **Konig, H., E. Nusser, and K. O. Stetter.** 1985. Glycogen in *Methanolobus* and *Methanococcus*. Fems Microbiol. Lett. **28:**265-269.

91. **Koning, S. M., M. G. Elferink, W. N. Konings, and A. J. Driessen.** 2001. Cellobiose uptake in the hyperthermophilic archaeon *Pyrococcus furiosus* is mediated by an inducible, high-affinity ABC transporter. J. Bacteriol. **183:**4979-84.

92. **Kyrpides, N. C., and C. A. Ouzounis.** 1999. Transcription in archaea. Proc. Natl. Acad. Sci.U S A **96:**8545-50.

93. **Labes, A., and P. Schonheit.** 2001. Sugar utilization in the hyperthermophilic, sulfate-reducing archaeon *Archaeoglobus fulgidus* strain 7324: starch degradation to acetate and CO2 via a modified Embden-Meyerhof pathway and acetyl-CoA synthetase (ADP-forming). Arch. Microbiol. **176:**329-38.

94. **Laderman, K. A., B. R. Davis, H. C. Krutzsch, M. S. Lewis, Y. V. Griko, P. L. Privalov, and C. B. Anfinsen.** 1993. The purification and characterization of an extremely thermostable alpha-amylase from the hyperthermophilic archaebacterium *Pyrococcus furiosus*. J. Biol. Chem. **268:**24394-401.

95. **Laksanalamai, P., D. L. Maeder, and F. T. Robb.** 2001. Regulation and mechanism of action of the small heat shock protein from the hyperthermophilic archaeon *Pyrococcus furiosus*. J. Bacteriol. **183:**5198-202.

96. **Lander, E. S.** 1999. Array of hope. Nat. Genet. **21:**3-4.

97. **Latimer, M. T., and J. G. Ferry.** 1993. Cloning, sequence-analysis, and hyperexpression of the genes encoding phosphotransacetylase and acetate kinase from *Methanosarcina thermophila*. J. Bacteriol. **175:**6822-6829.

98. **Lecompte, O., R. Ripp, V. Puzos-Barbe, S. Duprat, R. Heilig, J. Dietrich, J. C. Thierry, and O. Poch.** 2001. Genome evolution at the genus level: comparison of three complete genomes of hyperthermophilic archaea. Genome Res. **11:**981-93.

99. **Lee, S. J., A. Engelmann, R. Horlacher, Q. Qu, G. Vierke, C. Hebbeln, M. Thomm, and W. Boos.** 2003. TrmB, a sugar-specific transcriptional regulator of the trehalose/maltose ABC transporter from the hyperthermophilic archaeon *Thermococcus litoralis*. J. Biol. Chem. **278:**983-90.

100. **Leveque, E., S. Janecek, B. Haye, and A. Belarbi.** 2000. Thermophilic archaeal amylolytic enzymes. Enzyme Microb. Tech. **26:**3-14.

101. **Lindahl, P. A., and B. Chang.** 2001. The evolution of acetyl-CoA synthase. Origins Life Evol. B. **31:**403-434.

102. **Linden, A., O. Mayans, W. Meyer-Klaucke, G. Antranikian, and M. Wilmanns.** 2002. Differential regulation of a hyperthermophilic alpha -amylase with a novel (Ca,Zn)-dimetal centre by zinc. J. Biol. Chem.**:**M211339200.

103. **Ljungdahl, L. G., and J. R. Andreesen.** 1975. Tungsten, a component of active formate dehydrogenase from *Clostridium-thermoaceticum*. Febs Lett. **54:**279-282.

104. **Lundie, L. L., and J. G. Ferry.** 1989. Activation of acetate by *Methanosarcina thermophila* - purification and characterization of phosphotransacetylase. J. Biol. Chem. **264:**18392-18396.

105. **Ma, K., and M. W. Adams.** 2001. Hydrogenases I and II from *Pyrococcus furiosus*. Methods Enzymol. **331:**208-16.

106. **Ma, K., and M. W. W. Adams.** 2001. Ferredoxin NADP oxidoreductase from *Pyrococcus furiosus*. Methods Enzymol. **334:**40-5.

107. **Ma, K., A. Hutchins, S. J. Sung, and M. W. W. Adams.** 1997. Pyruvate ferredoxin oxidoreductase from the hyperthermophilic archaeon, *Pyrococcus furiosus*, functions as a CoA-dependent pyruvate decarboxylase. Proc. Natl. Acad. Sci.U S A **94:**9608-13.

108. **Ma, K., R. N. Schicho, R. M. Kelly, and M. W. W. Adams.** 1993. Hydrogenase of the hyperthermophile *Pyrococcus furiosus* is an elemental sulfur reductase or sulfhydrogenase: evidence for a sulfur-reducing hydrogenase ancestor. Proc. Natl. Acad. Sci.U S A **90:**5341-4.

109. **Macgregor, P. F., and J. A. Squire.** 2002. Application of microarrays to the analysis of gene expression in cancer. Clin. Chem. **48:**1170-1177.

110. **Maeder, D. L., R. B. Weiss, D. M. Dunn, J. L. Cherry, J. M. Gonzalez, J. DiRuggiero, and F. T. Robb.** 1999. Divergence of the hyperthermophilic archaea *Pyrococcus furiosus* and *P. horikoshii* inferred from complete genomic sequences. Genetics **152:**1299-305.

111. **Mai, X., and M. W. W. Adams.** 1996. Characterization of a fourth type of 2-keto acid-oxidizing enzyme from a hyperthermophilic archaeon: 2-ketoglutarate ferredoxin oxidoreductase from *Thermococcus litoralis*. J. Bacteriol. **178:**5890-6.

112. **Mai, X., and M. W. W. Adams.** 1994. Indolepyruvate ferredoxin oxidoreductase from the hyperthermophilic archaeon *Pyrococcus furiosus*. A new enzyme involved in peptide fermentation. J. Biol. Chem. **269:**16726-32.

113. **Mai, X., and M. W. W. Adams.** 1996. Purification and characterization of two reversible and ADP-dependent acetyl coenzyme A synthetases from the hyperthermophilic archaeon *Pyrococcus furiosus*. J. Bacteriol. **178:**5897-903.

114. **Makdessi, K., J. R. Andreesen, and A. Pich.** 2001. Tungstate uptake by a highly specific ABC transporter in *Eubacterium acidaminophilum*. J. Biol. Chem. **276:**24557-24564.

115. **Mukund, S., and M. W. W. Adams.** 1993. Characterization of a novel tungsten-containing formaldehyde ferredoxin oxidoreductase from the hyperthermophilic archaeon, *Thermococcus litoralis*. A role for tungsten in peptide catabolism. J. Biol. Chem. **268:**13592-600.

116. **Mukund, S., and M. W. W. Adams.** 1995. Glyceraldehyde-3-phosphate ferredoxin oxidoreductase, a novel tungsten-containing enzyme with a potential glycolytic role in the hyperthermophilic archaeon *Pyrococcus furiosus*. J. Biol. Chem. **270:**8389-92.

117. **Mukund, S., and M. W. W. Adams.** 1991. The novel tungsten-iron-sulfur protein of the hyperthermophilic archaebacterium, *Pyrococcus furiosus*, is an aldehyde ferredoxin oxidoreductase. Evidence for its participation in a unique glycolytic pathway. J. Biol. Chem. **266:**14208-16.

118. **Napoli, A., J. van der Oost, C. W. Sensen, R. L. Charlebois, M. Rossi, and M. Ciaramella.** 1999. An Lrp-like protein of the hyperthermophilic archaeon *Sulfolobus solfataricus* which binds to its own promoter. J. Bacteriol. **181:**1474-80.

119. **Oh, M. K., L. Rohlin, K. C. Kao, and J. C. Liao.** 2002. Global expression profiling of acetate-grown *Escherichia coli*. J. Biol. Chem. **277:**13175-83.

120. **Okinaka, Y., C. H. Yang, N. T. Perna, and N. T. Keen.** 2002. Microarray profiling of *Erwinia chrysanthemi* 3937 genes that are regulated during plant infection. Mol. Plant Microbe Interact. **15:**619-29.

121. **Paschos, A., A. Bauer, A. Zimmermann, E. Zehelein, and A. Bock.** 2002. HypF, a carbamoyl phosphate-converting enzyme involved in [NiFe] hydrogenase haturation. J. Biol. Chem. **277:**49945-51.

122. **Paustian, M. L., B. J. May, and V. Kapur.** 2001. *Pasteurella multocida* gene expression in response to iron limitation. Infect. Immun. **69:**4109-15.

123. **Peak, M. J., J. G. Peak, F. J. Stevens, J. Blamey, X. Mai, Z. H. Zhou, and M. W. W. Adams.** 1994. The hyperthermophilic glycolytic enzyme enolase in the archaeon, *Pyrococcus furiosus*: comparison with mesophilic enolases. Arch. Biochem. Biophys. **313:**280-6.

124. **Peters, J. W.** 1999. Structure and mechanism of iron-only hydrogenases. Curr. Opin. Struct. Biol. **9:**670-6.

125. **Peters, J. W., W. N. Lanzilotta, B. J. Lemon, and L. C. Seefeldt.** 1998. X-ray crystal structure of the Fe-only hydrogenase (CpI) from *Clostridium pasteurianum* to 1.8 angstrom resolution. Science **282:**1853-8.

126. **Peterson, J. D., L. A. Umayam, T. Dickinson, E. K. Hickey, and O. White.** 2001. The comprehensive microbial resource. Nucleic Acids Res. **29:**123-125.

127. **Pierik, A. J., W. Roseboom, R. P. Happe, K. A. Bagley, and S. P. Albracht.** 1999. Carbon monoxide and cyanide as intrinsic ligands to iron in the active site of [NiFe]-hydrogenases. $NiFe(CN)_2CO$, Biology's way to activate H_2. J. Biol. Chem. **274:**3331-7.

128. **Raffaelli, N., A. Amici, M. Emanuelli, S. Ruggieri, and G. Magni.** 1994. Pyridine dinucleotide biosynthesis in archaebacteria: presence of NMN adenylyltransferase in *Sulfolobus solfataricus*. FEBS Lett. **355:**233-6.

129. **Rashid, N., H. Imanaka, T. Kanai, T. Fukui, H. Atomi, and T. Imanaka.** 2002. A novel candidate for the true fructose-1,6-bisphosphatase in archaea. J. Biol. Chem. **277:**30649-55.

130. **Reeves, R. E., L. G. Warren, B. Susskind, and H. S. Loi.** 1977. Energy-conserving pyruvate to acetate pathway in *Entamoeba histolytica* - pyruvate synthase and a new acetate thiokinase. J. Biol. Chem. **252:**726-731.

131. **Reiter, W. D., U. Hudepohl, and W. Zillig.** 1990. Mutational analysis of an archaebacterial promoter: essential role of a TATA box for transcription efficiency and start-site selection in vitro. Proc. Natl. Acad. Sci.U S A **87:**9509-13.

132. **Revel, A. T., A. M. Talaat, and M. V. Norgard.** 2002. DNA microarray analysis of differential gene expression in *Borrelia burgdorferi*, the Lyme disease spirochete. Proc. Natl. Acad. Sci.U S A **99:**1562-7.

133. **Robinson, K. A., and H. J. Schreier.** 1994. Isolation, sequence and characterization of the maltose-regulated mlrA gene from the hyperthermophilic archaeum *Pyrococcus furiosus*. Gene **151:**173-6.

134. **Rosenthal, B., Z. M. Mai, D. Caplivski, S. Ghosh, H. delaVega, T. Graf, and J. Samuelson.** 1997. Evidence for the bacterial origin of genes encoding fermentation enzymes of the amitochondriate protozoan parasite *Entamoeba histolytica*. J. Bacteriol. **179:**3736-3745.

135. **Roy, R., and M. W. W. Adams.** 2002. Characterization of a fourth tungsten-containing enzyme from the hyperthermophilic archaeon *Pyrococcus furiosus*. J. Bacteriol. **184:**6952-6956.

136. **Roy, R., and M. W. W. Adams.** 2002. Tungsten-dependent aldehyde oxidoreductase: A new family of enzymes containing the pterin cofactor. Met. Ions Biol. Syst. **39:**673-697.

137. **Roy, R., A. L. Menon, and M. W. W. Adams.** 2001. Aldehyde oxidoreductases from *Pyrococcus furiosus*. Methods Enzymol. **331:**132-144.

138. **Roy, R., S. Mukund, G. J. Schut, D. M. Dunn, R. Weiss, and M. W. Adams.** 1999. Purification and molecular characterization of the tungsten-containing formaldehyde ferredoxin oxidoreductase from the hyperthermophilic archaeon *Pyrococcus furiosus*: the third of a putative five-member tungstoenzyme family. J. Bacteriol. **181:**1171-80.

139. **Sako, Y., N. Nomura, A. Uchida, Y. Ishida, H. Morii, Y. Koga, T. Hoaki, and T. Maruyama.** 1996. *Aeropyrum pernix* gen nov, sp nov, a novel aerobic hyperthermophilic archaeon growing at temperatures up to 100 degrees C. Int. J. Syst. Bacteriol. **46:**1070-1077.

140. **Sakuraba, H., and T. Ohshima.** 2002. Novel energy metabolism in anaerobic hyperthermophilic archaea: A modified Embden-Meyerhof pathway. J. Biosci. Bioeng. **93:**441-448.

141. **Sakuraba, H., I. Yoshioka, S. Koga, M. Takahashi, Y. Kitahama, T. Satomura, R. Kawakami, and T. Ohshima.** 2002. ADP-dependent glucokinase/phosphofructokinase, a novel bifunctional enzyme from the hyperthermophilic archaeon *Methanococcus jannaschii*. J. Biol. Chem. **277:**12495-8.

142. **Sanchez, L. B., and M. Muller.** 1996. Purification and characterization of the acetate forming enzyme, acetyl-CoA synthetase (ADP-forming) from the amitochondriate protist, *Giardia lamblia*. Febs Lett. **378:**240-244.

143. **Sapra, R., K. Bagramyan, and M. W. W. Adams.** The simplest respiratory system, proton reduction coupled to proton translocation. Submitted.

144. **Sapra, R., M. F. Verhagen, and M. W. W. Adams.** 2000. Purification and characterization of a membrane-bound hydrogenase from the hyperthermophilic archaeon *Pyrococcus furiosus*. J. Bacteriol. **182:**3423-8.

145. **Savchenko, A., C. Vieille, S. Kang, and J. G. Zeikus.** 2002. *Pyrococcus furiosus* alpha-amylase is stabilized by calcium and zinc. Biochemistry **41:**6193-201.

146. **Savchenko, A., C. Vieille, and J. G. Zeikus.** 2001. alpha-Amylases and amylopullulanase from *Pyrococcus furiosus*. Methods Enzymol. **330:**354-363.

147. **Schafer, G.** 1996. Bioenergetics of the archaebacterium *Sulfolobus*. Biochim. Biophys. Acta **1277:**163-200.

148. **Schafer, G., R. Moll, and C. L. Schmidt.** 2001. Respiratory enzymes from *Sulfolobus acidocaldarius*. Methods Enzymol. **331:**369-410.

149. **Schafer, T., and P. Schonheit.** 1992. Maltose fermentation to acetate, CO_2 and H_2 in the anaerobic hyperthermophilic archaeon *Pyrococcus furiosus* - evidence for the operation of a novel sugar fermentation pathway. Arch. Microbiol. **158:**188-202.

150. **Schafer, T., and P. Schonheit.** 1991. Pyruvate metabolism of the hyperthermophilic archaebacterium *Pyrococcus furiosus* - acetate formation from acetyl-CoA and ATP synthesis are catalyzed by an acetyl-CoA synthetase (ADP forming). Arch. Microbiol. **155:**366-377.

151. **Schafer, T., M. Selig, and P. Schonheit.** 1993. Acetyl-CoA synthetase (ADP-forming) in archaea, a novel enzyme involved in acetate formation and ATP synthesis. Arch. Microbiol. **159:**72-83.

152. **Schena, M., D. Shalon, R. W. Davis, and P. O. Brown.** 1995. Quantitative monitoring of gene-expression patterns with a complementary-DNA microarray. Science **270:**467-470.

153. **Schena, M., D. Shalon, R. Heller, A. Chai, P. O. Brown, and R. W. Davis.** 1996. Parallel human genome analysis: Microarray-based expression monitoring of 1000 genes. Proceedings of the National Academy of Sciences of the United States of America **93:**10614-10619.

154. **Schonheit, P., and T. Schafer.** 1995. Metabolism of hyperthermophiles. World J. Microb. Biot. **11:**26-57.

155. **Schramm, A., B. Siebers, B. Tjaden, H. Brinkmann, and R. Hensel.** 2000. Pyruvate kinase of the hyperthermophilic crenarchaeote *Thermoproteus tenax*: physiological role and phylogenetic aspects. J. Bacteriol. **182:**2001-9.

156. **Schummer, M., W. L. Ng, P. S. Nelson, R. E. Bumgarner, and L. Hood.** 1997. Inexpensive handheld device for the construction of high-density nucleic acid arrays. Biotechniques **23:**1087-&.

157. **Schut, G. J., S. Brehm, S. Datta, and M. M. W. Adams.** Submitted. Whole genome DNA microarray analysis of a hyperthermophile and and archaeon: *Pyrococcus furiosus* grown on carbohydrates or peptides.

158. **Schut, G. J., A. L. Menon, and M. W. W. Adams.** 2001. 2-ketoacid oxidoreductases from *Pyrococcus furiosus* and *Thermococcus litoralis*. Methods Enzymol. **331:**144-58.

159. **Schut, G. J., J. Zhou, and M. W. W. Adams.** 2001. DNA microarray analysis of the hyperthermophilic archaeon *Pyrococcus furiosus*: evidence for a new type of sulfur-reducing enzyme complex. J. Bacteriol. **183:**7027-36.

160. **Selig, M., K. B. Xavier, H. Santos, and P. Schonheit.** 1997. Comparative analysis of Embden-Meyerhof and Entner-Doudoroff glycolytic pathways in hyperthermophilic archaea and the bacterium *Thermotoga*. Arch. Microbiol. **167:**217-32.

161. **She, Q., R. K. Singh, F. Confalonieri, Y. Zivanovic, G. Allard, M. J. Awayez, C. C. Chan-Weiher, I. G. Clausen, B. A. Curtis, A. De Moors, G. Erauso, C. Fletcher, P. M. Gordon, I. Heikamp-de Jong, A. C. Jeffries, C. J. Kozera, N. Medina, X. Peng, H. P. Thi-Ngoc, P. Redder, M. E. Schenk, C. Theriault, N. Tolstrup, R. L. Charlebois, W. F. Doolittle, M. Duguet, T. Gaasterland, R. A. Garrett, M. A. Ragan, C. W. Sensen, and J. Van der Oost.** 2001. The complete genome of the crenarchaeon *Sulfolobus solfataricus* P2. Proc. Natl. Acad. Sci.U S A **98:**7835-40.

162. **Shieh, J. S., and W. B. Whitman.** 1987. Pathway of Acetate Assimilation in Autotrophic and Heterotrophic *Methanococci*. J. Bacteriol. **169:**5327-5329.

163. **Siebers, B., H. Brinkmann, C. Dorr, B. Tjaden, H. Lilie, J. van der Oost, and C. H. Verhees.** 2001. Archaeal fructose-1,6-bisphosphate aldolases constitute a new family of archaeal type class I aldolase. J. Biol. Chem. **276:**28710-8.

164. **Siebers, B., and R. Hensel.** 1993. Glucose catabolism of the hyperthermophilic archaeum *Thermoproteus tenax*. Fems Microbiol. Lett. **111:**1-8.

165. **Siebers, B., H. P. Klenk, and R. Hensel.** 1998. PPi-dependent phosphofructokinase from *Thermoproteus tenax*, an archaeal descendant of an ancient line in phosphofructokinase evolution. J. Bacteriol. **180:**2137-43.

166. **Siebers, B., V. F. Wendisch, and R. Hensel.** 1997. Carbohydrate metabolism in *Thermoproteus tenax*: in vivo utilization of the non-phosphorylative Entner-Doudoroff pathway and characterization of its first enzyme, glucose dehydrogenase. Arch. Microbiol. **168:**120-7.

167. **Silva, P. J., E. C. van den Ban, H. Wassink, H. Haaker, B. de Castro, F. T. Robb, and W. R. Hagen.** 2000. Enzymes of hydrogen metabolism in *Pyrococcus furiosus*. Eur. J. Biochem. **267:**6541-51.

168. **Soppa, J.** 2001. Basal and regulated transcription in archaea. Adv. Appl. Microbiol. **50:**171-217.

169. **Soppa, J.** 1999. Normalized nucleotide frequencies allow the definition of archaeal promoter elements for different archaeal groups and reveal base-specific TFB contacts upstream of the TATA box. Mol. Microbiol. **31:**1589-92.

170. **Stec, B., H. Yang, K. A. Johnson, L. Chen, and M. F. Roberts.** 2000. *Methanococcus jannaschii* MJ0109 gene product: An ancestral phosphatase? Faseb. J. **14:**A1386-A1386.

171. **Stetter, K. O.** 1996. Hyperthermophilic procaryotes. Fems Microbiol. Rev. **18:**149-158.

172. **Stetter, K. O., R. Huber, E. Blochl, M. Kurr, R. D. Eden, M. Fielder, H. Cash, and I. Vance.** 1993. Hyperthermophilic archaea are thriving in deep north-sea and alaskan oil-reservoirs. Nature **365:**743-745.

173. **Tersteegen, A., D. Linder, R. K. Thauer, and R. Hedderich.** 1997. Structures and functions of four anabolic 2-oxoacid oxidoreductases in *Methanobacterium thermoautotrophicum*. Eur. J. Biochem. **244:**862-8.

174. **Tolman, C. J., S. Kanodia, M. F. Roberts, and L. Daniels.** 1986. P-31-NMR spectra of methanogens - 2,3-cyclopyrophosphoglycerate Is detectable only in *Methanobacteria* strains. Biochim. Biophys. Acta **886:**345-352.

175. **Tracy, M. R., and S. B. Hedges.** 2000. Evolutionary history of the enolase gene family. Gene **259:**129-38.

176. **Tuininga, J. E., C. H. Verhees, J. van der Oost, S. W. Kengen, A. J. Stams, and W. M. de Vos.** 1999. Molecular and biochemical characterization of the ADP-dependent phosphofructokinase from the hyperthermophilic archaeon *Pyrococcus furiosus*. J. Biol. Chem. **274:**21023-8.

177. **van der Oost, J., M. A. Huynen, and C. H. Verhees.** 2002. Molecular characterization of phosphoglycerate mutase in archaea. FEMS Microbiol. Lett. **212:**111-20.

178. **van der Oost, J., G. Schut, S. W. Kengen, W. R. Hagen, M. Thomm, and W. M. de Vos.** 1998. The ferredoxin-dependent conversion of glyceraldehyde-3-phosphate in the hyperthermophilic archaeon *Pyrococcus furiosus* represents a novel site of glycolytic regulation. J. Biol. Chem. **273:**28149-54.

179. **Verhagen, M. F., and M. W. Adams.** 2001. Fe-only hydrogenase from *Thermotoga maritima*. Methods Enzymol. **331:**216-26.

180. **Verhees, C. H., J. Akerboom, E. Schiltz, W. M. de Vos, and J. van der Oost.** 2002. Molecular and biochemical characterization of a distinct type of fructose-1,6-bisphosphatase from *Pyrococcus furiosus*. J. Bacteriol. **184:**3401-5.

181. **Verhees, C. H., M. A. Huynen, D. E. Ward, E. Schiltz, W. M. de Vos, and J. van der Oost.** 2001. The phosphoglucose isomerase from the hyperthermophilic archaeon *Pyrococcus furiosus* is a unique glycolytic enzyme that belongs to the cupin superfamily. J. Biol. Chem. **276:**40926-32.

182. **Verhees, C. H., J. E. Tuininga, S. W. Kengen, A. J. Stams, J. van der Oost, and W. M. de Vos.** 2001. ADP-dependent phosphofructokinases in mesophilic and thermophilic methanogenic archaea. J. Bacteriol. **183:**7145-53.

183. **Vierke, G., A. Engelmann, C. Hebbeln, and M. Thomm.** 2003. A novel archaeal transcriptional regulator of heat shock response. J. Biol. Chem. **278:**18-26.

184. **Vignais, P. M., B. Billoud, and J. Meyer.** 2001. Classification and phylogeny of hydrogenases. FEMS Microbiol. Rev. **25:**455-501.

185. **Volbeda, A., M. H. Charon, C. Piras, E. C. Hatchikian, M. Frey, and J. C. Fontecilla-Camps.** 1995. Crystal structure of the nickel-iron hydrogenase from *Desulfovibrio gigas*. Nature **373:**580-7.

186. **Voorhorst, W. G., R. I. Eggen, E. J. Luesink, and W. M. de Vos.** 1995. Characterization of the *cel*B gene coding for beta-glucosidase from the hyperthermophilic archaeon *Pyrococcus furiosus* and its expression and site-directed mutation in *Escherichia coli*. J. Bacteriol. **177:**7105-11.

187. **Voorhorst, W. G., Y. Gueguen, A. C. Geerling, G. Schut, I. Dahlke, M. Thomm, J. van der Oost, and W. M. de Vos.** 1999. Transcriptional regulation in the hyperthermophilic archaeon *Pyrococcus furiosus*: coordinated expression of divergently oriented genes in response to beta-linked glucose polymers. J. Bacteriol. **181:**3777-83.

188. **Walden, H., G. S. Bell, R. J. Russell, B. Siebers, R. Hensel, and G. L. Taylor.** 2001. Tiny TIM: a small, tetrameric, hyperthermostable triosephosphate isomerase. J. Mol. Biol. **306:**745-57.

189. **Wettach, J., H. P. Gohl, H. Tschochner, and M. Thomm.** 1995. Functional interaction of yeast and human TATA-binding proteins with an archaeal RNA polymerase and promoter. Proc. Natl. Acad. Sci. U S A. **92:**472-6.

190. **Wilson, M., J. DeRisi, H. H. Kristensen, P. Imboden, S. Rane, P. O. Brown, and G. K. Schoolnik.** 1999. Exploring drug-induced alterations in gene expression in *Mycobacterium tuberculosis* by microarray hybridization. Proc. Natl. Acad. Sci.U S A **96:**12833-8.

191. **Woese, C. R., O. Kandler, and M. L. Wheelis.** 1990. Towards a natural system of organisms: proposal for the domains Archaea, Bacteria, and Eucarya. Proc. Natl. Acad. Sci. U S A **87:**4576-9.

192. **Xavier, K. B., L. O. Martins, R. Peist, M. Kossmann, W. Boos, and H. Santos.** 1996. High-affinity maltose/trehalose transport system in the hyperthermophilic archaeon *Thermococcus litoralis*. J. Bacteriol. **178:**4773-7.

193. **Xavier, K. B., R. Peist, M. Kossmann, W. Boos, and H. Santos.** 1999. Maltose metabolism in the hyperthermophilic archaeon *Thermococcus litoralis*: purification and characterization of key enzymes. J. Bacteriol. **181:**3358-67.

194. **Yamamoto, I., T. Saiki, S. M. Liu, and L. G. Ljungdahl.** 1983. Purification and properties of NADP-dependent formate dehydrogenase from *Clostridium thermoaceticum*, a tungsten-selenium-iron protein. J. Biol. Chem. **258:**1826-1832.

195. **Ye, R. W., W. Tao, L. Bedzyk, T. Young, M. Chen, and L. Li.** 2000. Global gene expression profiles of *Bacillus subtilis* grown under anaerobic conditions. J. Bacteriol. **182:**4458-65.

196. **Zillig, W., J. Tu, and I. Holz.** 1981. Thermoproteales - a 3rd order of thermoacidophilic archaebacteria. Nature **293:**85-86.

197. **Zirngibl, C., W. Van Dongen, B. Schworer, R. Von Bunau, M. Richter, A. Klein, and R. K. Thauer.** 1992. H_2-forming methylenetetrahydromethanopterin dehydrogenase, a novel type of hydrogenase without iron-sulfur clusters in methanogenic archaea. Eur. J. Biochem. **208:**511-20.

APPENDIX A

A KEY ROLE FOR SULFUR IN PEPTIDE METABOLISM AND IN THE REGULATION OF THREE HYDROGENASES IN THE HYPERTHERMOPHILIC ARCHAEON *Pyroccus furiosus*[1†]

[1]Adams, M.W.W., J.F. Holden, A.L. Menon, G.J. Schut, A.M. Grunden, C. Hou, A.M. Hutchins, E.F. Jenney, C. Kim, K. Ma, G. Pan, R. Roy, R. Sapra, S.V. Story, M.F. Verhagen. 2001. *Journal of Bacteriology*. 183:716-724.

[†]M.W.W. Adams, J. F. Holden, A. Lal Menon, and G. J. Schut contributed equally to the design, execution, and data interpretation of this study.

ABSTRACT

The hyperthermophilic archaeon *Pyrococcus furiosus* grows optimally at 100°C by the fermentation of peptides and carbohydrates. Growth of the organism was examined in media containing either maltose, peptides (hydrolyzed casein) or both as the carbon source(s), each with and without elemental sulfur (S°). Growth rates were highest on media containing peptides and S°, with and without maltose. Growth did not occur on the peptide medium without S°. S° had no effect on growth rates in the maltose medium in the absence of peptides. Phenylacetate production rates (from phenylalanine fermentation) from cells grown in the peptide medium containing S° with or without maltose were the same, suggesting that S° is required for peptide utilization. The activities of 14 of 21 enzymes involved in or related to the fermentation pathways of *P. furiosus* were shown to be regulated under the five different growth conditions studied. The presence of S° in the growth media resulted in the decrease in specific activities of two cytoplasmic hydrogenases (I and II) and of a membrane-bound hydrogenase, each by an order of magnitude. The primary S°-reducing enzyme in this organism and the mechanism of the S°-dependence of peptide metabolism are not known. This study provides the first evidence for a highly regulated fermentative-based metabolism in *P. furiosus* and a significant regulatory role for elemental sulfur or its metabolites.

INTRODUCTION

Hyperthermophiles are microorganisms that grow optimally at 80°C and above (46, 47). Virtually all of them are strict anaerobes and most are heterotrophs. All of the heterotrophs utilize peptides as a carbon source and most use elemental sulfur (S°) as a terminal electron acceptor leading to H_2S production. The most studied of the S°-reducing, heterotrophic hyperthermophiles are species of *Pyrococcus*. Most of these organisms only utilize peptide-related substrates as a carbon source and show no significant growth in the absence of S° (9, 12, 19, 36). Notable exceptions are *Pyrococcus furiosus*, *P. woesei*, and *P. glycovorans*, which are capable of metabolizing poly- and oligosaccharides, as well as peptides (2, 4, 10). *P. furiosus* and *P. woesei* can also grow to high cell densities in the absence of S°.

The pathways of peptide and carbohydrate metabolism have been well-studied in *P. furiosus* (1, 7). Glycolysis appears to occur via a modified Embden-Meyerhof pathway (Fig. A.1; 22, 35). This pathway is unusual in that the hexose kinase and phosphofructokinase steps are ADP- rather than ATP-dependent, and a novel tungsten-containing enzyme termed glyceraldehyde-3-phosphate oxidoreductase (GAPOR) replaces the expected glyceraldehyde-3-phosphate dehydrogenase and phosphoglycerate kinase. Amino acid catabolism in *P. furiosus* is thought to involve four distinct 2-keto acid oxidoreductases that convert transaminated amino acids into their corresponding CoA derivatives (Fig. A.2; 3, 15, 31, 32). These CoA derivatives, together with acetyl CoA produced from glycolysis via pyruvate, are then transformed to their corresponding organic acids by two acetyl-CoA synthetases, unique to archaea, with concomitant substrate-level phosphorylation to form ATP (33). Alternatively, it has been postulated

(26) that, depending on the redox balance of the cell, 2-keto acids are decarboxylated to aldehydes and then oxidized to form carboxylic acids by a second tungsten-containing enzyme, aldehyde:ferredoxin oxidoreductase (34). A third enzyme of this type, termed formaldehyde:ferredoxin oxidoreductase (FOR), is thought to be involved in the catabolism of basic amino acids (42).

During fermentative growth of *P. furiosus* on oligosaccharides such as maltose, the primary end products are H_2, CO_2 and acetate. When S° is present in the medium, it is reduced to H_2S with a corresponding decrease in the amount of H_2 produced (10). However, the precise mechanisms by which H_2 is evolved and S° is reduced are not known as this organism contains two cytoplasmic, NAD(P)H-dependent hydrogenases, both of which can reduce S° *in vitro* (6, 28, 29). In addition, *P. furiosus* contains an H_2-evolving, membrane-bound hydrogenase complex, the function of which is not clear, although it does not reduce S° to H_2S *in vitro* (44). To further complicate matters, the cell yield of *P. furiosus* (dry weight/mol of maltose utilized) increases almost two-fold if S° is added to a maltose-containing medium (45). It is not known if this organism contains a membrane-bound, respiratory sulfur reductase of the type found in mesophilic S°-reducing organisms (14).

While the fermentative pathways of *P. furiosus* are reasonably well established, the extent to which they are regulated by the carbon source and by S° has not been investigated. Similarly, it is not clear why this organism differs from most other S°-reducing, heterotrophic hyperthermophiles in being able to grow well in the absence of S°. Herein we report the growth properties of *P. furiosus* grown on various combinations of carbohydrate (maltose), peptides (casein hydrolysate) and S°. In addition, under each growth condition, the extent of peptide fermentation was assessed by phenylacetate

production and the activities of twenty-one enzymes involved in the fermentative pathways were measured. The results establish a link between S° reduction, peptide metabolism and the activities of several key enzymes, notably the hydrogenases, and readily explain some of the unusual properties of this species of *Pyrococcus*.

MATERIALS AND METHODS

Growth conditions. *P. furiosus* (DSM 3638) was grown in a 20-liter fermenter containing 15 liters of medium, which was prepared as described previously (49). Media components were prepared as separate sterile stock solutions and stored at 4°C. Stock solutions were as follows. 5X salts solution (per liter): NaCl, 140 g; $MgSO_4 \cdot 7H_2O$, 17.5 g; $MgCl_2 \cdot 6H_2O$, 13.5 g; KCl, 1.65 g; NH_4Cl, 1.25 g; $CaCl_2 \cdot 2H_2O$, 0.70 g. 100 mM $Na_2WO_4 \cdot 2H_2O$ (10,000X, per liter): $Na_2WO_4 \cdot 2H_2O$, 3.3 g. 1000X trace minerals solution (per liter): HCl (concentrated), 1 ml; Na_4EDTA, 0.5 g; $FeCl_3$, 2.0 g; H_3BO_3, 0.05 g; $ZnCl_2$, 0.05 g; $CuCl_2 \cdot 2H_2O$, 0.03 g; $MnCl_2 \cdot 4H_2O$, 0.05 g; $(NH_4)_2MoO_4$, 0.05 g; $AlK(SO_4) \cdot 2H_2O$, 0.05 g; $CoCl_2 \cdot 6H_2O$, 0.05 g; and $NiCl_2 \cdot 6H_2O$, 0.05 g. Potassium phosphate buffer, pH 6.8 (1000X, per liter): 1 M KH_2PO_4 (pH 4.3), 450 ml; add 1 M K_2HPO_4 until the solution reaches pH 6.8 (approx. 550 ml). 10% (w/v) yeast extract (per liter): yeast extract (Difco), 100 g; filter sterilized. 10% (w/v) casein hydrolysate (per liter): casein hydrolysate (USB, enzymatic), 100g; filter sterilized. 50% maltose (per liter): maltose (Sigma), 500 g; filter sterilized. Resazurin: 5 mg per ml.

Each medium was composed of 1X base salts solution containing the following (per liter): distilled water, 800 ml; 5X salts, 200 ml; 100 mM $Na_2WO_4 \cdot 2H_2O$, 0.1 ml; 1000X trace minerals, 1 ml; resazurin, 0.05 ml; and 10% yeast extract, 5 ml (except in the

maltose plus peptides media, see below). One of three combinations of carbon source (maltose or peptides) was added to the 1X base salts solution. The carbohydrate-based medium contained 0.5% (w/v) maltose, and 0.1% (w/v) elemental sulfur was added to give the maltose plus S° medium. The peptides plus S° medium contained 0.5% (w/v) casein hydrolysate (enzymatic) plus 0.1% (w/v) sulfur (cultures grew very poorly on casein hydrolysate without sulfur, see below). Cultures grew poorly on acid-hydrolyzed casein and did not grow on casamino acids as a peptide source (with or without sulfur). The peptides plus maltose medium contained 0.5% (w/v) maltose, 0.5% (w/v) casein hydrolysate, together with 0.5% (w/v) yeast extract. This medium matches that typically used by our laboratory to grow *P. furiosus* in large scale culture (6). Elemental sulfur (0.1%, w/v) was added to give the peptides plus maltose plus sulfur medium.

The headspace of the fermenter was flushed with N_2/CO_2 (80:20), and 7.5 g each of cysteine-HCl and $Na_2S•9H_2O$ were added in that order as reducing agents to remove residual O_2. The pH (measured at room temperature) was adjusted to 6.8 with 1 N NaOH and 15 ml of 1 M potassium phosphate (pH 6.8) was slowly added. The medium was stirred and heated to 95°C. The pH of the medium at 95°C was 5.9 and was maintained (± 0.1 pH unit) by the automatic addition of 5% (w/v) $NaHCO_3$. *P. furiosus* was grown under each of the five growth conditions in triplicate.

An exponential-phase culture of *P. furiosus* that had undergone four successive transfers on the experimental medium was used to inoculate the 20-liter fermenter. During growth, 15 ml samples were removed at 1 h intervals from the fermenter and used to measure cell counts, media pH (at room temperature), and phenylacetate concentration. Cells were counted using a Petroff-Hausser counting chamber and phase-contrast light microscopy. Growth rate was calculated by measuring the slope of a best-fit line through

the exponential portion of the growth curve. Cells were harvested in the late logarithmic phase of growth (1-2 x 10^8 cells•ml^{-1}). The culture was first cooled to room temperature by pumping 12 liters (at 1 liter•min^{-1}) from the fermenter through a glass cooling coil bathed in an ice water slurry, and into a stoppered, 20-liter glass carboy flushed with argon. The cooled cells were harvested by centrifugation at 10,000 x *g* for 15 min (Beckman J2-21 centrifuge, JA-10 rotor) at 4°C, resuspended in 15-20 ml of anoxic 50 mM Tris-HCl buffer (pH 8.0) containing 2 mM Na-dithionite (DT) and 2 mM dithiothreitol (DTT) (Buffer A) in an anaerobic chamber (VAC Atmospheres) and frozen under Ar at -80°C.

Phenylacetate measurements. Aliquots (1.5 ml) of media from each 1 h sample were spun at 16,000 x *g* for 10 min in a microcentrifuge (Eppendorf). The supernatant was decanted and preserved with 0.1 M H_2SO_4 (final conc.). Phenylacetate concentrations were determined using an HPLC (Waters 2690) separation module equipped with a photodiode array detector. Organic acids were separated on an Aminex HPX-87H column (Bio-Rad) at 60°C using 5 mM H_2SO_4 and acetonitrile (manufacturer's stock solution) as the eluent in the following gradient: 5% acetonitrile, 0-5 min; 5-25% acetonitrile, 5-30 min; 25% acetonitrile, 30-35 min. Acetate could not be determined accurately in casein hydrolysate-containing media due to a low signal-to-noise ratio. The specific phenylacetate production rate was calculated by plotting the product of phenylacetate concentration (nmol•ml^{-1}) times growth rate (h^{-1}) divided by 0.693 against cell concentration (cells•ml^{-1}) for each time point sample. The slope of the best-fit line through the points yielded the specific production rate. The production rates were normalized by growth rate to compare the rates from the various growth conditions.

Protein fractionation. All sample transfers and manipulations were carried out in an anaerobic chamber and all buffers were degassed with Ar and contained 2 mM DT and 2 mM DTT. The cell suspension was thawed and DNase I in buffer A was added to a final concentration of 0.0002% (w/v). The cell suspension was incubated at room temperature with shaking for 30 min. The cells were then disrupted anaerobically by sonication for 30 min (Branson Sonifier 450) by placing the sample vial in an ice-water slurry with the sonicator probe. Cell lysis was verified using phase-contrast microscopy. Debris and unbroken cells were removed by centrifugation (10,000 x *g* for 15 min in a Beckman L8-M ultracentrifuge, 60Ti rotor) and a portion of the supernatant was used as the whole-cell extract. The remainder was centrifuged at 100,000 x *g* for 45 min and the supernatant was used as the cytoplasmic protein fraction. The membrane pellet was resuspended in buffer A, homogenized using a glass tissue grinder and then centrifuged at 100,000 x *g* for 45 min. This procedure was repeated three times, where buffer A in the final step contained 4 M KCl. The supernatant from the 4 M KCl wash formed the membrane-associated protein fraction, while the washed membrane pellet was resuspended and homogenized in buffer A and this formed the membrane-bound protein fraction. Protein fractions that were not used immediately for enzyme assays were frozen in liquid N_2 and stored at -80°C.

Enzyme assays. Activities are expressed in units where 1 unit is equivalent to 1 µmole of substrate transformed min^{-1} at 80°C, unless otherwise stated. Protein concentrations were estimated using the Bradford method (5) with bovine serum albumin as a standard.

The following spectrophotometric assays were carried out anaerobically in rubber-stopper sealed glass cuvettes that had been degassed and flushed with Ar. The buffer

used was 50 mM EPPS buffer (pH 8.4) unless otherwise stated. Aldehyde:ferredoxin (Fd) oxidoreductase (AOR), formaldehyde:Fd oxidoreductase (FOR), and glyceraldehyde-3-phosphate:Fd oxidoreductase (GAPOR) activities were determined by measuring the reduction of 3 mM benzyl viologen (BV) at 600 nm (ε = 7400 $(M \cdot cm)^{-1}$) using 0.3 mM crotonaldehyde, 50 mM formaldehyde or 0.4 mM glyceraldehyde-3-phosphate, respectively, as substrates (34, 35, 42). Formate dehydrogenase (FDH) activity was determined by measuring the reduction of 5 mM BV at 600 nm in 100 mM EPPS (pH 8.4) using 10 mM sodium formate as the substrate (27). The activities of pyruvate:Fd oxidoreductase (POR), 2-ketoglutarate:Fd oxidoreductase (KGOR), indolepyruvate:Fd oxidoreductase (IOR), and 2-ketoisovalerate:Fd oxidoreductase (VOR) were determined by measuring the reduction of 1 mM methyl viologen (MV) at 578 nm (ε = 9700 $(M \cdot cm)^{-1}$) using 5 mM pyruvate, 2-ketoglutarate, indolepyruvate or 2-ketoisovalerate, respectively, as substrates (3, 15, 31, 32). The assay mixtures also contained 2.5 mM $MgCl_2$, 0.4 mM thiamine pyrophosphate (TPP), and 0.1 mM coenzyme A (CoA). NADPH:rubredoxin oxidoreductase (NROR) activity was determined by measuring the reduction of 20 µM rubredoxin at 494 nm (ε = 9220 $(M \cdot cm)^{-1}$) at 25°C in 100 mM EPPS (pH 8.0) using 0.3 mM NADPH as the substrate (25). The combined activities of ferredoxin:NADPH oxidoreductase (FNOR) and NROR were determined by measuring the reduction of 3 mM BV at 600 nm using 0.4 mM NADPH as the substrate (24). The activities of acetyl-CoA synthetases I and II (ACS I and II) in the direction of acetate formation were measured by coupling the reactions to *P. furiosus* POR and IOR, respectively (33). ACS activity was determined by measuring the reduction of 5 mM MV at 600 nm with 5 mM $MgCl_2$, 0.4 mM TPP, 0.025 mM CoA, 1

mM ADP, and 10 mM K_2HPO_4 using 40 µg of POR to generate acetyl CoA or 40 µg of IOR to generate indoleacetyl CoA. Hydrogenase activity was determined by following the H_2 evolution rate using 3 mM MV reduced with 30 mM DT as the electron donor (6, 44).

The following enzyme activities were measured under aerobic conditions. Glutamate dehydrogenase (GDH) activity was determined by the reduction of 0.4 mM $NADP^+$ measured at 340 nm (ε= 6200 $(M \bullet cm)^{-1}$) in 100 mM EPPS buffer (pH 8.4) using 6 mM sodium glutamate as the substrate (40). Superoxide reductase (SOR) activity was determined as apparent superoxide dismutase activity where one unit is the amount of enzyme required to obtain 50% inhibition of the rate of cytochrome *c* (20 µM) reduction due to superoxide produced aerobically at 25°C by 0.2 mM xanthine and 3.4 µg xanthine oxidase in 50 mM potassium phosphate buffer (pH 7.8) (20). Adenylate kinase (AK) and guanylate kinase (GK) activities were determined by measuring the rates of ADP and GDP formation, respectively (modified from 38). For AK, the sample was added to 4 mM AMP, 10 mM $MgCl_2$ and 100 mM KCl and incubated for 2 min. The reaction was initiated by the addition of ATP (4 mM) and quenched by placing the sample on ice. The ADP formed was measured by adding 1 mM phosphoenolpyruvate (PEP), 40 mM NADH, and 5 U of pyruvate kinase and 5 U of lactate dehydrogenase (Roche Molecular Biochemicals) and following NADH oxidation at 340 nm (at 25°C, ε = 6200 $(M \bullet cm)^{-1}$). GK activity was measured in a similar manner except 2 mM GMP was substituted for AMP. One unit of AK activity is equivalent to 0.5 µmol ADP formed min^{-1} (since 2 ADP are produced for each AMP phosphorylated) and one unit of GK activity equals 1 µmol ADP formed min^{-1}. Phosphoenolpyruvate synthetase (PpsA) activity was

determined by phosphate formation (18). The sample was added to 4 mM pyruvate, 10 mM $MgCl_2$, and 200 mM KCl and incubated for 2 min. The reaction was initiated by adding ATP (4 mM) and quenched after 2 min with 0.2 ml of 5 M H_2SO_4. The amount of phosphate produced was measured spectrophotometrically as described previously (13). Aminoacylase activity was determined by adding the sample to a 500 µl total volume containing 50 mM Bis-Tris HCl (pH 6.5) and 30 mM N-acetyl-L-methionine (S. V. Story, A. Grunden, and M. W. W. Adams, submitted for publication). The assay mixture was heated to 100°C for 5 min, mixed with 500 µl of 15% trichloroacetic acid, and then spun at 13,000 x *g* for 5 min. 500 µl of this solution was removed and 250 µl of ninhydrin reagent (3% ninhydrin in ethylene glycol monomethyl ether) and 250 µl of 0.2 mM sodium acetate cyanide were added. The mixture was heated at 100°C for 15 min. 1.5 ml of 50% isopropanol was then added and the absorbance of the mixture was read spectrophotometrically at 570 nm. Prolidase activity was determined by measuring the production of proline using the colorimetric ninhydrin method (11, 51) from the hydrolysis of 4 mM Met-Pro dipeptide at 100°C in 50 mM MOPS buffer (pH 7.0). One unit of prolidase or aminoacylase activity is defined as the amount of enzyme that liberates 1 µmole of amino acid min^{-1} at 100°C.

Statistical analyses. The culture growth rate data, the phenylacetate production rates, and each enzyme activity measurement were subjected to statistical analysis as described previously (52). The triplicate growth rate and enzyme activity data from the five growth conditions were first compared by an analysis of variance (ANOVA) test, and then by a Tukey test ($\alpha = 0.05$, or a 95% confidence). Individual groups of data for each condition are reported as means ± one standard deviation (SD). The results of the Tukey test are

presented as shaded growth rates and enzyme activities in Tables A.1 and A.2 such that the shaded values are significantly different from the non-shaded values. The phenylacetate production rates were compared using linear regression analysis, analysis of covariance (ANCOVA), and a Tukey test ($\alpha = 0.05$).

RESULTS

***P. furiosus* growth versus carbon source.** The growth rates (doubling times ± SD) for *P. furiosus* under each growth condition are summarized in Table A.1. All growth curves demonstrated that the cultures were in exponential growth phase throughout the experiment, and that there was no diauxic growth or cultures reaching stationary growth phase (data not shown). Growth was most rapid when cultures were grown on peptides in the presence of S° (both with and without maltose). The growth rates in media containing maltose, maltose plus S°, and maltose plus peptides were not significantly different from each other, but were much lower than the growth rates in peptides plus S° media with and without maltose. On a small scale (50 ml of medium in 120 ml bottles), growth was extremely poor when cultures were grown in the peptides medium without S° after the first transfer, and no significant growth occurred after a second transfer. No attempt was made to grow *P. furiosus* in the fermenter using this medium. These data suggested that S° was required for growth of *P. furiosus* on peptides, but not on maltose.

As a measure of the extent to which peptides were being fermented during the growth of *P. furiosus* under the various conditions, we used phenylacetate production as an indicator. Phenylacetate is readily determined in complex mixtures and is the specific product of phenylalanine fermentation via phenylpyruvate and phenylacetyl CoA (Fig.

A.2). As shown in Fig. A.3, phenylacetate is produced by cultures grown on the peptides plus S° medium with a rate of 1.34 ± 0.14 nmol $(h \cdot 10^6 \text{ cells})^{-1}$ (± 95% confidence interval, n=18). The rate of phenylacetate production in the peptides plus maltose medium in the presence of S° (0.98 ± 0.06 nmol $(h \cdot 10^6 \text{ cells})^{-1}$, n=11) was very similar to that measured in the same medium without maltose when normalized by dividing the production rates by their corresponding specific growth rates. Thus, the production rates in the peptides plus S° medium were not affected by the presence of maltose. In contrast, with cells growing with maltose only as the carbon source, there was very little phenylacetate produced (0.03 ± 0.01 nmol $(h \cdot 10^6 \text{ cells})^{-1}$, n=4). Hence, phenylacetate production appears to be a very good measure of peptide utilization. There was a low level of phenylacetate produced when cultures were grown on maltose plus S° (0.19 ± 0.25 nmol $(h \cdot 10^6 \text{ cells})^{-1}$, n=9) and on peptides plus maltose without sulfur (0.23 ± 0.02 nmol $(h \cdot 10^6 \text{ cells})^{-1}$, n=13). However, these rates were not significantly different from one another, but were higher than the rate measured for the maltose medium and lower than the rates measured in medium containing peptides and sulfur (with or without maltose). Thus, the production rates in the peptides plus S° medium were not affected by the presence of maltose, while the production rates in the maltose, maltose plus S° and maltose plus peptides media were all much lower than those seen during growth on peptides and S° both with and without maltose. Furthermore, the phenylacetate production data corroborated well with the growth data and confirmed that growth on peptides was to a large extent dependent upon sulfur availability.

Enzyme activities. In view of the differential utilization of peptides depending on the presence of S°, the activities of a variety of enzymes in the fermentative pathways were

measured in cells grown under the five growth conditions (Table A.1). In order to assess the activities of both cytoplasmic and membrane-bound enzymes, the proteins from whole-cell extracts (WCE) of cells were fractionated into defined cytoplasmic (CYT), membrane-associated (MA) and membrane-bound (MB) samples. Protein assays showed that of the total protein present in the WCE, 75% ± 8% (n=15) was recovered in the combined CYT and 50 mM Tris-wash fractions. Only a very small percentage of the total protein (3% ± 1%, n=14) was recovered in the MA fraction obtained by the high salt wash, while the MB fraction contained 12% ± 5% (n=15) of the total protein. The remaining protein (~ 10%) was presumably lost during sample transfer and manipulations. The washing procedure was effective at removing CYT protein from the MA and MB fractions as judged by the amount of glutamate dehydrogenase (GDH) activity in the various fractions. GDH is a soluble protein (40) and was used as a marker to establish that the wash protocol provided complete separation of CYT proteins from the membrane. Of the total GDH activity, 77% ± 15% (n=15) was recovered after the first centrifugation step (100,000 x *g*) and only a trace amount of activity could be measured in the MA and MB protein fractions (0.5% ± 0.5% and 0.1% ± 0.1%, respectively, n=15).

The specific activities and standard deviations for each of the 21 enzyme assays that were carried out using cytoplasmic and membrane fractions from cells derived from each of the five growth conditions are summarized in Table A.2. Notably, 14 of the 21 enzymes showed significant differences in activity with change in growth condition. Those that remained essentially unchanged under the five growth conditions were ferredoxin:NADP oxidoreductase (FNOR), acetyl CoA synthetase II (ACS II), adenylate

kinase (AK), guanylate kinase (GK), prolidase, aminoacylase, and superoxide reductase (SOR).

On the other hand, the specific activities of both the cytoplasmic and membrane-bound hydrogenases increased approximately 10-fold when S° was omitted from the media. This was independent of whether cells were grown on maltose or maltose plus peptides. To determine whether these differences were due to enzyme inhibition by residual S° (or its metabolites) in the protein sample, aliquots of the cytoplasmic protein fraction from cells grown on maltose in the absence of S° were combined separately with aliquots of cytoplasmic, membrane, and whole-cell extract fractions from cells grown with maltose plus S°. In each case, hydrogenase activities were additive showing that the extracts of S°-grown cells do not contain inhibitors of these enzymes.

The activities of the peptidolytic pathway-related enzymes, aldehyde:Fd oxidoreductase (AOR), formaldehyde:Fd oxidoreductase (FOR) and 2-ketoisovalerate:Fd oxidoreductase (VOR), were each unchanged during growth on maltose or peptides plus S° (with and without maltose) media, but decreased significantly when the organism was grown on maltose plus S° (Table A.2). In contrast, the specific activity of NADPH:rubredoxin oxidoreductase (NROR) was highest under this growth condition, slightly lower on the maltose only medium, and lower still in the three peptide-based media. When *P. furiosus* was grown on peptides plus S° medium, the specific activities of the peptidolytic pathway-related enzymes, 2-ketoglutarate:Fd oxidoreductase (KGOR) and glutamate dehydrogenase (GDH), were significantly higher than in cells grown under any other condition, which were all similar to each other. In addition, indolepyruvate:Fd oxidoreductase (IOR) activity was higher in cells from the peptides plus S° medium than it was in cells grown with maltose with and without S° or peptides, which were all similar

to each other. The specific activity of the glycolytic enzyme, glyceraldehyde-3-phosphate:Fd oxidoreductase (GAPOR), was lowest in the peptides plus S° medium, although the values obtained varied considerably with the different growth conditions probably because of the inhibitory effect of sodium dithionite (which was present in all buffers) on the enzyme (35). Both pyruvate:Fd oxidoreductase (POR) and phosphoenolpyruvate (PpsA) showed a significant trend towards higher specific activity when cultures were grown on the maltose medium, while the activity of acetyl-CoA synthetase I (ACS I) was significantly higher in the maltose plus peptides medium. The specific activity of formate dehydrogenase (FDH) was very low in cells grown without S°, and the enzyme could not be detected in cells grown in the presence of S°.

DISCUSSION

The results presented herein show for the first time that *P. furiosus* efficiently utilizes peptides for growth only if S° is present, and peptides (plus S°) appear to be more favorable for growth over maltose as the carbon source. Yet, S° appears to have little effect on the metabolism of maltose by *P. furiosus*. Similarly, peptides appear to have little effect on cell growth with maltose in the absence of S°. These conclusions are supported by the results showing that phenylacetate production increased six-fold when S° was added to the peptides plus maltose medium. Also, growth rates were highest when both peptides and S° were present in the medium. The presence of maltose in the peptides plus sulfur medium had no effect on the rate of phenylacetate production, suggesting peptidolysis coexists with glycolysis. This is the first study to demonstrate growth substrate preference by *P. furiosus* and a link between peptide utilization and S°

availability. Peptides are the favored carbon source presumably because they obviate the need for the likely energy-requiring, *de novo* synthesis of some amino acids necessary during growth on maltose. Moreover, a link between peptide utilization and sulfur availability enables rationalization of some previously reported data. For example, Raven and Sharp (37) have shown that *P. furiosus* does not grow after 20 h of incubation with 0.5% (w/v) peptone and 0.1% (w/v) yeast extract in the absence of S°, whereas growth occurred when the peptide source was replaced with 20 mM maltose. However, this apparent preference for maltose over peptides was determined without considering S°. The results presented here show that peptides could only be utilized in the presence of S°.

There have been several reports on the nutritional characteristics of *P. furiosus* but typically maltose is the carbon source and S° is omitted from growth media. For example, using a defined minimal medium for the continuous culture of *P. furiosus* on maltose (no S°), it was shown that biotin, proline, and cysteine are required (37), while other researchers have reported slower growth rates on the same medium (23) and that Ile and Val are also essential amino acids (16). In the present study, the low concentration of yeast extract satisfied the essential amino acid and vitamin requirements of the organism, and we show here that these were independent of S° during growth with maltose as the carbon source. Like *P. furiosus*, *P. woesei* and *P. glycovorans* are reported to grow on maltose as the main carbon source (2, 4) but, in contrast to the situation with these strains, the growth rates and cell yields of other *Pyrococcus* spp., including *P. abyssi*, *P. horikoshii*, *Pyrococcus* ES-4 and *Pyrococcus* GB-D, are low or zero in the absence of S° and peptides (9, 12, 19, 36). It seems that these organisms cannot grow without S° because they can only utilize peptides, and that this appears to be a S°-dependent process.

P. furiosus is therefore unusual among known *Pyrococcus* spp. in that it will grow to high densities using maltose as the carbon source in the absence of peptides and S°. Maltose utilization has been studied in the hyperthermophile *Thermococcus litoralis* (17, 50) which, like *P. furiosus*, grows on maltose without S° (39). Maltose binds to the membrane protein MalE and crosses the membrane via the MalFG ABC membrane transporter complex where, in *P. furiosus*, it is converted to glucose by a-glucosidase (50). As might be expected, homologs of *malEFG* are present in the genome sequence of *P. furiosus* (30), but they are absent in the genomes of *P. horikoshii* (30) and *P. abyssi* (www.genoscope.cns.fr/cgi-bin/Pab.cgi). This could explain the inability of these organisms to utilize maltose, and presumably these genes would not be present in the other known *Pyrococcus* spp. that can only grow on peptides plus S°.

It has been established that in media lacking S°, the rate of H_2 production by *P. furiosus* is similar to the combined rates of H_2 and H_2S (~ 40:60 ratio) produced in the same media containing S° (10, 45). These results suggest that S° reduction simply 'replaces' H_2 evolution as a means of disposing of excess reductant (10) and that, as previously suggested, the cytoplasmic hydrogenases reduce S° as well as produce H_2 (28, 29). However, the results presented herein show that S° reduction may not occur by this simplistic mechanism, since the activities of the cytoplasmic hydrogenases are dramatically reduced by the presence of S° (Table A.2). In fact, it is reasonable that the activities of the cytoplasmic hydrogenases, as well as that of the membrane-bound enzyme, increase in the absence of S° as this would allow increased rates of H_2 production to compensate for the loss of S° reduction activity. Therefore, it does not appear that the hydrogenases are responsible for significant S° reduction, at least under the conditions used to grow *P. furiosus* described herein. The question is, what does

catalyze this reaction? FNOR reduces S° (24) but its activity did not vary with S° availability (Table A.2) suggesting that this is probably a fortuitous reaction. A hyperthermophilic membrane-bound sulfur reductase has been purified and characterized from the autotroph *Pyrodictium abyssi* (8). We have been unable to detect any S°-reducing activity in the membranes of *P. furiosus* using H_2, reduced ferredoxin, or NAD(P)H as the electron donors (J. F. Holden, R. S. Sapra, and M. W. W. Adams, unpublished data), and the genome sequence of *P. furiosus* does not contain any obvious homologs of the three genes that encode the membrane-bound sulfur-reductase complex of mesophilic organisms (14). The S°-reducing entity of *P. furiosus* is therefore unknown at this time. The membrane protein composition of *P. furiosus* changed with sulfur availability (21, J. F. Holden, R. S. Sapra, and M. W. W. Adams, unpublished results), and characterization of these S°-responsive proteins may lead to an understanding of the role of sulfur in metabolism. Our results correlate well with those reported for the growth of *Thermococcus* sp. strain ES1 in a peptide-based medium where hydrogenase (and FDH) activity decreased with increasing amounts of S° (27).

In prior studies of *P. furiosus*, the only enzymes of the glycolytic and peptidolytic pathways that have been shown to be regulated are GAPOR and GAPDH (48). The activities of these enzymes increased 5-fold and decreased 7-fold, respectively, when *P. furiosus* was grown on cellobiose relative to growth on pyruvate (48). Expression of the GAPOR gene (*gor*) is regulated at the transcriptional level while the activity of GAPDH appears to be regulated post-translationally. Accordingly, from our analyses, the highest GAPOR activity was measured in cells grown on maltose, and this decreased when peptides were the sole carbon source (Table A.2). Of the other enzymes tested that are involved in carbohydrate metabolism, both POR (Fig. A.1) and the gluconeogenic

enzyme PEP synthetase (PpsA, Fig. A.1) showed higher activity in a maltose-only medium although the differences are not large. Expression of *ppsA* is reported to be higher in cells grown on maltose and tryptone cells than in cells grown on tryptone only (41). PEP synthetase comprises about 5% of the cellular protein in maltose-grown *P. furiosus* and it has been suggested that it might function under high carbohydrate concentrations to rid the cell of excess energy, which can be harmful to the cell (18, 43).

We show here that several of the enzymes involved in the metabolism of peptides by *P. furiosus* are also regulated. KGOR, IOR, and GDH (Fig. A.2) show higher activities in cells grown on the peptides plus S° medium compared to cells using maltose as the sole carbon source (Table A.2). On the other hand, the activities of FOR and VOR (Fig. A.2) are largely unaffected by the growth conditions, except in cells grown on maltose plus sulfur when both decrease significantly. The same is true for AOR, an enzyme that is postulated to be involved in removing aldehydes generated in both the peptidolytic (via IOR, VOR and POR) and saccharolytic (via POR) pathways. The specific effector that is generated only by the metabolism of maltose and S° (and not by maltose only) is not known. The other enzyme that appears to undergo regulation is NROR, which catalyzes the NADPH-dependent reduction of rubredoxin possibly as part of a defense mechanism against oxygen toxicity (20, 25). Its activity increases when cultures are grown in the absence of peptides (with or without sulfur) but the reason for this is unclear.

Aside from GAPOR (48), it is not known if the regulation of the various enzymes listed in Table A.2 occurs at the transcriptional, translational, or post-translational level. Protein and mRNA analyses using two-dimensional gel electrophoresis and DNA microarrays are underway to address this issue. What is clear is that the metabolism of

sugars, peptides and S° by *P. furiosus* is not as straightforward as previously thought (Figs. A.1 and A.2) as key enzymes are tightly regulated and particularly those involved in the disposal of excess reductant.

ACKNOWLEDGMENTS

We thank H. Dailey for the use of his microscope. This research was funded by grants from the National Science Foundation (MCB 9904624, MCB 9809060 and BES-0004257), the National Institutes of Health (GM 60329) and the Department of Energy (FG05-95ER20175 and contract 992732401 with Argonne National Laboratory).

REFERENCES

1. **Adams, M. W. W.** 1999. The biochemical diversity of life near and above 100°C in marine environments. J. Appl. Microbiol. Sym. Suppl. **85:**108S-117S.

2. **Barbier, G., A. Godfroy, J.-R. Meunier, J. Quérellou, M.-A. Cambon, F. Lesongeur, P. A. D. Grimont, and G. Raguénes.** 1999. *Pyrococcus glycovorans* sp. nov., a hyperthermophilic archaeon isolated from the East Pacific Rise. Int. J. Syst. Bacteriol. **49:**1829-1837.

3. **Blamey, J. M., and M. W. W. Adams.** 1993. Purification and characterization of pyruvate ferredoxin oxidoreductase from the hyperthermophilic archaeon *Pyrococcus furiosus*. Biochim. Biophys. Acta **1161:**19-27.

4. **Blamey, J., M. Chiong, C. López, and E. Smith.** 1999. Optimization of the growth conditions of the extremely thermophilic microorganisms *Thermococcus celer* and *Pyrococcus woesei*. J. Microbiol. Meth. **38:**169-175.

5. **Bradford, M. M.** 1976. A rapid and sensitive method for the quantitation of microgram quantities of protein utilizing the principle of protein-dye binding. Anal. Biochem. **72:**248-254.

6. **Bryant, F. O., and M. W. W. Adams.** 1989. Characterization of hydrogenase from the hyperthermophilic archaebacterium, *Pyrococcus furiosus*. J. Biol. Chem. **264:**5070-5079.

7. **de Vos, W. M., S. W. M. Kengen, W. G. B. Voorhorst, and J. van der Oost.** 1998. Sugar utilization and its control in hyperthermophiles. Extremophiles **2:**201-205.

8. **Dirmeier, R. M., M. Keller, G. Frey, H. Huber, and K. O. Stetter.** 1998. Purification and properties of an extremely thermostable membrane-bound sulfur-reducing complex from the hyperthermophilic *Pyrodictium abyssi*. Eur. J. Biochem. **252:**486-491.

9. **Erauso, G., A.-L. Reysenbach, A. Godfroy, J.-R. Meunier, B. Crump, F. Partensky, J. A. Baross, V. Marteinsson, G. Barbier, N. R. Pace, and D Prieur.** 1993. *Pyrococcus abyssi* sp. nov., a new hyperthermophilic archaeon isolated from a deep-sea hydrothermal vent. Arch. Microbiol. **160:**338-349.

10. **Fiala, G., and K. O. Stetter.** 1986. *Pyrococcus furiosus* sp. nov. represents a novel genus of marine heterotrophic archaebacteria growing optimally at 100°C. Arch. Microbiol. **145:**56-61.

11. **Ghosh, M., A. Grunden, R. Weiss, and M. W. W. Adams.** 1998. Characterization of the native and recombinant forms of an unusual cobalt-dependent proline dipeptidase (prolidase) from the hyperthermophilic archaeon *Pyrococcus furiosus*. J. Bacteriol. **180:**4781-4789.

12. **González, J. M., Y. Masuchi, F. T. Robb, J. W. Ammerman, D. L. Maeder, M. Yanagibayashi, J. Tamaoka, and C. Kato.** 1998. *Pyrococcus horikoshii* sp. nov., a hyperthermophilic archaeon isolated from a hydrothermal vent at the Okinawa Trough. Extremophiles **2:**123-130.

13. **Hasegawa, H., M. Parniak, and S. Kaufman.** 1982. Determination of the phosphate content of purified proteins. Anal. Biochem. **120**:360-364.

14. **Hedderich, R., O. Klimmek, A. Kröger, R. Dirmeier, M. Keller, and K. O. Stetter.** 1999. Anaerobic respiration with elemental sulfur and with disulfides. FEMS Microbiol. Rev. **22:**353-381.

15. **Heider, J., X. Mai, and M. W. W. Adams.** 1996. Characterization of 2-ketoisovalerate ferredoxin oxidoreductase, a new and reversible coenzyme A-dependent enzyme involved in peptide fermentation by hyperthermophilic archaea. J. Bacteriol. **178:**780-787.

16. **Hoaki, T., M. Nishijima, M. Kato, K. Adachi, S. Mizobuchi, N. Hanzawa, and T. Maruyama.** 1994. Growth requirements of hyperthermophilic sulfur-dependent heterotrophic archaea isolated from a shallow submarine geothermal system with reference to their essential amino acids. Appl. Environ. Microbiol. **60:**2898-2904.

17. **Horlacher, R., K. B. Xavier, H. Santos, J. DiRuggiero, M. Kossmann, and W. Boos**. 1998. Archaeal binding protein-dependent ABC transporter: Molecular and biochemical analysis of the trehalose/maltose transport system of the hyperthermophilic archaeon *Thermococcus litoralis*. J. Bacteriol. **180:** 680-689.

18. **Hutchins, A. M., J. F. Holden, and M. W. W. Adams.** Phosphoenolpyruvate Synthetase from the Hyperthermophilic Archaeon *Pyrococcus furiosus*. J. Bacteriol. (in press, JB 373-00).

19. **Jannasch, H. W., C. O. Wirsen, S. J. Molyneaux, and T. A. Langworthy.** 1992. Comparative physiological studies on hyperthermophilic archaea isolated from deep-sea hot vents with emphasis on *Pyrococcus* strain GB-D. Appl. Environ. Microbiol. **58:**3472-3481.

20. **Jenney, Jr., F. E., M. F. J. M. Verhagen, X. Cui, and M. W. W. Adams.** 1999. Anaerobic microbes: oxygen detoxification without superoxide dismutase. Science **286:**306-309.

21. **Kelly, R. M., and J. W. Deming.** 1988. Extremely thermophilic archaebacteria: biological and engineering considerations. Biotechnol. Progr. **4:**47-62.

22. **Kengen, S. W. M., F. A. M. de Bok, N.-D. van Loo, C. Dijkema, A. J. M. Stams, and W. M. de Vos.** 1994. Evidence for the operation of a novel Embden-Meyerhof pathway that involves ADP-dependent kinases during sugar fermentation by *Pyrococcus furiosus*. J. Biol. Chem. **269:**17,537-17,541.

23. **Krahe, M., G. Antranikian, and H. Märkl.** 1996. Fermentation of extremophilic microorganisms. FEMS Microbiol. Rev. **18:**271-285.

24. **Ma, K., and M. W. W. Adams.** 1994. Sulfide dehydrogenase from the hyperthermophilic archaeon *Pyrococcus furiosus*: a new multifunctional enzyme involved in the reduction of elemental sulfur. J. Bacteriol. **176:**6509-6517.

25. **Ma, K., and M. W. W. Adams.** 1999. A hyperactive NAD(P)H:rubredoxin oxidoreductase from the hyperthermophilic archaeon *Pyrococcus furiosus*. J. Bacteriol. **181:**5530-5533.

26. **Ma, K., A. Hutchins, S.-H. Sung, and M. W. W. Adams.** 1997. Pyruvate ferredoxin oxidoreductase from the hyperthermophilic archaeon, *Pyrococcus furiosus*, functions as a coenzyme A-dependent pyruvate decarboxylase. Proc. Natl. Acad. Sci. **94:**9608-9613.

27. **Ma, K., H. Loessner, J. Heider, M. K. Johnson, and M. W. W. Adams.** 1995. Effects of elemental sulfur on the metabolism of the deep-sea hyperthermophilic archaeon *Thermococcus* strain ES-1: characterization of a sulfur-regulated, non-heme iron alcohol dehydrogenase. J. Bacteriol. **177:**4748-4756.

28. **Ma, K., R. N. Schicho, R. M. Kelly, and M. W. W. Adams.** 1993. Hydrogenase of the hyperthermophile *Pyrococcus furiosus* is an elemental sulfur reductase or sulfhydrogenase: evidence for a sulfur-reducing hydrogenase ancestor. Proc. Natl. Acad. Sci. USA **90:**5341-5344.

29. **Ma, K., R. Weiss, and M. W. W. Adams.** 2000. Characterization of hydrogenase II from the hyperthermophilic archaeon *Pyrococcus furiosus* and assessment of its role in sulfur reduction. J. Bacteriol. **182:**1864-1871.

30. **Maeder, D. L., R. B. Weiss, D. M. Dunn, J. L. Cherry, J. M. González, J. DiRuggiero, and F. T. Robb.** 1999. Divergence of the hyperthermophilic archaea *Pyrococcus furiosus* and *P. horikoshii* inferred from complete genomic sequences. Genetics **152:**1299-1305.

31. **Mai, X., and M. W. W. Adams.** 1994. Indolepyruvate ferredoxin oxidoreductase from the hyperthermophilic archaeon *Pyrococcus furiosus*. J. Biol. Chem. **269:**16,726-16,732.

32. **Mai, X., and M. W. W. Adams.** 1996. Characterization of a fourth type of 2-keto acid oxidizing enzyme from hyperthermophilic archaea: 2-ketoglutarate ferredoxin oxidoreductase from *Thermococcus litoralis*. J. Bacteriol. **178:**5890-5896.

33. **Mai, X., and M. W. W. Adams.** 1996. Purification and characterization of two reversible and ADP-dependent acetyl coenzyme A synthetases from the hyperthermophilic archaeon *Pyrococcus furiosus*. J. Bacteriol. **178:**5897-5903.

34. **Mukund, S., and M. W. W. Adams.** 1991. The novel tungsten-iron-sulfur protein of the hyperthermophilic archaebacterium, *Pyrococcus furiosus*, is an aldehyde ferredoxin oxidoreductase. J. Biol. Chem. **266:**14,208-14,216.

35. **Mukund, S., and M. W. W. Adams.** 1995. Glyceraldehyde-3-phosphate ferredoxin oxidoreductase, a novel tungsten-containing enzyme with a potential glycolytic role in the hyperthermophilic archaeon *Pyrococcus furiosus*. J. Biol. Chem. **270:**8389-8392.

36. **Pledger, R. J., and J. A. Baross.** 1991. Preliminary description and nutritional characterization of a chemoorganotrophic archaeobacterium growing at temperatures of up to 110°C isolated from a submarine hydrothermal vent environment. J. Gen. Microbiol. **137:**203-211.

37. **Raven, N. D. H., and R. J. Sharp.** 1997. Development of defined and minimal media for the growth of the hyperthermophilic archaeon *Pyrococcus furiosus* Vc1. FEMS Microbiol. Lett. **146:**135-141.

38. **Rhoads, D. G., and J. M. Lowenstein.** 1968. Initial velocity and equilibrium kinetics of myokinase. J. Biol. Chem. **243:**3963-3972.

39. **Rinker, K. D., and R. M. Kelly.** 1996. Growth physiology of the hyperthermophilic archaeon *Thermococcus litoralis*: development of a sulfur-free defined medium, characterization of an exopolysaccharide, and evidence of biofilm formation. Appl. Environ. Microbiol. **62:**4478-4485.

40. **Robb, F. T., J.-B. Park, and M. W. W. Adams.** 1992. Characterization of an extremely thermostable glutamate dehydrogenase: a key enzyme in the primary metabolism of the hyperthermophilic archaebacterium, *Pyrococcus furiosus*. Biochim. Biophys. Acta **1120:**267-272.

41. **Robinson, K. A., F. T. Robb, and H. J. Schreier.** 1994. Isolation of maltose-regulated genes from the hyperthermophilic archaeum, *Pyrococcus furiosus*, by subtractive hybridization. Gene **148:**137-141.

42. **Roy, R., S. Mukund, G. J. Schut, D. M. Dunn, R. Weiss, and M. W. W. Adams.** 1999. Purification and molecular characterization of the tungsten-containing formaldehyde ferredoxin oxidoreductase from the hyperthermophilic archaeon *Pyrococcus furiosus*: the third of a putative five-member tungstoenzyme family. J. Bacteriol. **181:**1171-1180.

43. **Russell, J. B.** 1998. Strategies that ruminal bacteria use to handle excess carbohydrate. J. Animal Sci. **76:**1955-1963.

44. **Sapra, R., M. F. J. M. Verhagen, and M. W. W. Adams.** 2000 Purification and characterization of a membrane-bound hydrogenase from the hyperthermophilic archaeon *Pyrococcus furiosus*. J. Bacteriol. **182:**3423-3428.

45. **Schicho, R. N., K. Ma, M. W. W. Adams, and R. M. Kelly.** 1993. Bioenergetics of sulfur reduction in the hyperthermophilic archaeon *Pyrococcus furiosus*. J. Bacteriol. **175:**1823-1830.

46. **Stetter, K. O.** 1996. Hyperthermophilic procaryotes. FEMS Microbiol. Rev. **18:**149-158.

47. **Stetter, K. O.** 1999. Extremophiles and their adaptation to hot environments. FEBS Lett. **452:**22-25.

48. **van der Oost, J., G. Schut, S. W. M. Kengen, W. R. Hagen, M. Thomm, and W. M. de Vos.** 1998. The ferredoxin-dependent conversion of glyceraldehyde-3-phosphate in the hyperthermophilic archaeon *Pyrococcus furiosus* represents a novel site of glycolytic regulation. J. Biol. Chem. **273:**28,149-28,154.

49. **Verhagen, M. F. J. M., A. Lal Menon, G. J. Schut, and M. W. W. Adams.** *Pyrococcus furiosus*: large scale cultivation and enzyme purification. Meth. Enzymol. (in press).

50. **Xavier, K. B., R. Peist, M. Kossmann, W. Boos, and H. Santos.** 1999. Maltose metabolism in the hyperthermophilic archaeon *Thermococcus litoralis*: purification and characterization of key enzymes. J. Bacteriol. **181:**3358-3367.

51. **Yaron, A., and D. Mlynar.** 1968. Aminopeptidase-P. Biochem. Biophys. Res. Commun. **32:**658-663.

52. **Zar, J. H.** 1996. Biostatistical Analysis, Third Edition. Prentice Hall, Upper Saddle River, New Jersey.

Table A.1. Growth rates of *P. furiosus* on various media[a].

Sulfur (S°)	Doubling time (min)[a] in medium with:		
	Maltose	Peptides	Peptides plus Maltose
Present	65.1 ± 1.6	**40.5 ± 4.8**	**47.6 ± 1.4**
Absent	63.3 ± 0.8	No growth	64.1 ± 5.8

[a]Results are means ± SDs. Boldfaced values are significantly different ($P < 0.05$) from all values that are not boldfaced (see Materials and Methods).

Table A.2. Specific activities of selected glycolytic, peptidolytic and related enzymes of cells grown with various substrates.

Enzyme	Sp act (U mg^{-1})[a] on the following growth medium:				
	Maltose + Peptides	Maltose	Maltose + Peptides + S°	Maltose + S°	Peptides + S°
Glycolysis:					
GAPOR	1.63±0.71	4.35±3.21	1.22±0.83	2.25±0.85	0.42±0.38
Peptidolysis:					
Prolidase	8.35±3.16	9.20±0.82	9.64±0.94	11.43±5.20	6.86±3.57
Aminoacylase	1.53±0.71	1.81±0.16	0.80±0.16	1.03±0.78	1.03±0.55
GDH	2.81±1.08	1.73±0.77	1.73±0.20	0.73±0.20	**5.70±0.67**
KGOR	0.20±0.06	0.13±0.05	0.26±0.06	0.20±0.03	**0.44±0.02**
IOR[b]	0.17±0.04	0.06±0.03	0.10±0.01	0.02±0.01	0.25±0.09
VOR	2.12±0.45	2.16±0.23	1.88±0.37	**0.79±0.08**	1.80±0.61
FOR	2.36±0.18	2.37±0.49	3.58±0.93	**0.83±0.22**	3.99±0.56
Both Pathways:					
POR[c]	7.90±1.27	9.70±1.12	6.81±0.15	4.89±0.87	4.95±1.60
AOR	2.30±0.47	2.48±0.37	2.42±0.75	**0.99±0.22**	2.19±0.42
ACS I	**0.57±0.08**	0.24±0.07	0.21±0.05	0.15±0.01	0.35±0.12
ACS II	0.14±0.11	0.06±0.00	0.07±0.01	0.08±0.04	0.08±0.02
H_2ase I+II	**4.17±1.72**	**2.57±0.87**	0.45±0.12	0.16±0.10	0.39±0.06
MB H_2ase	**18.06±8.15**	**14.52±7.37**	2.64±0.53	0.51±0.09	1.09±0.46

Other:					
NROR	0.019±0.015	**0.033±0.013**	0.004±0.002	**0.053±0.007**	0.012±0.002
NROR+FNOR	1.55±0.49	1.35±0.07	0.99±0.01	0.96±0.20	0.81±0.09
SOR	32.33±9.88	31.53±23.51	30.22±5.79	25.98±5.66	25.98±6.49
FDH	0.01±0.01	0.02±0.02	0	0	0
PpsA[d]	1.13±0.12	2.27±0.29	1.49±0.21	1.02±0.55	1.59±0.09
AK	0.27±0.10	0.37±0.01	0.32±0.03	0.22±0.06	0.31±0.05
GK	0.06±0.04	0.06±0.01	0.06±0.00	0.03±0.02	0.07±0.02

[a]All enzyme activities were measured using the cytoplasmic protein fraction except for the MB hydrogenase (H_2ase). All values means ± SDs. Boldfaced values are significantly different ($P < 0.05$) from all values that are not boldfaced.
[b]Statistical trend: peptides + S° > maltose = maltose + S° = peptides + maltose + S°
[c]Statistical trend: maltose > maltose + S° = peptides + S°
[d]Statistical trend: maltose > maltose + S° = peptides + maltose

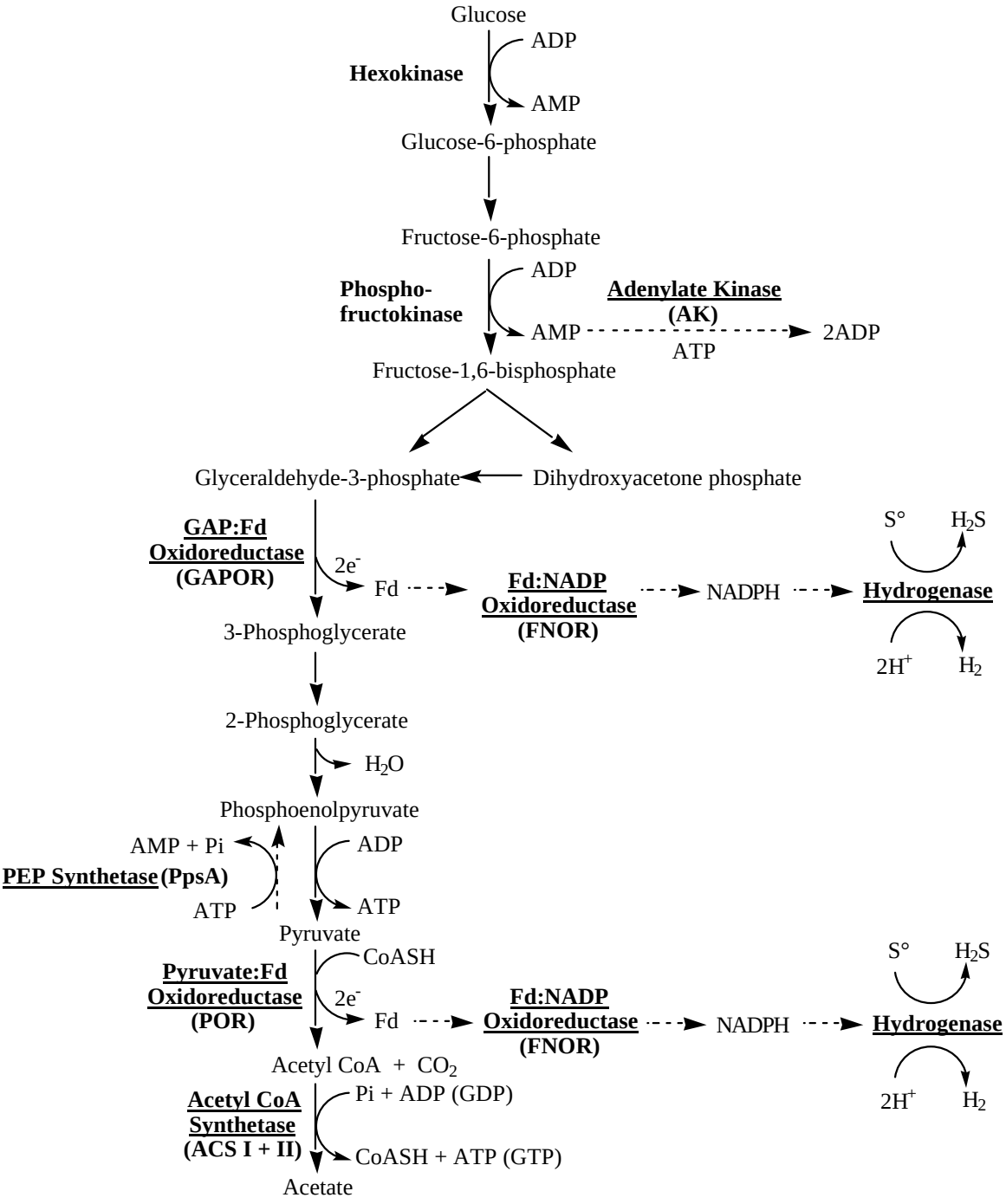

Figure A.1. Proposed glycolytic pathway in *Pyrococcus furiosus*. The enzymes whose activities were measured in this study are underlined. Fd represents the electron carrier ferredoxin. Modified from ref. 35.

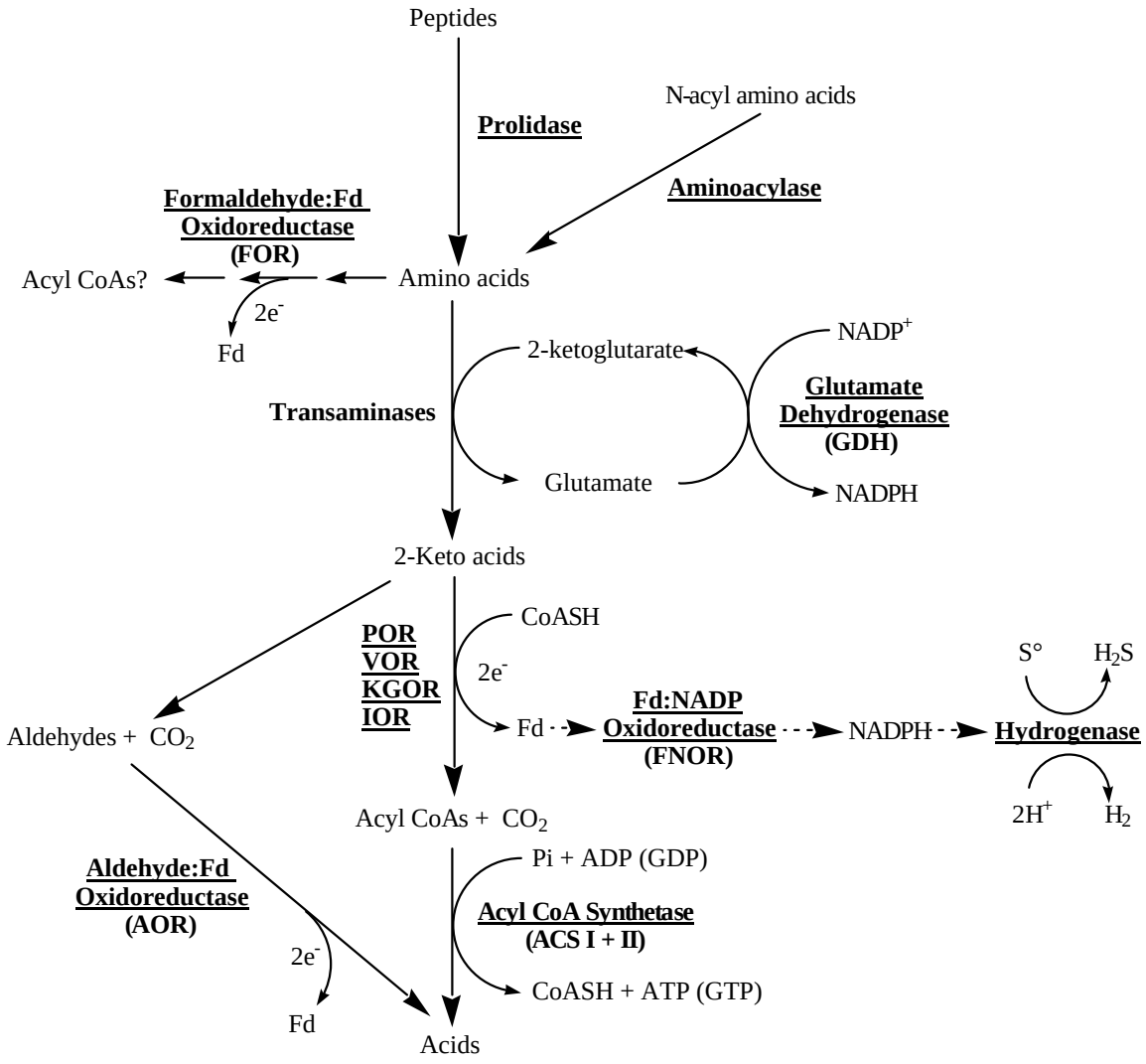

Figure A.2. Proposed peptidolytic pathway in *Pyrococcus furiosus*. The enzymes whose activities were measured in this study are underlined. FOR is thought to be involved in the metabolism of basic amino acids although the pathway involved is not known (42). Modified from refs. 15 and 34.

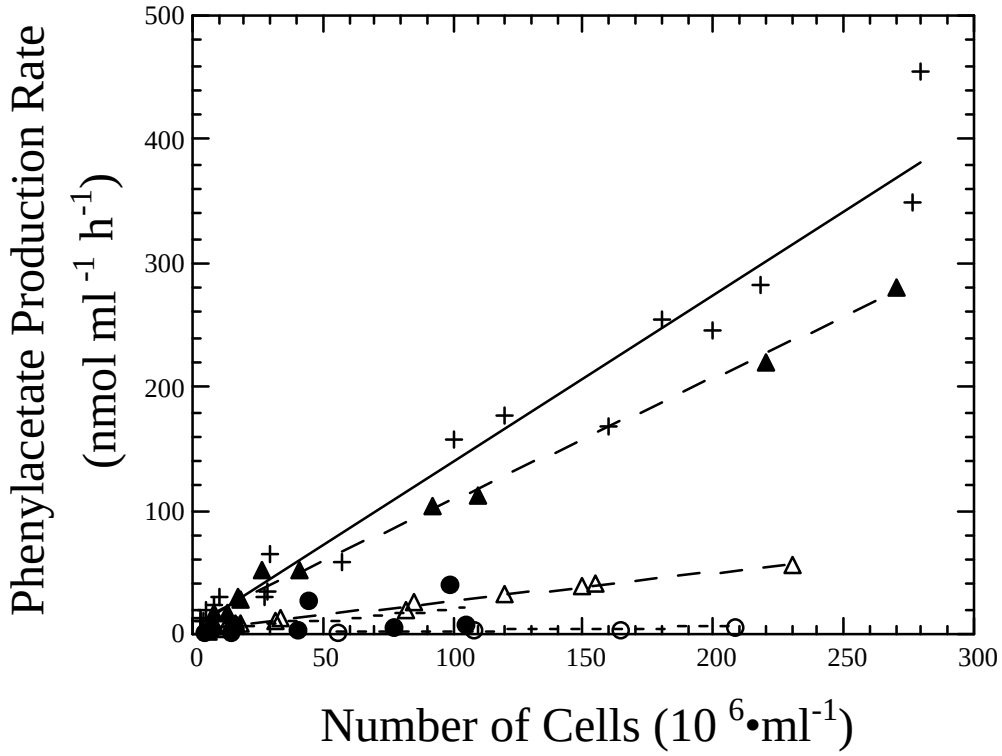

Figure A.3. Phenylacetate production rates when cultures were grown on peptides + S° (+, solid line), maltose (open circles, short-dashed line), maltose + S° (solid circles, short-dashed line), maltose + peptides (open triangles, long-dashed line), and maltose + peptides + S° (solid triangles, long-dashed line) media.